REAL INSTITUTO Y OBSERVATORIO DE LA ARMADA EN SAN FERNANDO
BOLETÍN ROA N.º 3/2013

PROCEEDINGS OF THE XVth IAGA WORKSHOP ON GEOMAGNETIC OBSERVATORY INSTRUMENTS, DATA ACQUISITION, AND PROCESSING

MINISTERIO DE DEFENSA

REAL INSTITUTO Y OBSERVATORIO DE LA ARMADA EN SAN FERNANDO
BOLETÍN ROA N.º 3/2013

PROCEEDINGS OF THE XVth IAGA WORKSHOP ON GEOMAGNETIC OBSERVATORY INSTRUMENTS, DATA ACQUISITION, AND PROCESSING

Extended Abstract Volume

Edited by:
Pavel Hejda
Arnaud Chulliat
Manuel Catalán

MINISTERIO DE DEFENSA

CATÁLOGO GENERAL DE PUBLICACIONES OFICIALES
http://publicacionesoficiales.boe.es/

Edita:

MINISTERIO DE DEFENSA
SECRETARÍA GENERAL TÉCNICA

www.bibliotecavirtualdefensa.es

NIPO: 083-13-199-X (impresión bajo demanda)
ISSN: 1131-5040
Fecha de edición: septiembre 2013

NIPO: 083-13-200-2 (edición libro-e)

Foto portada:

Cuarto de Círculo, J. Sisson (Londres, fines del siglo XVIII), N.º INV ROA 0023/B7.

PROCEEDINGS OF THE XVth IAGA WORKSHOP ON GEOMAGNETIC OBSERVATORY INSTRUMENTS, DATA ACQUISITION, AND PROCESSING

Extended Abstract Volume

June 4th – 14th, 2012
Real Instituto y Observatorio de la Armada
San Fernando, Cádiz, Spain

SPONSORED BY:

GOBIERNO DE ESPANA
MINISTERIO DE ECONOMIA Y COMPETITIVIDAD

GOBIERNO DE ESPAÑA
MINISTERIO DE DEFENSA

Spanish Navy

City of San Fernando

Royal Institute and Observatory of the Spanish Navy

CONTENTS

SESSION III: OBSERVATORIES

SESSION IV: Networks, Surveys, Repeat Stations and Satellites

SESSION V: DATA PROCESSING AND MANAGEMENT

PREFACE

The relationship of the Royal Observatory of the Spanish Navy (ROA) with Geomagnetism is old. Our first absolute observations were performed in 1879, and a continuous time recording began in 1891. From then onward it has been carried out with short periods of disruptions. We have been affected, as other geomagnetic observatories around the world, by urban growth, railway electrifying, and anthropogenic noise. It led us to move twice searching for new observatory sites. First in 1978, and lately in 2004. This last site, inside the Army stud farm of Garrapilos in La Barca de la Florida (Jerez-Cádiz) is located about 60km NE from San Fernando staff building.

In August 2009, IAGA requested to San Fernando geomagnetic observatory to assume the responsibility for the organization, the "*XVth Workshop on Geomagnetic Observatory, Instruments, Data acquisition and Processing*", finally celebrated from June 4th to June 14th, 2012. From my point of view there is no doubt that this will mark a remarkable event for geomagnetism in Spain as it was the first time that this workshop has been hosted by a Spanish institution.

More than 90 researchers from the five continents have participated in the Workshop. In general terms, the scheme has been as follows:

- Measurement sessions on Garrapilos Geomagnetic Observatory between 4 and June 8.
- Opening Ceremony in the morning of June 11, chaired by the Admiral of the Spanish Fleet, by the Major of San Fernando as local representative, and by Dr. Pavel Hejda as IAGA representative.
- Scientific sessions in "Bahía Sur" hotel at San Fernando between June 11 and 13.
- Visit to the Royal Observatory of the Spanish Navy in the evening of June 12, and an official dinner at Naval Officer's Club.

This was followed by a three-day scientific sessions (oral and poster), which began on June 11. This programme was divided in six sessions as follows:

- Topic I: Absolute measurements.
- Topic II: Magnetometers.
- Topic III: Observatories.
- Topic IV: Networks, surveys, repeat stations and satellites.
- Topic V: Data processing and management.
- Topic VI: Applications.

To complement the scientific oral sessions, Dr. Monika Korte, and Dr. Alan Thomson gave two keynotes lectures. The first addressed issues related to the evolution of geomagnetic observatories currently underway, and the second was devoted to space weather studies.

We would like to thank the help of the International Organizing Committee chaired by Arnaud Chulliat, and formed by Mioara Mandea, Aude Chambodut, Jeffrey J. Love, Pavel Hejda, Juan J. Curto, Christopher W. Turbitt, Manuel Catalán and particularly to Hans-Joaquim Linthe, Anca Isac and Errol Julies for their help during the measurement and training sessions.

All these actions could not have ever been fulfilled without the invaluable support of the Spanish Department of Defense and particularly the Spanish Marine Corps. We thank also our sponsors, the Spanish Navy, the Spanish Ministry of Economy and Competitiveness, the IAGA, and San Fernando city council.

Director of the Royal Observatory of the Spanish Navy

- Fernando Belizón Rodríguez -

GROUP PHOTOS OF ATTENDEES

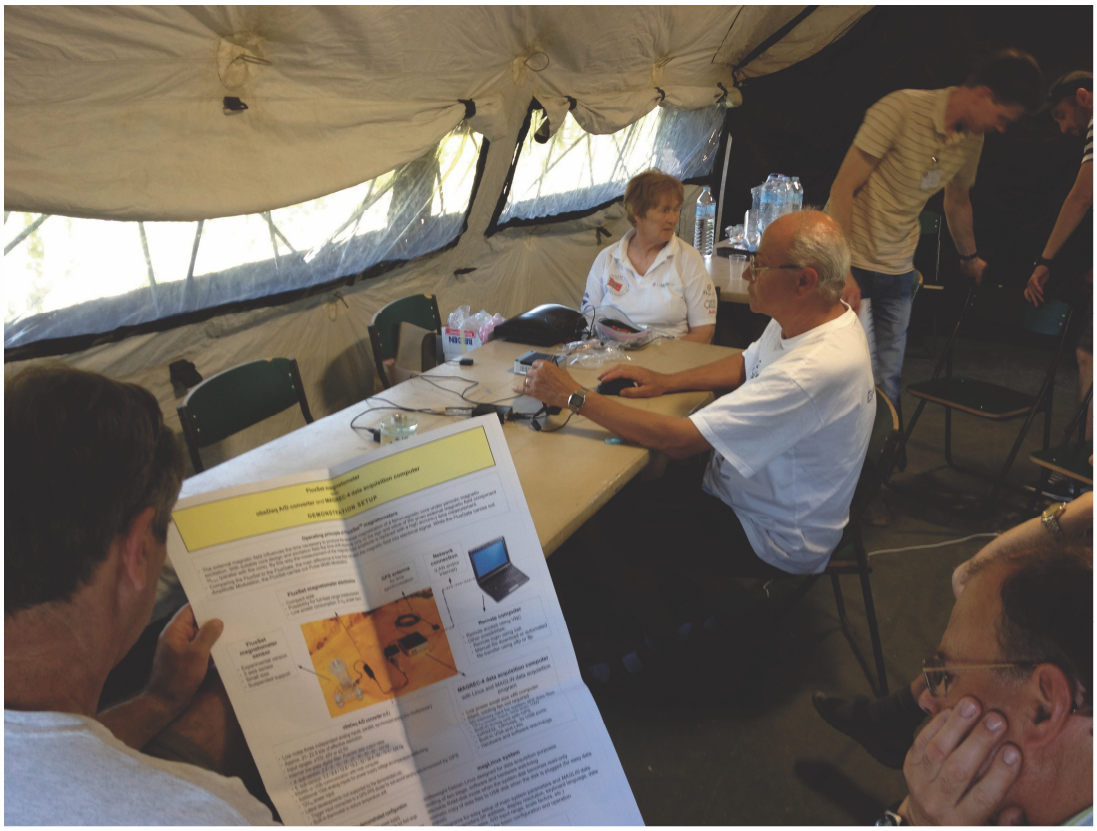


IAGA
XVth IAGA WORKSHOP
ON GEOMAGNETIC OBSERVATORY INSTRUMENTS,
DATA ACQUISITION AND PROCESSING
2 0 1 2
www.armada.mde.es


2 0 1 2
www.armada.mde.es


12/6/2012


12/6/2012

MEASUREMENT SESSION RESULTS

M. Catalán [(1)], M. Larrán [(1)]

[(1)] Royal Observatory of the Spanish Navy, San Fernando 11100, Spain, mcatalan@roa.es

1. INTRODUCTION

The absolute measurement session of the XV IAGA Workshop was held at San Fernando Magnetic Observatory (SFS) [June 5-8, 2012] at Garrapilos. The main focus of this session was for observers to make and compare measurements using DI-Flux magnetometers, scalar magnetometers and variometers. The session also included absolute measurement training carry out by Anca Isac (Geological Institute of Romania) and Errol Julies (SANSA Space Science, South Africa).

Testing and demonstration of three instruments under development were also carried out during the absolute measurement session:

- The auto DI Flux - Dr. Jean Rasson (Royal Meteorological Institute of Belgium).
- A triaxial DI Flux – Uli Auster (TU Braunschweig, Germany).
- A delta Declination/delta Inclination (dIdD) magnetometer - Laszlo Hegymegi (Mingeo Ltd, Hungary).

2. SCALAR MAGNETOMETER FREQUENCY TEST AND COMPARISON

The procedure consisted on a frequency test based on a checking through standard frequencies (instrument provided by H.J. Linthe - Niemegk Geomagnetic Observatory, Germany) and an inter-comparison with our master for a period of about 20 minutes with a sampling rate of 10 sec.

Scalar magnetometers, participants and results in this measurement session are listed below in Table 1.

Table 1– List of scalar magnetometers, observers and differences with master (model GSM-90F1)

No	NAME	COUNTRY	INSTRUMENT	DATE	DIFFERENCE (nT)
1	B. Leichter	Austria	Elsec 820 S/N 002084	06/06/2012	1.86+/-0.67
2	H.J. Linthe	Germany	GSM-19 S/N 410376	06/06/2012	0.48+/-0.09
3	L. Iancu(*)	Romania	Geometrics G-856 AX S/N 277996	06/06/2012	-0.08+/-0.32
4	J.L. Marin	Belgium	GSM-19W S/N 9053243	07/06/2012	0.58+/-0.10
5	S. Marsal	Spain	GSM-19 S/N 1041065	08/06/2012	-0.28+/-0.08
6	P. Covisa	Spain	GSM-19 S/N 707714	08/06/2012	-0.13+/-0.18
7	P. Covisa	Spain	G-856 S/N 50453	08/06/2012	-0.08+/-0.14

(*) This instrument was subjected to a frequency test. This checking shows an average error of -0.43 nT.

3. VARIOMETER COMPARISON

The procedure consisted of an inter-comparison using as masters SFS's variometers during one night period. These instruments are located inside the variometer hut, which is thermally isolated using an external air conditioning system. The orientation for the variometers used as masters were HDZ with a 5 sec.-sampling rate. The instruments to be checked were located on an external pier under a tent without temperature control. LOC performed absolute observations at the beginning and end of the intercomparison period to base the analysis on absolutes values, minimizing the effect of misorientations.

Two variometers have been brought for intercomparison: A. Marusenkov (Lviv Centre of Institute for Space Research, Ukraine)

model LEMI-031 low power (called **Var1** from now onward), and by U. Auster and Sandra Suarez (Magson GmbH, Germany) (called **Var2** from now onward).

We have compared both variometers registers against our two, which were installed on a Temperature controlled house as previously stated.

The temperature register shows three phases, which are delimited by two black vertical lines. The first period cover from the beginning of register until sunset. It shows a variation of 12ºC (approx.). A second period covers nighttime. During this period of time, temperature varied in a smoothly way. A third period starts at sunrise and extends until completion of register. This last period shows the strongest rate in temperature variation (7ºC/hr approx.). See figure 1.

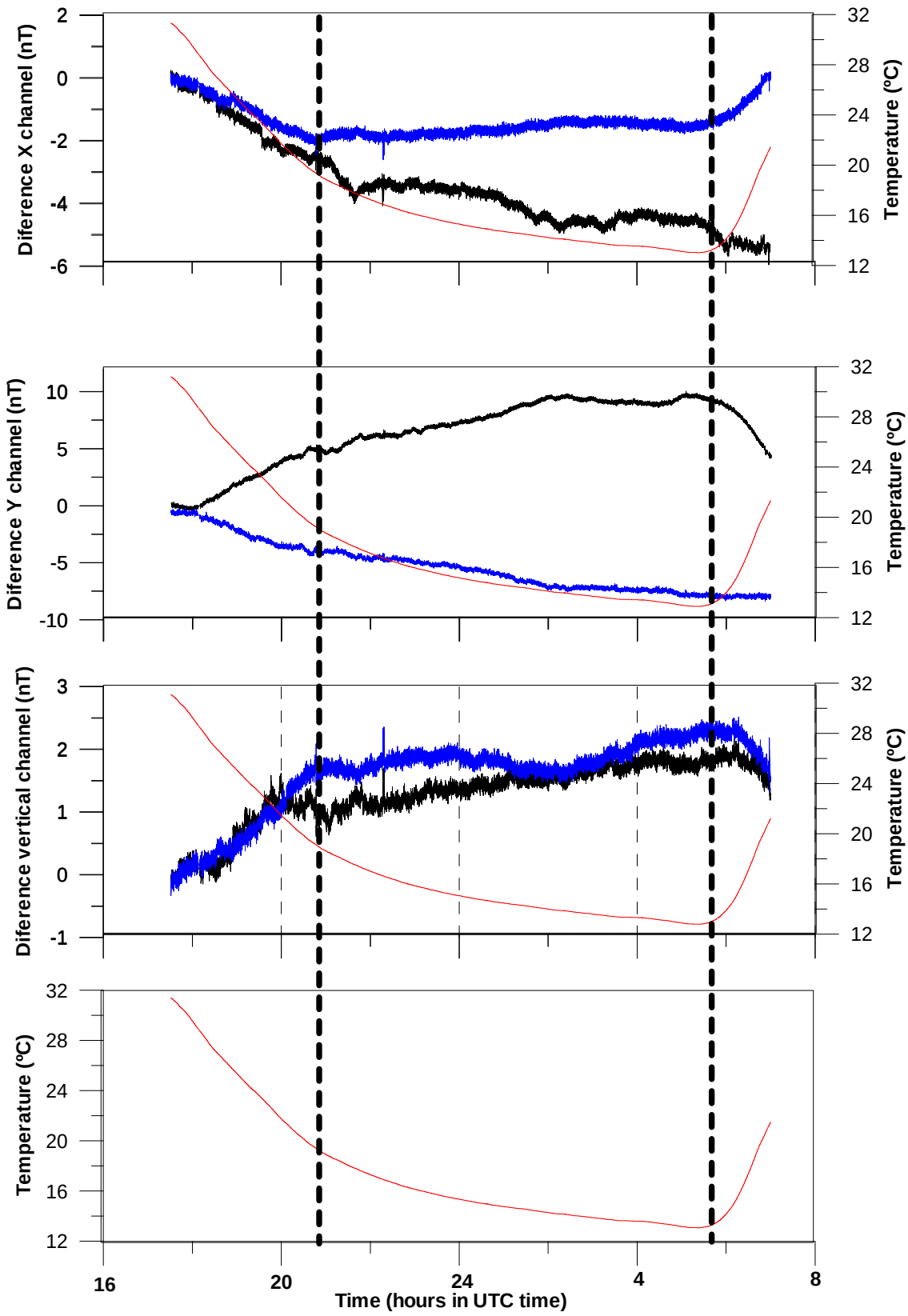

Figure 1–Black color corresponds to Var1. Blue color corresponds to Var2. In red the temperature variation is plotted. Uppermost, mid-upper and mid-lower plots denote residuals obtained after comparison against one of our variometers. Lowermost plot shows the variation of Temperature along the whole period of analysis.Two black dotted vertical lines divide the analysis in three segments: before sunset (First period),nighttime (Second period), and after sunrise (third period).

We include in Table 2 some temperature coefficient where possible, avoiding those periods where the rate of temperature variation was not uniform, as it distorted the correlation between both variables (magnetic component residual and temperature).

Table 2 – Variometers Temperature Coefficients

		First Period	Second period	Third period
X residual (T. Coeff. - nT/°C)	**Var1**	0.23	0.25	-0.02
	Var2	0.16	-0.04	0.18
Y residual (T. Coeff. - nT/°C)	**Var1**	-0.55	-0.68	-0.68
	Var2	0.33	0.64	0.005
Z residual (T. Coeff. - nT/°C)	**Var1**	-0.13	-0.12	-0.04
	Var2	-0.11	Not clear	-0.09

4. DI FLUX COMPARISON

Prior to the workshop several Total field and absolute measurements of declination and inclination were made at pillars 1, 2, 3, 4, 5 and 6 to calculate D (declination), H (horizontal intensity), and Z (vertical intensity) and scalar differences between pillars. Measurements were made by SFS staff, using their absolute instrumentation (MAG01H fluxgate magnetometer, and GEM Systems GSM-90F1 scalar magnetometer). The location of pillars 1 through 6 is showed in Figure 2 and the adopted D, H, Z, and F differences are shown in Table 3. Pillar 1 was chosen as reference. Offset between pillars were measured again after installation of the tents to assure that they do not introduce any magnetic bias or noise.

Figure 2 –pillar locations. V.H.: Variometer Hut., E.H.: Electronic House, A.H.: Absolute House.

Table 3 – D, H, Z and F differences for measurements pillars

	CorrD to Pillar 1 (min)	CorrH to Pillar 1 (nT)	CorrZ to Pillar 1 (nT)	CorrF to Pillar 1 (nT)
Pillar 2	0.57	0.70	-0.99	-0.30
Pillar 3	0.29	-1.05	1.45	0.40
Pillar 4	0.59	-0.14	-3.78	-3.10
Pillar 5	0.81	-1.28	-2.26	-2.50
Pillar 6	3.56	-7.58	-4.14	-8.05

During the workshop was detected that the window near pier 6 (absolute house) could interfere when opened. After the workshop SFS staff performed absolute measurements with the window completed closed and completed opened to quantify this effect. No differences were appreciated.

In the afternoon of June 5th and during 15 minutes, a car inadvertently parked close to the variometer house. It caused interferences. Four observations in that period were rejected (they affected to the following observers: A. Csontos, M. Sale and U. Auster).

The reference levels (zero level) for D, H, and Z were adopted from the average of all the measurements performed by the session's participants once referred to pillar 1, and the series of absolutes observations performed prior the workshop. Measurements outside two standard deviations were discarded. The reference level for D is 145.9±0.94 minutes; H is 27349.2±3.96 nT; Z is 33054.9±3.26 nT.

41 magnetometers and 35 observers participated in the DI-Flux absolute measurement session. The DI-Flux magnetometers and observers that participated in the absolute measurement session are listed below in Table 4.

Table 4 – List of DI-Flux instruments and observers

No	NAME	COUNTRY	INSTRUMENT
1	A. Berarducci	United States	Zeiss-Theo 020 DTU fluxgate magnetometer S/N 313836
2	A. Berarducci	United States	Zeiss-Theo 020 DTU fluxgate magnetometer (Compass Rose Surveying, Inc) S/N 616061
3	A. Berarducci	United States	Zeiss-Theo 020 DTU fluxgate magnetometer (Samoa) S/N 618312
4	A. Berarducci	United States	Zeiss-Theo 010 (L. Hegymegi´s fluxet magnetometer-Mingeo) S/N 107702
5	A. Csontos	Hungary	Theo-010B / S/N 107702 (L. Hegymegi´s fluxet prototipe)
6	A. Csontos	Hungary	Theo-010A / S/N 398205
7	A. Muslim	Maldives	Zeiss-Theo 020 DTU fluxgate magnetometer (Compass Rose Surveying, Inc) S/N 616061
8	B Harbour	United States	Zeiss-Theo 010 S/N 109648 / DTU Fluxgate S/N 0145
9	B. Leichter	Austria	Zeiss-Theo 010B S/N 154167 / MAG01H S/N 0619H
10	B. Worthington	United States	Zeiss-Theo 010 S/N 109648 / DTU Fluxgate S/N 0145
11	C. Turbitt	United Kingdom	Theo 010A S/N 814835 / Mag01H 0754H
12	D. Calp	Canada	Jena/Zeiss-Theo 010A S/N 392476 / Bartington MAG01H S/N 000772H
13	E. Cabrera	Argentina	Theo 010A S/N 814635 / MAG01H S/N 0754H
14	E. Julies	South Africa	Zeiss-Theo 010B S/N 152471
15	E. Nahayo	South Africa	Zeiss-Theo 010B S/N 152471
16	F. Valach	Slovakia	Theo-3T2KPNM S/N 39601 / LEMI-203
17	G. Cifuentes	México	Zeiss-Theo 020A S/N 3047
18	H.J. Linthe	Germany	Zeiss-Theo 010B S/N 105958 / MAG01H Bartington S/N 0714H
19	J. Horacek	Czech Republic	Theo 010B / MAG 01H Bartington S/N 154031
20	J.E. Hernández	México	Zeiss-Theo 010A S/N 200059
21	J.L. Marin	Belgium	Zeiss-Theo 020A S/N 616124 / FLM2/A
22	K. Pajunpää	Finland	Theo 010B S/N 153456
23	L. Iancu	Romania	Zeiss-Theo 010B S/N 160496 / MAG 01H S/N 402, S/N 0658H
24	L. Wang	Australia	Zeiss-Theo 010B S/N 160459 / MAG01H S/N 0610H
25	L.W. Perdersen	Denmark	Zeiss 010B S/N 107591 / D-I Fluxgate magnetometer, model G
26	M. Lim	Republic of Korea	Zeiss-Theo 010B S/N 105963 MAG01H Bartington S/N 788H
27	M. Vaczyova	Slovakia	Theo-3T2KPNM S/N 39601 / LEMI-203
28	M. Vlk	Czech Republic	Theo 010B / MAG 01H Bartington S/N 154031
29	Me Sale	Samoa	Zeiss-Theo 020 DTU fluxgate magnetometer S/N 313836
30	Me Sale	Samoa	Zeiss-Theo 020 DTU fluxgate magnetometer (Samoa) S/N 618312
31	P. Covisa	Spain	Zeiss-Theo 010B S/N 154747
32	R. Leonhardt	Austria	Theo-Leica F.-Nr: 231067 / MAG01H, S/N 562 Electronic S/N 1024H
33	S. Marsal	Spain	Zeiss-Theo 010B S/N 152076 / Elsec
34	S. Nagamachi	Japan	Theo 010B S/N 0624H
35	T. Bayer	Czech Republic	Theo 010B / MAG 01H Bartington S/N 154031
36	T. Raita	Finland	Theo 010B S/N 153456
37	T. Shanahan	United Kingdom	Carls-Zeiss Jena 010A S/N 814835 / Bartington MAG-01H S/N 0754H
38	U. Auster	Germany	Zeiss-Theo 010B S/N 101245 / Magson GmbH 3D fluxgate magnetometer
39	U. Auster	Germany	Zeiss-Theo 020 S/N 618312 / Magson GmbH 3D fluxgate magnetometer
40	W.S. Kim	Republic of Korea	Zeiss-Theo 010A S/N 811815
41	Y. Lipko	Russian Federation	Zeiss-Theo 010B S/N 152471

Results of the absolute measurement session of D, H, and Z are displayed in figures 3, 4, and 5 respectively. Results are shown in tabular form in Tables 5, 6, and 7.

Yellow cells in Tables 5, 6, and 7 show values which were excluded from the calculation of averages (these values were outside two standard deviations and are shown for information only), in the same Tables some values in red, clearly out of range, have been disregarded.

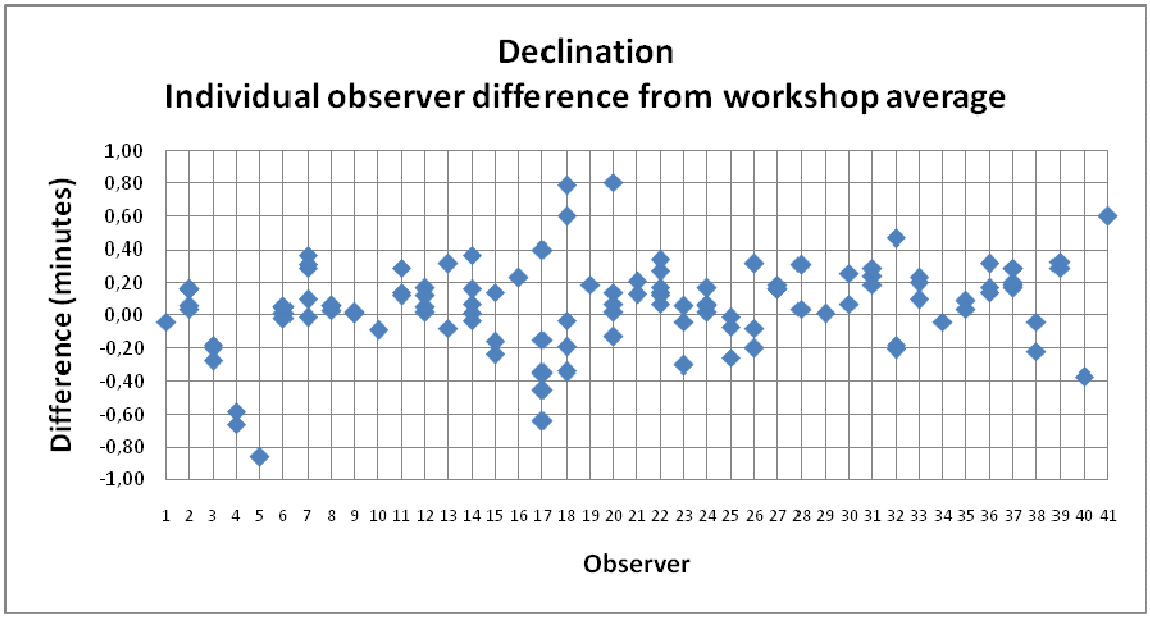

Figure 3–Individual observer differences from workshop average (Declination) referred to pillar 1. All measurements outside two standard deviations have been removed.

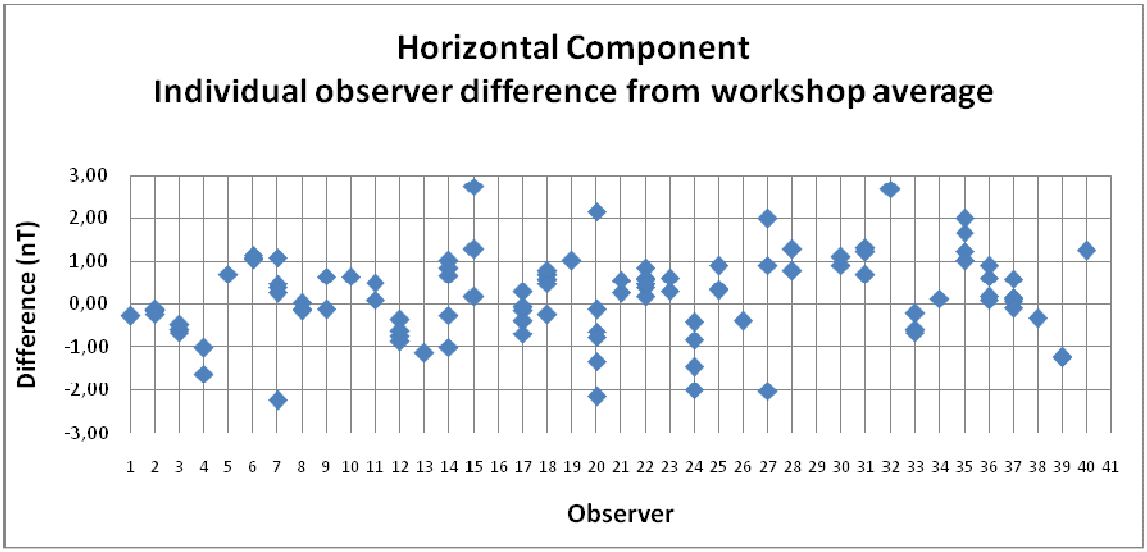

Figure 4 –Individual observer difference from workshop average (Horizontal component) referred to pillar 1.All measurements outside two standard deviations have been removed.

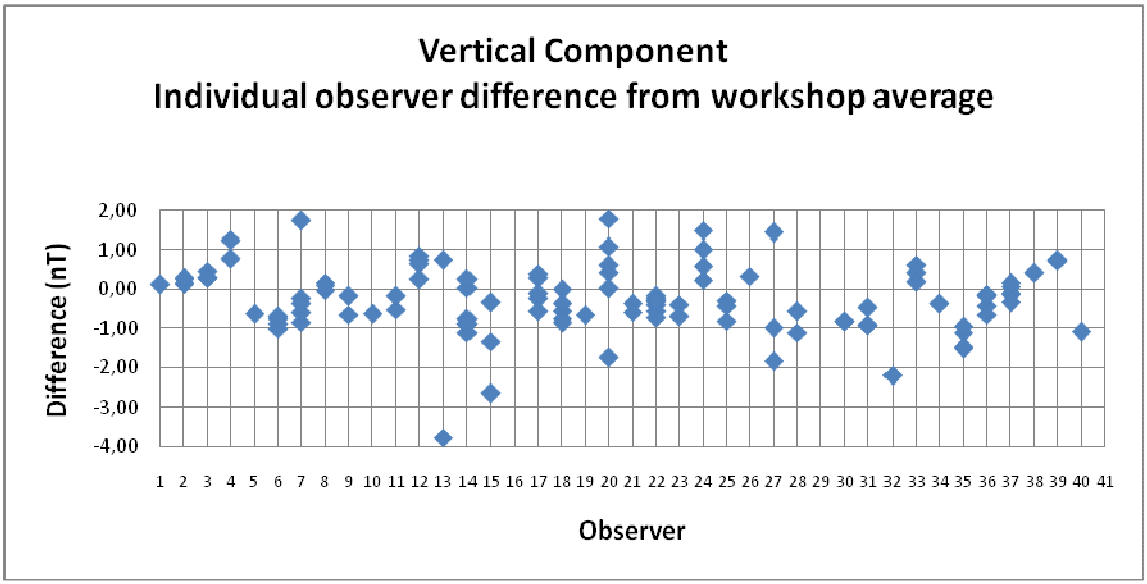

Figure 5 –Individual observer difference from workshop average (Vertical component) referred to pillar 1.

All measurements outside two standard deviations have been removed.

Table 5 – Individual observer difference from workshop average (declination). Measurements outside two standard deviations were not used in calculating workshop averages. Units in minutes. Obs: Observation

No	Obs 1	Obs2	Obs 3	Obs 4	Obs 5	Obs 6	Obs 7	Average	Std
1	-0.04							-0.04	0.00
2	0.06	0.04	0.16	0.16				0.10	0.06
3	-0.18	-0.20	-0.28					-0.22	0.05
4	-0.66	-0.58						-0.62	0.06
5	-0.86							-0.86	0.00
6	0.01	-0.02	0.05	0.05				0.02	0.03
7	0.1	0.29	0.37	-0.01	0.31			0.21	0.16
8	0.03	0.06	0.06					0.05	0.02
9	0.01	0.02						0.02	0.01
10	-0.09							-0.09	0.00
11	0.14	0.29	0.12					0.18	0.09
12	0.02	0.05	0.17	0.12				0.09	0.07
13	-0.08	0.32						0.12	0.28
14	-0.03	0.07	0.01	0.16	0.37			0.12	0.16
15	-0.24	-0.16	0.14					-0.09	0.20
16	0.23							0.23	0.00
17	-0.64	0.4	-0.15	-0.35	-0.45			-0.24	0.40
18	0.79	-0.34	-0.19	0.6	-0.03			0.17	0.50
19	0.19							0.19	0.00
20	0.81	0.02	0.14	-1.48	0.07	-0.13		0.18	0.36
21	0.21	0.13						0.17	0.06
22	0.14	0.27	0.34	0.07	0.14	0.12	0.17	0.18	0.09
23	-0.30	0.06	-0.04					-0.09	0.19
24	0.17	0.02	0.06	0.07				0.08	0.06
25	-0.07	-0.01	-0.26					-0.11	0.13
26	0.32	-0.08	-0.2					0.01	0.27
27	0.19	0.16	0.16					0.17	0.02
28	0.04	0.31						0.17	0.19
29	0.01							0.01	0.00
30	0.26	0.07						0.16	0.13
31	0.24	0.19	0.29					0.24	0.05
32	0.47	-0.18	-0.21					0.03	0.38
33	0.10	0.23	0.20					0.18	0.07
34	-0.04							-0.04	0.00
35	-2.76	-2.90	0.09	0.04				0.07	0.04
36	0.32	0.14	0.17	0.14				0.19	0.09
37	0.17	0.29	0.19	0.20	0.29			0.23	0.06
38	-0.22	-0.04						-0.13	0.13
39	0.29	0.33						0.31	0.03
40	-138.58	-0.37						-0.37	0.00
41	0.60							0.60	0.00

Table 6 – Individual observer difference from workshop average (Horizontal component). Measurements outside two standard deviations were not used in calculating workshop averages. Units in nT.

No	Obs 1	Obs2	Obs 3	Obs 4	Obs 5	Obs 6	Obs 7	Average	Std
1	-0.26							-0.26	0.00
2	-0.14	-0.14	-0.12	-0.22				-0.16	0.04
3	-0.57	-0.67	-0.47					-0.57	0.10
4	-1.02	-1.62						-1.32	0.42
5	0.71							0.71	0.00
6	1.05	1.07	1.14	1.04				1.07	0.05
7	0.38	1.08	0.45	0.25	-2.24			-0.02	1.28
8	-0.15	0.03	-0.13					-0.08	0.10
9	-0.13	0.65						0.26	0.55
10	0.64							0.64	0.00
11	0.49	0.09						0.29	0.28
12	-0.36	-0.88	-0.76	-0.62				-0.66	0.22
13	4.28	-1.14						-1.14	0.00
14	1.01	0.68	0.84	-0.25	-1.01			0.25	0.86
15	2.74	1.27	0.17					1.39	1.29
16	-48.03								
17	-0.14	-0.39	0.29	-0.7	-0.06			-0.20	0.37
18	0.69	0.58	0.77	0.47	-0.24			0.45	0.40
19	1.01							1.01	0.00
20	2.16	-0.63	-0.13	-2.15	-0.78	-1.33		-0.48	1.46
21	0.26	0.54						0.40	0.20
22	0.39	0.46	0.6	0.83	0.58	0.17	0.46	0.50	0.20
23	-8.70	0.30	0.60					0.45	0.21
24	-1.45	-1.99	-0.42	-0.84				-1.18	0.69
25	0.90	0.31	0.35					0.52	0.33
26			-0.38					-0.38	0.00
27	1.99	-2.02	0.91					0.29	2.07
28	0.78	1.27						1.02	0.35
29	-12.76								
30	0.91	1.09						1.00	0.13
31	0.69	1.31	1.22					1.07	0.34
32		-9.27	2.68					2.68	0.00
33	-0.21	-0.59	-0.68					-0.49	0.25
34	0.12							0.12	0.00
35	1.23	1.65	1.01	1.99				1.47	0.44
36	0.62	0.10	0.89	0.17				0.45	0.38
37	0.07	0.15	0.11	-0.09	0.58			0.16	0.25
38		-0.33						-0.33	0.00
39	-1.24	-1.23						-1.23	0.01
40	-202.23	1.25						1.25	0.00
41	-36.81								

Table 7 – Individual observer difference from workshop average (Vertical component). Measurements outside two standard deviations were not used in calculating workshop averages. Units in nT.

No	Obs 1	Obs2	Obs 3	Obs 4	Obs 5	Obs 6	Obs 7	Average	Std
1	0.12							0.12	0.00
2	0.15	0.25	0.16	0.3				0.21	0.07
3	0.29	0.47	0.31					0.36	0.10
4	0.79	1.26						1.02	0.33
5	-0.63							-0.63	0.00
6	-0.75	-1.00	-0.87	-0.70				-0.83	0.13
7	-0.24	-0.84	-0.59	-0.35	1.74			-0.06	1.03
8	0.17	-0.02	0.10					0.08	0.10
9	-0.17	-0.65						-0.41	0.34
10	-0.62							-0.62	0.00
11	-0.52	-0.17						-0.35	0.25
12	0.26	0.86	0.76	0.66				0.64	0.26
13	-3.76	0.76						-1.50	3.20
14	-1.10	-0.75	-0.90	0.05	0.25			-0.49	0.60
15	-2.63	-1.33	-0.33					-1.43	1.15
16	39.79								
17	0.3	0.41	-0.23	-0.1	-0.56			-0.04	0.40
18	-0.57	-0.74	-0.85	-0.36	0.00			-0.50	0.34
19	-0.67							-0.67	0.00
20	-1.74	0.44	0.03	1.78	0.62	1.09		0.37	1.20
21	-0.36	-0.58						-0.47	0.16
22	-0.22	-0.3	-0.55	-0.73	-0.4	-0.16	-0.29	-0.38	0.20
23	6.90	-0.38	-0.69					-0.54	0.22
24	1.01	1.49	0.24	0.59				0.83	0.54
25	-0.81	-0.29	-0.41					-0.50	0.27
26			0.34					0.34	0.00
27	-1.85	1.44	-0.99					-0.47	1.71
28	-0.56	-1.10						-0.83	0.38
29	10.38								
30	-0.81	-0.83						-0.82	0.01
31	-0.47	-0.93	-0.91					-0.77	0.26
32		7.51	-2.19					-2.19	0.00
33	0.20	0.42	0.63					0.42	0.22
34	-0.36							-0.36	0.00
35	-1.11	-1.51	-0.95	-1.49				-1.26	0.28
36	-0.41	-0.12	-0.64	-0.16				-0.33	0.24
37	0.06	-0.14	-0.11	0.16	-0.34			-0.07	0.19
38		0.43						0.43	0.00
39	0.75	0.74						0.75	0.01
40	166.58	-1.08						-1.08	0.00
41	29.87								

RESULTS OF ABSOLUTE MEASUREMENTS PERFORMED IN THE NIEMEGK GEOMAGNETIC OBSERVATORY USING THE DI3-FLUX INSTRUMENT

H.U. Auster [(1)], M. Korte [(2)]

[(1)] TU-Braunschweig, Mendelssohnstrasse 3, 38106 Braunschweig, Germany, uli.auster@tu-bs.de
[(2)] GFZ Potsdam, S. 2.3., Telegrafenberg, 14473 Potsdam, Germany, monika@gfz-potsdam.de

SUMMARY

Since 1980 the DI-Flux measurement is the commonly used procedure for determining the Earth's magnetic field components absolutely. The instrument used for this procedure consists of a non-magnetic theodolite equipped with a single axis fluxgate sensor. We replaced the single component fluxgate by a three component sensor which allows the measurement of the full Earth vector at each setting. The additional information can be used to characterize the instrument, to recover measurement errors and to calculate for the first time error bars of an absolute measurement. During the Changchun workshop this advanced method was successfully applied. For two years measurements with the DI3 Fluxgate have been continuously performed in the Geomagnetic Observatory Niemegk. We will present a comparison to the standard absolute measurement, instrument characteristics and error bars, which represent the observation quality.

1. INTRODUCTION

Three axes fluxgate magnetometers with sensors, small enough to be accommodated on top of a theodolite are developed by TU-Braunschweig for various space missions. Those magnetometers are used for measuring the magnetic field under harsh environmental conditions. The fluxgate magnetometer onboard the Lander of the ESA Rosetta mission (Auster et al., 2003) has to measure small magnetic field signals on the surface of a comet at a distance to Sun of 3 astronomical units (AU) at temperatures of about -100°C. The identical fluxgate sensors are used for the ESA BepiColombo mission (Glassmeier et al., 2011), measuring the turbulent plasma environment of Mercury at 0.3AU at a temperature of +180°C. The operation in a large temperature range requires high stability on offsets and sensor stiffness (e.g. stable axis alignment by using materials with similar thermal expansion coefficients only). Even for missions in the terrestrial magnetosphere with low perigees, which require the measurement in the full Earth field range, those magnetometers are used. Measuring in the Earth field range with the resolution which is needed at large Earth distances requires a high level of linearity. On spinning spacecrafts a high dynamic range is needed for performing precise measurements on systems moving with respect to the external field,.

We combined this type of fluxgate magnetometer featuring high dynamic range, low non linearity and high stability with the equipment usually needed for an absolute measurement. With a non magnetic theodolite for providing the horizontal leveling and the orientation versus azimuth mark and a scalar magnetometer for measuring the field magnitude, the magnetic field vector can be measured with a 3D magnetometer absolutely by each sample. The excess of information is usable to calculate error bars and to extend the robustness of the absolute measurement. Therefore, this method must have an advantage compared the DI-Flux measurement with a single component magnetometer used as (close) zero indicator only.

The method, briefly described in the following chapter (details see Geese et al. 2011) has been successfully compared with the standard method during the recent two workshops. A continuous application of this method has been run in the Niemegk observatory since 2010. Parameters characterizing the measurement quality, retrieved from this data set, are discussed in chapter 3.

2. MEASUREMENT PROCEDURE AND DATA PROCESSING

In contrast to the standard procedure, the theodolite has to be rotated completely independent of the local magnetic field conditions and measurements are taken independent of discrete time steps. A step to step procedure is programmed in a hand held computer (PDA). In

the beginning, middle and end of the procedure the azimuth mark has to be accessed in sensor up and down positions and the angles have to be typed into the PDA using a touch screen. For all other settings preselected angles have to be piloted. Vertical (VC) and horizontal (HC) angles are given by the software and have to be acknowledged. In analogy to the standard procedure first HC angles are varied and VC is kept constant followed by constant HC and varying VC angles. At each position (in the current procedure 54 in total) the magnetic field vector is measured by the fluxgate magnetometer.

During the measurement procedure the sensor is oriented in many different numbers of orientations with respect to the Earth field vector. Since we know the field magnitude from scalar magnetometer readings, we can use the relation between the field magnitude calculated by the components of the fluxgate magnetometer and the true field magnitude for calibrating the fluxgate magnetometer. The well-defined rotation about two theodolite axes can be exploited to calculate the orientation of the fluxgate magnetometer versus the theodolite reference system. Thus, after calibration and reorientation each fluxgate magnetometer is a single absolute measurement. Finally, variometer data is used to reduce the measurement to a certain measurement time.

3. TEST RESULTS

Absolute measurements with the DI3-Flux instrument have been performed in the Niemegk observatory continuously since December 2010. The results are shown in Figure 1. The measurements taken by the DI3 method (black dots) are compared with the standard absolute measurement in Niemegk (red dots). Procedure and data processing have been tested and improved in the course of the two years. After synchronizing the fluxgate data acquisition by the DCF clock in 2012 larger differences due to wrong timing as seen in 2011 could be eliminated.

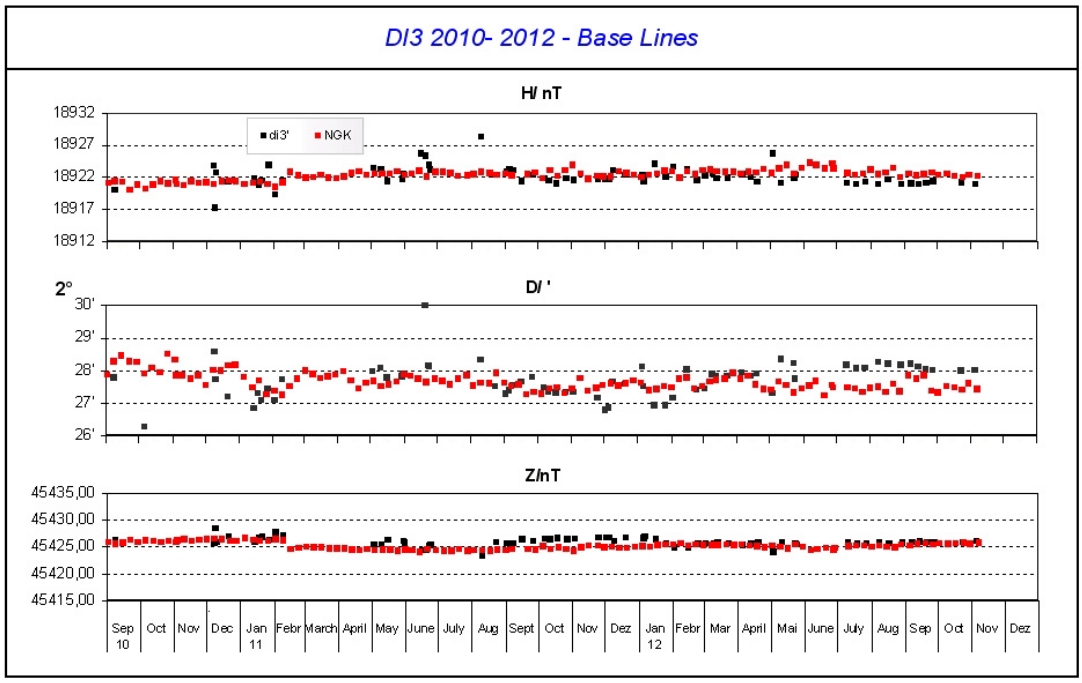

Figure 1 –Comparison between measurement by DI3 method and standard absolute measurement in Niemegk

A DI3 absolute measurement consists of 54 single vector readings each representing the complete field vector. The investigation of the variability of this set of measurement allows the characterization of the measurement error. The standard deviation can be used as an error bar and outliers are indicators of measurement errors like wrong adjusted theodolite settings or magnetic interferences. Thus, error bars (which should be provided for any measurement) can be given for the first time. The averaged errors for all Niemegk measurements are 3nT in D, 2nT in H and 1nT in Z. If the residues (deviation of each single measurement and averaged measurement result) are subsumed in an epoch time plot (see Figure 2, upper left panel) a common structure is visible. The averaged values, representing the systematic error, are plotted in the upper right panel. Reasons for systematic errors might be caused by the instrumentation, the magnetometer or the theodolite. For separating those two sources we have performed in San Fernando two measurements with a Zeiss Theo 010 from GFZ and two measurements with a Zeiss Theo 020 from USGS. The results are plotted in the lower right panel. Some features (see yellow circle) are visible in all four measurements. They are similar to the structure seen in the Niemegk statistics and can be therefore related to the magnetometer. Other features (see red circle) are clearly different for the Zeiss Theo 010 and 020. Those effects might be

related to more or less precision of the angular scales of the theodolites. Even if the statistics with different hardware are still weak, they indicate that both, magnetometer and theodolite quality can be investigated and monitored by the DI3 method.

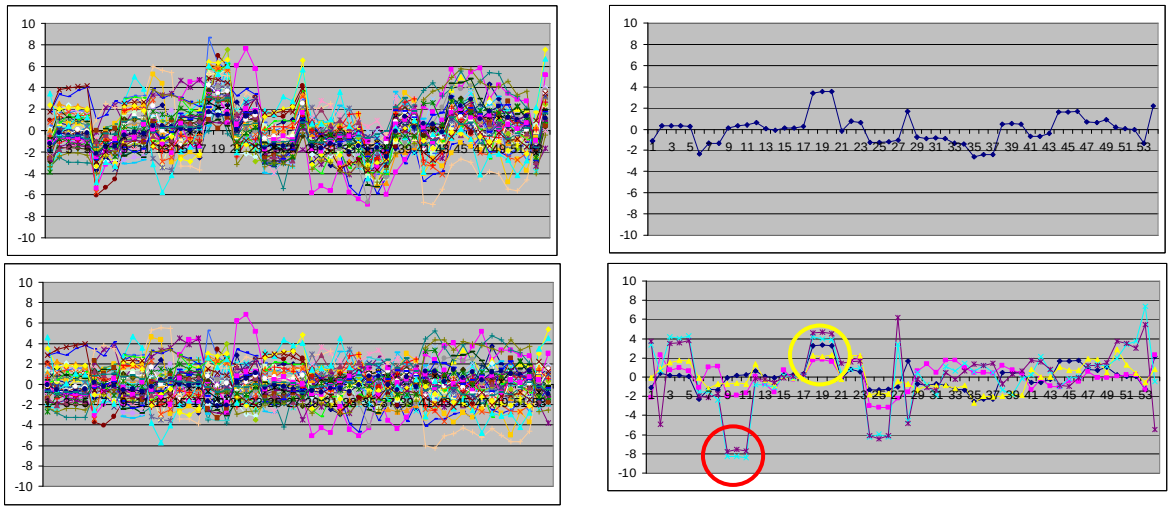

Figure 2 –In the upper left panel a super epoch plot of the 54 single measurements of the H component of each absolute measurement (different colors) performed during the last two years in Niemegk is shown. The averaged data (systematic error) is plotted in the upper right panel, the difference between original and averaged data (stochastic error) is plotted in the left bottom panel. In the bottom right panel the systematic error derived from Niemegk (blue) is plotted together with the errors of the San Fernando measurements performed with the GFZ theodolite (red and yellow) and performed with the USGS theodolite (light blue and purple). A signature common for all measurements is marked with a yellow circle, a signature which only occurs during the measurement by the USGS theodolite is marked with a red circle.

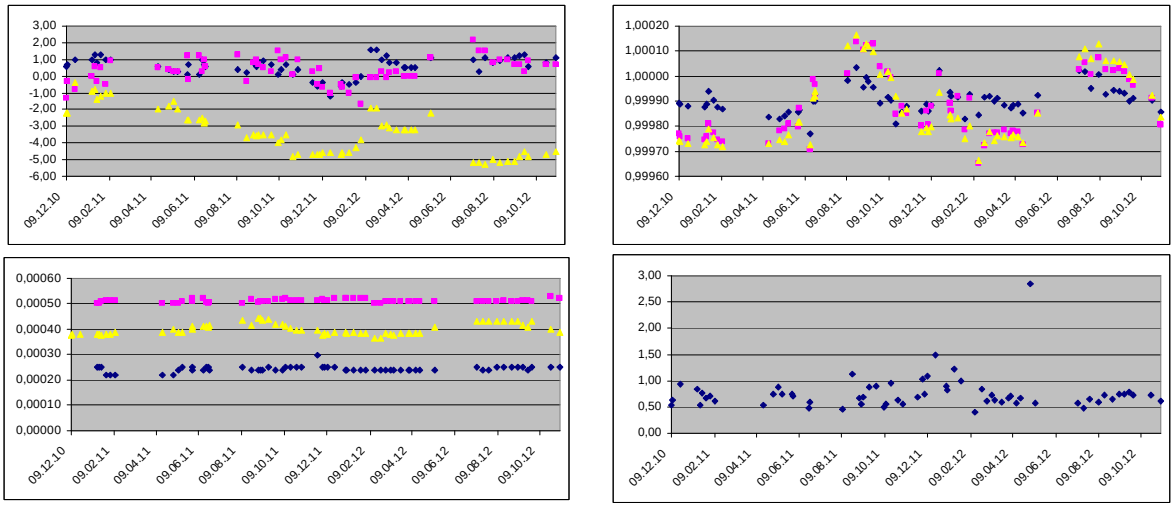

Figure 3 –Results of calibration: Upper left panel: offsets (x blue, y red, z yellow, in nT); Upper right panel: scale values (x ,y, z); Bottom left panel: orthogonality (xy, xz, yz); Bottom right panel: quality of the calibration (standard deviation of residues in nT).

As a spin-off product the calibration parameters of the magnetometer (offset, scale value and axis orientation, see Figure 3) can be derived. Offsets are varying within 3nT arbitrarily, scale values depend on environmental temperature due to the thermal expansion coefficient of the feedback coil system (see yearly variation) and the axes alignment is as expected almost stable. The quality of the calibration is plotted in the bottom right panel of Figure 3. A bad calibration seems to be performed beginning of May 2012. If the calibration is wrong, it has to be assumed that the absolute measurement is disturbed as well. This can be confirmed by checking the results in Figure 1. The value of the absolute measurement on May 03rd is the only one in 2012 (after improvement of timing) which deviates from all other by more than 2nT in the H component.

The possibility to detect measurement errors is one of the advantages of the DI3 method. The software checks automatically four different error sources. The consistency of the observatory data is checked by comparing the variation of the field magnitude measured by

the proton magnetometer and calculated from the variometer data, e.g. during our first measurement set in San Fernando the error flag turned red when a car interfered the variometer instrument. The quality of the calibration is checked by the difference between field magnitudes measured by the proton magnetometer and the field magnitude calculated from the DI3 magnetometer. Additionally, the drift of this difference is investigated because this is a measure for the temperature stability during the measurement, which might be not sufficiently preexisting soon after switching on. The fourth parameter is the consistency of the azimuth mark readings. Three angle readings are done and all of them should be within an acceptable tolerance interval. Beside this automated detection, data can by verified offline. Even if they are partly wrong they can still be recovered due to the high level of redundancy.

4. CONCLUSIONS

The test series in Niemegk shows the feasibility of the method. Compared to the standard one the method has two major advantages. The usage of the 3D magnetometer allows the determination of an error bar of an absolute measurement for the first time, and the substitution of the 3D magnetometer for a single component one on the theodolite improves the reliability of the absolute measurement. The spread of the large number of single measurements can be split into a systematic behavior related to theodolite and magnetometer properties and into a stochastic part, which is a measure for the accuracy of angle settings, which depend on observer and/or type of the theodolite. Because stochastic errors can be minimized by averaging, the DI3 method is particularly suitable for using less precise theodolites and semi professional observers. Guiding all measurement steps by a PDA-software makes the procedure even more error tolerant.

5. ACKNOWLEDGMENTS

We would like to thank Manuel Catalan and Manuel Larran for providing variometer and total force data as well as for their efforts in translating our results into the San Fernando comparison form. Furthermore we want to thank Katrin Tornow for doing the measurement in Niemegk during the recent two years and Alan Berarducci for providing the Zeiss Theo 020 in San Fernando on short notice.

6. REFERENCES

Auster, H.U., Apathy, I., Berghofer, G., Remizov, A., Roll, R., Fornacon, K.H., Glassmeier, K.H., Haerendel, G., Hejja, I., Kührt, E., Magnes, W., Moehlmann, D., Motschmann, U., Richter, I., Rosenbauer, H., Russell, C.T., Rustenbach, J., Sauer, K., Schwingenschuh, K., Szemerey, I. & Waesch, R. 2007, "ROMAP: Rosetta magnetometer and plasma monitor", *Space Science Reviews*, vol. 128, no. 1-4, pp. 221-240.

Geese, A., Auster, U., & Korte, M. (2011). DI3 - A new procedure for absolute directional measurements. *Data Science Journal*, *10*

Glassmeier, K.H., Auster, H.U., Heyner, D., Okrafka, K., Carr, C., Berghofer, G., Anderson, B.J., Balogh, A., Baumjohann, W., Cargill, P., Christensen, U., Delva, M., Dougherty, M., Fornacon, K.H., Horbury, T.S., Lucek, E.A., Magnes, W., Mandea, M., Matsuoka, A., Matsushima, M., Motschmann, U., Nakamura, R., Narita, Y., O'Brien, H., Richter, I., Schwingenschuh, K., Shibuya, H., Slavin, J.A., Sotin, C., Stoll, B., Tsunakawa, H., Vennerstrom, S., Vogt, J. & Zhang, T. 2008, "The fluxgate magnetometer of the BepiColombo Mercury Planetary Orbiter", *Planetary and Space Science*.

AUTODIF: AUTOMATIC ABSOLUTE DI MEASUREMENTS

A. Gonsette[(1)], J. Rasson[(1)], J.-L. Marin[(1)]

[(1)] Royal Meteorological Institute, rue du centre de physique 3 – 5670 Dourbes, Belgium, agonsett@meteo.be

SUMMARY

After a first presentation of the AUTODIF MKII instrument at the XIV IAGA workshop in Changchun (Rasson et al., 2011) we are back with a first time series. We start this paper with a brief description of the instrument. In particular, we explain how theodolite motion is achieved and how the directions of the reference frame are determined. In the second part we show the results obtained during the first semester 2012 in Dourbes. A comparison is done with the manual measurements. We finish by presenting some absolute MKII measurements during the XV IAGA workshop in San Fernando.

1. INTRODUCTION

In all geomagnetic observatories the absolute DI measurements remain a manual procedure executed by means of a theodolite, either natively non-magnetic or "cleaned" with varying degrees of success by a reverse engineering process. Such instruments are more and more difficult to find and relatively expensive to process so that a great number of observatories continue to use old ones and even ones in disrepair. Training and hiring people to execute the absolute measurements is not always easy. Sometimes even the environment is too hostile for an attended observatory. The AutoDIF aims to overcome those problems by performing automatically the absolute DI measurements. It opens the way for future full automatic geomagnetic observatories.

2. TECHNICAL DESCRIPTION

The device is similar to traditional non-magnetic theodolites on witch a fluxgate sensor has been mounted on its telescope. It is composed of two orthogonal axes mounted on ceramic bearings with reduced play. Three foot-screws are adjusted manually during the setup in order to align the vertical axis to the local vertical. The tilt sensor is a non-magnetic electrolytic level with a resolution better than 0.5 arcsec. The true North is determined by means of a target consisting of a corner cube set-up in a known azimuth (Figure 1). A laser mounted on Autodif points that target and a couple of photocells placed on both side of the laser receives the returning light beam. If the beam points the center of the corner cube, both photocells receive the same light and the beam materializes the target direction.

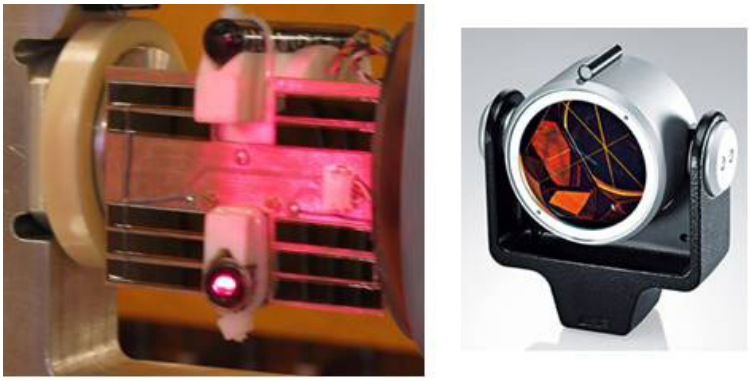

Figure 1 –Left: laser and photocells mounted on Autodif. Right: corner cube Leica GPH1P (source: Leica Geosystems website)

Each axis is actuated by piezoelectric motors. They consist of a ceramic rod excited by 280Vrms at 39.6 kHz. That frequency is high enough so as to be considered harmless for the DC magnetic measurements. When the AC current is applied, a wave motion occurs. A finger

placed at the end of the rod describes a circular path (*Figure* 2). The motion is transmitted to the axis through a ceramic ring by friction. The housing is in anodized aluminum so that the motor is non-magnetic. Two different displacement modes are possible. The first one is a traditional motion with a PID regulation used for relatively big angular displacements while the second is a very high resolution step-by-step motion providing 0.001° incremental steps. The motors were the Achilles' heel of the Autodif MK I with a life time of only a few months. The new motors are running now for two years without any sign of wear nor malfunction. They have performed thousands of measurements.

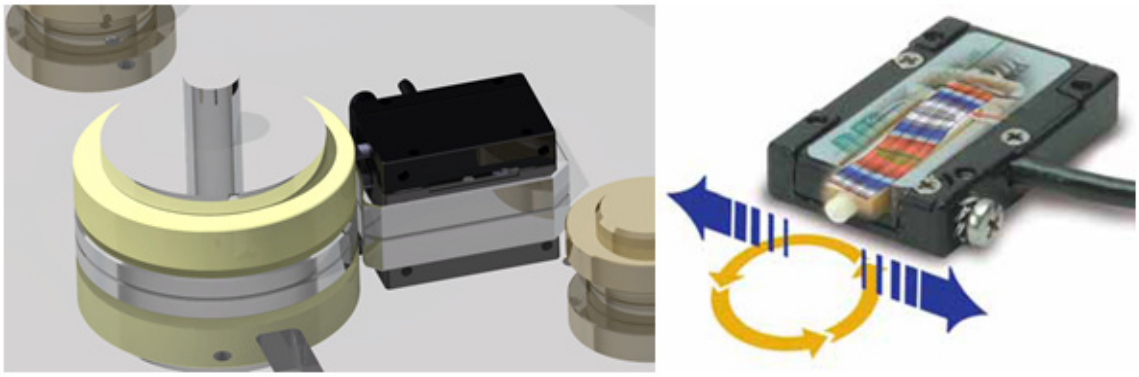

Figure 2 –Left: CAD representation of the motor and the ceramic ring of the vertical axis. Right: the wave motion of the rod and the circular path of the finger.

The traditional operator-read graduated circles of the theodolite are replaced by optical encoders (*Figure* 3). The principle is based on the optical moiré effect. A glass disc with 2048 lines is mounted on the rotor. A stator reading station with an IR led, optical reticle and a photodiode array generates three signals: one reference signal providing the zero position of the circle and a sin/cos couple allowing an interpolation between two lines. Two reading stations are positionned on the circle at 180° in order to remove the excentricity error of the disc set-up. It is therefore possible to read angles with a resolution of 1 arcsec and an accuracy of 6 arcsec. All original magnetic parts have been removed and replaced by non-magnetic ones. In particular the electronic boards have had to be completely redesigned.

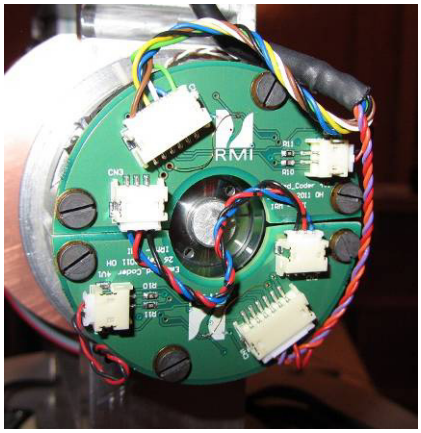

Figure 3 –Optical encoder measuring the rotation angle of the vertical circle.

3. MEASUREMENT

The Autodif follows the same sequence as a manual DIFlux (Rasson, 2005). The procedure starts with a target pointing probe up and down that gives a reference to the true North direction. The second pointing is done by reversing both axes of the instrument in order to remove the pointing error due to the mechanical defects, photocells eccentricity and offset. It continues with the four declinations measurements. As the fluxgate sensor is never exactly aligned with the optical axis of the telescope, a collimation (vertical and horizontal) error appears. On top of that the material composing it is magnetic, generating therefore a magnetization error. Actually, any magnetic part in the fluxgate frame participates to this error (Gilbert et al., 1996). If stable over the whole measurement sequence, it is removed from the final result by performing and averaging the four possible magnetic meridian measurements. A target pointing is done again to check the orientation stability of the instrument and the pillar/tripod. The protocol finishes with four inclinations measurements determining again and independently the magnetization and collimation errors.

The instrument was tested in Dourbes during the first semester of 2012. A complete measurement protocol was scheduled every 30 minutes so that we obtained 48 absolute measurements per day. For comparison a traditional sequence was performed on the same pillar by means of our observatory non-magnetic Zeiss 010B theodolite. Autodif was halted and removed from its pillar. After the Zeiss had performed its absolute measurement, AutoDIF was replaced on the pillar by the observer without any re-leveling. The corner cube was placed at about 100 m from the pillar just behind the target used for the manual measurement. This distance is large enough to ensure that a localization using 120° V-groove crapaudines does not affect the error budget. Indeed a simple trigonometric calculation shows that 1 mm misalignment in the worst direction (perpendicular to the target direction) generates 2'' azimuth error at that distance.

The variometer that we measure the baselines of is a DFI oriented Lama with name "LAMADOU" sampling at a 5 sec rate. We suppose that the magnetic field does not change significantly between two samples so we do not synchronize exactly Autodif with the variometer but we use the closest value which has therefore a 2.5 sec maximum time mismatch.

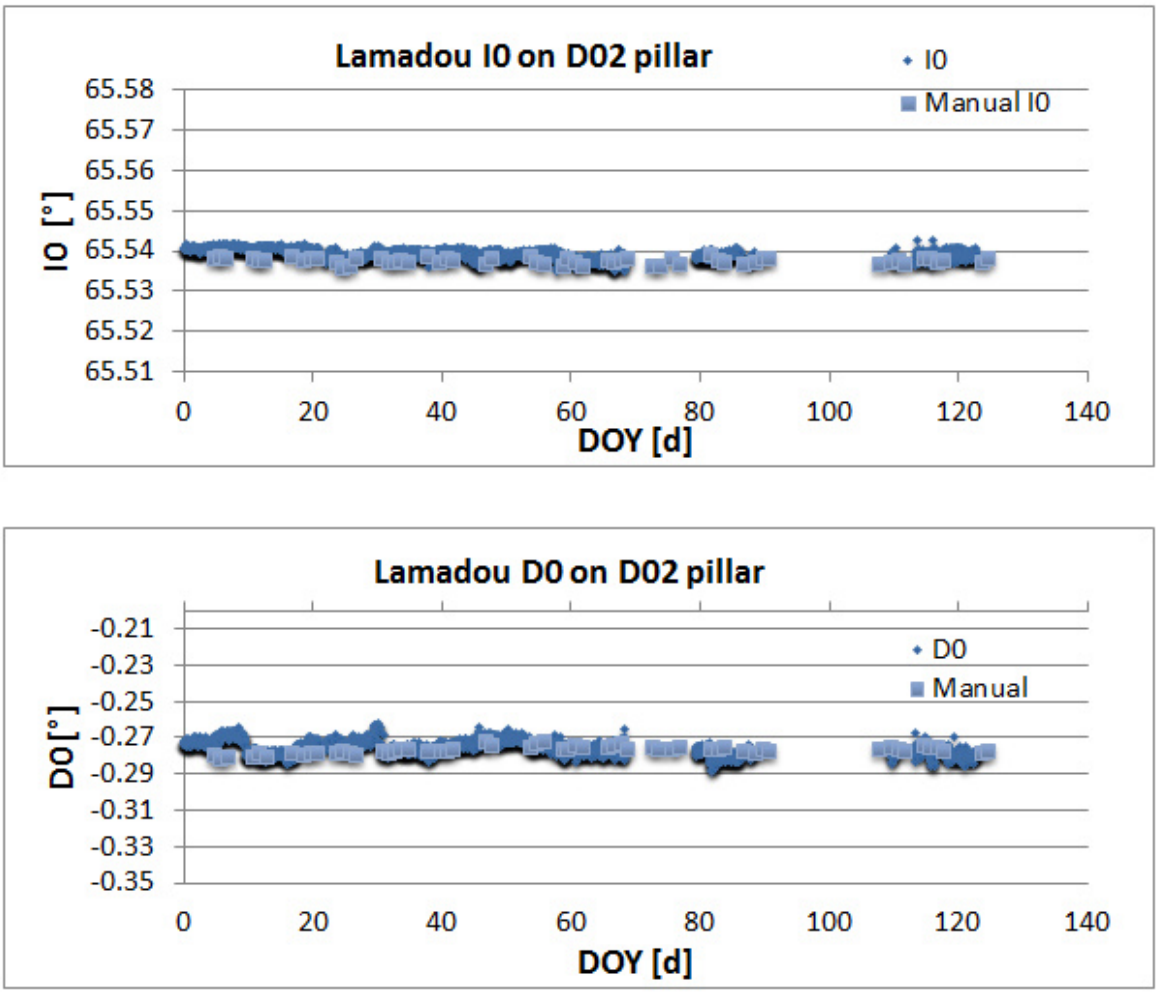

Figure 4 –D0 and I0 Lamadou baselines. Comparison between the Autodif and the Zeiss 010B measurements.

Figure 4 shows a comparison between the declination and inclination baselines of the variometer computed from the AutoDIF and the manual ZEISS010 results. The two data gaps correspond to a temporary installation of the instrument in other observatories (Manhay and Islamabad) during which no automatic measurements were performed in Dourbes. It seems that the international travel in the aircraft hold had no influence on the instrument results. The inclination graph indicates a difference of less than 0.002° (0.12') while the declination is less than 0.005° (0.3'). The examination of the comparison graphs (Figure 5) shows a good fitting between the collimation and magnetization errors each computed from D and I measurements. This is an indication of a good measurement process.

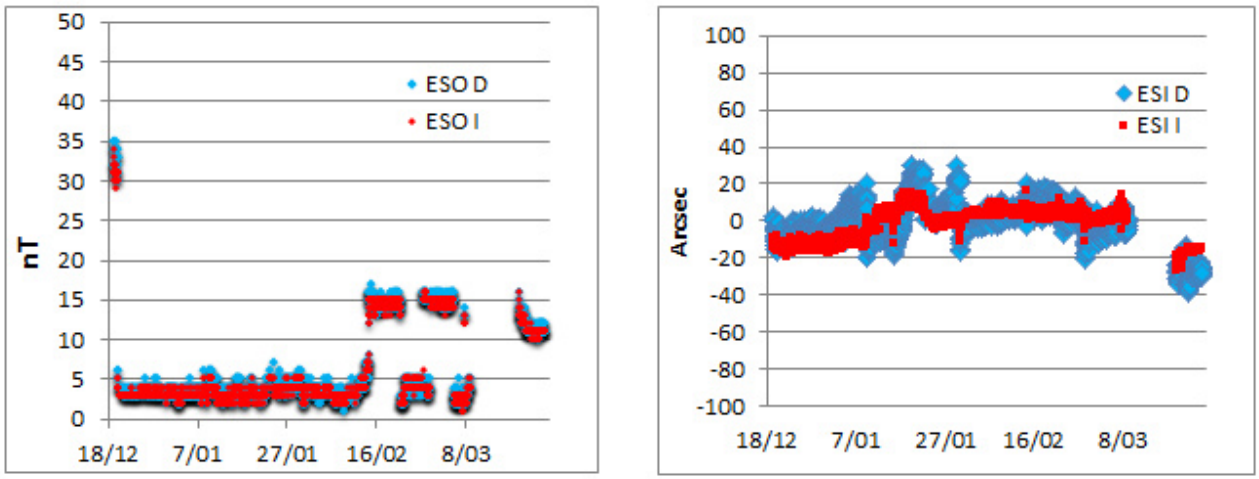

Figure 5 –Magnetization (left) and vertical collimation (right) errors computed from D (in blue) and I (in red).

During the XVth IAGA workshop in San Fernando, the AutoDIF was placed in a tent shelter on a field tripod and was set-up to perform a complete measurement every 30 min (Figure 6). The instrument, its electronics and the data logging laptop were all deployed rather close to each other into the same tent which was at 50m from the absolute house. Therefore, comparison with the observatory reference measurements were not supposed to be valid. However, the graphs below indicate a good stability and a low dispersion of the measurements. It was almost impossible to point the target because of excessive twisting of the tripod mainly due to the temperature variations. That explains why we do not have good D0 measurements to show.

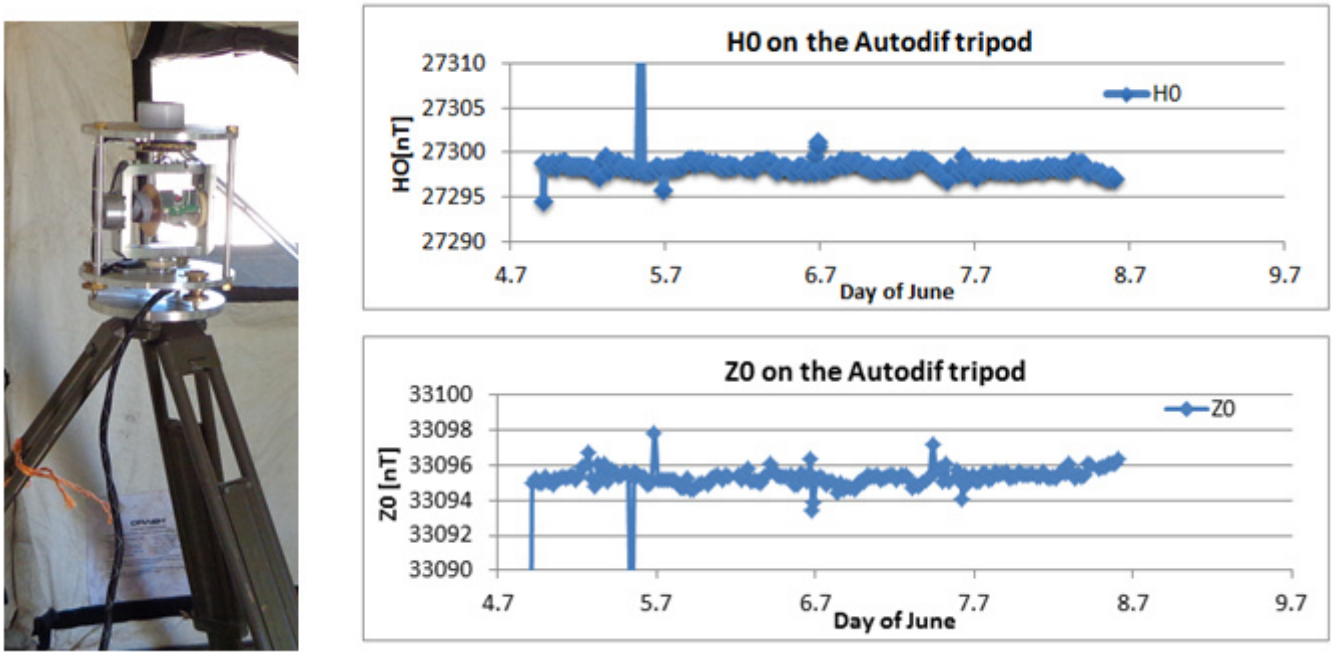

Figure 6 –AutoDIF on a tripod during the XVth IAGA workshop in San Fernando and the H0 and Z0 corresponding baselines.

4. REFERENCES

Gilber, D., Rasson, J.L. (2001): "Effect on DIflux Measuring Accuracy due to a Magnet Located on it". Scientific Technical Report STR98/21, pp168-171, GeoForschungsZentrum Potsdam.

Rasson, J.L. (2005): "About Absolute Geomagnetic Measurements in the Observatory and in the Field". Publication scientifique et technique no 40, Institut Royal Meteorologique de Belgique.

Rasson, J.L., Gonsette, A. (2011): "*The Mark II Automatic DIFlux*", Data Science Journal, Vol10.

STATUS OF THE GEOMAGNETIC AUTOMATED SYSTEM GAUSS

M. Korte [(1)], H.-P. Brunke [(1)], O. Bronkalla [(1)], E. Pulz [(1)]

[(1)] Helmholtz-Zentrum Potsdam, Deutsches GeoForschungsZentrum GFZ,Telegrafenberg, 14473 Potsdam, Germany, monika@gfz-potsdam.de

SUMMARY

The GAUSS instrument (Geomagnetic AUtomated SyStem) for automatic observatory absolute measurements has been running in long-term test at the Niemegk observatory since 2008 very reliably with very few mechanical problems. The accuracy of the directional results, however, requires a highly precise monitoring of the orientation. In contrast to the standard DI-flux measurement, the determinations of absolute declination by GAUSS are more precise than those of horizontal intensity. At present, we have obtained very satisfactory results, comparable to the quality of the traditional manual method, for time intervals of several months. However, for some other time intervals we still struggle to understand some offsets and artificial variations in the GAUSS directional results.

1. INTRODUCTION

Geomagnetic observatories have to provide data that only reflect the natural variations of the Earth's magnetic field and are not influenced by any other factors. This applies in particular to the long-term stability of the data series. Data from magnetometers continuously recording the geomagnetic field vector often are subject to other influences like e.g. from temperature variations or pillar tilts. Regular absolute vector measurements are mandatory to control the base-lines of the continuously recording magnetometers (Jankowski and Sucksdorff, 1996). While it nowadays is easy to obtain absolute scalar values, e.g. from Overhauser magnetometers, the determination of the absolute directional values remains a task that has to be performed manually and very carefully by means of DI-flux theodolite. This requirement hampers the installation of high-quality, automated magnetic observatories in remote regions to fill gaps in the global network.

The Geomagnetic AUtomated SyStem GAUSS, developed in cooperation between GFZ and TU Braunschweig, automatically determines the field intensity in two horizontal directions by means of rotations of a three-axis fluxgate magnetometer. Together with total intensity and standard variation recordings the method allows for a full calibration of the sensor, providing absolute values for all components. The orientation of the instrument with regard to a geographic reference frame is controlled by an optical set-up. A prototype instrument was presented at the IAGA Workshop in 2006 in Belsk (Auster et al., 2007). In the following years, some important mechanical improvements were implemented (Hemshorn et al., 2009). The instrument has been running in its present design for much of the time since 2008 at the Adolf-Schmidt Observatory for Geomagnetism in Niemegk. Here, we report on the latest status in terms of mechanical reliability and output data quality of the instrument.

2. MEASUREMENT PRINCIPLE AND INSTRUMENT SETUP

The measurement principle of GAUSS is based on a three-component fluxgate sensor, which is rotated around an arbitrary, but very stable axis. The field strength in the direction of the axis can be determined from the vector recordings in three positions, without knowledge of the rotation angles (Auster and Auster, 2003). The rotation is performed about two axes in the horizontal plain, so that together with absolute intensity recordings the full field vector can be determined. A full calibration of the fluxgate sensor is achieved if the sensor is rotated in various orientations with respect to the geomagnetic field vector and compared to absolute total intensity recordings (Auster et al., 2002). The various orientations are obtained from the rotations about the two axes and an additional rotation of the sensor by 90° for each of the axis directions. A variation correction similar to the one used in the standard DI-flux absolute measurements to take account of the field change during the measurement procedure is also implemented. The present protocol provides a redundancy of eight field component values per rotation axis.

All the rotations of the instrument are performed by non-magnetic piezo-motors (Fig. 1). The vector fluxgate sensor is housed in a “basket”. The sensor can be rotated inside the basket for redundancy and calibration purposes. The main part of the operation is the rotation around the axis of the basket, which is defined by a fibre-optics laser, pointing at a position sensitive device (PSD). In our present setup the

two axis directions lie in the horizontal plain and approximately 135° degrees apart. The instrument is rotated into the second direction by means of a turn-table. The laser beam describes small circles on the PSDs, which in the present setup are ca. 11 and 17 m away. The centres of the circles are the directions of the measured field components, and provide the information by how much the actual measurement deviates out of the horizontal plain and from the azimuths given by the centres of the PSDs.

The accuracy requirements of the geographic orientation are high: for a resolution of 1 nT an accuracy of 4 seconds of arc in the orientation is required, which corresponds to 0.3 mm on a PSD in 15 m distance. The pillars for the PSD are made from ceramics with very low thermal coefficient.

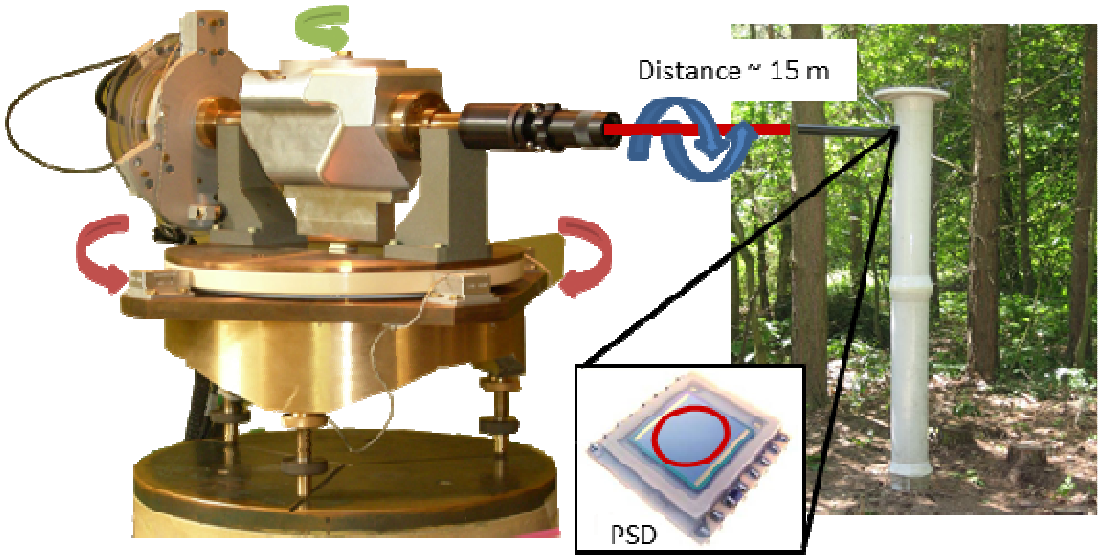

Figure 1 –The GAUSS instrument. A three-component fluxgate magnetometer can be rotated inside its basked (green arrow). Field intensity in one direction is obtained by rotation of the sensor about a fixed axis (blue arrows). The instrument is turned in a second direction by a turn-table (red arrows). All rotations are performed by non-magnetic piezo-motors. A combination of laser inside the main rotation axis and position sensitive devices (PSD) provides the orientation with regard to the geographic reference frame.

3. RECENT RESULTS

The instrument has been in operation, performing one set of measurements per night, for nearly four years in the absolute house of the Niemegk observatory. The reliability of the current mechanical design is excellent. Two times, the optical cable broke due to unforeseen rotations. This is prevented now both by software improvements and mechanical “emergency stops”. Occasionally, though, problems with dirt or animals disturbing the PSD recordings required manual intervention. Unfortunately a continuous processing of the produced data was not done due to a shortage of personnel. A few bugs in the processing software, particularly a timing error, were only detected in 2011 and impeded an efficient processing of previously collected data.

The baseline determinations for horizontal intensity (H), declination (D) and vertical intensity (Z) from the GAUSS measurements once a night compared to the standard Niemegk observatory baseline values from April 2011 to July 2012 are shown in Fig. 2. The GAUSS results are reduced to the standard absolute pillar, so that both measurements are directly comparable. Note also that only two components are determined by GAUSS (like declination and inclination are by the standard DI-flux method), while the third component is given by the absolute intensity (F) recordings at the observatory. Here, two horizontal components, which can be translated to H and D, are measured, and Z is calculated from F and H, thus is directly dependent on the quality of the GAUSS H determination.

From April to July 2011 (days 100 to 200) GAUSS provides very good declination baseline results, with even less scatter than the standard manual observations. The scatter in H is higher, but acceptable. The gap up to day 260 is due to a breaking of the optical cable, which occurred as consequence of a software bug after some modifications. While D looks acceptable after the interruption, there is an apparent offset of about 7 nT in H from days 260 to 340, which, however, disappears for the rest of December 2011. We do not understand the reason for that offset yet, as no modifications to the setup were done either before or after.

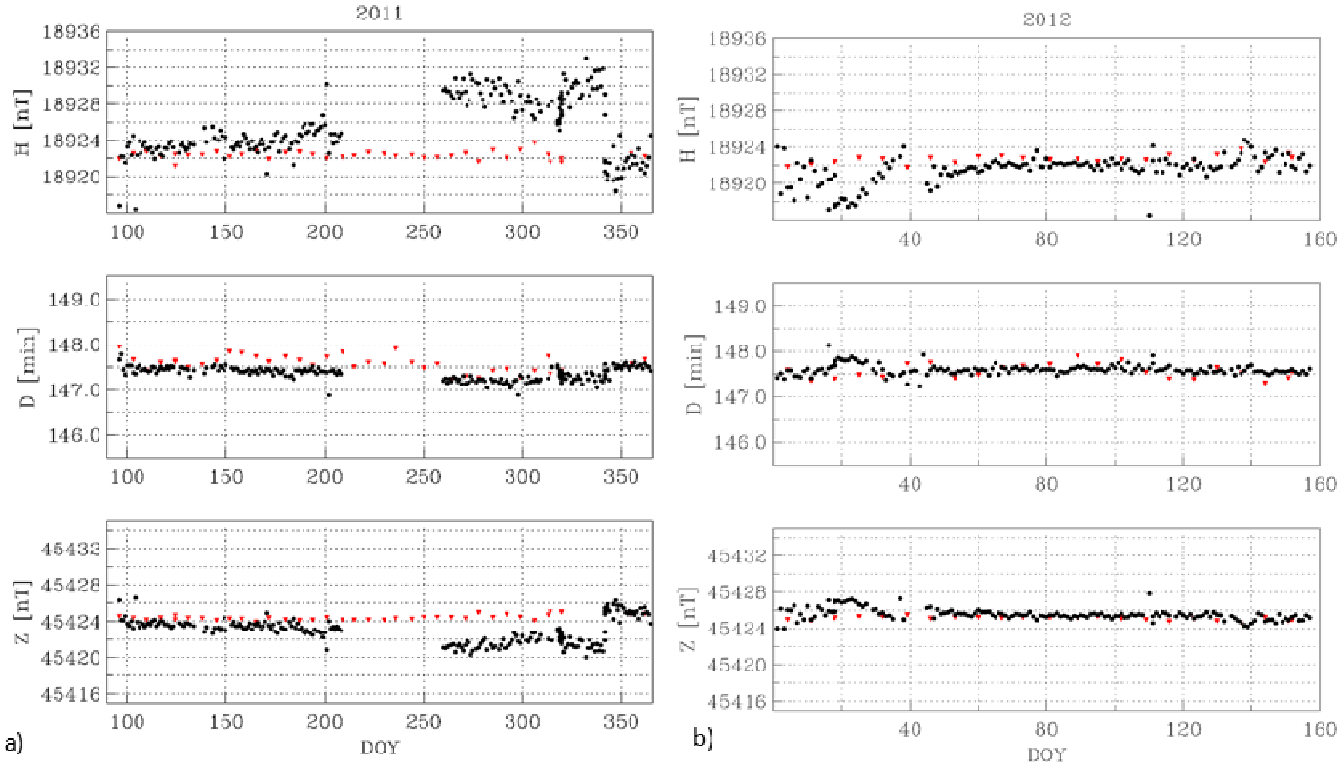

Figure 2 –a) Baselines for Niemegk observatory determined by GAUSS (black dots) once a night and by the standard DI-flux method (red triangles)once a week for April to December 2011, for horizontal component (H, top), declination (D, middle) and vertical intensity (Z, bottom). Only H and D are independent results from GAUSS, Z results are inferred from H with the standard observatory total intensity recordings. Vertical scales are the INTERMAGNET recommended ranges of 20 nT for H and Z and 4' for D. b) The same for January to June 2012.

For 2012, the declination results up to June look good, with an overall scatter of similar order as in the standard baseline determination by DI-flux. The H results are very satisfactory from the middle of February (~ day 45) to June, while the results from the beginning of the year show an unsatisfactory variation.

Vertikal intensity baseline values determined by GAUSS look good to very good most of the time. They are not independent, though. They depend on the quality of the H results, but are less sensitive to small axis orientation errors due to the strong influence of absolute intensity in this field component determination.

4. DISCUSSION

The GAUSS instrument provides absolute values for two nearly horizontal field components, for which the exact orientation with regards to the geographic reference frame and the horizontal plain has to be determined by a combination of a laser in the rotation axis of the instrument and fixed PSDs. We have obtained good to very good results for much of the time from April 2011 to June 2012 for the two components, represented here as baseline values of H and D and compared to the standard DI-flux results. However, a few apparent "jumps" and artificial variations on the order of a few nT, particularly in H, cannot be explained yet. We suppose that these are effects of small inaccuracies of exact rotation axis determination.

The determination of the geomagnetic H component is much more sensitive to small inaccuracies in rotation axis orientation than the declination. The variation observed in January 2012 seems to correlate roughly with a variation in night time temperatures, which were very low about the end of that month. The temperature coefficient of the PSD pillars is too small to account for such a temperature effect, but it seems conceivable that strong differences at the border between the rather warm and nearly constant temperature in our absolute house and the outside temperature affect the laser beam and lead to slightly erroneous values for the critical value of deviation of the rotation axis from the horizontal plain. However, this cannot explain the "jumps" that occurred after the gap around day 260 and back again around day 340 of the year 2011. We are now working on investigating any temperature dependence and other possible sources of error for the exact axis orientation determination.

5. CONCLUSIONS

The GAUSS instrument has been in operation at Niemegk observatory for nearly four years, performing one set of measurements each night. All mechanical parts of the present set-up have shown very good reliability. Very good to satisfactory baseline results for declination have been obtained for much of the time since April 2011. Highly accurate control of the orientation of the rotation axes with respect to geographic reference frame, in particular horizontal plain, is necessary to achieve the desired accuracy. Particularly the results for horizontal intensity are very sensitive to small inaccuracies of axis orientation and the obtained data quality is unsatisfactory at several times. We are still working on understanding the reasons for several apparent “jumps” or artificial variations on the order of a few nT. A mostly reasonable Z baseline is obtained from the GAUSS H recordings and observatory absolute intensity recordings, as Z determined in this way is less sensitive to the small inaccuracies of orientation control that have a strong effect on H alone.

We conclude that the mechanical design of the instrument itself is quite adequate to operate in a fully automated observatory, but improvements to the axis orientation control are still necessary to achieve the desired data quality for geomagnetic observatories in all vector components.

6. REFERENCES

Auster, H.U., K.H. Fornacon, E. Georgescu, K.H. Glassmeier and U. Motschmann (2002). “Calibration of fluxgate magnetometers using relative motion”. *Meas. Sci. Technol.*, **13**, 1124-1131.

Auster, H.U. and V. Auster (2003): "A new method for performing absolute measurements of the geomagnetic field". *Meas.Sci. Technol*., **14**, 1013-1017.

Auster, H.U. , M. Mandea, A. Hemshorn, M. Korte and E. Pulz (2007): "GAUSS: Geomagnetic Automated System ". *Publ. Inst. Geophys. Pol. Acad. Sci.*, **C-99** (389), 49-59.

Hemshorn, A., E. Pulz and M. Mandea (2009): “GAUSS: Improvements to the Geomagnetic AUtomated SyStem”. *USGS Open File Report* **2009-1226**, 100-103.

Jankowski, J. and C. Sucksdorff (1996): “Guide for magnetic measurements and observatory practice”. *IAGA*, Warsaw.

TEMPERATURE SENSITIVITY OF VARIOMETERS: LESSONS LEARNT FROM LIVINGSTON ISLAND GEOMAGNETIC OBSERVATORY

S. Marsal [(1)], J. M. Torta [(1)], J. J. Curto [(1)]

[(1)] Observatori de l'Ebre, *(OE), CSIC - Universitat Ramon Llull*, Horta Alta, 38, 43520 Roquetes, Spain, smarsal@obsebre.es

SUMMARY

Data from geomagnetic observatories deployed at remote sites, such as in Antarctica, which are only manned during restricted periods of time (e.g. in summer), are subject to great uncertainties during periods with no absolute control, and assumptions must be made concerning the baselines evolution during those periods. When different kinds of variometers are simultaneously operating and temperature is also recorded, data comparisons help to assess the validity of such assumptions. In this paper, we describe our experiences at Linvingston Island Observatory, LIV (Antarctica), where the two main instruments in the automatic magnetic observatory are a proton vector magnetometer (PVM) designed by the British Geological Survey, and a suspended tri-axial fluxgate magnetometer (model FGE). It has been revealed that both instruments are sensitive to temperature variations, but in a dynamic way, and differently depending on the magnetic element. Intercomparisons of quiet-day, midnight values from LIV and Argentine Island (AIA), the nearest INTERMAGNET magnetic observatory (i.e. having full absolute control), for the last years of corrected data available provide other qualitative and quantitative tests.

1. INTRODUCTION

The Livingston Island geomagnetic observatory (LIV, 62.67º S, 60.39º W), a partly manned settlement located in the South Shetland Islands, to the north of the Antarctic Peninsula (Torta et al., 1991), was renewed in 2008 with the inclusion of a suspended DMI fluxgate magnetometer (FGE). The new instrument is complemented by the existing Proton Vector Magnetometer (PVM), consisting of a *Geomag SM90R* Overhauser magnetometer mounted at the center of a pair of dual axis Helmholtz coils in δD/δI configuration (Riddick et al., 1995; Marsal et al., 2007) (see *Figure 1*).

Figure 1 –The two variometers operating at Livingston Island geomagnetic observatory: the PVM (left) and the FGE (right).

The PVM was designed by the British Geological Survey (BGS) and the size of the coils is about 80 cm in diameter. Unlike fluxgate magnetometers, the fact that the PVM is based on a scalar magnetometer makes it suitable, in principle, for instrument cross-calibrations, as it is not affected by scale factors; moreover, it is subject to just one orthogonality error, which reduces the total number of degrees of freedom (Heilig, 2007). Marsal et al. (2009) describes the procedure that was carried out to set up and calibrate the new FGE instrument,

where it was assumed that the PVM was a semi-absolute instrument, not being affected by temperature variations, or in any case not in the short term (up to several days, in which case it would be corrected by absolute measurements); however, the continuation of that study up to the present moment, i.e., with four more years of data available, arose some suspicions about the thermal stability of the PVM. The tests carried out to review that assumption are described in the following sections.

2. RESULTS OF TEMPERATURE TESTS

In order to figure out the thermal sensitivity of our new fluxgate sensor, the differences between the FGE and the PVM (after transforming the corresponding variations of F, D, I to variations of X, Y, Z) were plotted alongside temperature changes. The results for April 2010 are shown in Figure 2, where the blue line corresponds to the differences and the green line to temperature. Both lines show a clear correlation for the Y component (in the middle panel); this is also the case for the X component (upper panel) until day of year (DOY) 114 approximately, whereas no apparent correlation exists for the vertical component (lower panel). Assuming that the PVM is not sensitive to temperature variations, the thermal sensitivity of the fluxgate sensors could readily be calculated. However, a closer look to the graphs reveals that a similar change of tendency appears suddenly in both the X and Z components beyond DOY 114, corresponding to a severe temperature decrease (red circles in Figure 2). This fact arose suspicion about the PVM, as both components derive from the magnetic Inclination (I).

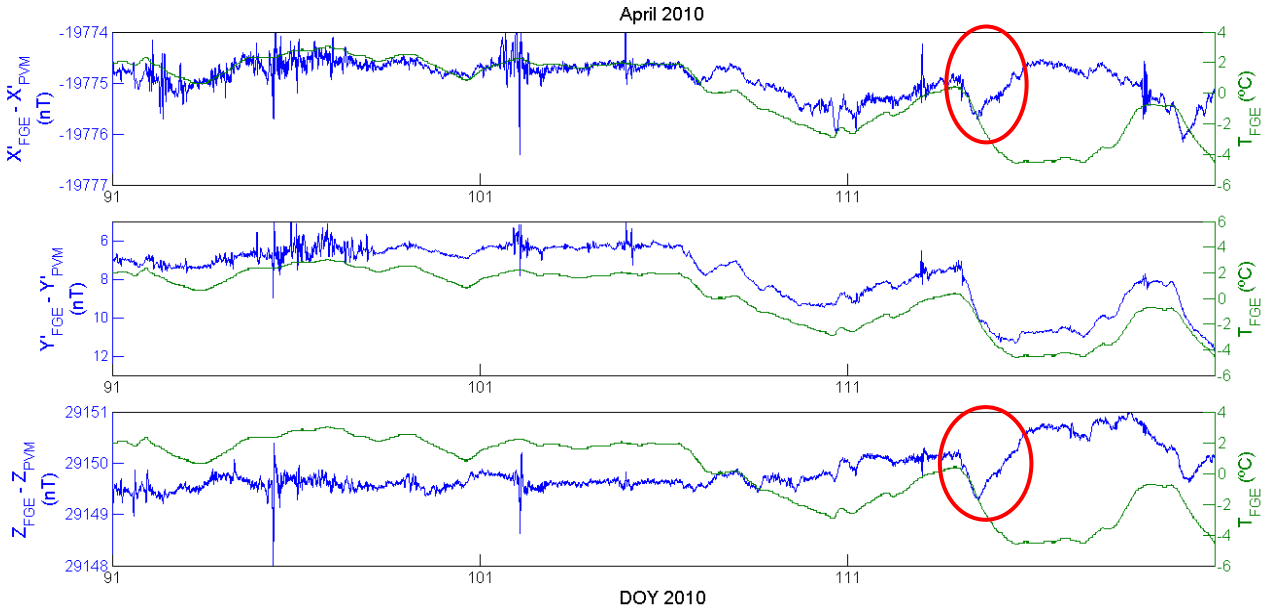

Figure 2 –Time evolution of the differences between the FGE and the PVM for the different components during April 2010 (blue line) alongside temperature (green line). The prime on the components (e.g., X') indicates magnetic orientation rather than geographic.

A similar test was carried out for the whole year 2010. However, we now aimed at isolating the specific weight of temperature in causing instrumental dependencies. Thus, we selected only spot midnight values from geomagnetically quiet days with extreme temperatures so as to minimize the external geomagnetic variations (such as geomagnetic storm effects or daytime Sq variations) and maximize the effect of temperature on the variometers. The direct differences between the FGE and the PVM for the selected periods again showed a good correspondence with temperature changes, except for a superimposed long term variation. Such long periods could be related to slow pillar movements not necessarily owing to temperature changes, so in order to remove such low frequencies a high-pass-filter was applied to both data series. The results for the Y component are displayed in Figure 3, where the correspondence between the two series is outstanding.

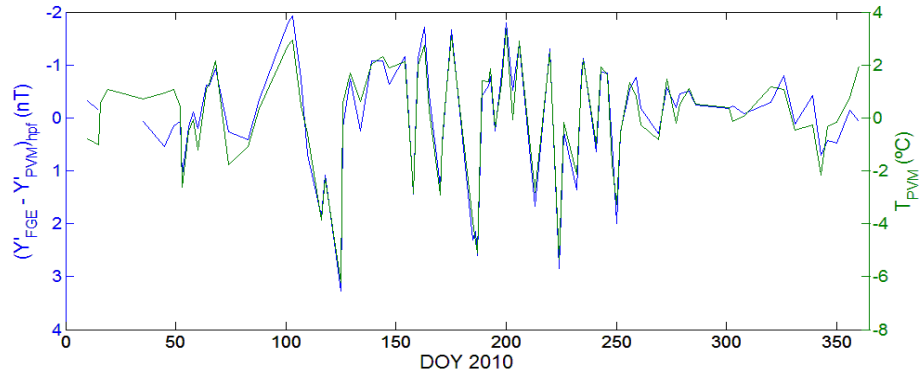

Figure 3 –Differences between the Y' (magnetic east) components of the two LIV variometers at local midnight for selected quiet days with extreme temperatures (blue line) alongside temperature (green line). A high-pass-filter has been applied to the data.

To quantify this correlation, Figure 4 plots the filtered differences against temperature. The correlation coefficient equals -0.95 for the Y component, with a temperature sensitivity of the differences of -0.49 nT/ºC. However, the same procedure applied to the other components gives poorer correlation coefficients, especially for Z, in agreement with what was seen in Figure 2.

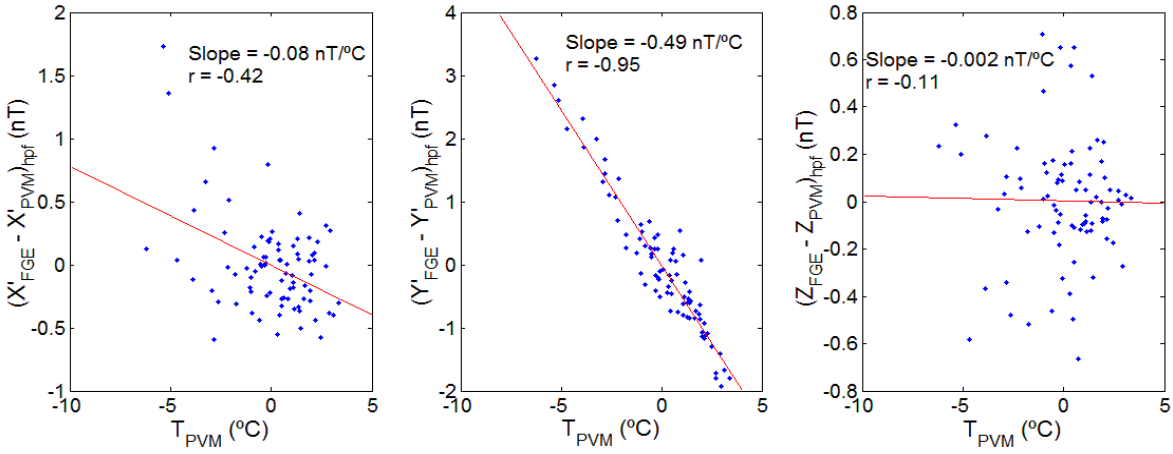

Figure 4 –Differences between the components of the two LIV variometers at local midnight for selected quiet days with extreme temperatures versus temperature. The different panels correspond to the three components.

It is worth to emphasize that the previous tests provide information about the difference between the FGE and the PVM, but we still lack a test to determine the weight of each of the two variometers as far as the temperature sensitivity is concerned. As a possible solution to that issue, we opted to compare our two data sets with definitive data from Argentine Island (AIA), which is about 350 km southwest from LIV; furthermore, this observatory belongs to INTERMAGNET, so absolute control during the whole year is assumed, as well as the accomplishment of a high quality standard. However, questions could arise concerning the resemblance of the magnetic variations between the two locations. In particular, we are again interested in quiet days and local midnight values (about 04 UT). Figure 5 presents an example of the differences between the simultaneous horizontal component (H) of the magnetic field at LIV and AIA for a quiet day (July 10, 2010). The differences range in the 4 nT interval for this winter day. The same procedure applied to other quiet days shows a typical deviation of the differences of the minute values during a 1-hour interval around midnight of the order of 1 nT. Thus, the election of AIA for comparison purposes seems reasonable despite the inherent uncertainty due to the distance between the two observatories. Once the suitability of AIA had been evaluated, we applied a similar method to that in Figure 4, but we used definitive data from Argentine Island as a reference instead of making the differences between our two variometers. This led us to Figure 6, where the upper row shows differences between our fluxgate and AIA, and the lower row differences between our PVM and AIA. These differences are plotted against temperature in all cases, and the different columns correspond to X, Y and Z components. Following this approximate method, our fluxgate sensitivities would be around 0.15 nT/ºC (in reasonable agreement with the instrument specifications), while our PVM sensitivities would be somewhat higher (between 0.1 and 0.4 nT/ºC). The best correlation with temperature is seen to happen for the Y component of the PVM, with a sensitivity of 0.37 nT/ºC.

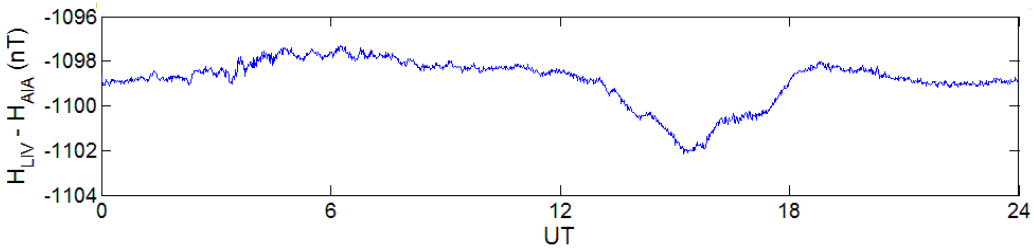

Figure 5 –Differences between the horizontal (H) component at LIV and AIA for the quiet day July 10, 2010.

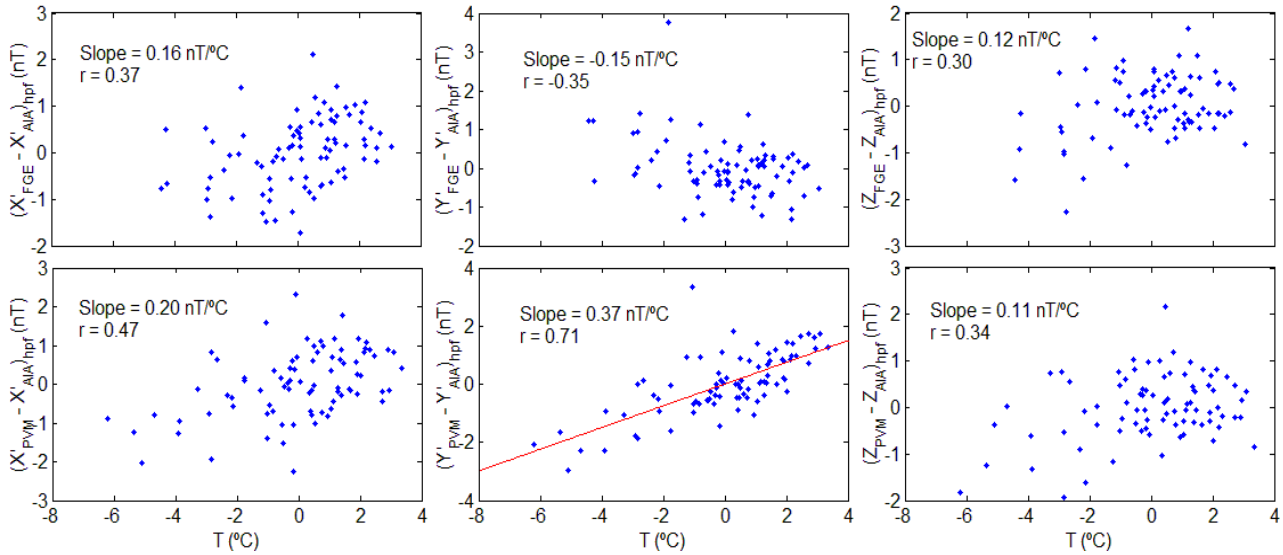

Figure 6 –Same as Figure 4, but using AIA definitive data as a reference instead of making the difference between the two variometers at LIV.

Finally, we made a comparison between the total field (F) measured by the PVM and a Gem Systems GSM90-F1 scalar magnetometer in a nearby location (about 38 m distance from each other). The differences between the two (not shown here) showed a clear dependence with temperature, though only of the order of 0.02 nT/ºC. Though we initially thought that such differences were due to instrument inaccuracies, we were suggested that they could be related to differential magnetic thermal sensitivity of rocks in the volcanic island where LIV observatory is deployed.

3. SHORT DISCUSSION AND CONCLUSIONS

Tests have been conducted about the temperature sensitivity of the FGE and the PVM magnetometers in use at the Livingston Island geomagnetic observatory. Results in general show a somewhat higher temperature sensitivity of the BGS PVM than that of the FGE. A possible explanation for this is the large size of the PVM coils, which are thus more affected by thermal expansions. Variable natural gradients due to differential magnetic thermal sensitivity of the rocks where the two instruments are deployed could explain only a small part of the observed temperature dependence, as this effect is expected to be in the order of a few hundredths of a nanotesla per degree for the different vector components (as it is the case for F). Although it must be emphasized that the results presented here are only valid for the instruments operating at LIV, we believe that observatories can benefit from our results in the sense that they question that proton vector magnetometers are less sensitive to temperature than fluxgate-based variometers, as it is sometimes assumed. We encourage other observatories to carry out similar tests. A thermal coefficient of several tenths of a nanotesla per degree or more is considerable, and care should be taken to thermally insulate any instrument with these characteristics. Unfortunately, this is not much the case at LIV, where the instruments are placed in huts that attenuate the daily temperature variations, but are transparent to the annual thermal wave. A total error of up to 4 to 6 nT (depending on the component) might have been produced at LIV during the past years at the middle of the winter season, when no absolute control exists.

4. REFERENCES

Heilig, B. (2007): "Intercalibration of dIdD and Fluxgate Magnetometers". *Publs. Inst. Geophys. Pol. Acad. Sc., C-99 (398)*, 144-151.

Marsal, S., J. M. Torta and J. C. Riddick (2007): "An assessment of the BGS δD/δI Vector Magnetometer". *Publs. Inst. Geophys. Pol. Acad. Sc., C-99 (398)*, 158-165.

Marsal, S., J. J. Curto, J. C. Riddick, J. M. Torta, O. Cid and M. Ibañez (2009): "Livingston Island Observatory Upgrade: First Results". *Proceedings of the XIIIth IAGA Workshop on geomagnetic observatory instruments, data acquisition, and processing: U.S. Geological Survey Open-File Report 2009–1226*, edited by J. J. Love, 154-161.

Riddick, J. C., C. W. Turbitt and J. McDonald (1995): "The BGS Proton Magnetometer (δD/δI) Observatory System Mark II. Installation Guide and Technical Manual". *British Geological Survey Technical Report WM/95/32*. BGS Geomagnetism Series, Edinburgh.

Torta, J. M., L. R. Gaya-Pigué, J. G. Solé, I. Blanco and A. García (1991): A new geomagnetic observatory in at Livingston Island (South Shetland Islands): Implications for future regional magnetic surveys. Annali di Geofisica, **42**, 2, 141-151.

ACCURACY OF OUR DIFLUX MEASUREMENTS AND CAN WE IMPROVE IT?

J. Rasson [(1)]

[(1)] Institut Royal Météorologique, Centre de Physique du Globe, Rue du Centre de Physique 2, 5670 DOURBES, Belgium, jr@oma.be

SUMMARY

Absolute measurements are at the very base of our observatory data production. Therefore a good understanding and monitoring of the performance and quality of our absolute instruments is necessary. The IAGA observatory workshops adress this concern by organizing periodically (every two years) intercomparison sessions of absolute instrumentation. We will discuss here the Diflux theodolite: the instrument able to perform absolute measurements of the magnetic declination and inclination.

The paper will first examine the accuracy limiting factors of a typical Diflux. Based on past experience, we will try to evaluate how those factors may affect the quality of our Diflux measurements. The methods used for improving the Diflux's accuracy will be mentioned.

We will then examine the results of the Difluxes which have measured in past IAGA workshop intercomparison sessions when they have been made available. We will try to extract all useful accuracy information relating to these past intercomparison sessions. We will discuss what can be done for Difluxes/observers which do badly at the intercomparison.

Finally we will propose that intercomparison sessions in our IAGA workshops have a more standardised approach and be recorded faithfully in an ad hoc database, coordinated by the IAGA working group V-OBS. One innovation would be that the participating Difluxes be clearly identified together with the operating observers and their Observatory. One idea here is to be able to follow the DIflux instruments over their life and take the necessary steps to improve the failing ones

1. INTRODUCTION

Absolute measurements are important because at the very base of our observatory data production. Therefore a good understanding and monitoring of the performance and quality of our absolute instruments is essential. The IAGA observatory workshops address this concern by organizing periodically intercomparison sessions for absolute instruments.

The outline of this paper is as such:

- Accuracy limiting factors of a typical DIflux, based on past experience and tips for improving the DIflux accuracy
- Results of the DIfluxes in past IAGA workshop intercomparison sessions and how it is reported.
- Proposal for follow-up on intercomparison sessions in our IAGA workshops

2. ACCURACY LIMITING FACTORS OF A TYPICAL DIFLUX

Past intercomparison workshops have shown that for the Diflux, the quality of our absolute measurements vary widely. Intercomparisons are usually performed using the host observatory variometer as an intercomparison transfer standard. The lack of quality may be due to the less than perfect absolute instruments, low observer skills, unclean magnetic environment, variometer instability etc... For the measurements performed with the Diflux, we identify these most important accuracy limiting factors:

- Magnetism in the theo + observer.
- Telescope parallax error
- Tribrach co-rotation
- Circle reading interpolator errors
- Eccentricity error due to vertical axis wobble

Note: many DIflux defects (collimation errors, non-orthogonality of axes, sensor and reticule offset,…) are eliminated by the standard DIflux measurement protocol and are not discussed here: they are not compromising the accuracy.

1. Magnetism in the theodolite* (and observer)

Detection:

- Theo pollution will affect inclination I measurement mainly
- I gradient (= $I_{sensorup} - I_{sensordown}$) will quantify the effect
- During IAGA ws intercomparison
- By a magnetic signature measurement (provided we remove the fluxgate)
- Motion of an unclean observer close to Diflux will produce magnetic signals

Mitigation:

- Replace magnetic elements by non-magnetic ones
- Observer precaution: Good measurement practice / use residue method

* excluding the parts rotating with the fluxgate sensor

2. Parallax Error: Adjusting the Eyepiece and Telescope

The telescope must be adjusted to eliminate the parallax error**.** how? By bringing the focus of the eyepiece and the focus of the objective lens to the plane of the reticule.

Method:

- Adjust eyepiece[1]: Point the telescope toward a neutral background and rotate the knurled ring of the telescope eyepiece until the reticule crosslines are sharp.
- Adjust distance[2]: Point the telescope on the target and, still focusing the eye on the crosslines, bring the target into a sharp image by rotating the knurled focusing ring on the telescope.
- Check for parallax error: Move the eye back and forth across the eyepiece. If the parallax has been improperly adjusted, the target will move with respect to the reticule

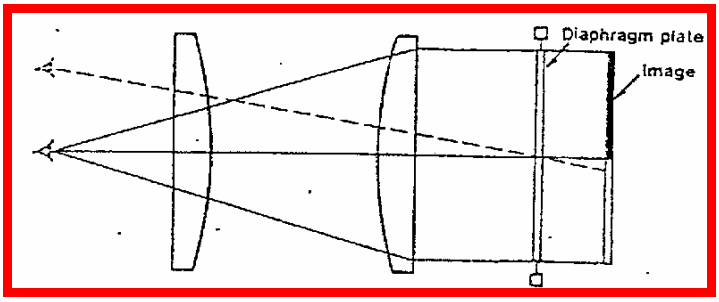

Figure 1 –Incorrect parallax: diaphragm (with reticule on it) and image do not coincide

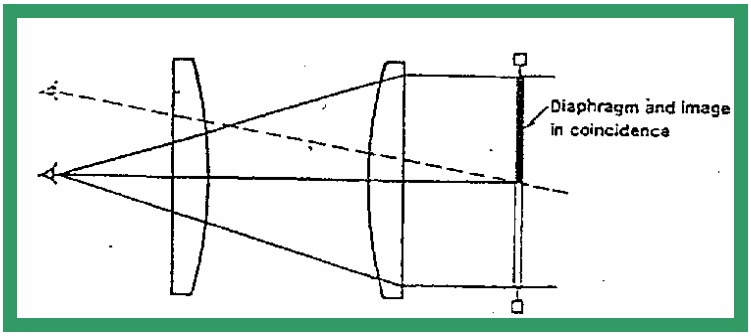

Figure 2 –When diaphragm and image coincide, a motion of the eye in front of the eyepiece will not produce a motion of image with respect to the reticule on the diaphragm

[1] This adjustment setting is dependent upon observer's eye

[2] This adjustment setting is dependent upon the targets distance

3. Tribrach co-rotation

- The tribrach connects the angle reading device to the referential (pillar, tripod,…)
- The tribrach should not rotate nor move with respect to the referential (see Fig 3)
- Unwanted motions of tribrach take place when the leveling screws are loose (too much play from maladjustment or wear – see Fig 4 for suppressing it)

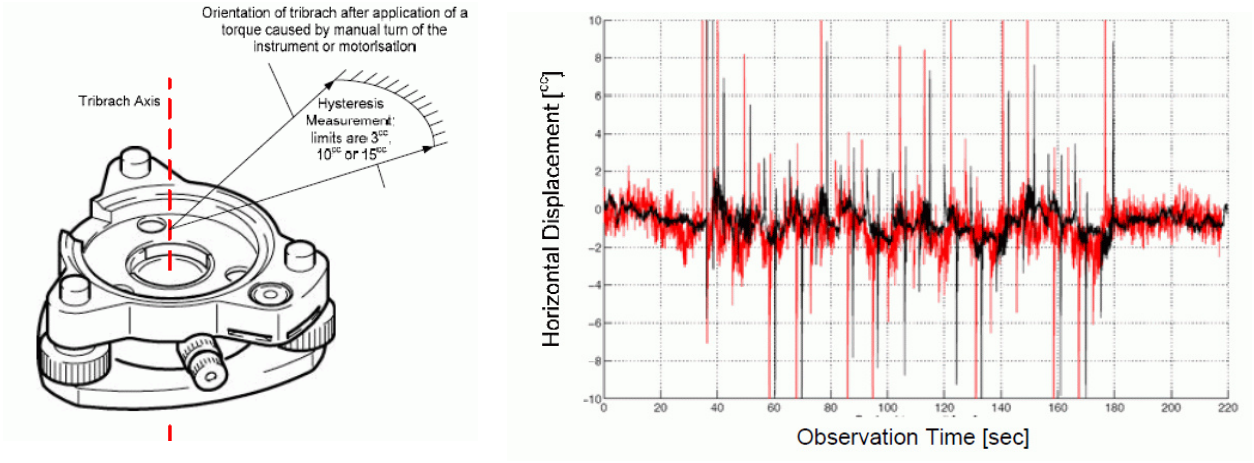

Figure 3 –Red: tribrach co-rotation, Black: tripod head co-rotation. 1cc=0.3", Source: Surveying tribrachs, White Paper, Characteristics and Influences, Leica Geosystems, March 2010

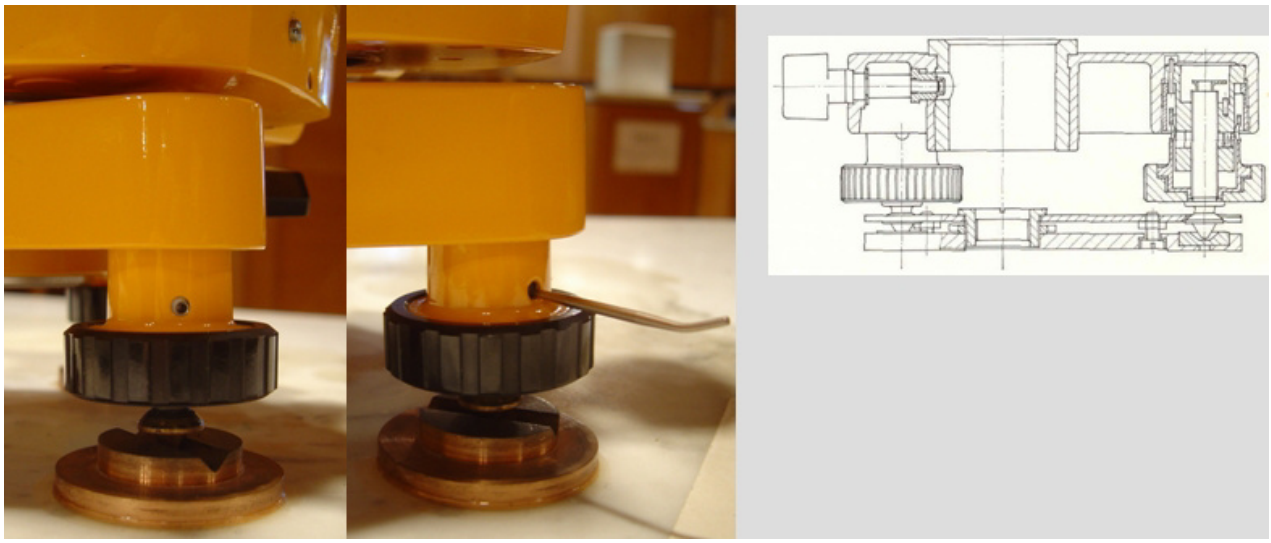

Figure 4 – Foot-screw adjustment for play suppression

4. Circle reading interpolator errors

Here the problem experienced by the observer is that the coincidence bars in the microscope eyepiece cannot coincide because the upper and lower separation of the bars are not identical. This is a common maladjustment, usually provoked by vibrations experienced by the theodolite during transport, handling etc. While this can be readjusted in a theodolite service shop, it is often not done, for reason of costs or unavailability of a capable workshop.

Therefore some solution may be sought to the problem of setting the lines in an equivalent way to coincidence. As explained on Fig. 5, the problem originates in a different magnification of the microscopes reading the circle at diametrically opposed reading stations on the divided circle. Finding a position equivalent to true coincidence is as shown: the difference in coincidence should be averaged over the viewing window and no particular bars except in the centre of the window should be singled out for coincidence.

5. Excentricity error due to axis wobble

- Only in theodolites with extreme wear or with bad rotation axes
- Remedy: buy new theodolite and/or have it fixed

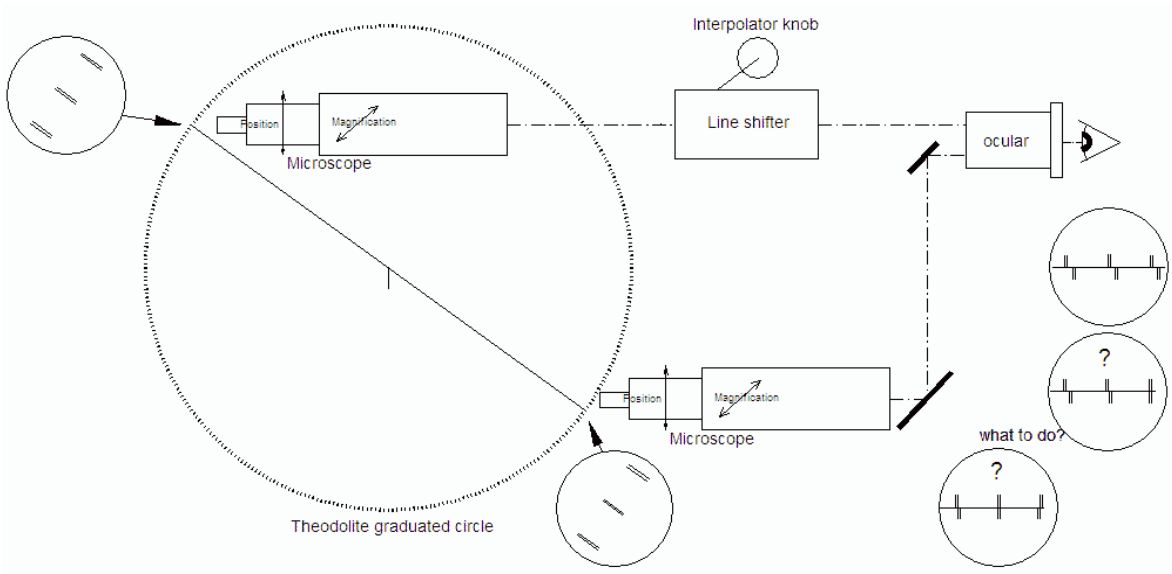

Figure 5 –Optical schematic of a Zeiss 010 circle reading set-up with a wrong magnification of one of the microsvopes. The answer to the question "what to do?" is to obtain coincidences as in the lower circular window.

3. RESULTS OF THE DIFLUXES IN PAST IAGA WORKSHOP INTERCOMPARISON SESSIONS: HOW IT WAS REPORTED.

It can be seen in table 1 that the way of reporting the comparison results in our past IAGA workshops has evolved towards a more complete description, but is still far from standardized. The representation of the comparison results does not allow to follow a specific instrument from one intercomparison to the next.

Table 1 – IAGA Workshops Reporting Particulars

Year	WS Place	Reporting & Publishing								
		Reference	D errors	I errors	# measurements	Error bars	Theo type	Theo ID	Flxg El. type	Operator & Obs ID
1986	Ottawa	obs	x	x	x					
1987	Chambon									
1989	Nurmijrvi	obs	x	x	x					x
1991	Tihany									
1992	Paris									
1994	Dourbes	Clean mean	x	x	x	x	x			x
1996	Niemegk	clean mean	x	x	x	x	x			x
1997	Huancayo	clean mean	x	x	x	x	x			x
1998	Vassouras	clean mean	x	x	x	x	x	x	x	x
2000	Hurbanovo									
2002	Hermanus	clean mean	x	x	x	x				x
2004	Kakioka	mean	x	x	x		x			x
2006	Belsk	clean mean	x	x	x		x	x	x	x
2008	Boulder	clean mean	x	H & Z	x		x			x
2010	Changchun	clean mean	x	x	x		x		x	x

4. PROPOSAL FOR FOLLOW-UP ON INTERCOMPARISON SESSIONS IN OUR IAGA WORKSHOPS

DIfluxes should be precisely identified when being intercompared in IAGA WS. Minimum information should include:

I. Theo type
II. Theo ID (serial numbers of alidade and tribrach)
III. Fluxgate sensor type
IV. Fluxgate electronics type
V. Operator ID (Name)
VI. Observatory where used

Results of intercomparison sessions should include

I. Mean errors for D and I in arc-seconds
II. Amount of measurements per observer and error bars
III. Reference used: observatory reference or (cleaned) mean or other

This **information** should be collected in a database and updated after each workshop. This would clearly be a task for the IAGA working group V-OBS.

NOISE REDUCTION OF FLUXGATE DATA BY COMMON INTERPRETATION WITH INDUCTION COIL DATA

H.-P. Brunke [(1)], M. Korte [(1)]

[(1)] Helmholtz-Zentrum Potsdam, DeutschesGeoForschungsZentrumGFZ,Telegrafenberg, 14473 Potsdam, Germany, brunke@gfz-potsdam.de

SUMMARY

Traditional fluxgate magnetometers used at geomagnetic observatories often show a rather high noise level in data with one second time resolution. Here,data from a three axis induction coil system are used to significantly reducethe noise of fluxgate data. The time integral of induction coil data is fitted to the fluxgate measurements. Ascaling factor, an offset in the voltage induced in the coils, and the integration-constant are determined by a least squares approach. The resulting field values show a clear improvement in the signal to noise ratio. In contrast to usual filtering, e.g., by a Gaussian filter as proposed in Jankovski and Sucksdorff(1996)our method causes no loss of information. A $\Delta \boldsymbol{F}$ *test using a very low noise K-magnetometer as reference shows a noise reduction from about 80pT of unprocessed to about 25pT of processed data at one standard deviation.The used K-magneter is described in: Pulz, E.; Jäckel, K.-H.; Linthe, H.-J. (1999).*

1. INTRODUCTION

Modern geomagnetic satellites offer a time resolution of one second. The same is now desired for magnetic observatories. Due to physical reasons, traditional fluxgate vector magnetometers often have a high noise level at this resolution: Musmann and Afanassiev (2010). Induction coil data give a measure of the difference between consecutive values of the magnetic field at high temporal sampling rates. We take advantage of the data from a three component induction coil system operated at the Niemegk observatory and use it to improve the signal to noise ratio of the standard fluxgate readings.

2. METHOD

Our method is formulated for X as an example but it can also be used for Y and Z. The premise is to integrate induction coil data over time. The functionresulting by this integration, which depends on some unknown parameters, is used as a spline curve to the fluxgate measurements. The three unknown parametersare:

- Scaling factor C linking the measured induced voltages to dX/dt
- Constant offset Off in the data of induced voltages
- Integration constant

A number (here 200) of fluxgate measurements are taken into account and the parameters are chosen sothat residuals to the fluxgate measurements are minimized by a least squares approach. This reduces the noisecomparable to using a spline-fit. But unlike a normal spline, the integral of the induction coil data implicitly contains the shape of the time series of the magnetic field. Whereas spline-fitting always implicates low pass filtering and loss of information, there is no loss of information and no phase shift to any spectral component of the signal in our method.The method exploits the low noise of induction coil data at high frequencies. One set of the three parameters is obtained for each second.

3. MATHEMATICAL FORMULATION

A magnetic field component measurement $X(t_0)$ made at the time $t_0$is linked to measurements $X(t_i)$ at times t_i shortly before or after the time t_0 by the field derivatives measured by induction coils:

$$X(t_i)|_{Fluxgate} - X(t_0) = \int_{t_0}^{t_i} \dot{X}|_{Coil} \quad (1)$$

With $\dot{X} = C * U_{COIL} + Offset$ (C a scaling factor and *Off* the offset of the coil voltages measurement) this writes as

$$X(t_i)|_{Fluxgate} - X(t_0) = \int_{t_0}^{t_i} (C \cdot U_{Coil} + Off)\, dt \quad (2)$$

Replacing the integral by the discrete sum and re-arranging leads to

$$C\,\Delta t \cdot \sum_{k=0}^{i} U_k + Off\; i\,\Delta t + X(t_0) = X(t_i)|_{Fluxgate} \quad (3)$$

This is an (over-determined) linear system in *C*, *Off* and $X(t_0)$. For convenience we set $S_i = \sum_{k=0}^{i} U_k$.

Assuming that Δt = 1s and considering i = {-N,…+N} we get the following linear system of equations:

$$\begin{aligned} C \cdot S_N + Off \cdot N + X(t_0) &= X(t_N)|_{Fluxgate} + r_N \\ &\vdots \\ C \cdot S_i + Off \cdot i + X(t_0) &= X(t_i)|_{Fluxgate} + r_i \\ &\vdots \\ C \cdot S_{-N} + Off \cdot (-N) + X(t_0) &= X(t_{-N})|_{Fluxgate} + r_{-N} \end{aligned} \quad (4)$$

The number N is much greater than 3 and a solution for the unknowns *C*, *Off* and $F(t_0)$ exists only in the sense of a least squares solution minimizing the sum of the r_i^2.We assume that r_i mainly consists of noise from the fluxgate magnetometer. Written in matrix form we get:

$$\begin{pmatrix} S_N & N & 1 \\ S_i & i & 1 \\ S_{-N} & -N & 1 \end{pmatrix} \cdot \begin{pmatrix} C \\ Off \\ X(t_0) \end{pmatrix} = \begin{pmatrix} X(t_N) \\ X(t_i) \\ X(t_{-N}) \end{pmatrix}\Big|_{Fluxgate} + \begin{pmatrix} r_N \\ r_i \\ r_{-N} \end{pmatrix} \quad (5)$$

To find the set of parameters minimizing the sum of the squared residuals, this equation is multiplied from the left with the transpose of the matrix on the left hand side to get the normal equations:

$$\begin{pmatrix} \sum_{i=-N}^{N} S_i^2 & \sum_{i=-N}^{N} i \cdot S_i & \sum_{i=-N}^{N} S_i \\ \sum_{i=-N}^{N} i \cdot S_i & \sum_{i=-N}^{N} i^2 & \sum_{i=-N}^{N} i \\ \sum_{i=-N}^{N} S_i & \sum_{i=-N}^{N} & 2(N+1) \end{pmatrix} \cdot \begin{pmatrix} C \\ Off \\ X(t_0) \end{pmatrix} = \begin{pmatrix} \sum_{i=-N}^{N} S_i X(t_i) \\ \sum_{i=-N}^{N} i\, X(t_i) \\ \sum_{i=-N}^{N} X(t_i) \end{pmatrix} \quad (6)$$

This simple 3x3 system turned out in practice to be well conditioned and can be solved for the three parameters in *C*, *Off* and $X(t_0)$:

$$\begin{pmatrix} C \\ Off \\ F(t_0) \end{pmatrix} = \begin{pmatrix} \sum_{i=-N}^{N} S_i^2 & \sum_{i=-N}^{N} i \cdot S_i & \sum_{i=-N}^{N} S_i \\ \sum_{i=-N}^{N} i \cdot S_i & \sum_{i=-N}^{N} i^2 & \sum_{i=-N}^{N} i \\ \sum_{i=-N}^{N} S_i & \sum_{i=-N}^{N} & 2(N+1) \end{pmatrix}^{-1} \cdot \begin{pmatrix} \sum_{i=-N}^{N} S_i F(t_i) \\ \sum_{i=-N}^{N} i\, F(t_i) \\ \sum_{i=-N}^{N} F(t_i) \end{pmatrix} \quad (7)$$

The third parameter $X(t_0)$is justthe noise reduced value of Xat time t_0 . The number N was chosen by empirical tests of time intervals from N=500 to N=10 and set to N=100 in the following examples.Figure 1a and b showintegrated induction coil data before and after fitting them to fluxgate data, respectively.

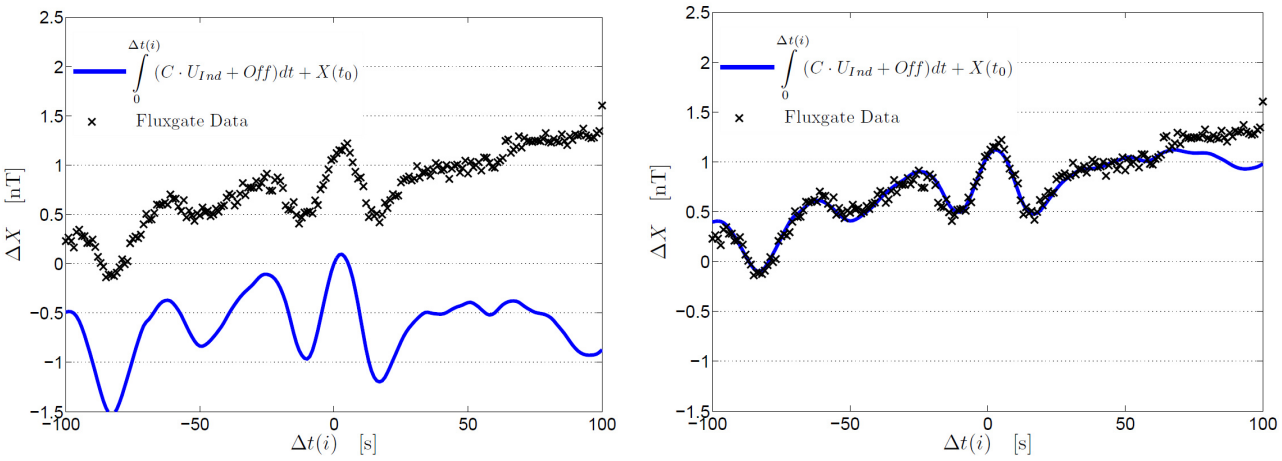

a) ***b)***

Figure 1 –Fluxgate data and integrated induction coil data, with the parameters C, Off and X(t_0), a) not yet fitted to fluxgate data and b) fitted to the fluxgate data.

4. RESULTS

Figure 2shows the effect of noise reduction. The data in Figure 2a show a period with low magnetic activity, but include pulsations withsmall amplitudesof less than 0.5nT. These small pulsations, almost vanishing in the noise produced by the fluxgate, are clearly resolved after taking induction coil data into account. The application of the method to a typical SSC (sudden storm commencement)in Figure 2b showsthat abrupt variations are not blurred out, as would be expected from simple low-pass filtering. The original shape of the SSC is perfectly preserved. To test the fidelity of the data produced by the method we use the Δ**F** test (The intensity data calculated from the three fluxgate components are compared with data from an absolute scalar magnetometer. Here, a very low noise, high resolution K-magnetometer has been used for comparison.)Even at the time of the SSC the method performs well. The Δ**F** test shows that a noise reduction from 80pT to about 25 pT can be reached.

5. CONCLUSIONS

We have presented a method to reduce the noise in high frequency fluxgate magnetometer data by means of combining it with induction coil data. For instruments installed at the Niemegk observatory we have reduced noise from 80 pT to 25 pT. Our method can provide an easy way to obtain low-noise one second data at any observatory that operates inductions coils in addition to standard observatory instrumentation.

6. REFERENCES

Jankovski, J. and C. Sucksdorff (1996): “Guide for magnetic Measurements and Observatory Practice”.

Pulz, E.; Jäckel, K.-H.; Linthe, H.-J. (1999): A new optically pumped tandem magnetometer: principles and experiences. Measurement Science and Technology, 10, 11, 1025-1031.

G. Musmann and Afanassiev, V. (2010): "Fluxgate Magnetometers for Space Research”.

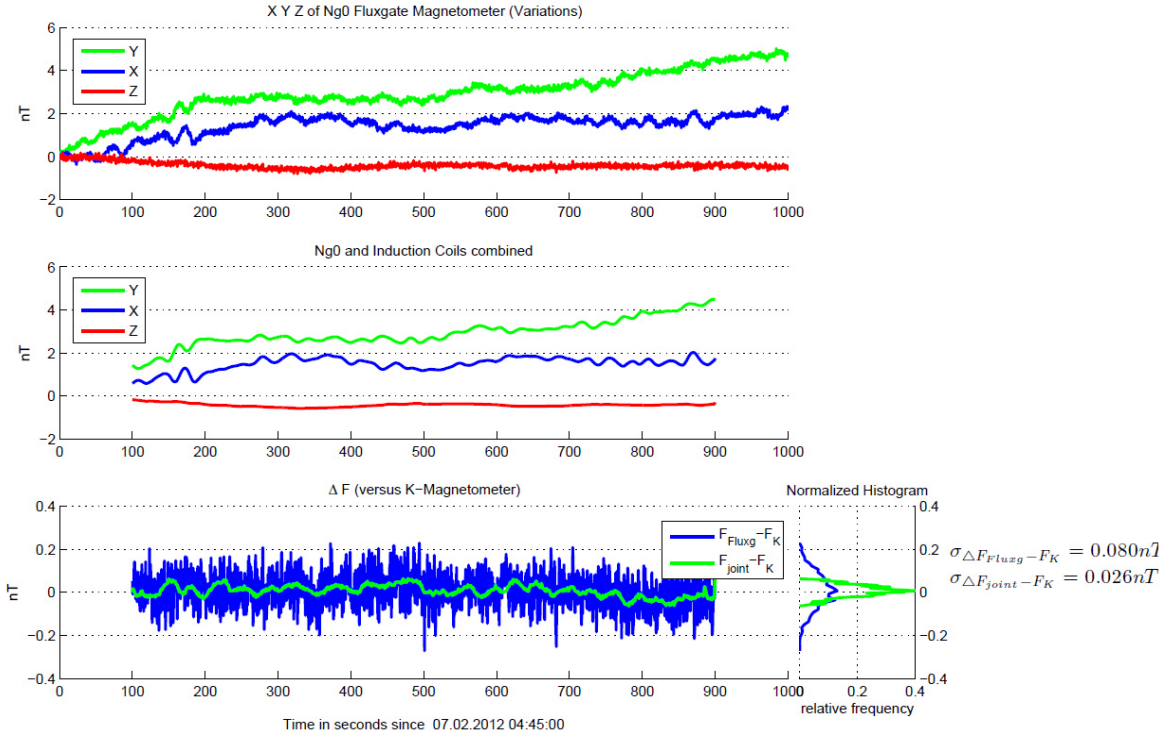

a)

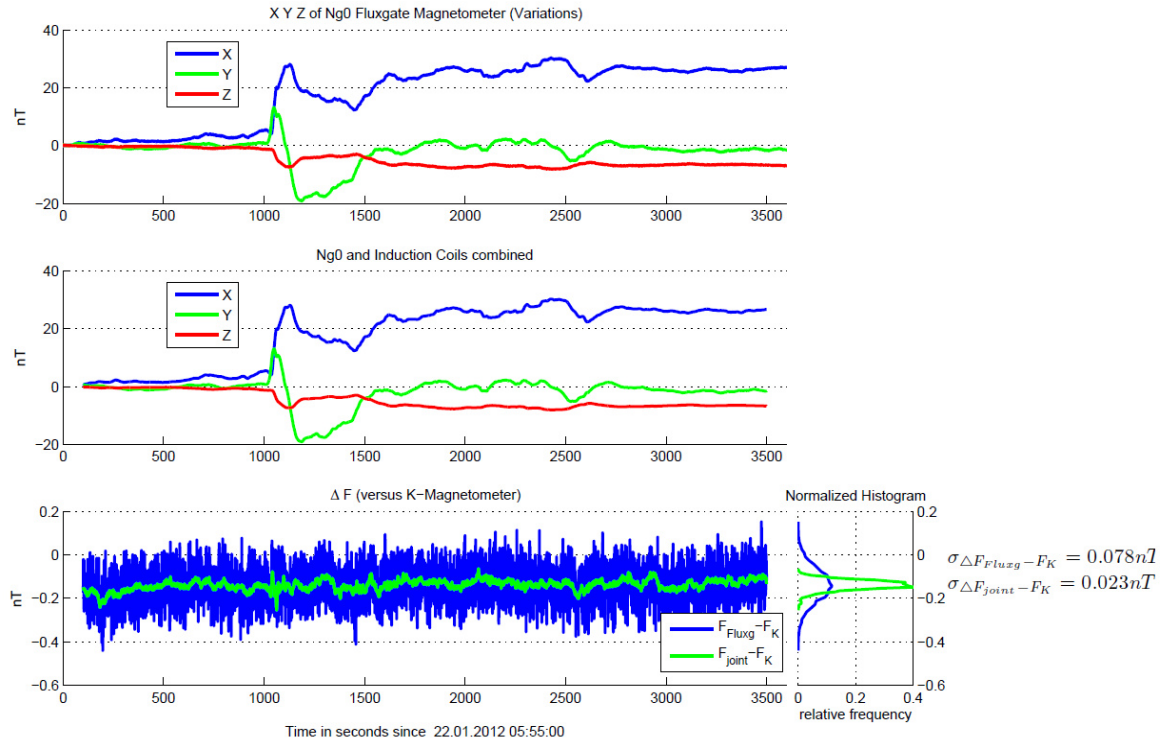

b)

Figure 2 – Fluxgate data (top panels) and data resulting of the joint interpretation with induction coil data (middlepanels) for a) a quite period with pulsations and b) a sudden storm commencement. The bottom panels show the respective noise determined by ΔF test using a K-magnetometer as reference.

METHODS FOR MEASURING THE GRADIENT OF THE MAGNETIC FIELD USING STANDARD OBSERVATORY INSTRUMENTATION

A. Csontos [(1)]

[(1)] Geological and Geophysical Institute of Hungary, H-1143 Stefánia út 14, Budapest, Hungary, csontos.andras@mfgi.hu,

SUMMARY

The practice of geomagnetic observation requires new methods if the spatial gradient of the geomagnetic elements vary in time. This circumstance can arise for example in areas with anomalous conductivity. In such a case the accuracy of the absolute control of variometers is decreased, because the baseline values become dependent not only on the mechanical instabilities of the devices but also on the influences of the varying geomagnetic field. Presently there are no general instructions available how to separate the influences of the different sources and correct the dataset.

This paper presents a procedure based on the measurement of magnetic gradient in order to suggest a new way of data analysis for potential use in observatory practice. As a result of the proposed procedure the geomagnetic field becomes known not only in discrete points, but in a volume of space in which the field can be presumed to vary uniformly.

The paper demonstrates the capability of the DIM instrument for this task, and a case study on repeat station measurements is presented.

1. INTRODUCTION

The direction and the intensity of geomagnetic elements are measured in many ways in current observatory practice. Several of the methods implicitly suppose that the magnetic field is homogeneous, and additionally, that the spatial gradient of the field is constant. The observers try to keep away the recording instruments from strong magnetic anomalies to reach the best result. (The degradation of the proton signal of a proton magnetometer caused by high magnetic gradient is well known.) However, there are a few phenomena (for instance the sea-side effect) which create special circumstances for the measurements, e.g. when the spatial differences of the geomagnetic elements vary in time. In that case the accuracy of the absolute control of variometers is decreased, because the baseline values become dependent on the varying fields. Since all records are reduced to the absolute pillar of the observatory, the effects of the varying external magnetic field on the measured magnetic field are hardly separable from instabilities of the devices. Without taking these phenomena into account, the evolution of the baseline could be corrupted, but there could be a lot of other reasons of a baseline drift. There are no general instructions available how to separate the influences of the different sources and correct the dataset in such a case.

As it will be shown, standard observatory instrumentation gives the observer a chance to identify any change of the magnetic gradient. The variation of the geomagnetic gradient observed by different instruments can help to identify external sources.

2. SOME POSSIBILITIES FOR OBSERVATION THE VARIATION OF GEOMAGNETIC GRADIENT

The focus of this paper is the gradient of geomagnetic field which may vary in the time. The spatial gradients of the magnetic components are not necessarily constant values. These circumstances generate the need for the development of new methods making the geomagnetic measurement with high long term stability possible.

a.) The use of nuclear gradiometers is a very common solution recently. These devices can measure the total field difference between two points directly. An important advantage of this method is the reliability of the applied magnetometers. The use of this method is limited, however, because we only know the differences of the intensities of the sites, but it does not yield information on the direction of the gradient.

b.) One can also start from the difference of the corresponding components of two tri-axial magnetometers. In this case the observer has to be careful, because the difference of two independent tri-axial devices can be a function of several other factors (e.g. orientation of

the devices, temperature etc.). In an ideal case a pair of vector magnetometers records not only the magnetic field components, but also the gradient of these components.

We mention here the difference of absolute instruments for component measurement and variometers (baseline of variometer). In this case the absolute device ensures always perfect record.

An ideal solution would be a gradiometer based on two independent absolute instruments.

c.) DIM as a gradiometer (see 3. for the details)

3. DIM AS A GRADIOMETER

In this section all procedures and calculations relate to absolute measurements taken by a DIM instrument with null reading method. We suppose that the theodolite and the environment are totally free from artificial magnetic impurities, and that the variations of geomagnetic elements are practically zero during an absolute measurement.

A complete set of an absolute measurement consists of eight independent samples taken by a one-component fluxgate (DI) device. In general, the samples represent the geomagnetic field in eight separate points of the space, since none of the theodolite axes intersect the "centre" of the DI sensor. The angles measured by the theodolite define the position of the "centre" of the DI sensor.

The intensity and the direction of the geomagnetic field can be different in the above mentioned eight points. The fluxgate device measures the geomagnetic field component which is parallel to the magnetic axis of the DI sensor. This feature of the device ensures a possibility for measuring the field gradient. From the eight samples gives several quantities can be derived. We will present the behaviour of two quantities in this study to demonstrate the utility of the method.

3.a) Definitions and measurement in vertical gradient field

Positions of observations are the following:

A_1= Eup, A_2= Wup, A_3 =Edn, A_4 =Wdn, V_1= Nup, V_2= Sdn, V_3 =Ndn, V_4 =Sup

The calculated parameters from the observed positions:

$$I= (V_1+V_2-V_3-V_4)/4+ \pi/2 \quad (1)$$

$$D=(A_1+ A_2+A_3+A_4)/4 – (B-A_Z) \text{ Where } (B-A_Z) \text{ is the azimuth mark correction} \quad (2)$$

$$\delta = (A_3+A_4- A_1- A_2)/4 \quad (3)$$

$$\varepsilon_D =(A_1- A_2- A_3+A_4\pm 2\pi)/4*\tan I \quad (4)$$

$$S_{0D}=(A_1- A_2+ A_3- A_4)*H/4 *180/\pi \quad (5)$$

$$\varepsilon= \pi- (V_1+V_2+V_3+V_4)/4 \quad (6)$$

$$\varepsilon_1= (V_1+V_3)/2-180 \quad (7)$$

$$\varepsilon_2= (V_2+V_4)/2-180 \quad (8)$$

$$S_0= -[(V_1-V_2-V_3+V_4)/4+90]*F*180/\pi \quad (9)$$

$$S_{01}= -[(V_1-V_2)/2+90]*F*180/\pi \quad (10)$$

$$S_{02}= -[(V_4-V_3)/2+90]*F*180/\pi \quad (11)$$

Where I is the inclination, D is the declination, δ is the misalignment of the sensor in the horizontal plane, ε_D is misalignment of sensor in the vertical plane calculated from the declination readings, S_{0D} is the offset calculated from the declination readings, H is the horizontal intensity of the geomagnetic field, ε is the misalignment of the sensor in the vertical plane, ε_1 is the misalignment of the sensor in the vertical plane calculated from V_1 and V_3 positions, ε_2 is the misalignment of the sensor in the vertical plane calculated from V_2 and V_4 positions, S_0 is the offset calculated from the inclination readings, F is the total intensity of the field, S_{01} is the offset calculated from V_1 and V_2 readings, S_{02} is the offset calculated from V_3 and V_4 readings. *(Kring-Lauridsen, 1985.)*

The appearance of a gradient can be detected on the course of the inclination measurement by comparing the two independent values of the observed offset (S_{01} and S_{02}). If we want to understand the reason for the difference between the two values, then have a look at Fig 1. Suppose that there is a difference (γ) between the directions of the magnetic field observed in the up and down positions.

The measured positions without gradient: V_1, V_2, V_3, V_4, and V_1, $V_2+\gamma$, $V_3-\gamma$,V_4 with gradient (V_2,V_3 are the down positions)

The result of the measurement with gradient is $I = (V_1 +V_2 -V_3 -V_4)/4 +\pi/2+\gamma/2$ → the result has an error (= $\gamma/2$)

The measured $S_{01}= (V_2+\gamma-(V_1 -180))*180*F/2\pi$ and $S_{02}= (180-V_4 -(360-(V_3 -\gamma)))*180*F/2\pi$ → $S_{01} = -S_{02}$ if $S_0=0$. The original value of S_0 can also be expressed by the mean of S_{01} and S_{02}, since $(S_{01} + S_{02})/2 = (V_2+\gamma-(V_1 -180)+ 180-V_4 -(360-(V_3 -\gamma))*180*F/4\pi=-[(V_1 -V_2 -V_3 +V_4)/4+90]*180*F/ \pi$, which gives the offset according to its definition.

Thus we can express $\gamma/2 = (S_{01} - S_0)/F*180/ \pi$, and although ε_1 and ε_2 will differ, $\varepsilon = (\varepsilon_1 + \varepsilon_2)/2$ remains unaffected.

Note: We can conclude that the γ value is a derived from two independent absolute inclination measurements of V_1,V_2,V_3,V_4 readings, so this value is absolute, too. We can express the intensity of the measured gradient as (sin(γ/2)*F)/d where d is the distance of the sensor up and sensor down positions. The resulting vector lies in the meridional component of the gradient vector, and is nearly perpendicular to the total field vector.

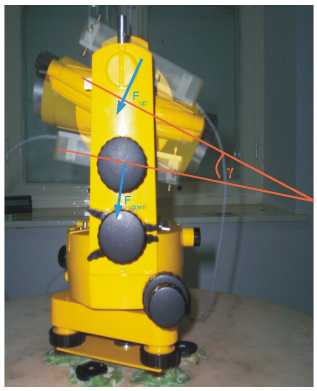

Figure 1 –The definition of the field direction gradient and the γ value in the V_3 and V_4 positions (F_{up} and F_{down} are the vectors of total intensity. Vectors are not to scale)

3.b Declination measurement in horizontal direction gradient

Now let us suppose, that there is a gradient in the horizontal field also, and the "centre" of the sensor lies on the vertical axis of the theodolite. Moreover, it is supposed that ε = 0, and S_{0D} = 0, or at least we know ε and S_{0D}, and hence we can correct all the four readings with them. In this case the difference between the readings in the two up positions should be ideally 180°, and this is valid also for the difference of the down positions.

In the cases when the "center" of the sensor lies not exactly on the vertical axis of the theodolite, the measurement will be corrupted by the horizontal gradient. The measured difference between the upper readings as well as the difference of the down readings will differ from 180° (observed S_{0D} will be a function of the gradient). This behaviour appears similarly when the original value of S_{0D} is not equal to zero.

The difference of the observed and the true offset will be proportional to the intensity of the measured gradient. The direction of the observed gradient vector component is horizontal and nearly perpendicular to the total field vector (i.e. parallel to the east-west direction). In this case the measured gradient is not an absolute value because we have only one declination measurement during the procedure of absolute measurement.

Generally, the effects described above appear only if the sensor is mounted neither on the optical axis nor on the vertical axis of the theodolite. In order to avoid the effect caused by the magnetic field gradient, the sensor should be built into the telescope at the intersection of the two axes. On the other hand, one can take advantage from the gradient sensitivity of the theodolite, depending on the motivation of the observation.

Note: Several different cases (for example effects on a magnetic theodolite) are described by Marsal et. al. 2007.

4. ELECTROMAGNETIC INDUCTION AT A LAND-SEA BORDER (SEASIDE EFFECT) IN THE MIRROR OF DIFFERENT GRADIENT MEASUREMENTS

In the middle of July 2010 we performed a four days long reoccupation at KRBavsko Polje repeat station. The site is in Dinaric mountain 50 km away from the Adriatic see. Portable DIDD system was installed in the nearest forest. The absolute instrument was a Zeiss 20A theodolite equipped with a DMI D&I one component fluxgate sensor. We used a GSM-19 magnetometer for total field measurement on an auxiliary point. A lot of sets of absolute measurements were performed in the morning and in the evening.

Due to closeness of the Adriatic Sea a strong induction effect is noticed as a consequence of the enormous land-sea conductivity contrast. This phenomenon is well know and has been repeatedly investigated theoretically. We observed the temporal change of the magnetic field gradient. The ocean effect can be the reason for the spatial field variations at small spatial and temporal scales, even at large distances. *(Soyer 2002)*

The above described environment was ideal for the test of the gradient measurement methods. Typical marks of the induction effect can be seen in Fig. 2. The first information is that the spatial differences of the geomagnetic elements are not constant. This fact is a strong limitation for the accuracy of the whole measurement.

The most important advantage of the above methods is that they make the detection of gradient effects possible for the observer. It gives the observer a further chance to find the source of the external effect. On the other hand the results can help to distinguish between an external field influence and a technical problem.

In order to demonstrate the relation of the field fluctuations observed by different instruments, we applied a correction. The difference of the measured total field between the site of the DIDD and the repeat station was corrected with the observed declination offset values. The result is presented in Fig 3.

It can be concluded that the external influences appeared mostly in the horizontal gradient of the field. This experience is in good agreement with theoretical predictions, i.e. the north-west direction of the coast implies an effect in the horizontal plane at a relatively large distance from the sea.

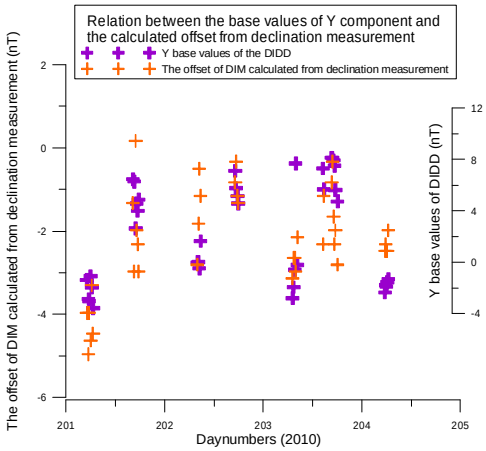

Figure 2 –Relation between the base values of Y component and the calculated S_{0D} of the DIM

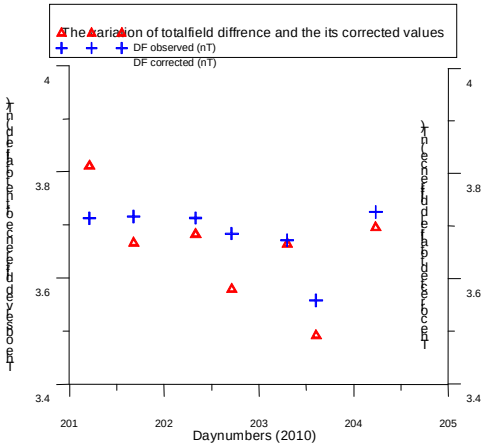

Figure 3 –The measured (red) and the corrected (blue) total field differences

5. CONCLUSIONS

The paper demonstrates different methods for gradient measurement based on standard observatory instrumentation. We presented that the DIM instrument, which measure the magnetic field in a volume of the space, is capable to detect the gradient or the variation of the spatial gradient of the geomagnetic field.

The comparison of different methods was presented in a case study from an area with anomalous conductivity. The similar behaviour of the observed fluctuations in the gradient field gives a chance to identify the source of the influence. In the presented case the correction of the dataset was also possible. The results fit well to the theoretical models.

6. ACKNOWLEDGMENTS

This work was supported by a US-Hungarian joint project funded by the Hungarian Science and Technology and by OTKA (K-75640). The DIDD system was provided by MINGEO Ltd. and GEM Systems Inc. Balázs Heilig is specially acknowledged for valuable discussions, remarks.

7. REFERENCES

Kring-Lauridsen E. Experiences with the DI-fluxgate magnetometer inclusive theory of the instrument and comperson with other methods, Geophysical Papers R-71, Danish Meteorological Institute, Copenhagen, 30 pp. 1985.

Marsal S. and J. M. Torta,: An evaluation of the uncertainty associated with the measurement of the geomagnetic field with a D/I fluxgate theodolite Meas. Sci. Technol. 18 2143 2007.

Soyer W.: Analysis of geomagnetic variations in the Central and Southern Andes. Dissertation zur Erlangung des Doktorgrades im Fachbereich Geowissenschaften an der Freien Universität Berlin. 2002.

MEASURING THE ORTHOGONALITY ERROR OF COIL SYSTEMS

B. Heilig [(1)], A. Csontos [(1)], K. Pajunpää [(2)], D. Gouws [(3)], T. White [(4)], B. St-Louis [(5)], D. Calp [(5)]

[(1)] Geological and Geophysical Institute of Hungary, H-1143 Stefánia út 14, Budapest, Hungary, heilig.balazs@mfgi.hu,
[(2)] Finnish Meteorological Institute, Helsinki, Finland,
[(3)] South African National Space Agency, Hermanus, South-Africa,
[(4)] United States Geological Survey Geomagnetism Group, Golden, CO, USA
[(5)] Geological Survey of Canada, Ottawa, Canada

SUMMARY

Recently, a simple method was proposed for the determination of pitch angle between two coil axes by means of a total field magnetometer. The method is applicable when the homogeneous volume in the centre of the coil system is large enough to accommodate the total field sensor. Orthogonality of calibration coil systems used for calibrating vector magnetometers can be attained by this procedure. In addition, the method can be easily automated and applied to the calibration of delta inclination–delta declination (dIdD) magnetometers. The method was tested by several independent research groups, having a variety of test equipment, and located at differing geomagnetic observatories, including: Nurmijärvi, Finland; Hermanus, South Africa; Ottawa, Canada; Tihany, Hungary. This paper summarizes the test results, and discusses the advantages and limitations of the method.

1. INTRODUCTION

For the calibration of fluxgate magnetometers, mostly large room-sized coil systems are used. The precision of the calibration procedure depends on how accurately the orthogonality of the calibration coil system is known. The method considered to be the most reliable for the determination of the misalignment angles of the calibration coils is based on measurements made by a DI-flux magnetometer on a pillar in the centre of the coils (Pajunpää et al 2007). The coils should be large enough to have room for the instrument and the observer executing the measurements. The measurement is time-consuming. Here, a more time-efficient process is introduced which can be easily automated and can also be used with small-sized (15–20 cm in diameter) coils.

2. DESCRIPTION OF THE PROCEDURE

In this section the proposed method is summarized based on Heilig (2012). The procedure is based on a well-known method introduced by Alldredge and Saldukas (1964) to measure the magnitude of the magnetic field generated by a coil using a scalar magnetometer. Let $\boldsymbol{A}_{1+}$ and $\boldsymbol{A}_{1-}$ denote the bias fields created by positive and negative currents, respectively, in the coil C_1. These bias fields are collinear and equal in magnitude but oppositely directed. During a data acquisition sequence, the magnitude of the total field ($\boldsymbol{F}$) and the deflected fields ($\boldsymbol{F} + \boldsymbol{A}_{1+}$ and $\boldsymbol{F} + \boldsymbol{A}_{1-}$) are measured. The corresponding readings are F, F_{1+} and F_{1-}, respectively. Since the resulting vectors are coplanar, the magnitude of the bias field $A_1 = |\boldsymbol{A}_{1+}| = |\boldsymbol{A}_{1-}|$ can be easily obtained (Alldredge and Saldukas 1964) from the triangles formed by $\boldsymbol{F}$, $\boldsymbol{F}_{1+}$, $\boldsymbol{A}_{1+}$ and $\boldsymbol{F}$, $\boldsymbol{F}_{1-}$, $\boldsymbol{A}_{1-}$, respectively, by applying the law of cosines:

$$A_1 = \sqrt{\left(F_{1+}^2 + F_{1-}^2 - 2F^2\right)/2}\,, \tag{1}$$

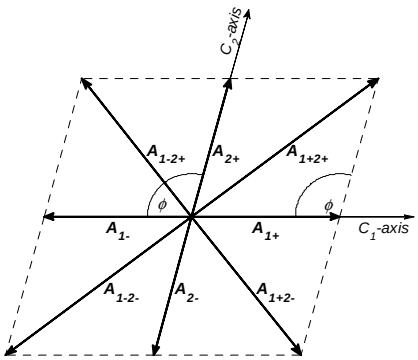

Figure 1 –Bias fields generated by the coils and their combinations (from Heilig, 2012)

If the current I_1 introduced in the coil is known, the coil constant can also be derived as A_1/ I_1.

Let C_1 and C_2 be two coils between which the pitch angle has to be determined. Let A_{2+}/A_{2-} denote the bias fields created by positive/negative currents in the C_2 coil. The corresponding magnetometer readings are F_{2+} and F_{2-}. The magnitude of the deflection field, A_2, in the coil C_2 can be calculated in the same way as A_1 in Equation (1). If A_{1+} and A_{2+} are applied simultaneously, a new combination bias field is created: the vector sum of A_{1+} and A_{2+}. Let us denote it by A_{1+2+} (Fig. 1). By changing the direction of the current in both coils, we get another bias field, A_{1-2-}. The two opposite bias fields are again of equal magnitude and coplanar, hence their magnitude (A_{12}) can be determined in the same way as in the single-coil case by Equation (1), namely

$$A_{12}=\sqrt{\left(F_{1+2+}^2+F_{1-2-}^2-2F^2\right)/2}, \tag{2}$$

where $F_{1+2+} = |\boldsymbol{F} + \boldsymbol{A}_{1+2+}|$ and $F_{1-2-} = |\boldsymbol{F} + \boldsymbol{A}_{1-2-}|$. In Fig. 1, $A_1 = |\boldsymbol{A}_{1+}|$, $A_2 = |\boldsymbol{A}_{2+}|$ and $A_{12} = |\boldsymbol{A}_{1+2+}|$ form a triangle, and are related through the law of cosines as

$$A_{12}^2 \;=\; A_1^2 \;+\; A_2^2 \;-\; 2\,A_1 A_2 \cos\;\varphi\;, \tag{3}$$

from which φ can be easily calculated

$$\varphi = \arccos\left(\frac{A_{12}^2 - A_1^2 - A_2^2}{-\,2\,A_1 A_2}\right), \tag{4}$$

Coils C_1 and C_2 are orthogonal if $\varphi = \pi/2$. Any deviation from this value is the degree to which the coil system is non-orthogonal. The orthogonality error is therefore defined as $\varepsilon = \varphi - \pi/2$. Applying the other combination of the bias fields, the angle φ' can be determined from

$$A_{21}^2 \;=\; A_1^2 \;+\; A_2^2 \;+\; 2\,A_1 A_2 \cos\;(\varphi') \tag{5}$$

where $A_{21} = |\boldsymbol{A}_{1+} + \boldsymbol{A}_{2-}| = |\boldsymbol{A}_{1-} + \boldsymbol{A}_{2+}|$ is the magnitude of the other combination of the bias fields. If all assumptions are valid, then $\varphi = \varphi'$ (or $\varepsilon = \varepsilon'$). Conversely, if $\varphi \neq \varphi'$, the symmetry of the system has been violated. Such cases are discussed in the following section.

3. TEST MEASUREMENTS AND RESULTS

The proposed method was tested by independent groups at different locations using different coil systems. The total field magnetometer applied for testing was a GEM System GSM-19 Overhauser magnetometer (using tuned mode at THY and using auto-tune mode elsewhere) in all locations, except for NUR, where a PMP-7 proton magnetometer was used. Here we summarize and discuss the most important test results.

Case 1: varying coil current (recorded): ELSEC Helmholtz coil pair at THY

A Helmholtz coil pair (C_V – vertical, C_H – horizontal) was driven by a current generator, and the current strength was recorded throughout the experiment. While the range of the current variation was about 1.8 mA (1.7 %), the magnitude of the opposite currents differed only a few tenths of a μA. Table 1 summarizes the observations. The bias fields computed using Eq. (1) were as follows: A_V = 15849.90 nT and A_H = 15636.78nT; the combined bias fields from Eq. (2): A_{VH} = 22330.28 nT and A_{HV} = 21810.56 nT. The difference between the two estimations of the orthogonality error, $|\varepsilon-\varepsilon'|$ was close to 2°. This large difference indicates that the measurements were contaminated, possibly by current strength variation. However, the temporal variation of the coil currents can be easily corrected by reducing all bias fields to the same current level according to $A_{xcorr} = A_x(I_{ref}/I)$, where I_{ref} is an arbitrarily chosen reference current strength (in our case 100 mA). The corrected values are: A_{Vcorr} = 15301.86 nT, A_{Hcorr} = 15353.28 nT, etc. With this simple correction the difference

between the two estimations of the orthogonality error decreased below 0°01' (ε = 1°20'41", ε'=1°19'49") ! This example suggests that even slight current variations could corrupt the results if not taken into account.

***Table 1* – Example of a measurement cycle**

Comp.		Current	Comp.		Current
	[nT]	[mA]		[nT]	[mA]
F	48158.34	0.000	F	48158.94	0.000
F_{V+}	62729.07	+103.582	F_{H+}	50789.71	+101.847
F_{V-}	34726.85	-103.582	F_{H-}	50477.62	-101.847
F	48159.13	0.000	F	48160.04	0.000
F_{V+H+}	64616.48	+101.828	F_{V+H-}	64191.42	+101.807
F_{V-H-}	38217.77	-101.828	F_{V-H+}	38335.9	-101.807

Case 2: varying, unknown coil current, semi-automated measurement, dIdD coil system at THY

With the same method, the orthogonality error of the *dIdD* coils can be measured directly, without any additional instrumentation. At the time of the test presented here, the magnitude of the ambient magnetic field, F, was about 48,200 nT, the inclination, $I \approx 63.5°$, and the declination, $D \approx 3.5°$. The applied bias field was about 11,800 nT (~ 25% of F). The absolute accuracy of the measurement of the bias fields is estimated to be better than 1 nT. At first, the instrument was run in the normal *dIdD* mode to derive A_d and A_i. In the second step, the current was introduced into both coils simultaneously. The C_D- and C_I-coils were connected in series to ensure the same current in both coils. From these measurement sequences the combination bias fields, A_{di} and A_{id} were then calculated. A full measurement sequence (10 readings) lasted less than 1 minute. Altogether 30 sequences were completed. The difference between the two estimations, $|\varepsilon-\varepsilon'|$ ranged between 0' and 5', likely again due to the variation of the current strength. GEM Systems' *dIdD* uses 10 mA current for generating the bias field in the coils. A 4 μA variation in the bias current could account for the observed differences. However, even if the current was not recorded during this experiment, the results can be corrected supposing that $I_D = I_I \neq I_{DI} = I_{ID}$ (which is reasonable if the current strength depends on the resistivity of the coils, since the resistivity of C_D- and C_I-coils are similar). If all four currents were equal, then the following equality (derived from the sum of Eqs. (3) and (5)) should be satisfied:

$$A_{di}^2 + A_{id}^2 = 2\left(A_i^2 + A_d^2\right), \tag{6}$$

Eq. (6) does not apply in the case of varying current. However, if the above assumptions on the bias currents ($I_D = I_I \neq I_{DI} = I_{ID}$) are valid, a constant γ (= I_{DI}/I_D) can be found that satisfies the following modified equation:

$$A_{di}^2 + A_{id}^2 = 2\gamma^2\left(A_i^2 + A_d^2\right), \tag{7}$$

This γ can then be used to correct the computed bias fields ($A_{xcorr} = \gamma A_x$).

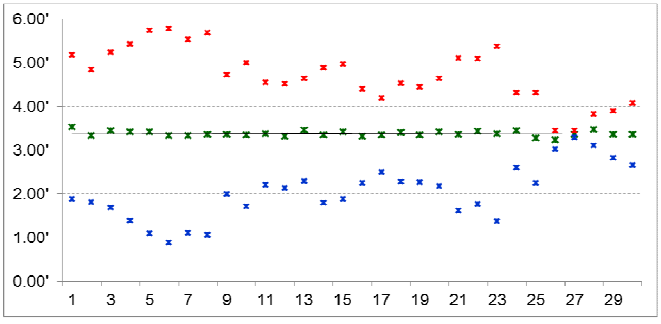

Figure 2 –The results of the orthogonality error measurements of dIdD without (red and blue) and with (green) corrections

Figure 2 shows the results of the test without corrections (red and blue x) and with corrections (green x) for current variations. Note that the corrected values are close to the arithmetic means of the uncorrected results. The mean of the 30 corrected observations is very stable, with a 0'04" standard deviation about 3'23".

Absolute accuracy

For practical applications, the most important consideration is absolute accuracy of the measurement. That is why the orthogonality error values obtained by the new method were compared to the values obtained by the well-proven FMI method. The FMI method is based on DIM absolute measurements carried out by an observer in the centre of the coil system (Pajunpää et al, 2007). At GSC, the FMI measurements were taken immediately before the new method was used. This ensures the highest level of consistency between the two

methods. Table 2 summarizes the results of these comparisons, which were carried out by three different groups, FMI, SANSA, and USGS variously at the three locations, Nurmijärvi (Finland, NUR), Hermanus (South Africa, HER), Ottawa (Canada, OTT).

***Table 2* – Comparison of the results of the new method and the FMI method**

Coils	**OTT**	**USGS**		**HER**	**SANSA**		**NUR**	**FMI**	
	FMI	**new**	**nr**	**FMI**	**new**	**nr**	**FMI**	**new**	**nr**
HD (XY)	-2'07"±06"	-2'01"±01"	3*20	2'37"	2'42"±51"	6*1	0'04"±2"	0'10"±5"	3*1
HZ (XZ)	1'33"±06"	1'19"±02"	3*20	0'04"	n.a.	6*1			0
DZ (YZ)	1'48"±06"	1'34"±01"	3*20	0'04"	0'14"±31"	6*1			0

The difference was, in all cases, less than 10"-15". However, the scatter of the results varies. At OTT, an extremely stable current generator was used, and the results published in Table 2 were achieved without any corrections. Also, during the three full tests, 20 magnetometer readings ('nr' in Table 2) were taken at each bias field applied. We therefore assume these two reasons as explanations for the lowest scatter in the results here

At HER, measurement sequences at two different current strengths were carried out for all dual combinations (HD, HZ, DZ) of the three calibration coils. Current strengths were recorded, and all measurements were later corrected for current changes. The angle between the HZ pair could not be determined because one of the deflected fields was too low (15-18 μT) to be measured accurately, since it is out of the measurement range of the Overhauser magnetometer. This failed test with the Hz coils occurred because the ambient field at HER is in the 25,700 nT range, being among the lowest of all observatories world-wide, and points to one of the limitations of the procedure. However, we think that the method could be modified for use in such circumstances simply by activating a third coil to increase the effective ambient field. But this modification has not yet been tested.

In NUR, only the XY coil pair was used for the test. Three measurement sequences were completed. Bias fields were corrected for the temporal variation of the coil currents. After the temporal variation correction, the mean result (0'06"±7") was quite close to the reference value. However, we were not satisfied with large differences found between ε and ε'. In remediation, we corrected all magnetometer readings for the time variation of the geomagnetic field. The time series used for the correction, then, was calculated from the observed variations in the ambient field and from the corresponding constant bias fields. This correction resulted in the difference $|\varepsilon-\varepsilon'|$ decreasing from 3'-5' to below 1'.

4. CONCLUSIONS

The tests show that the proposed method is suitable to measure the misalignment errors of coil systems. The procedure is much faster than the previous method based on DIM observations, and can be easily automated. With this method an accuracy close to 10" can be achieved for both the *dIdD* and the calibration coil system configurations.

However, there are limitations of the applicability of the method. The test results showed that the stability of the driving current is crucial. Only one of the tested current generators was stable enough to avoid having to apply a correction in the computed bias fields for current strength variation. At low magnetic latitudes, the low total field values of ambient field limit the applicability of the method. Also, in the low latitude zone measurements made in the meridional plane are critical. The procedure should be applied in quiet conditions. In moderately disturbed conditions the time variation of the geomagnetic field should be taken into account. In general, it is recommended to take many measurements and use the mean of all ε and ε' to arrive at the primary result. The method described here augments pre-existing practices but does not completely replace them. This method does not yield any information on the absolute orientation of the coils.

5. ACKNOWLEDGEMENT

This work was supported by the US-Hungarian (OMFB-00890/2008), and the South African-Hungarian (TÉT_10-1-2011-0025) bilateral projects. We thank R.E. Bracken, E. A. Sauter, C. A. Finn, L. Loubser, J. McCarthy, and P. Crosthwaite for reviewing this document.

6. REFERENCES

Alldredge, L. R. and I. Saldukas (1964) An automatic standard magnetic observatory *J. Geophys. Res.*, **69** 1963.

Heilig, B (2012) Determining the orthogonality error of coil systems by means of a scalar magnetometer: application to delta inclination–delta declination (dIdD) magnetometers, *Meas. Sci. Technol.*, **23**, 037001

Pajunpää, K., E. Klimovich,V. Korepanov, P. Posio, N. Nevanlinna, W. Schmidt, M. Genzer, A.-M.Harri and Lourenço (2007) Accredited vector magnetometer calibration facility, *Geophysica* **43**, 59

THE IN-SITU CALIBRATION OF THE NURMIJARVI OBSERVATORY VARIOMETER

A. Marusenkov [(1)], V. Korepanov [(1)], K. Pajunpää [(2)]

[(1)] Lviv Centre of Institute for Space Research, 5A Naukova Str., 79000, Lviv, Ukraine, marand@isr.lviv.ua

[(2)] Finnish Meteorological Institute, Nurmijärvi Geophysical Observatory, Finland, kari.pajunpaa@fmi.fi

SUMMARY

Using a reference instrument the attempt to calibrate in-situ the observatory variometer without interruption its regular operation have performed. The special procedure of the virtual pointing of the reference sensor to the geographic axes is applied. It makes possible to check the observatory sensor orientation. The allowable level of the methodical error – 0.1 % for scale factors and 0.1 deg. of arc for non-orthogonality and orientation angles – has been achieved. Besides calibrating parameters of the observatory magnetometer the synchronization error of its time scale relatively the Universal coordinated time is revealed.

1. INTRODUCTION

Magnetic observatories are continuously striving to improve the accuracy of the magnetic field measurements. The majority of the observatories are still equipped with flux-gate or even photoelectric variometers. The baselines of these types of variometers are estimated using well-known absolute measurements, whereas the scale factors and orientation of the sensor reference frame, which are implicitly involved into the computation of the absolutes values of the field, usually are poorly known and in almost every case are not regularly calibrated, as should be required. The lack of periodic calibrations can be partly explained by the fact that the metrological certification of the instruments must be carried out in a special laboratory by means of calibration coils. This check requires interrupting the measurements, transporting the instrument to and from the calibration site and reinstalling it in the observatory. This method is absolutely unacceptable, especially for remote observatories, because the time taken by the whole procedure can be very long, resulting in large gaps in the records. For these reasons, in-situ calibrations are much more advisable.

In this report we continue to discuss the possibility of calibrating *in-situ* the observatory instrument by means of the comparison of its records with the field recorded simultaneously by a reference magnetometer. The first stage of the experiment included calibration of the two low noise magnetometers LEMI-025 #04 and #06 in the Magnetic Calibration and Test Laboratory of Nurmijarvi geomagnetic observatory and performing simultaneous records of geomagnetic variations by these instruments as well as the standard observatory magnetometer (Danish suspended flux gate magnetometer FGE-89). The inter-calibration of the two LEMI-025 by processing its quite short records (about 3 days) was in good agreement with the Coil calibration results (Marusenkov (2011)). While one of the LEMI-025 magnetometers was removed at the third day of the operation the other continued to record more than 10 days. The latter was used as a reference instrument with the aim to calibrate standard observatory magnetometer, which parameters are not known exactly. The peculiarities of the magnetometers' data processing as well as the main obtained results are given below.

2. THE REFERENCE SENSOR ORIENTATION

During both the coil calibration procedure and the variations' measurements the sensor of the reference magnetometer LEMI-025 #04 was oriented at the same position respectively to the horizontal plane. It was achieved using the precise (≈0.1 min of arc) spirit level installed on the rotating support of the sensor. While the axis Z of the calibration coils is perfectly directed vertically (<0.1 min of arc after the proper calibration using DI-flux, K. Pajunpaa, (2007)), the correction matrix calculated during the calibration could be used for the virtual rotation of the sensor to the required horizontal position (Figure 1).

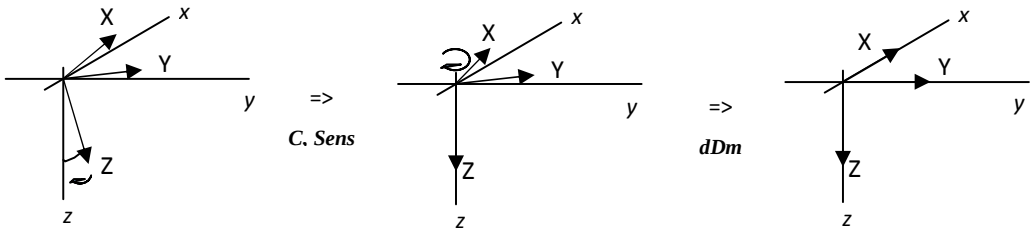

Figure 1 –The virtual orientation of the reference magnetometer axes.

So, we use outcome of the Coil calibration: the vector-row of the scale factors **Sens** and the matrix of the axes' misalignment **C,** which implicitly contains information on the non-orthogonality and orientation errors. Applying **Sens** and **C** to the initial magnetometer data **R** we expected to obtain perfectly scaled data along the orthogonal directions, two of which located in the horizontal plane: $\mathbf{R1}=\mathbf{R}\cdot\mathbf{Sens}^{-1}\cdot\mathbf{C}^{-1}$.

The next step is a precise orientation of the X and Y components to the geographic North and East respectively. For this purposes we exploited the absolute measurements, which were performed on September, 08th 2010 (Table 1).

Table 1 **– Comparison of the absolute measurements and the reference magnetometer data**

The results of the absolute measurements		LEMI-025 #004	
		before rotation	after rotation
X	14857.38 nT	14830.58 nT	14887.87 nT
Y	1882.49 nT	2293.62 nT	1886.32 nT
Z	49888.26 nT	49838.30 nT	49838.30 nT
T	52087.66 nT	52048.66 nT	52048.66 nT
D	7.221 deg of arc	8.791 deg of arc	7.221 deg of arc
I	73.291 deg of arc	73.242 deg of arc	73.242 deg of arc

If we assume, that the declination of the magnetic field vector in the variometer hut is the same as in the absolute one, it is necessary virtually rotate the data **R1** at the angle dD=Dm-D=8.791-7.221= 1.570 deg of arc. Using the rotation matrix **dDc** the records of the LEMI-025 virtually oriented to the geographic frame could be computed by the expression $\mathbf{R2}=\mathbf{R1}\cdot\mathbf{dDc}$.

After virtual rotation (see Table 1) there are still some discrepancy with the absolute measurements in the inclination (≈ 3 min of arc) and the total field (≈ 39 nT). However, we believe that the reference magnetometer axes are oriented with the similar level of accuracy - better than 0.1 deg of arc respectively to the geographic frame, if our assumption about declination equality in the absolute and variometer huts is true.

3. DATA PROCESSING PARTICULARITIES

The data of LEMI-025, collected with the sample rate 10 Hz, were preliminary processed for excluding spikes and step-like interferences. After this the filtration and decimation to 1 Hz sample rate was performed. The observatory magnetometer recorded data with sample frequency 1 Hz. Comparison of the magnetometers' records reveals some traces of both the diurnal variations and the variations during the disturbed day (September, 24th) in the difference signals. There are no observable long-term drifts – the mutual stability of the magnetometers baselines is very good.

To compare the magnetometers' records we use the method, which was successfully applied for inter-calibration of the both LEMI magnetometers (Marusenkov (2011)). The magnetometer readings are shaped into N x 3 matrixes **T** and **R2** and incorporated into the following linear regression equation:

$$\mathbf{T}=\left(\mathbf{R}2-\mathbf{d_r}\right)\cdot\mathbf{n}+\mathbf{d_t}\ , \qquad (1)$$

where **n** is the 3 x 3 matrix mapping the reference signal onto the tested one and $\mathbf{d_r}$ and $\mathbf{d_t}$ the reference and tested instrumental noise respectively. The further decomposition of **n** provides the scale factors ratios, the angles of non-orthogonality and orientation of the tested instrument respectively the geographic frame (in our case we believe that the reference magnetometer had been properly oriented). The estimation of regression parameters matrix may be found by the multivariate extension of the formula given by Nielsen (2005):

$$\mathbf{n}^{\mathrm{est}}_{\gamma,m}=\left(\sum_{j=m_0}^{m}\lambda_j^{\gamma}\cdot\mathrm{Re}\left(\mathbf{I_{RR}}\left(\lambda_j\right)\right)\right)^{-1}\cdot\sum_{j=m_0}^{m}\lambda_j^{\gamma}\cdot\mathrm{Re}\left(\mathbf{I_{RT}}\left(\lambda_j\right)\right)\ , \qquad (2)$$

where $I_{RR,kl}(\lambda_j) = w_{R(\bullet,k)}(\lambda_j) \cdot w^*_{R(\bullet,l)}(\lambda_j) \in \mathbb{C}$ unless $k = l$, $\dim(\mathbf{I_{RR}}) = 3 \times 3$ – elements of the cross-periodogram matrix $\mathbf{I_{RR}}$ between time series measured by the reference magnetometer;

$I_{RT,kl}(\lambda_j) = w_{R(\bullet,k)}(\lambda_j) \cdot w^*_{T(\bullet,l)}(\lambda_j) \in \mathbb{C}$ unless $k = l$, $\dim(\mathbf{I_{RT}}) = 3 \times 3$ – elements of the cross-periodogram matrix $\mathbf{I_{RT}}$ between time series measured by the reference and tested magnetometers; the asterisk (*) denotes complex conjugation;

$w_{R(\bullet,k)}(\lambda_j) = \frac{1}{\sqrt{2\pi N}} \cdot \sum_{t=1}^{N} R(t,k) \cdot e^{it\lambda_j}$ and $w_{T(\bullet,k)}(\lambda_j) = \frac{1}{\sqrt{2\pi N}} \cdot \sum_{t=1}^{N} T(t,k) \cdot e^{it\lambda_j}$ – discrete Fourier transforms of the time series recorded by the reference and tested magnetometers accordingly;

$\lambda_j = 2\pi j/N$ – normalized frequency of discrete Fourier transform; $m=m(N)$, $m_0= m_0(N)$ – bandwidth parameters;

γ – parameter, which takes into account the power law dependence of spectral density of regression errors. According to a priori information about spectral characteristics of the magnetometers noises, the parameter γ has to be selected in the range [0.8; 1].

We had performed set of the preliminary calculations using Eq. (2) with different values of the m_0, m and γ in order to understand the influence of each of them and to select the proper values. While the parameters m_0, m define in fact the analyzing frequency band we rather use the lower and upper limit frequencies (f_l, f_u) of this band, which is connected with the parameters m_0, m through the record duration. For all preliminary estimations we operated with the whole record data. The estimations are almost invariant to the upper limit of the frequency band f_u, if it is not exceed 2-5 mHz. It has to be noted that the confidence intervals quite weakly depends on the upper limit of the frequency band, then it is possible to decrease f_u without loss of accuracy. The estimations also depend on the lower limit of the frequency band, but not so considerable as for the upper one. The confidence intervals of the estimations gradually increase with increasing f_l higher than 10-20 μHz. The influence of the parameter γ on the estimations (at the different values f_l, f_u) is a very weak, if the parameter γ lies in the expected range [0.8; 1].

4. DISCUSSION OF THE OBTAINED RESULTS

Basing on the obtained dependencies of the estimations on the frequency band limits and the parameter of the spectral density correction the following values were adopted for calculations: γ =0.9; f_l = [1; 10] μHz; f_u = [0.5; 1] mHz. The estimations performed in the four intersected frequency bands are given with a 95% confidence interval in Table 2 for the detailed comparison.

Table 2 **– The estimations computed in the different frequency bands**

Estimated parameter	$f_l = 10^{-6}$ Hz ; $f_u = 0.5 \cdot 10^{-3}$ Hz ;	$f_l = 10^{-6}$ Hz ; $f_u = 10^{-3}$ Hz ;	$f_l = 10^{-5}$ Hz ; $f_u = 0.5 \cdot 10^{-3}$ Hz	$f_l = 10^{-5}$ Hz ; $f_u = 10^{-3}$ Hz ;
Kxt/Kxr	1.00144 ± 0.00059	1.00142 ± 0.00051	1.00162 ± 0.00067	1.00158 ± 0.00057
Kyt/Kyr	1.00186 ± 0.00053	1.00187 ± 0.00046	1.00191 ± 0.00057	1.00192 ± 0.00051
Kzt/Kzr	1.00211± 0.0012	1.00220 ± 0.0011	1.00223 ± 0.0014	1.00233 ± 0.0013
ε_{xy}	0.125 ± 0.066	0.126 ± 0.056	0.117 ± 0.073	0.119 ± 0.062
ε_{xz}	0.031 ± 0.097	0.031 ± 0.088	0.029 ± 0.11	0.032 ± 0.099
ε_{yz}	0.047 ± 0.088	0.044 ± 0.082	0.048 ± 0.098	0.044 ± 0.092

As it follows from the Table 2 the estimations are mutually consistent and its maximum deviations do not exceed 0.022% for the scale factors and 0.01 deg of arc for the non-orthogonality errors, that are an order of magnitude less than the respective confidence intervals.

From the obtained results we can conclude that the scale factors of the observatory magnetometer are slightly exceed (appr. 0.2 %) the rated values. The non-orthogonality error between axes X and Y has also a considerable deviation from the zero (appr. 0.12 deg. of arc). The most noticeable difference had been found in the mutual orientation of the observatory and reference sensors. The observatory sensor has to be rotated in the horizontal plane at the angle about 0.37 deg of arc clockwise (X to the East and Y to the South). The mutual misalignment of the sensors' axes caused the considerable discrepancy in the corrected and non-corrected difference signals (Figure 2). However, even the corrected difference signals contain some disturbances connected with the geomagnetic activity. These disturbances appeared in the amplitude spectra at the frequencies around 7 and 30 mHz and well matched with the local extremum on the geomagnetic variations spectrum (Figure 2). Moreover, the detailed consideration of these disturbances had revealed, that they are strongly correlated with the derivatives of the geomagnetic pulsations along the respective components. In order to correct possible phase or time shifts the

matrix **R2** was supplemented with 3 columns of the first-order difference of itself and the estimation of the new regression parameter matrix **n1** (with 6x3 dimension) was found. The latter and the supplemented matrix **R2s** were used for computing the difference signals corrected simultaneously for the scale factors and axes orientation, as well as for time shifts. As a result, such double corrected difference signals are free from the geomagnetic variations (Figure 2) and could be used for estimation of the observatory magnetometer noise level: 100 pT/Hz$^{1/2}$ at 0.1 Hz and 515 pT/Hz$^{1/2}$ at 0.001 Hz for X and Y components and 150 pT/Hz$^{1/2}$ at 0.1 Hz and 790 pT/Hz$^{1/2}$ at 0.001 Hz for Z one.

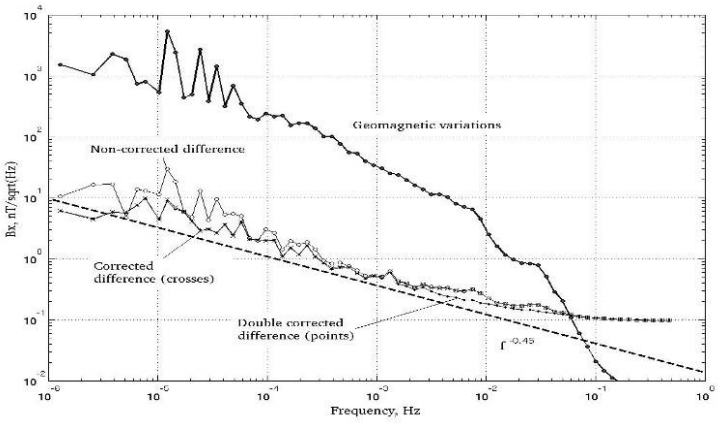

Figure 2 –The spectral density of the geomagnetic variations and difference signals along the component X.

5. CONCLUSIONS AND FUTURE WORKS

The attempt to calibrate in-situ the observatory variometer without interruption its regular operation have performed. For this purpose, the comparison of its records with the field recorded simultaneously by a reference magnetometer was exploited. The low-noise flux-gate magnetometer LEMI-025 was used as a reference instrument. It was calibrated in the three-component Coil system, which magnetic axes were aligned to the geographical frame. Keeping the same tilt of the reference sensor respectively horizontal plane during the Coil calibration procedure and further records of the geomagnetic variations and applying data of the absolute measurements let to know the exact orientation of the sensor axes respectively the geographic frame.

After the Coil calibration the magnetometer LEMI-025 have been installed in the variometer hut of the observatory and more than two week records were acquired. In this work the last 9 days, when the baselines of the reference magnetometer had stabilized, were analyzed and processed. Due to the quite long record and few geomagnetically disturbed days the allowable level of the methodical error (0.1 % for scale factors and 0.1 deg. of arc for non-orthogonality and orientation angles) was achieved. The detailed scope of the difference signals has also revealed a possible asynchronism in the magnetometers' records. Then, it is highly advisable to check independently the synchronisation accuracy of the observatory magnetometer, introduce the time shift corrections and repeat computations presented above. In order to confirm the obtained estimations it is also desirable to repeat the described calibration procedure more carefully calibrating the compensator scale factors of the reference magnetometer and pointing its sensor as precise as possible. For solving these tasks we intend to keep the reference instrument inside the Calibration Coils during the record period and to repeat calibration after this interval.

6. ACKNOWLEDGEMENT

Authors express sincere gratitude to the IAGA 2012 Workshop organizers for the financial support.

REFERENCES

Marusenkov A., A. Chambodout, J.-J. Schott, V. Korepanov (2011): "Observatory Magnetometer In-Situ Calibration". *Data Science Journal*, **10**, 102-108.

Nielsen, M.O. (2005): "Semiparametric estimation in time-series regression with long-range dependence". *Journal of Time Series Analysis*, **26**, 279 – 304.

Pajunpaa K. (2007): "Accredited Vector Magnetometer Calibration Facility". *Geophysica*, **43**, 59 – 76.

PREPARATION OF QUASI-DEFINITIVE (QD) DATA FOR THE OBSERVATORIES NARSARSUAQ, QEQERTARSUAQ AND TRISTAN DA CUNHA

J. Matzka [(1)]

[(1)] DTU Space, Elektrovej 327, DK-2800 Kgs. Lyngby, Denmark, jrgm@space.dtu.dk

SUMMARY

On a monthly basis, DTU Space is preparing quasi-definitive (QD) data for three of its geomagnetic observatories: Narsarsuaq (NAQ) and Qeqertarsuaq (GDH) in Greenland and Tristan da Cunha (TDC) in the South Atlantic Ocean. The data processing is based on a near-real time data stream of 1-Hz samples from a FGE variometer and usually 2 absolute measurements per week. The QD-data prepared so far is identical to the definitive data in terms of visual quality control, including despiking and removing of artificially disturbed data. Thus, all data processing is already performed for the QD-data, with the exception of a minor baseline-revision when preparing the definitive data. For TDC, the QD-baselines are expected to be within 1 nT of the definitive baselines, and similar results are achieved for the observatories in Greenland. This article describes the scheme implemented for calculating the QD-data at DTU Space and the experience we have made with the processing of this data type. The scheme is rather simple and does not add significantly to the operational workload, it rather brings certain tasks forward in time.

1. INTRODUCTION

INTERMAGNET (St-Louis, 2011) has introduced a new data-type to support dissemination of high quality geomagnetic observatory minute mean value data with a time lag of months rather than years, in order to match the time lag of satellite derived geomagnetic data. The main motivation is to provide timely observatory data in parallel to the European Space Agency's Swarm satellite mission (Friis-Christensen, 2006). The data type is called quasi-definitive, and here it is for convenience referred to as QD-data. The one-letter data type code is Q. Citing from St-Louis (2011; p. 63): "Quasi-definitive data are defined as data that have been corrected using provisional baselines. Processed soon after their acquisition, their accuracy is intended to be very close to that of an observatory's definitive data product. 98% of the differences between quasi-definitive and definitive data (X, Y, Z) monthly mean values should be less than 5nT."

QD-data processing at Institute de Physique du Globe de Paris (IPGP) and British Geological Survey (BGS) were presented by Chulliat et al. (2009) and Baillie et al. (2009). The IPGP method is also described in Peltier and Chulliat (2010).

In 2012, DTU Space started to prepare this data type for three of its geomagnetic observatories: Narsarsuaq (NAQ) and Qeqertarsuaq (GDH) in Greenland and Tristan da Cunha (TDC) in the South Atlantic Ocean. These are the observatories, for which the 1-second sample stream intended for definitive data production is available in near-real time. No QD-data is prepared for the geomagnetic observatory Qaanaaq (THL), where currently near-real time data transmission is based on a 1-Hz sample stream and definitive data production is based on 20-second means derived from another data logger. Neither is it prepared for Brorfelde (BFE), where the horizontal component is artificially disturbed by up to 6 nT and the vertical component by up to 3 nT (Fox Maule et al., 2009). For NAQ, QD-data is prepared monthly since September 2012, after a major maintenance visit, and starts on March 12, 2012, after a major temperature instability. For NAQ, definitive data is available until 2008. For GDH, QD-data is prepared monthly since May 2012, and starts from January 2012, while definitive data is available until 2011 (with a gap for 2007 and 2008). For TDC, QD-data is prepared monthly since May 2012 and starts on January 2011. Definitive data is available until December 2011. Therefore, TDC allows for a comparison between QD-data and definitive data for the year 2011. In principle, a temperature dependency of the variometer sensor and/or electronics can be compensated mathematically in the programs used for processing. However, no temperature correction was applied to the data discussed here.

2. METHOD FOR QD-DATA PROCESSING AT DTU SPACE

Following the nomenclature introduced by Peltier and Chulliat (2010), the DTU Space method involves these three steps: (1) preprocessing of the variation data from month M, (2) calculation of the temporary baseline for month M, and (3) calculation and validation of the baseline-corrected data for month M. Here, we denote the start time of month M by t_M and the start time of month M+1 by t_{M+1}. We consider four types of baselines: measured baselines ($H0^{meas}$, $D0^{meas}$, $Z0^{meas}$), preliminary baselines ($H0^{prel}$, $D0^{prel}$, $Z0^{prel}$), QD-baselines ($H0^{QD}$, $D0^{QD}$, $Z0^{QD}$), and definitive baselines ($H0^{def}$, $D0^{def}$, $Z0^{def}$) for the horizontal component H, magnetic declination D and vertical component Z. Our baseline adoption method is identical for all three components and we use B0 (pronounce 'b-zero') to denote a baseline irrespectively of the component in question.

Step (1) is typically performed weekly, but latest around day 7 of month M+1. It involves visual check of daily plots of the 1-Hz variometer samples and of first differences of the 1 Hz samples with a graphical user interface programmed under Matlab. Spikes larger than 1 nT, most conveniently seen in the first differences, are replaced by missing data code by using the graphical user interface. However, in the auroral zone in Greenland spikes of up to 10 nT (possibly 20 nT) could be masked by fast changes of the magnetic field under magnetically disturbed conditions. Artificially disturbed data is also removed. Identification of spikes and artificially disturbed data is facilitated by plotting differences between calibrated variometer data and absolute scalar data (only available for TDC), by plotting differences between collocated variometers, and by comparing first differences to those of neighbouring variometers (typically separated by 200 km).

Step (2) is typically performed around day 15 of month M+1, when usually two sets (with two absolute measurements each) are available for NAQ and GDH and one set of absolutes is available for TDC. At that time, $B0^{QD}(t_M)$ is known and $B0^{QD}(t)$ for $t_M < t \leq t_{M+1}$ has to be adopted. The adoption process is very simple and entirely controlled by an operator: a number N of linear segments are visually fitted to the measured baselines. The operator visually checks a plot of the measured baselines versus time, and decides on the number N of linear segments to be used and the starting and end point for each segment. The first segment starts at t_M and Nth segment stops at t_{M+1}. In practical terms, for N segments the operator defines N points in times and N values for $B0^{QD}$ and adds these to a 'linear segment table' with existing $B0^{def}$ and $B0^{QD}$ values for the respective component. A program is then creating a 'adopted baseline table' very similar to that in Intermagnet BLV-files, i.e. containing all three components, however with much higher time resolution and 0.02 nT baseline resolution.

In step (3) the 'adopted baseline table' is used to calculate baseline-corrected data (or, in our terminology, absolute data) from the variometer data. The 1-Hz samples are filtered to minute means and are saved as QD-data in IAGA-2002 files and Intermagnet IAF-files (i.e. binary files usually used for definitive data). For validation, a program is reading absolute values from all absolute measurements of month M and then calculates differences to the minute means absolute data in the IAF-files. In this way, the final QD-data product calculated from the variometer and the adopted baseline is directly compared to the original absolute measurement with theodolite and scalar magnetometer. In this way, we can check for any errors introduced in the data processing. In order to make this test, absolute measurements performed at DTU Space observatories are designed such that the absolute values of the geomagnetic field can be determined for one defined point in time (chosen to be at the top of the minute at the start of the absolute measurements). In contrast, other frequently used schemes for absolute measurements only allow to calculate a mean value for D over the times used for declination measurement and a mean for H and Z over the times used for inclination measurements. Our scheme allows for more direct comparison to the Intermagnet minute means, which are also centred on the top of the minute.

3. COMPARISON OF QD- AND DEFINITVE DATA

Only for TDC we have an overlapping period (the year 2011) for QD-data and definitive data. However, the QD-baselines for the observatories in Greenland are of comparable quality. Figure 1 shows all available measured baselines, adopted QD-data baselines and adopted baselines for TDC from February 2011 to the time of writing (November 2012). Baselines for January are omitted for convenience, because on January 31st, 2011, the FGE variometer electronics at TDC was shifted, leading to a significant jump in the baseline of H and Z. The measured baselines in Fig. 1 show a scatter of about 2 nT for H0meas and D0meas, while Z0meas has a scatter of about 1 nT. The drift of the baseline is about 3 nT for $H0^{meas}$ and $D0^{meas}$, and about 2 nT for $Z0^{meas}$ in the whole period. The difference between $H0^{QD}$ and $H0^{def}$, as well as the difference between $D0^{QD}$ and $D0^{def}$, is below 1 nT. The difference between $Z0^{QD}$ and $Z0^{def}$ is below 0.5 nT.

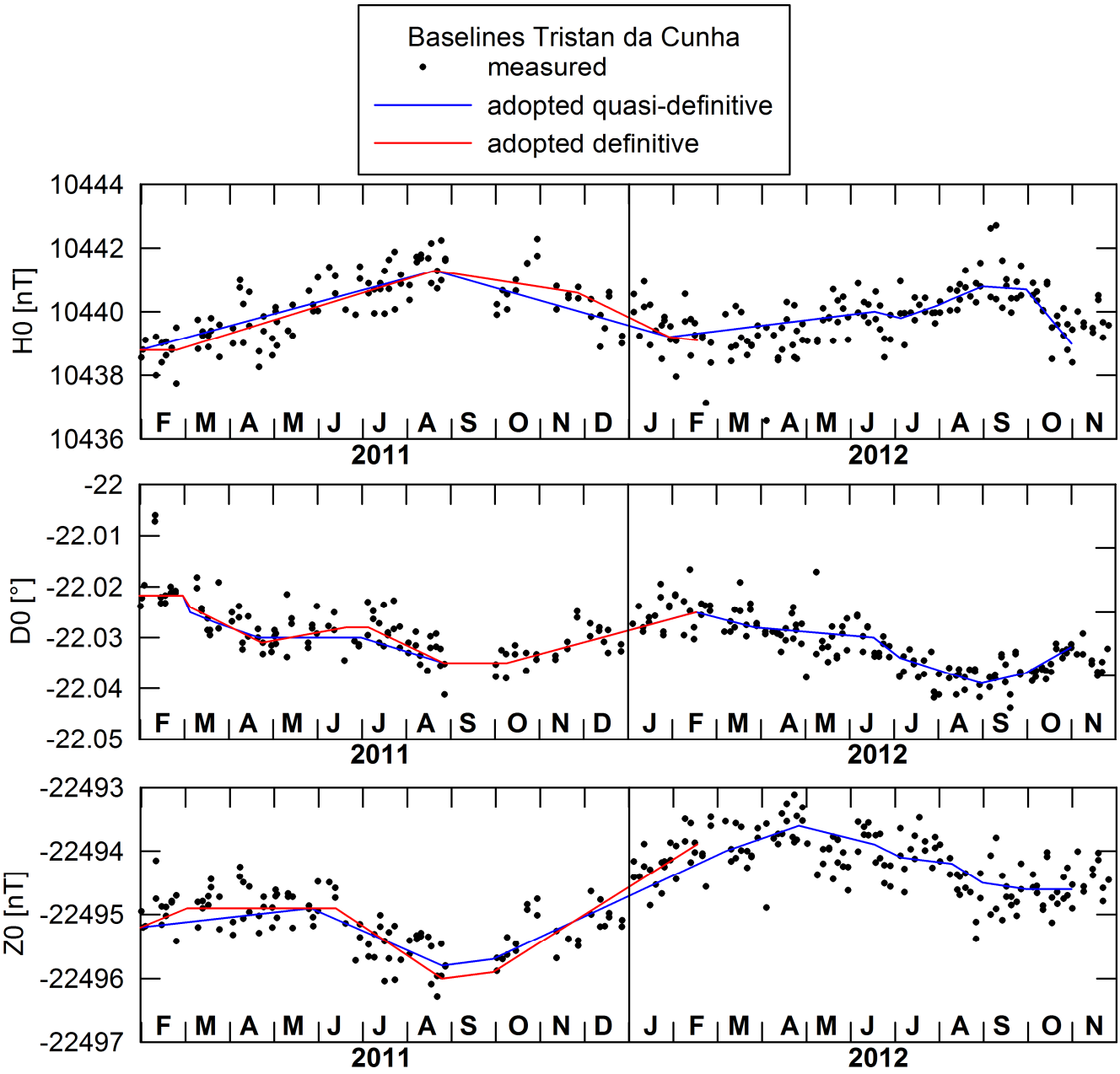

Figure 1 –Baselines for Tristan da Cunhafrom February 2011 to November 2012: measured (black dots), adopted for QD-data (blue line), adopted for definitive data (red line). Note that the scale for Z0 is two times larger than for H0 and D0 (0.01° corresponds to about 2 nT).

4. DISCUSSION

The comparison of QD-baselines and definitive baselines in Fig. 1 is not necessarily a significant measure for the quality of monthly processed QD-data since the QD-data was processed first in May 2012, when measured baselines were already available for the whole year of 2011 and part of 2012. However, comparing monthly processed QD-baselines from May 2012 onwards (for which no knowledge on the future development of the baselines was available at the time of processing) with the measured baselines clearly indicates that a similar good agreement of QD-baselines and definitive baselines can be expected.

The presented baseline adoption technique is very simple, and applying a smooth curve (polynomial or spline) for baseline adoption would be a physically more appropriate approximation for a process like instrument drift. However, the length of each linear segment can be chosen freely and can be shortened to better fit the measured baselines and to avoid strong kinks in the function that represents the adopted baselines.

An important experience from operating remote geomagnetic observatories over the last years is that it is advisable to have only one data stream to work with. In previous years, for example, we had at each observatory real-time data from a logger with real-time capability but

with no back-up in case of data loss. Definitive data however was produced from another type of logger with back-system, leading to significantly less data gaps. Any work on the real-time data stream (e.g. repeated download from the remote system of data, that got lost during transmission; visual control; despiking; baseline calculation and adoption) had to be duplicated for the real time and definitive data stream. Also, in our experience, 1-Hz samples are much more efficient for despiking and general visual data control than 1-minute means. Therefore, we have deliberately chosen to process QD-data only for observatories for which we have fast access to the data that will be used for the definitive data, and for which this data is available as 1-Hz samples. The geomagnetic observatory Qaanaaq (THL) is currently being re-equipped to fulfil these conditions and it is planned to process QD data for THL from 2013.

We conclude that processing of QD-data can be a simple task, leading to an excellent data product on a monthly rather than yearly basis. For an observatory with stable variometer, that is operated in a period without major technical changes, the monthly QD-data can easily be within 1 nT of the definitive data. This is expected to be satisfactory for secular variation studies based on monthly means. From this angle, Intermagnet's requirement for QD-data to be within 5 nT from the definitive data seems to be easy to outperform.

5. ACKNOWLEDGEMENT

I would like to thank Anni Dahl, Robin Repetto, Jason Green and the Ice Patrol in Greenland for their diligent absolute measurements and care for the observatories.

6. REFERENCES

Baillie, O., E. Clarke, S. Flower, S. Reay and C. Turbitt (2009):" Reporting quasi-definitive observatory data in near real-time". Presentation at the 11th IAGA Assembly, Sopron, 24th August 2009, unpublished.

Chulliat, A., A. Peltier, F. Truong and D. Fouassier (2009) Proposal for a new observatory data product: quasi-definitive data. Presentation at the 11th IAGA Assembly, Sopron, 24th August 2009, unpublished.

Fox Maule, C., P. Thejll, A. Neska, J. Matzka, L.W. Pedersen and A. Nilsson (2009) "Analyzing and correcting for contaminating magnetic fields at the Brorfelde geomagnetic observatory due to high voltage DC power lines". Earth Planets Space, **61**, 1233 – 1241.

Friis-Christensen, E., H. Lühr and G. Hulot (2006) "Swarm: a constellation to study the Earth's magnetic field". Earth Planets Space **58**, 351–358.

Peltier, A. and A. Chulliat (2010): "On the feasibility of promptly producing qusai-definitive magnetic observatory data". Earth Planets Space, **62**,e5-e8.

St-Louis, B. (2011): "Intermagnet Technical Reference Manual, Version 4.5". Intermagnet, www.intermagnet.org.

GEOMAGNETIC DATA ACQUISITION SYSTEM DEVELOPED FOR THE PLASMON PROJECT

L. Merényi [(1)], B. Heilig [(1)], L. Szabados [(1)]

[(1)] Geological and Geophysical Institute of Hungary, H-1143 Stefánia út 14, Budapest, Hungary, merenyi.laszlo@mfgi.hu

SUMMARY

PLASMON is a global collaboration of 11 institutions, funded by the EU (FP7-SPACE), addressing near real-time monitoring of the state of the plasmasphere based on ground VLF and ULF wave observations. A geomagnetic data acquisition (DAQ) system has been developed in Geological and Geophysical Institute of Hungary to fulfill the requirements of the ULF pulsation stations of the PLASMON project. Hardware elements of the DAQ include fluxgate magnetometer, A/D converter, additional data acquisition electronics, embedded computers, GPS unit and power supply unit. The DAQ software incorporates a DOS program used as a real-time interface towards the A/D converter, and a Linux system with a graphical data acquisition program and networking scripts. In this paper we present the hardware and software elements, and some test results related to the estimated noise of the A/D converter and settling time of the magnetometer.

1. INTRODUCTION

A geomagnetic data acquisition (DAQ) system has been developed to fulfill the requirements for ULF pulsation stations of the PLASMON project. In this system care has been taken to achieve high timing accuracy and to get high resolution, low noise magnetic data. Stable and robust operation, small size and very low power consumption were also critical design issues for a reliable system running at unmanned stations powered by solar PV panels. Linux was selected as the operating system for the main acquisition computer of the DAQ. Linux is a trusted and stable system that runs efficiently on low-power computers having limited computational power, memory and disk space. Moreover, Linux allows easy implementation of the networking functions required for automated quasi real-time data transfer and remote access. Four identical DAQ systems have been built and operated successfully in Tihany Observatory, Hungary and at other PLASMON sites.

2. HARDWARE AND SOFTWARE ELEMENTS

Figure 1 presents the schematics of the DAQ system. The magnetometer noise level should be low, below 10 pT at 1 Hz, moreover, the amplitude response of the magnetometer at the analogue output should be flat from DC to several Hz. Long term base-line stability and low temperature sensitivity – that are generally important factors for geomagnetic observatories – are less important for this application. Lawson Labs M250 type 23 bit A/D converter was selected for fast and low noise A/D conversion. Three input channels from the six 23 bit multiplexed channels are used to sample the fluxgate analogue output signals. The remaining three spare input channels can be used for additional recordings, such as temperature monitoring. The Lawson Labs M250 converter communicates with the host computer through the parallel (LPT) port. A PC/104 industrial computer running a DOS program (in a FreeDOS system) is interfaced between the A/D converter and the main acquisition computer. The task of this DOS computer is to realize the parallel port communication in real-time and to buffer the raw digitized data before it is retrieved and processed by the main computer.

For high accuracy timing, a micro-controller based device with a GPS module is used (“GPS electronics” in Figure 1). A Trimble LassenIQ type GPS module provides timing information in NMEA format messages; moreover, it outputs accurate Pulse-Per-Second (PPS) signals. The PPS output is wired to the M250 A/D converter trigger input to restart the A/D sampling every second. Between two PPS events, the sampling is based on the M250’s internal clock. The GPS electronics has a buffer to temporarily store GPS NMEA messages, PPS events and headers of data records from the A/D converter, coming through the DOS interface PC. All these data and events are time

stamped in the buffer by the electronics' internal clock. The data acquisition program on the main data acquisition computer periodically retrieves the contents of the GPS electronics buffer and the digitized raw data from the DOS program running on the PC/104 computer. GPS time stamps are then calculated for each digitized raw datum.

Both the PC/104 DOS computer and the main Linux computer are compact size XCore86 based computer systems, with onboard hardware watchdog function. Xcore86 (also called Vortex86MX) is an x86 compatible system-on-chip, with very low power consumption.

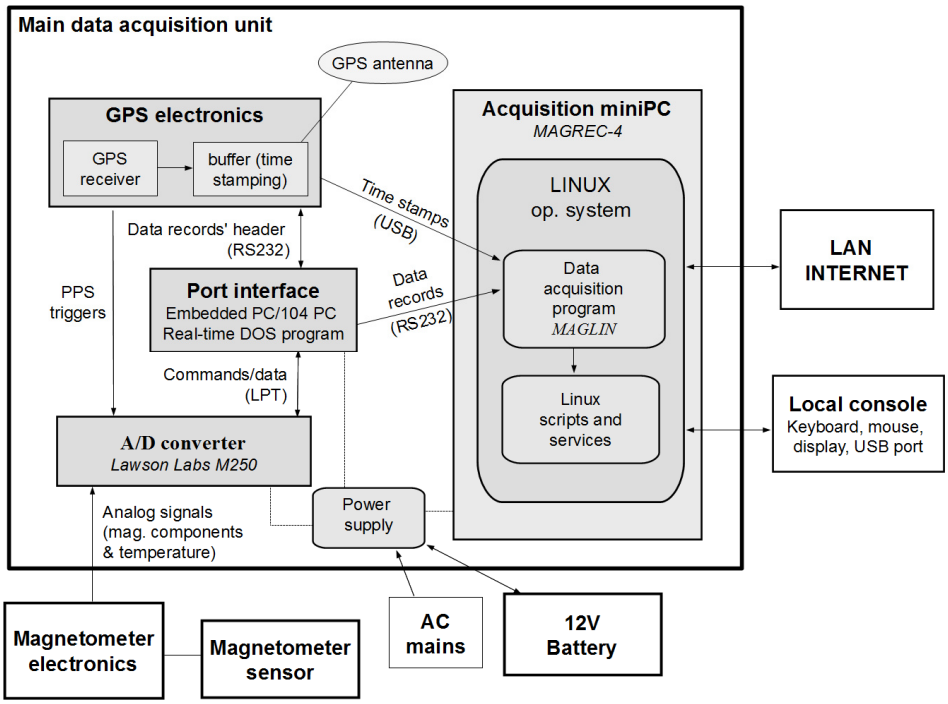

Figure 1 –Schematics of the data acquisition system

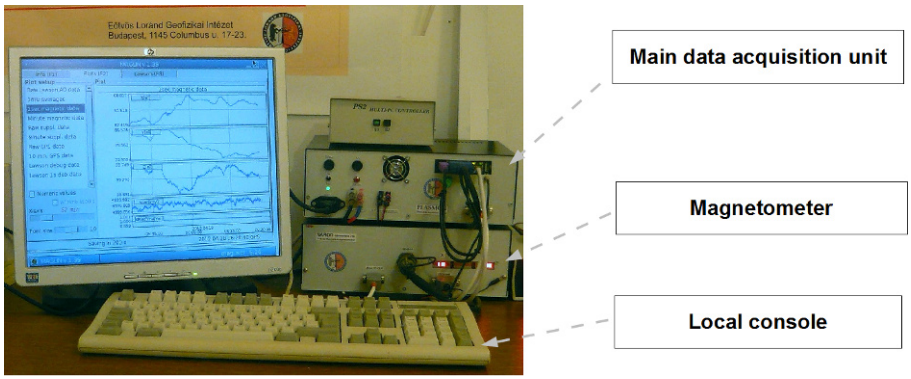

Figure 2 –Photo of a running system

An AC/DC power supply unit was designed and built to supply all DC power requirements of the hardware elements (+15Vdc, -15Vdc, +12Vdc, +5Vdc). Surge protection with varistors and transient suppressors on the AC line have been added. The measured overall power consumption of the DAQ system is 18.5 W when operated from 230 VAC, and 16-17 W when operated from 12 V battery. Automatic charging of a 12 V lead-acid battery (9- 55Ah) with over-discharge protection is possible. The system can automatically switch to battery operation in case of power outages. A solar cell (PV) driven version has also been built and is under test.

The raw sampling rate was chosen as 128 Hz. Time stamped raw samples are filtered in the data acquisiton program by two subsequent digital Gaussian filters. The first filter has a flat response up to 3 Hz (16 Hz data product), while the second filter used to produce the 1 Hz data cuts off at 0.25 Hz. The filters have zero phase shift.

The MAGLIN data acquisition program is used in the main data acquisiton computer. MAGLIN is a graphical program designed for continuous, long term data acquisition. It features modular acquisition configuration, one or more different instruments with one or more

components can be added to the system. MAGLIN can calculate arithmetic averages or filtered values with user selectable averaging windows and user defined filter coefficients. MAGLIN not only saves, but also plots raw data, filtered/averaged data and GPS timing and positional information data in different time scales. This helps the operator to check the system either on the local console or through a remote access connection.

3. FILE STORAGE AND NETWORKING

1 Hz filtered data, and optionally also the 16 Hz filtered data and raw 128 Hz data are saved in compact binary format files using a simple compression algorithm. Then gzip compression is applied to these binary files to further reduce file size. Using the compact binary format and gzip in sequence performs better than applying zip compression to simple binary or text files. 1 Hz data files are automatically sent to PLASMON's server every 5 or 10 minutes, using FTP and/or SFTP protocol. {Comment: Perhaps information on the average compressed size of a file could be included here?} The high file-size reduction rate with the double-compression has been found very beneficial when files are transferred from stations having a limited network connection (slow bandwidth and/or limited total monthly amount of data, typical of mobile Internet network services). Files are also archived locally on the main flash disk of the data acquisition computer. Oldest data files are automatically deleted when disk space goes too low. Disk space is sufficient to store at least 1 year of 1 Hz data files.

The automated file transfer works for stations having Internet services with either a static or dynamic IP address. However, sometimes it is neccessary to log in to stations for manual system checks and for making configuration changes and remote login is generally not possible for stations with a dynamic IP address. To overcome this limitation we intend to update the Linux system and implement a remote access service supporting connections to computers with a dynamic public IP address.

4. SOME TEST RESULTS

The measured time delay of the whole system with a LEMI magnetometer is about 32 ms in the frequency range of interest. The error of this delay estimation is about 1-2 ms, probably due to the timing errors of emitted magnetic signals. According to comparison of different tests, the delay is probably due mainly to the magnetometer. The 32 ms delay corresponds to approximately four samples (31.25 ms) of the raw data, and hence could easily be corrected with a simple shift of the filter. However, since this small delay causes only 2° phase delay in a 200 mHz signal (and even less at lower frequencies) we decided not to correct the data for this delay. The delay will be added to the time-stamps instead. {Comment: I find this sentence confusing, you decide not to correct for the time delay, but then state “The delay will be added to the time-labels”?} The other reason for not correcting the data is that a known time delay (supposing linear phase delay) can easily be corrected for during data processing if required..

Noise on the A/D converter was evaluated by measuring zero voltage on shorted analog inputs. Noise on raw 128 Hz data were examined in windows containing 100 samples. Noise on 1 Hz filtered data (produced by the two subsequent digital Gaussian filters) were also examined, in 30 seconds wide windows. Typical (average) noise on raw 128 Hz data is 8.9 μV_{RMS}, and noise on the 1 Hz filtered data is about 1.4 μV_{RMS}. Typical (average) peak-to-peak noise is 44.5 μV and 4.0 μV for raw 128 Hz and filtered 1 Hz data respectively.

5. ACKNOWLEDGEMENT

The research leading to these results has received funding from the European Union Seventh Framework Programme (FP7/2007-2013) under grant agreement no 263218.

6. REFERENCES

PLASMON FP7-Space project: A new, ground based data-assimilative model of the Earth’s Pasmasphere – a critical contribution to Radiation Belt modeling for Space Weather purposes. http://plasmon.elte.hu

J. Lichtenberger, M. Clilverd, B. Heilig, M. Vellante, J. Manninen, C. Rodger, A. Collier, A. Jørgensen, J. Reda, R. Holzworth, and R. Friedel (2012) First results on plasmasphere in PLASMON project, (submitted to Journal of Space Weather and Space Climate)

MODERNIZING OF THE NURMIJÄRVI MAGNETOMETER CALIBRATION SYSTEM

K. Pajunpää [(1)], E. Klymovych [(2)], J. Rynö[(1)], A. Prystaj [(2)]

[(1)] Finnish Meteorological Institute, Nurmijärvi Geophysical Observatory, Observatoriontie 125, 05100 Röykkä, Finland, kari.pajunpaa@fmi.fi

[(2)] Lviv Centre of Institute of Space Research, 5-A Naukova str., 79000 Lviv, Ukraine, klimovich@isr.lviv.ua

SUMMARY

The three-component magnetometer calibration system at the Nurmijärvi Geophysical Observatory has served for calibration of satellite and geophysical magnetometers for couple of decades. This calibration system is the only known accredited by European metrological community what gives confidence to high reliability of its calibration results. The electronics that was made in 1990's suffered of out-of-date components and was therefore modernized in 2010-2011 by a joint team of Nurmijärvi Geophysical Observatory and Lviv Centre of Institute for Space Research.

The modernized system is based on electronic components that communicate through a local computer network. Computer dependent hardware is no more needed. The system components were carefully calibrated and the measurement uncertainty was estimated to further meet the requirements of the accreditation. The capability of the system and first calibrations results will be presented.

1. INTRODUCTION

The three-component coil system, following an article by Alldred and Scollar (1967), was built at the Nurmijärvi observatory in 1986. The coil system together with DC power sources and current meters was used manually until the middle of 1990's when automatic control and measuring system was built for magnetometer calibrations. The work was made in 1990's as well as in 2010-2011 in collaboration with the Lviv Centre of Institute of Space Physics. A quality system was built for the laboratory and the Finnish Accreditation Services accredited the magnetometer calibration (together with compass calibration and compass swing base measurement) in 2007 (Pajunpää et al. 2007).

The electronics of the calibration system was out-of-date few years ago. The computer had to have the ISA bus to accommodate a lab card with analog and digital connections for current control and measuring system etc. Such computers were no more available. Also other electronic components were more than 10 years old and had some other limitations. The architecture of the new system (Fig. 1) was built on units that are connected through the local network. The long analog connections were removed (except the electric current wires). Both current measuring system and the analog magnetometer have their own AD-converters.

The modernized electronics was ready at the end of 2010 and the software of the calibration system was up-dated in the spring 2011. Next the current measuring system and the AD-converter were calibrated and also the coil constants and magnetic directions of the coils were measured. The method guides were corrected for the new system and especially the estimate of the measurement uncertainty was calculated once again.

2. MEASUREMENT UNCERTAINTY ESTIMATION

The calibration laboratory has a program for internal calibrations of the various parts of the calibration system. These include calibration of current measurement, temperature drift of the current measuring resistors, AD-converters, coil constants and coil directions. The coil constants are approximately 42.40, 48.27 and 36.97*nT/mA* for X, Y and Z, respectively. The coil constant is a combination of the current measurement and the coil structure.

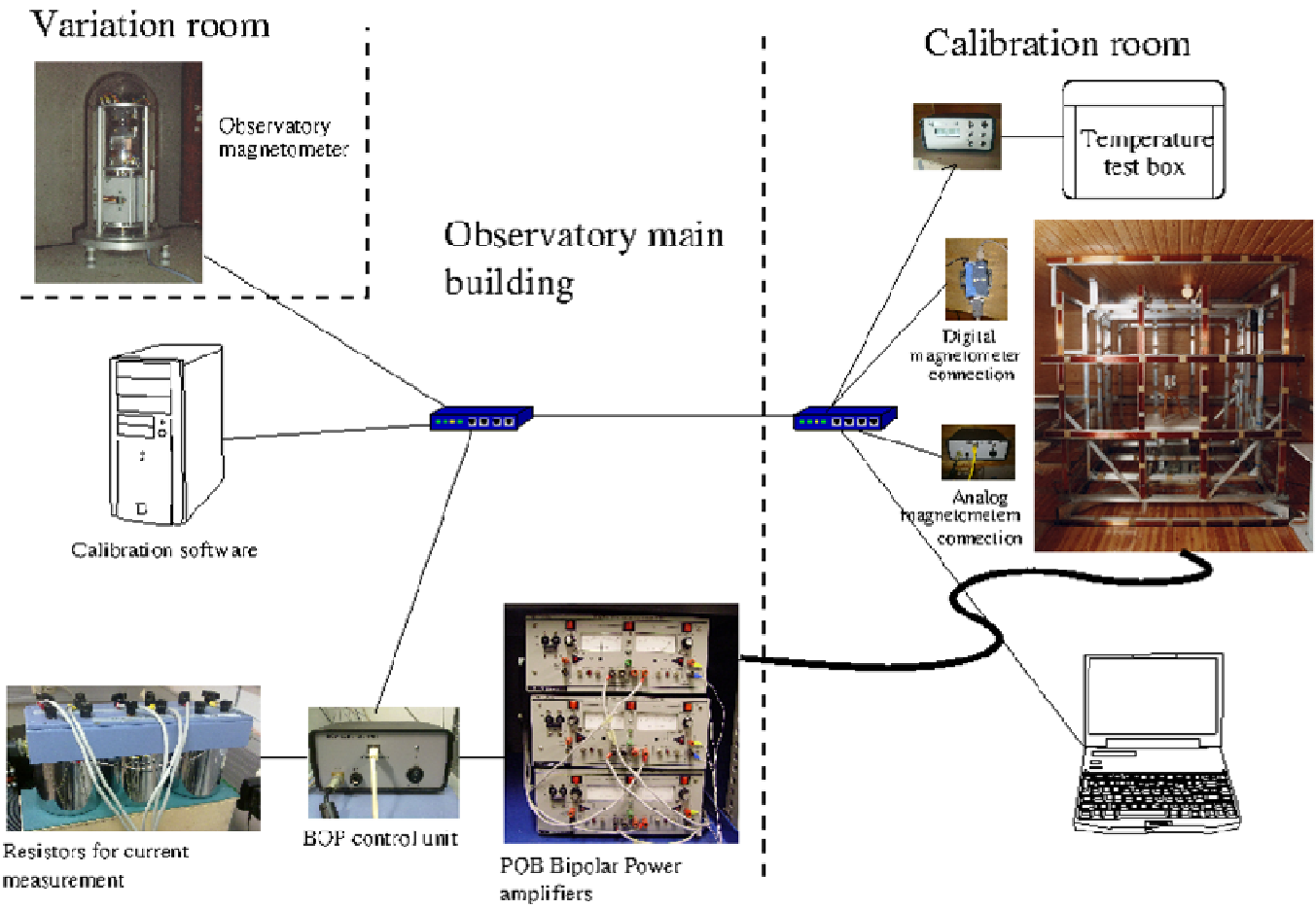

Figure 1 –The equipment and the local area network connections.

The angles between the magnetic directions of the orthogonal coils differ from 90° by less than half minute of arc. These angles are measured once in two years with the DI-fluxgate instrument. In 2012 the measurement gave the numbers: $X \leftrightarrow Y : 90°00'04"$; $X \leftrightarrow Z : 89°59'40"$; $Y \leftrightarrow Z : 90°00'12"$; $Z \rightarrow North : +10"$ and $Z \rightarrow East : +8"$. The positive direction of the Z is down and therefore the tilts are from down to North and East.

An electric multimeter, a thermometer and a 2*kHz* frequency transmitter are calibrated regularly at an external accredited laboratory. The frequency transmitter is used to calibrate the proton magnetometer. The trace for the magnetic direction measurement with the DI-fluxgate comes from the comparison measurements at the IAGA workshops and at the Nordic observatory meetings.

After all the calibrations the measurement uncertainty budget was calculated (Tables 1 and 2). The standard uncertainty of the scale value of an analogue magnetometer is about 0.01%. This value is multiplied by the coverage factor *k=2* to get the expanded standard uncertainty 0.02%. The best measurement capability is the expanded uncertainty of measurement, which for a normal distribution corresponds to a coverage probability of approximately 95%. The scope of accreditation can be found in the web page of the Finnish Accreditation Services: http://www.finas.fi/frameset.aspx?url=finas.aspx%3fpageID=0%26categoryID=2&langID=uk (Accredited bodies – Calibration laboratories – Magnetic quantities). The best measurement capability for the transfer functions of a magnetometer is ±(0.02% + 0.5*nT*) and for the angle measurements ±0.02°. The angles between magnetic and mechanical axes of a magnetometer can be measured with an optical orientation method. The best measurement capability for these angles is ±0.03°.

The fluxgate magnetometer LEMI-004-cle has been calibrated with the system many times in the years 2007 … 2012. Fig. 2 shows the results of these calibrations: transfer functions in the unit *nT/mV* and angles between the sensors in degrees. The two last calibrations are made with the modernized system. The results show that no change in the results occurred due to the modernization. The best measurement capability (0.02%) for the transfer functions would be ±0.0001*nT/mV* and for the angles ±0.02degrees. All the results are within the limits.

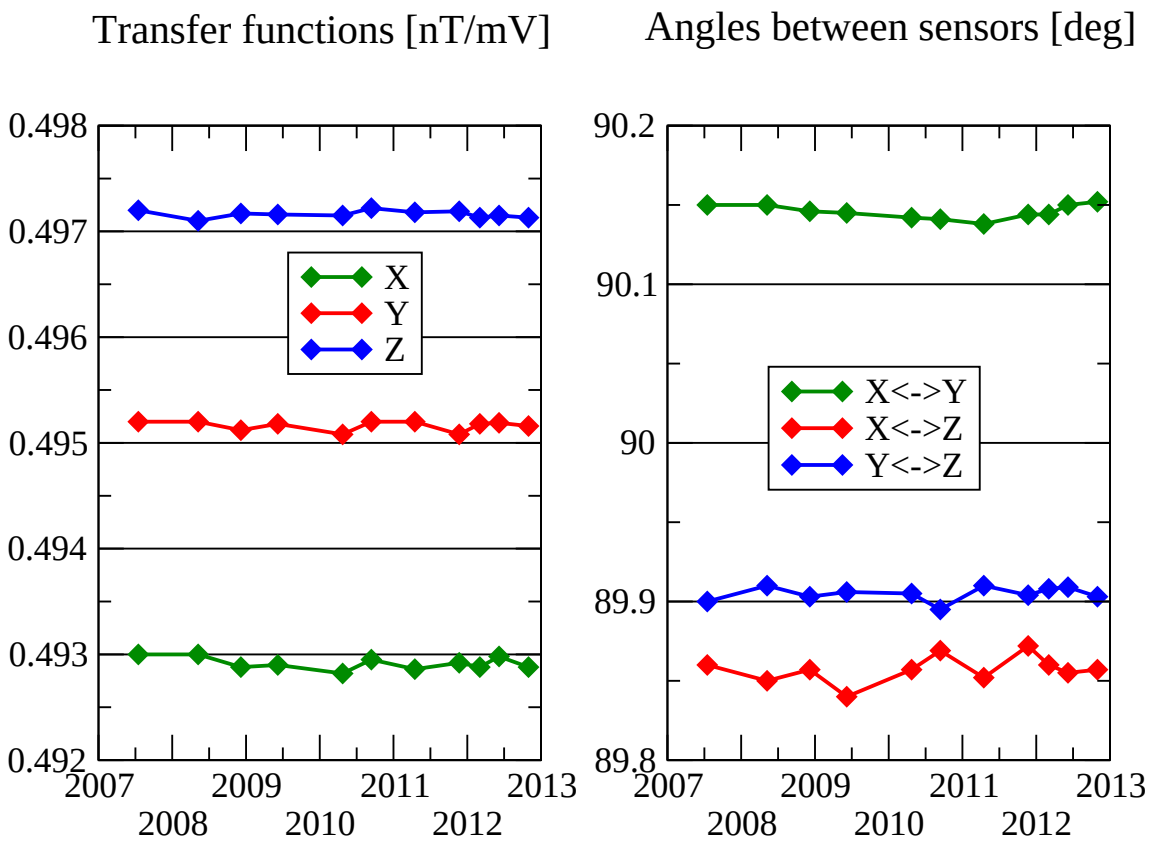

Figure 2 –Calibration results of the LEMI-004-cle fluxgate magnetometer at the Nurmijärvi observatory in 2007 … 2012.

Table 1 – The uncertainty budget for a transfer function measurement of an analog magnetometer.

Quantity **X-comp.**	**Estimate** x_i	**Standard Uncertainty** $u(x_i)$	**Probability distribution**	**Sensitivity coefficient** c_i	**Contribution to the standard uncertainty** $u_i(y)$
Coil current	$80\,mA$	$0.0039\ mA$	U-shape	$0.0063\ \frac{nT}{mVmA}$	$0.000025\frac{nT}{mV}$
Coil constant	$42.40\ \frac{nT}{mA}$	$0.00109\ \frac{nT}{mA}$	normal	$0.012\ \frac{mA}{mV}$	$0.000013\frac{nT}{mV}$
Magnetometer output voltage	$6784\,mV$	$0.23\ mV$	rectangular	$-0.00007\ \frac{nT}{mV^2}$	$-0.000016\frac{nT}{mV}$
Magnetic field	$3392\ nT$	$0.16\ nT$	normal	$0.00015\ \frac{1}{mV}$	$0.000024\frac{nT}{mV}$
Tranfer function	$0.5\,\frac{nT}{mV}$				$\pm\,0.000039\,\frac{nT}{mV}$ 0.0078%

Table 2 – The uncertainty budget for an angle measurement.

Quantity **X-comp.**	**Estimate** x_i	**Standard Uncertainty** $u(x_i)$	**Probability distribution**	**Sensitivity coefficient** c_i	**Contribution to the standard uncertainty** $u_i(y)$
D	90°	30"	rectangular	1	30"
C	90°	10"	normal	1	10"
α	90°				± 32"

3. OPERATION PRACTICE

The software of the calibration system was written in C++ and Tcl/Tk languages in a Linux computer. Analog or digital output of the tested magnetometer can be connected to the calibration system. A calibration is usually run in an automatic mode where the software chooses random coil currents in predefined ranges. Also a predefined file with current or magnetic field values can be run. The ranges of the three components can be around zero fields or around the Earth's field and their magnitude is usually somewhere between $\pm 1000nT$ and $\pm 50000nT$. In one measurement cycle the three currents, the three outputs of the tested magnetometer and the three temperatures of the current measuring resistors are measured. The number of measurement cycles can be limited or unlimeted (until stopped). The calibration can be performed in different (sensor) temperatures from $-20°C$ (dry ice) up to $+60°C$. The angles between the mechanical and the magnetic axes of the magnetometer sensor can be measured after an optical orientation of the sensor. A laser beam at a distance of $60m$ can be directed to a mirror that is attached to the sensor. The returning light beam is observed with a theodolite. The calibration result will be measured at the end of the calibration and can be calculated also always after a predifined number of observations .

4. MAGNETOMETER CALIBRATION RESULTS

We have calibrated magnetometers used in space, on the Earth's surface and underwater. As an example we show here result of a reacent calibration. The magnetometer had a sensor support with a mirror fixed to it. The sensor position was such that the X-component was towards North, Y to West and Z up. The optical method was used to adjust the mirror surface in orthogonal position to the laser light beam coming from the south axis of the coil system. The following angles between the components were observed: $X \leftrightarrow Y : 89.46° ; Y \leftrightarrow Z : 90.42°$ and $X \leftrightarrow Z : 90.40°$. The angles between the magnetic and mechanical axes of the magnetometer are in the Table 3.

Table 3 – Angles between magnetic and mechanical axes..

X-sensor [degrees]	Y-sensor [degrees]	Z-sensor [degrees]
$North \rightarrow West(Y)$	$West \rightarrow North(X)$	$Up \rightarrow North(X)$
+0.18	+0.36	+0.05
$X-Y-plane \rightarrow up(Z)$	$X-Y-plane \rightarrow up(Z)$	$Up \rightarrow West(Y)$
-0.46	+0.71	-1.12

The magnetometer was calibrated with up to 300 hundred measurements at varios field ranges (e.g. $\pm 5000nT$; $\pm 50000nT$ round zero fields). In the ranges random field values were generated. The observed transfer functions were 12.967, 13.060 and 12.803 nT/mV for X, Y and Z components. The standard deviations of the diffrences of the fields calculated from the coil currents and from the tested magnetometer output, were between about 1 and 2 nT.

5. CONCLUSIONS

The magnetometer calibration system of the Nurmijärvi Geophysical observatory was successfully modernized in 2010 ... 2011. The new system is based on units that are connected with the computer network and operated with the special calibration software. After carefull calibrations of the calibration system units the uncertainty estimate of the calibration was calculated and the Finnish Accreditation Service gave the permission to proceed accredited calibrations with the new system. The calibration results of the LEMI-004-cle magnetometer show the stability of the system.

6. REFERENCES

Alldred, J.C. and I. Scollar (1967): Square cross section coils for production of uniform magnetic fields ". *J. Sci. Instrum.*, **44**, 755-760.

Pajunpää, K., E. Klimovich, V. Korepanov, P. Posio, H. Nevanlinna, W. Schidt, M. Genzer, A.-M. Harri and A. Lourenco (2007): " Accredited vector magnetometer calibration facility ". *Geophysica*, **1-2**, 59-76.

DETECTION OF MECHANICAL INSTABILITY IN DI-FLUXGATE SENSORS

L.W. Pedersen [(1)], J. Matzka [(1)]

[(1)] Danish National Space Center, DTU Space, Elektrovej, Building 327 DK-2800, Kgs. Lyngby, Denmark, lawp@space.dtu.dk

SUMMARY

An important part of the declination-inclination (DI) measurement with the theodolite is to calculate the sensor parameters (horizontal and vertical misalignment, sensor offset). It is crucial to track these parameters over time, since the sensor has to be stable to give correct DI results. The Danish Meteorological Institute and now DTU Space have for many years produced DI-fluxgate electronics and used fluxgate sensors from Pandect. Some sensors were found to be unstable due to loose ferromagnetic cores inside, i.e., the vertical misalignment changes when the sensor is turned 'upside down' during the DI-measurement. We have found a way to glue the ferromagnetic cores within the new sensors to make them mechanically stable. All sensors are tested very carefully before being used. Since the observed erroneous sensor offset due to loose sensor usually is extremely high, we can use a fast method (called 'double offset') for a first check of the sensor. However, the definitive test of a sensor is the comparison of its offset measured in a zero-field chamber with the offset calculated from an absolute measurement.

1. DI-MEASUREMENT

A full DI-measurement with 4 positions for measuring declination (D), 4 positions for measuring inclination (I) and properly reading of azimuth marks will give the actual Earth magnetic field vector, helping to define variometer baselines, theodolite stability and sensor parameters (Lauridsen, 1985): Baselines: H0, D0 and Z0; magnetic field: D, I and F; azimuth mark angle; telescope misalignment; sensor scale factor; sensor offset: S0; horizontal sensor misalignment: ð or ð*H; vertical sensor misalignment: ε or ε*Z. Sensor offset is a combination of offset owing to the fluxgate sensor, cables and electronics. Sensor offset and misalignment can easily be plotted over time to keep track of changes.

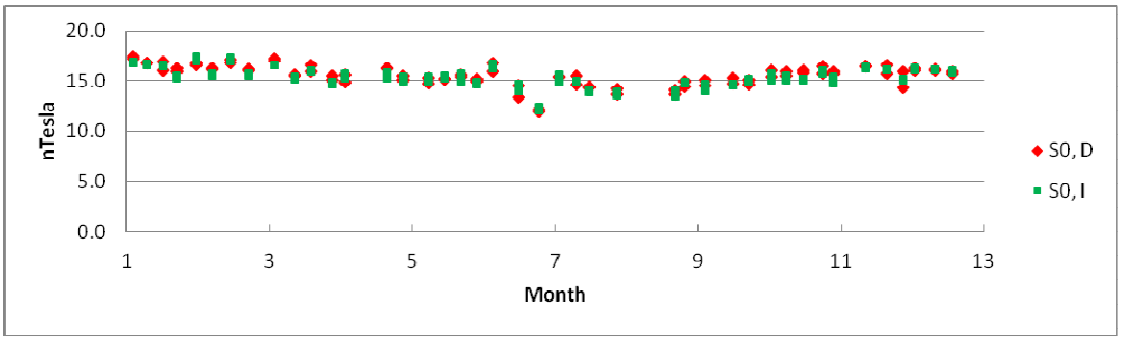

Figure 1 –Sensor offset S0 [nT] from D and I measurements, an example from Qaanaq (THL) observatory, Jan-Dec 2008.

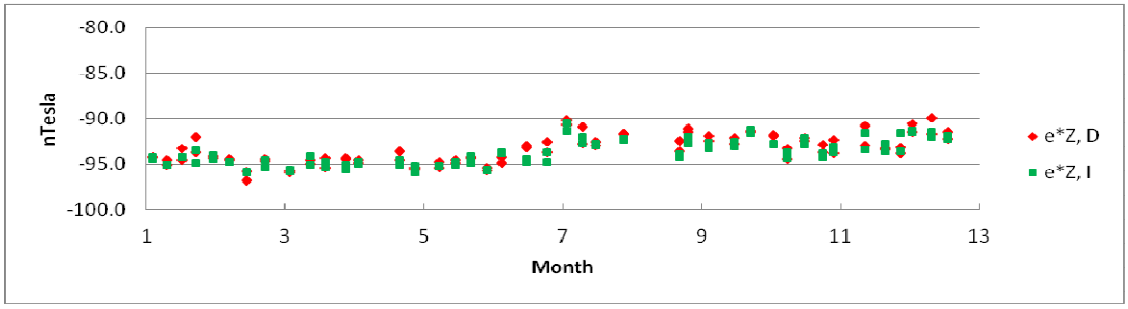

Figure 2 –Vertical misalignment ε*Z [nT] from D and I measurements. Qaanaq (THL) observatory Jan-Dec 2008

Figure 1 and 2 give an example of almost stable sensor offsets and misalignments from THL observatory in Northern Greenland.

The DI-measurement following the method described by Lauridsen (1985) is an absolute measurement and not a relative one like with the 3-axial variometer. But its accuracy can be affected by many factors.

- **Timing:** the time of the DI-readings should be synchronized with variometer and proton magnetometer readings to a few seconds to avoid effects of changes in the magnetic field.
- **Magnetic cleanliness:** If the theodolite or other parts around it are magnetic, they will affect the local magnetic field and measured angles will be wrong.
- **Stability:** If pillars, telescope, sensor or azimuth marks are not stable, this will affect the DI-measurement.

Often, only baselines are plotted and controlled, and errors from other sources may not be seen in the data, and the variometer will be assumed to be unstable, even though this might not be the case. By plotting DI-parameters over time it should be possible to judge on the stability of the theodolite and the fluxgate sensor.

2. THE UNSTABLE DI-SENSOR

The Pandect sensor LDC-A20 is a widely used fluxgate sensor for DI-measurements. During the last 20 years DTU Space and DMI have produced more than 150 DI-instruments using this sensor.

In 2005 Pandect Company probably has made changes in the production of the sensor. In later years, high scatter in misalignment data from DI-measurement was seen for some instruments, without identifying the reason. In 2008, we received a theodolite from the Geological Survey of Sweden (SGU) back for inspection (unit LYC) that gave unstable readings of the offset (Figure 3).

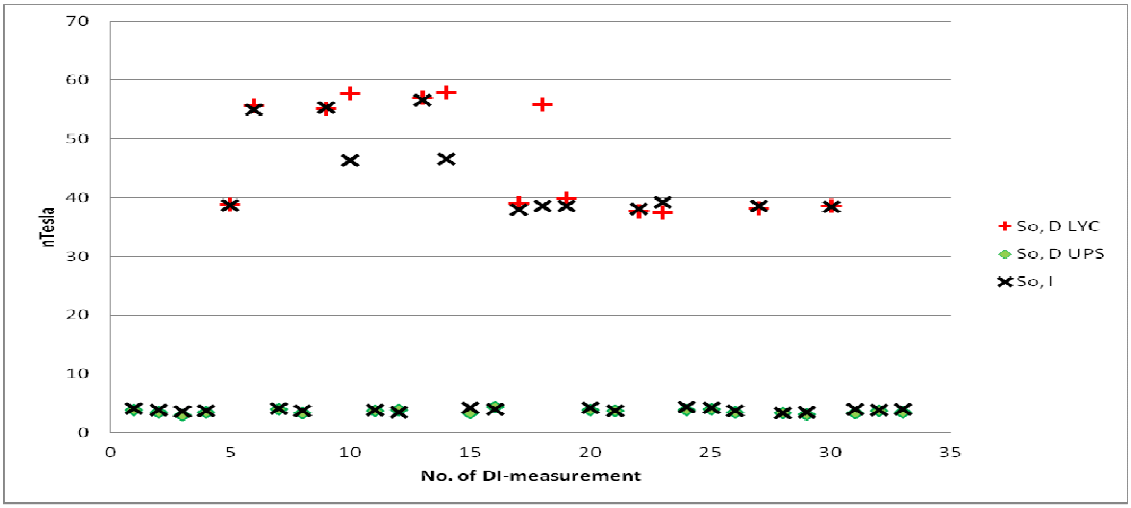

Figure 3 –Sensor offset S0 [nT], measured by SGU during 5 month in summer 2008 with the LYC and the UPS DI-fluxgate.

Large discrepancies were observed in data from the LYC–system itself compared to the ordinary UPS-system.

Measuring with the LYC theodolite, we found a big discrepancy between S0(D), the sensor offset from D measurement and S0(I), the sensor offset from I measurement and S0 measured in zero field. We recognized that the problem could be due to loose ferromagnetic cores, as we could move the end of the core sticking out of the sensor with a very thin nonmagnetic stick. When we did this test with the Earth magnetic field perpendicular to the sensor we saw a big change in the output signal. In zero field, we observed no changes. This test indicated that the moving core changed the misalignment of the sensor but not the sensor offset. In the next paragraph we will show that it is difficult to distinguish between offset error and misalignment error during absolute measurements.

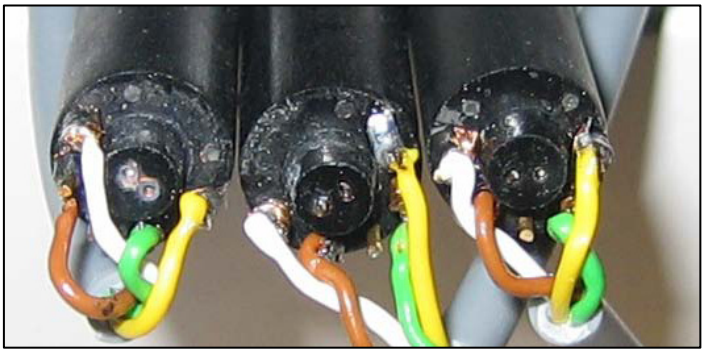

Picture 1 –Pandect sensors, in the middle of each sensor the 2 ferromagnetic cores can be seen.

Normally movements of the core in its tube are too small to be visible. But, we have observed this behaviour when rotating a sensor with loose core ‘upside down’.

3. DOUBLE OFFSET METHOD

Before discussing how to measure the effect of loose sensors, we will describe the method for measuring the offset in a fast way, so that it can be done many times on each sensor.

With the sensor mounted on a theodolite in position ’North-up’ and turned to position ’South-down’, the sensor offset can be measured. (Actually it works in all 4 I-positions.) As output, we get the residual that can be read on the display of the DI-electronics.

1: Adjust output to zero in position ’North-up’ Example:

Then the misalignment angle ε times F will be equal to the offset, i.e., **ε *F = S0**

Output = S0 – ε*F = 0 Output = 0.0nT

2: Turn precisely 180 degrees to position ’South-down’ Output = -6.2nT

The misalignment is now opposite, i.e., -ε *F:

Output = S0 + ε*F = **2*S0** (1)

S0 = output/2 S0 = -3.1nT

If the core is tilting at angle α, misalignment will be α+ε

Output = S0 + (α+ε) *F

Output = 2*S0 + α*F Output=-32nT

Offset, S = S0 + α/2 * F

Since the tilting angle α will vary over time depending on the handling of the telescope, the measured ’Double offset’ will change over time. The ’Double offset’ method can also be applied when changing from position ’South-down’ to ’North-up’, i.e., when the theodolite is turned back into starting position. It will then give a second reading of offset and sensor tilting.

4. REPAIR AND CONTROL OF SENSORS

Measurements show that cores are only loose at one end, here called the ‘top’. At the ’bottom’, the cores are glued by the producer, but not at the top to allow for temperature expansion. We now glue the core in the top with silicone in vacuum, so the silicone can penetrate into the thin tube. By using silicone and not a ’hard’ glue, we avoid mechanical stress in the cores and observe no temperature drift of the sensor output (offset).

After glueing we now control the sensors in the following ways:

- Each sensor is visually inspected under the microscope to check that cores are not loose.
- Sensors are placed in our ‘zero field’ cylinder and the offsets are measured to see stability over time.
- In the observatory sensors are mounted on a test theodolite, and offsets are measured using the ’Double offset’ method to see if cores are stable. The sensors are rotated 4 times in steps of 90 degrees during this test, with the label (showing the serial number) being oriented ‘text up’, text right’, ‘text down’ and ‘text left’.
- Accepted sensors and DI-electronics are combined and adjusted to low offset with the sensor in the zero-field chamber.
- A careful DI-measurement is made as a final test for each sensor and its electronics. If the ferromagnetic core is tilting when the telescope is inverted, this results in an erroneously high sensor offset. By comparing the sensor offset determined in zero field (true value) with a regular DI-measurement (erroneous value), loose ferromagnetic cores can be identified.

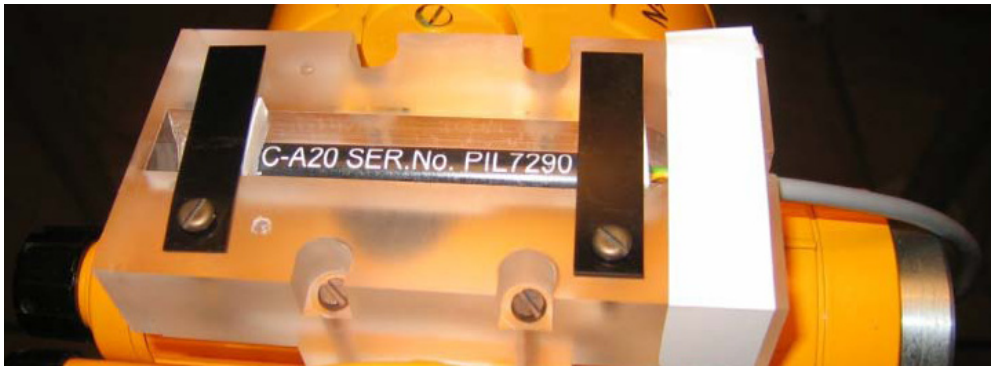

Picture 2 –Pandect sensor mounted in a cradle with nonmagnetic springs for fast replacement or rotation.

5. RESULTS

Table 1 –offset [nT] measured with 'Double offset' method

Sensor	Good /bad	Offset in zero-field		Measured 'Double offset', sensor is rotated into 4 positions					Half DO
No		start	end	0 degr.	90 degr.	180 degr.	270 degr.	360 degr.	mean/2
7365	/	-3.4	-3.6	-5.6	-5.5	-7.2	-5	-5.2	-2.9
7399	v	-4.9	-4.9	-8.1	-7.9	-8.3	-8.3	-8.0	-4.1
7400	v	-4.6	-4.4	-8.5	-7.1	-7.4	-8.4		-3.9
7401	v	1.8	1.9	5.0	3.5	4.5	3.8	4.5	2.1
7402	v	-3.8	-3.8	-7.1	-6.4	-6.1	-7.0		-3.3
7403	/	-1.9	-2.2	2.4	5.5	6.2	2.2		2.0
7406	v	-4.7	-4.7	-8.0	-8.1	-8.0	-7.9	-8.1	-4.0
7407	v	-2.7	-2.6	-5.7	-4.5	-6.6	-5.0		-2.7
7408	v	-6.4	-6.7	-9.8	-10.9	-9.4	-9.7		-5.0
7409	v	-4.2	-4.2	-8.2	-8.1	-8.8	-7.2		-4.0

Table 1 shows the offset from both good and bad sensors. The offset of sensor 7403 (bad sensor) is changing a lot (4 nT) when tested in different positions and in zero field. In the same way, we have measured 10 older sensors produced before 2005. They all deliver very stable results.

6. CONCLUSIONS

It is possible to repair most sensors with loose cores. With the described test routine, we can find all bad sensors. The 'Double offset' method is a quick but not a precise method to determine sensor offset without completing a full DI-measurement. The varying Earth magnetic field is not considered in this procedure. Therefore, measuring the offset has to be done fast to avoid errors in readings due to changing magnetic field. The adjustment of the angles of the theodolite has to be very precise, better than 2 seconds of arc.

For a conclusive test of the sensor, the sensor offset is measured in a zero-field chamber and calculated from a normal DI-measurement as well.

7. REFERENCES

Lauridsen, E.K., 1985. Experiences with the DI-fluxgate magnetometer. Geophysical Papers R-71. Danish Meteorological Institute, Copenhagen.

EXPERIENCES IN DESIGNING A LOW-COST TEMPERATURE CONTROLLED VARIOMETER ENCLOSURE

T. Shanahan [(1)], C. Turbitt [(1)], S. Flower [(1)]

[(1)] British Geological Survey, Murchison House, West Mains Road, Edinburgh, EH9 3LA, UK, tjgs@bgs.ac.uk

SUMMARY

Magnetic observatories have traditionally used small buildings or huts to provide stable and temperature controlled environments for housing sensitive magnetometer instruments. As magnetometer technology has developed, instruments have reduced in size and become less reliant on mechanical pier stability, whilst still relying on adequate temperature control. Temperature control in large, older, buildings can be challenging and expensive due to their volume, thermal losses and undefined thermal properties of construction materials. This report describes a modern instrument housing comprising a small-scale enclosure and low-power, non-magnetic heating element controlled by a proportional–integral–derivative (PID) temperature controller. Operating magnetometers in a compact environment requires careful selection of heating elements and minimising any sources of local interference. The specifications, thermal calculations, materials and temperature control system for the enclosure are presented with results of long term temperature stability and overall performance in comparison with traditional observatory housings. The disadvantages and benefits of operating instruments in small enclosures are also discussed.

1. INTRODUCTION

The British Geological Survey (BGS) operates three magnetic observatories in the UK and four overseas. The original observatory buildings were designed to accommodate larger instruments and as a result have become inefficient for housing modern instruments; Eskdalemuir observatory requires over 4 kW of heating to maintain the temperature in the building that houses the primary instrument.

The BGS operates Danish Technical University (DTU) FGE fluxgate magnetometers for all of its variometers. BGS has developed a new low-cost enclosure which is currently used to house backup variometer systems at Lerwick, Hartland and Eskdalemuir. This type of enclosure is also used at the recently re-established observatory on the island of South Georgia. To quantify performance of the new enclosure, a comparison was carried out between the primary variometer (GDAS1) at Lerwick (which continues to use the old-style of building for instruments) and the new enclosure that houses a backup variometer (GDAS2), for 2011 data. Design of the new enclosure focussed on minimising the volume and heating requirements whilst still ensuring a stable, magnetically clean and low-noise environment for long-term magnetic recordings.

2. CONSTRUCTION

The foundations for the enclosure are formed from a shallow raft (0.5 m) of non-magnetic concrete (all materials were tested for magnetic ‘hygiene’ before construction). This construction provides adequate stability, providing the fluxgate sensor has a tilt-compensation system. The enclosure is fabricated from a two-layer fibre-glass wall with a 15 mm polystyrene core of insulation. This combination gives the structure strength and durability whilst still remaining light enough to transport by hand. The inside walls and floor of the enclosure are clad with 75 mm, foil-backed polyurethane insulation panels to further reduce heat loss and all seams are sealed with silicone rubber to minimise heat loss through air exchange. The fluxgate electronics and heater are located at the opposite end of the enclosure from the sensor to reduce interference and promote a more stable temperature gradient across the sensor block. The fluxgate sensor is mounted directly on the concrete raft through a gap in the insulation to de-couple any wind vibration on the main structure from the instrument. The external dimensions of the enclosure are: Height: 1.5 m, Width: 1.0 m, Length: 2.0 m (tapered sides to reduce wind vibration).

3. THERMAL STABILITY

Given the simple construction and materials of the enclosure, it is possible to calculate the thermal loss characteristics of the system. The thermal characteristics are dominated by a combination of conductive and convective (air change) heat losses. Radiation losses are negligible due to the low emissivity foil on all inside surfaces. The rate of heat lost due to conduction (dQ_c/dt) is related to the material thermal conductivity (k), surface area (A), temperature gradient (ΔT) & material thickness (x) by equation 1. For a wall construction using a combination of different materials and thicknesses, a total thermal resistance (R-value) can be determined by combining the individual thermal resistance values for each layer of material (equation 2 & 3). The total thermal resistance of the enclosure walls and floor is summarised in Table 1 (the R-value for the insulation board was provided by the manufacturer's specifications).

$$\frac{dQ_c}{dt} = \frac{k_m A \Delta T}{x} \tag{1}$$

$$R_v = \frac{x}{k_m} \tag{2}$$

$$R_v = R_{v1} + \ldots + R_{vn} \tag{3}$$

Table 1 – Total Thermal Resistance Value

Material	**Usage**	**x (mm)**	**k_m (W/mK)**	**R_v (m^2K/W)**
Fibre-glass	Wall	03	0.040	0.075
Polystyrene	Wall	15	0.030	0.500
Fibre-glass	Wall	03	0.040	0.075
Insulation board	Wall & floor	75	-	3.450
Total walls:	-	*96*	-	*4.100*
Total floor:	-	*75*	-	*3.450*

The total thermal transmittance (Ut) for the enclosure construction is the reciprocal of the total thermal resistance (0.243 W/m2K and 0.290 W/m2K for the walls and floor respectively). The thermal transmittance values allow calculation of the combined conductive losses (equation 4). The heat lost via convection or natural ventilation (dQ_v/dt) is calculated (equation 5) as the rate of thermal energy lost due to air exchanges (N), for the volume of space being heated (V), volumetric heat capacity of air at 20 °C (C_v) and the temperature gradient (ΔT).

$$\frac{dQ_c}{dt} = U_t A \Delta T \tag{4}$$

$$\frac{dQ_v}{dt} = NVC_v \Delta T \tag{5}$$

Assuming a set-point temperature of 20 °C, winter external temperature of -10 °C, enclosure volume of approximately 3 m^3, wall area of 11 m^2, floor area of 2 m^2, C_v = 1.297 $kJ/m^3/K$ and a conservative 1 air exchange per hour (N), the total predicted thermal losses can be summarised in Table 2. A result of the low thermal losses (<140 W) is that a low-power heating system can be designed to run from lower voltages, simplifying many aspects of the enclosure design.

Table 2 – Total Thermal Losses at 20 °C Internal, -10 °C External

Loss Type	**Rate of Thermal Loss (W)**
Conductive (walls)	80.5
Conductive (floor)	17.4
Ventilation	32.4
Total:	130.3

4. HEATING ELEMENT

A non-magnetic and non-inductive heater is essential when the magnetometer and heater are in such close proximity. Sourcing commercial non-magnetic, low-voltage, heaters is a common problem so BGS chose to construct tailored heater elements specifically for this application. The heating element comprises four Vishay 50 W (56 Ohm) thick-film power resistors mounted in parallel on 1.3 °C/W anodised aluminium heat sinks. The heat sinks are then mounted in a standard 19" aluminium vented rack with all magnetic parts removed. The use of standard parts simplifies fabrication and future proofs availability of components whilst keeping the cost low. Powering the heating element at 48 VAC (RMS), produces a maximum power output of 160 Watts. The magnetic susceptibility of the heater is undetectable at distances > 0.5 m from the variometer sensor. This type of heater has proved to be very reliable over the long-term, having been operated at several of the BGS observatories without failure.

5. PID CONTROLLER

The enclosure temperature is regulated using a Eurotherm 2404 PID process controller. The controller proportions power to the non-magnetic heating element in the enclosure via a TE10S solid state relay (SSR), and step down (220 VAC to 48 VAC) transformer (Figure 1). The TE10S relay ensures zero-voltage switching to ensure that the supply is switched on and off at zero points in the AC cycle. Zero-voltage switching prevents harmonics of the supply frequency being generated (a common source of noise) and also extends the operating life of the heater element by reducing high-frequency currents. For optimal performance, the PID control parameters are tuned, on installation, to the operating environment and response time of the system. The Eurotherm 2404 does this using a tuning cycle that forces the temperature in the enclosure to oscillate, allowing it to determine the ideal PID settings [2]. The 48V AC supply is chosen for safety to provide Separated Extra Low Voltage (SELV) protection from electric shock [1]. SELV permits un-armored power cables, due to the low voltage and electrical isolation provided by the transformer. This relaxes the power cable specifications and prevents introducing magnetic contamination associated with steel armored cable.

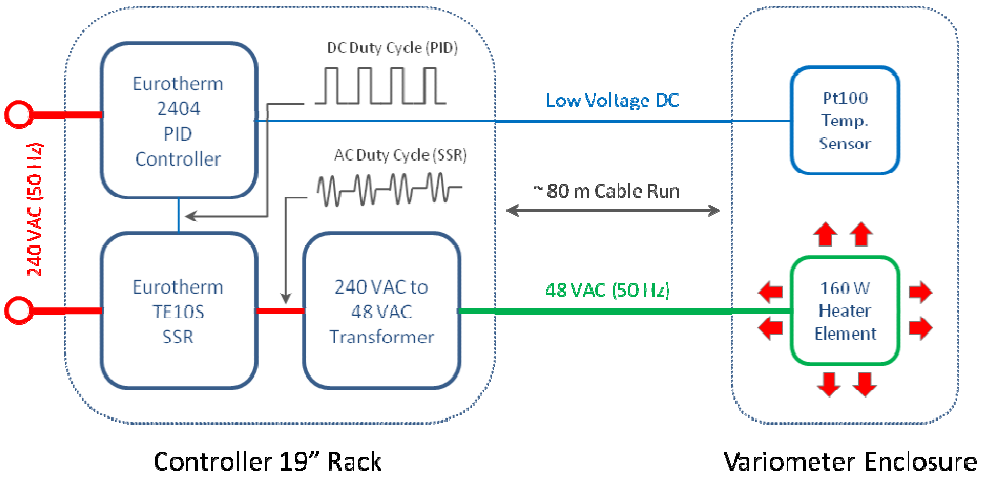

Figure 1 –Temperature Control System for Enclosure

6. PERFORMANCE

To assess the performance of the enclosure, both the short-term and long-term temperature stability of the system have to be considered. Figure 2 is a statistical view of the temperature stability of the new enclosure. The histogram shows that for 358 days of the year (98%) the temperature in the enclosure (1-minute samples) did not deviate by more than 1 °C from the chosen set-point. This was during a period where, the average external daily range was 4.2 °C and the maximum daily range was 11.0 °C.

To quantify the quality of the new variometer enclosure (GDAS2), a comparison of the final data was carried out using the primary recording system at Lerwick observatory (GDAS1), with the assumption that this is a low-noise and stable (temperature & baselines) reference system. Comparing the variometer data in this way gives a measure of the total system performance taking into account any possible sources of contamination, noise or instability of the new enclosure. Figures 3 show the final data quality of this system compares well to the primary system with over 95% of minute samples from 2011 differing by less than +/- 0.5 nT in the Horizontal (H) and Vertical (V) components and +/- 0.5 arc-mins in Declination (D).

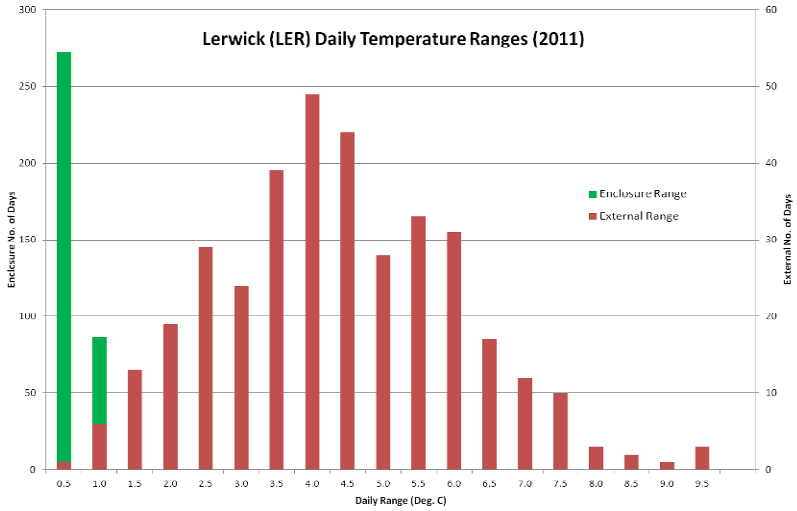

Figure 2 –Daily Temperature Stability of New Enclosure for Lerwick (2011)

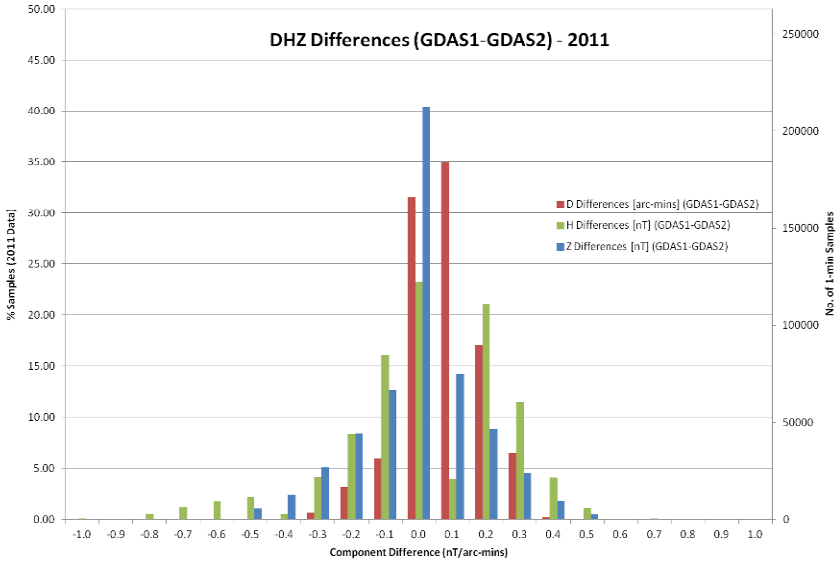

Figure 3 –Comparison of Primary & New Enclosure Variometer Systems for Lerwick (2011)

7. CONCLUSIONS

In general, tilt-compensated fluxgate sensors don't require pillars mounted on bedrock, and a shallow raft of concrete provides sufficient stability, reducing the cost and installation time. However, the concrete raft can be susceptible to excessive tilt in locations where the soil is particularly soft, and this was briefly seen at Lerwick when a fault developed with the sensor tilt-compensator; a situation that would not typically affect more traditional installations.

Experience from operating the temperature control system shows the PID controller typically drives the heating element with a duty cycle of between 30-60 % over most of the year and has always been able to deliver sufficient power over the coldest periods. This equates to 50-100 Watts nominal power consumption which agrees well with the modelled thermodynamic performance of the system and the observed temperature variations (external) for 2011 at Lerwick. Due to the low thermal mass of the enclosure, temperature over-ranging can occur in the summer, but this could be reduced by adding more thermal mass to the system by banking earth around the enclosure. The data quality analysis confirms that the low-cost enclosure successfully provides a low-noise environment for making high quality magnetic recordings and that any long-term temperature variations are being adequately removed by the baselines used to produce the final data.

8. REFERENCES

[1] British Standards Institute, The IEE. (2004): "Requirements for Electrical Installations". *Wiring Regulations 16th Edition (BS7671:2001).*

[2] Eurotherm. (2004): "Eurotherm 2404 Installation & Operation Handbook, Issue 10.0".

VARIOMETER USING A TEMPERATURE STABILIZED SENSOR

S. Suárez [(1)], M. Wiedemann [(1)], R. Kroth [(1)]

[(1)] Magson GmbH, Carl Scheele Strasse 14, 12489 Berlin, Germany, sandra.suarez@magson.de

SUMMARY

Avoiding thermal drifts can be achieved by using material with low thermal expansion coefficient or by keeping the sensor in a thermally stabilized environment. Since our sensor has a very low thermal capacity (consist of 25 g aluminium and copper only) the second option has been selected particularly for magnetic field measurements under harsh environmental conditions. The digital fluxgate technique permits a synchronised heating which allows the cancellation of magnetic stray field generated by the heater. The heater power is small due to the low mass and small volume of the sensor. The design is completed by the option to stabilize the electronics temperature as well. Furthermore the instrument has a network interface for remote controlling of heater and all other parameters as well as for analysing data online. The variometer has been compared with the observatory standard in San Fernando. Results of the tests will be presented.

1. INTRODUCTION

Temperature control of magnetometer sensors has been done for many applications. In geomagnetic observatories the whole variometer house is typically kept at constant temperatures. On board space missions only magnetometer sensors have to be heated because they are exposed to deep space and during eclipses it has to be ensured that some types of sensors not exceed a certain survival temperature.

We intent to combine those approaches and have tested a sensor for observatory applications equipped with a heater design developed for space missions.

2. SENSOR DESIGN

The magnetic field is measured by a vector compensated ringcore fluxgate sensor. The sensor consists of two crossed ringcores, three pick-up coils and a tri-axial Helmholtz coil system for field feedback. The field sensitive ringcores are kept always in zero field by the feedback system. This vector compensation allows the measurement of all three components of the magnetic field vector in the center of the sensor. Details of sensor design and data acquisition by the digital fluxgate technique can be found in Auster at al., 2008.

The stability of the offsets depends on the individual characteristics of the ringcores, whereas scale values and non-orthogonalities depend on stability of the feedback coil system. The isotropic design and the usage of material with very similar expansion coefficients (only copper and aluminum) ensures an extremely high axis stability (alteration < 0.02° total) and the possibility to use the sensor in a very large temperature range (-100°C…+200°C). However the temperature sensitivity of the scale value (depends on the expansion coefficient of the feedback system) is relatively high (17.5 ppm/°C +/- 1.5 ppm/°C) compared to sensors based on ceramic supports. Therefore a thermal control of the sensor seems to be obvious. The small mass (25 g only) and the small volume make a thermal isolation easily possible. Furthermore OSR's (second surface mirrors) are used to reflect the sunlight for the case that the sensor is directly exposed to the sunlight while passing through the infrared radiation (see Figure 1a). The sensor is accommodated in a water proven tripod. All screws for leveling are accessible from the topside to have the option for installing the sensor in a hole in the ground.

3. HEATING PHILOSOPHY

The sensor heating is performed by a DC current led through a Constantan wire which is twisted to minimize induced magnetic fields. The remaining field induced by the heater current (could be some nT) is compensated by switching the current direction symmetrically. This heater current is fully synchronized with excitation and signal acquisition. In our digital fluxgate electronics the field sensitive second harmonics (19.2 kHz) of the excitation signal is sampled in its maximum and minimum with 38.4 kHz. ADC data are

averaged over 5 ms before a new DAC value is set for adapting the feedback field. Positive and negative heater currents are applied within this 5 ms.

Figure 1a –Temperature stabilized sensor accommodated in a well isolated tripod for field applications.

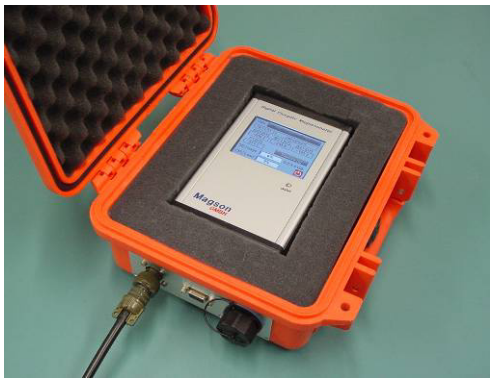

Figure 1b –Digital fluxgate electronics with touch screen and WEB interface. Can be thermally controlled as well.

During setting of heater currents and DAC values the ADC measurement is interrupted to avoid interferences on the measurement. Thus the data acquisition is arranged in 5 ms sequences with two interruptions in between, the longer one for switching heater and feedback and the shorter one for switching the heater only. Thus 5 ms is the fundamental period for a heating sequence and data acquisition sequence. Figure 2 shows the excitation signal, the ADC sampling and the heater current. In this example, the heater is active for two out of 256 heating sequences (two 5 ms periods with and 254 without heating). The DPU (Data Processing Unit) controls how often the heater is activated. Thus the number of heating sequences can be commanded from 0% (no heating) to 100% (heater activated at each 5 ms interval).

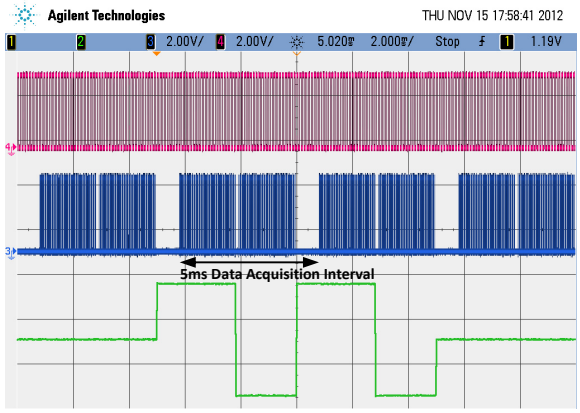

Figure 2 –Oscillogram of excitation (purple), ADC sampling (blue) and Heater current (green). Four 5 ms intervals are shown. The heater is activated during the second and third interval. Data sampling is done half during positive and half during negative heater current. During current switching the data acquisition is interrupted. During the longer interruptions the new feedback currents are set.

Although the digital fluxgate technique permits switching of the heater synchronously with the excitation, which allows a nearly perfect cancellation of magnetic stray field, heater disturbances up to 100 pT might remain e.g. due to different currents in positive and negative direction. Even those interferences can be removed mathematically during the internal calculation of the magnetic field value since timing of heating is exactly known.

Furthermore the electronics box is equipped with foil heaters. It is installed inside a water proof case which decouples the electronics box from the ambient temperature conditions and makes temperature control of the electronics possible (see Figure 1b). Tests show that the temperature for the electronics has to be set higher than the temperature of the sensor. Reasons are the internal power dissipation (which of course minimise the necessary heating power) and the less reflecting surface properties. In San Fernando the set temperature of 50°C was still too low. Directly illuminated by the southern sun it has been exceeded by 8°C at noon whereas the set temperature of 40°C was sufficient for the sensor. This proves the perfect thermal-optical properties of the sensor housing.

The temperature control of both, sensor and electronics is done by digital PID controllers. In Figure 3 the functionality of the control algorithm is shown. At t=0 the sensor heater was enabled with a setpoint temperature of 45°C. At an ambient temperature of 25°C it takes

about 1.5 h for getting stable conditions. When the setpoint temperature is reached, the stability of the temperature is less than 0.05°C. The offset drift over the temperature difference of 20 °C is between 0 nT (Y) and 2 nT (X and Z). Offset variation during heating due to instable temperature conditions is about 1nT in all components. The noise in all components is nearly independent from the heater power.

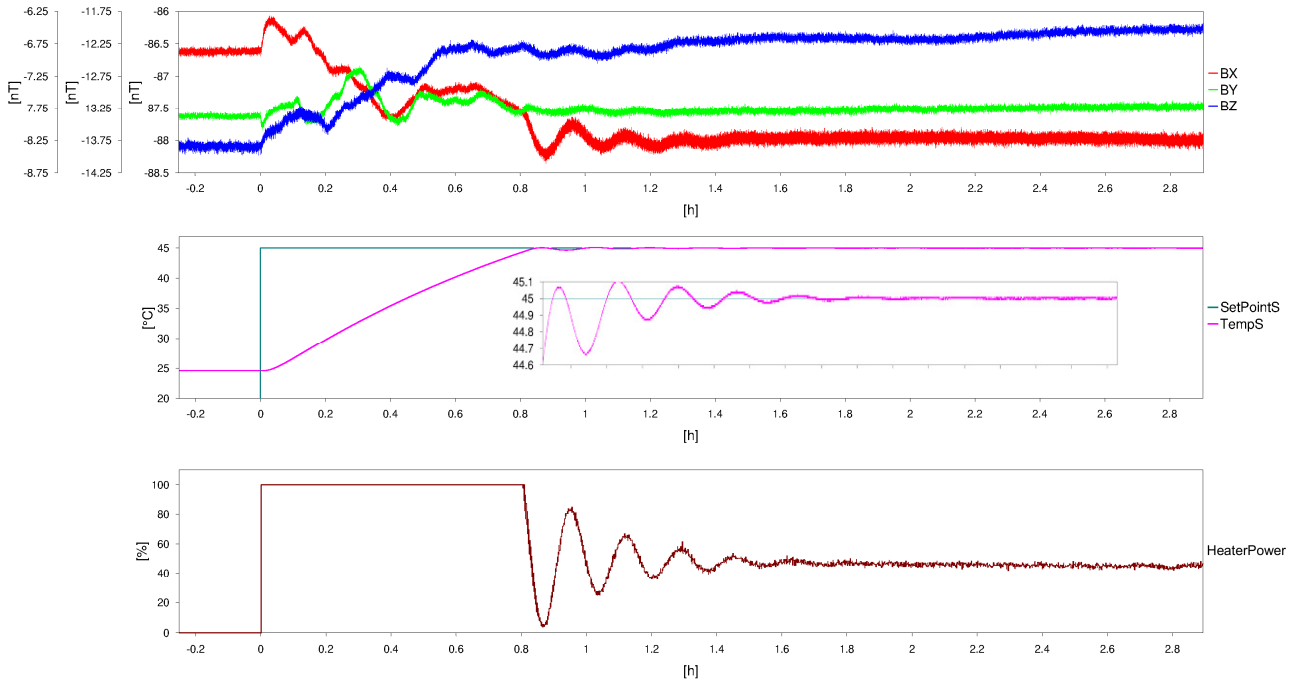

Figure 3 –The top panel shows the magnetic field components X (red), Y (green), Z (blue), the middle panel the temperature of the sensor and the bottom panel the heater power. The temperature variation after achieving the setpoint temperature for the first time shows the efficiency of the PID control algorithm. The variation (zoom out in the middle panel) is less than 0.5°C and becomes less than 0.05°C within the next hour.

4. INSTRUMENT CONTROL

The magnetometer can be controlled stand-alone via a touch screen or remotely over a TCP/IP network connection or a serial link. The heaters are only one of the options which can be operated by the electronics. A second magnetic field sensor for using the device as a gradiometer, a GPS receiver, inclinometers or a rotary encoder can also be added. The Magnetometer itself, all interface options and add-ons are controlled by an ARM9 microcontroller with a Linux operation system. It has the following features:

- Measurement of 3 or 6 magnetic field components (Measurement range ±65000 nT)
- Adjustable data rates of 200 Hz, 100 Hz, 50 Hz, 10 Hz, 1 Hz
- Measurement of electronics and sensor temperature
- Optional: measurement of inclination (2 axis each sensor)
- Optional: measurement of rotary encoder angle
- Magnetometer control and data output via touch screen, network services (Webpage, socket connection, FTP) and serial interface
- Data recording on an internal SD card (ASCII or binary data format)
- Manually triggered measurement including geographical position
- Simultaneous data access and recording
- Synchronization of time and position determination with a GPS receiver
- Optional: temperature control

The network services grant device control via network (LAN) or internet. Thus the temperature settings can be adjusted remotely. Both touch screen and WEB page allow the graphical display of currently measured data. The FTP server gives access to data stored on the internal SD card.

5. TEST RESULTS FROM SAN FERNANDO VARIOMETER COMPARAISON

The variometer has been tested during the San Fernando workshop. The Magnetic field has been measured in comparison with the observatory standard on a pillar inside a tent and on the outer pillar. Results are published in this proceedings. The highest temperature gradient has been measured during sunrise on June 6th. The temperature increases (measured by LEMI sensor) from 13 °C to 20 °C within 1 hour. The comparison between the temperature stabilized sensor and the observatory in XYZ coordinates is shown in the measurement session results. With the increasing temperature the X component drifts with less than <0.2 nT/°C (0.16 nT/°C during sunset and 0.18 nT/°C during sunrise) and the Z component with less than -0.13 nT/°C (-0.11 nT/°C during sunset and -0.09 nT/°C during sunrise). Transforming the data into spherical coordinates (see Figure 4), we can see that the field magnitude calculated by the components of the sensor depends not on temperatures (drifts by 0.4 nT continuously within 3 hours, but not in correlation with the temperature). That attests that the scale values are perfectly stabilized. The drift seen in the X and Z components in in the measurement session results can be clearly related to a drift in the inclination (-0.02 arcmin/°C, see lower right panel in Figure 4).

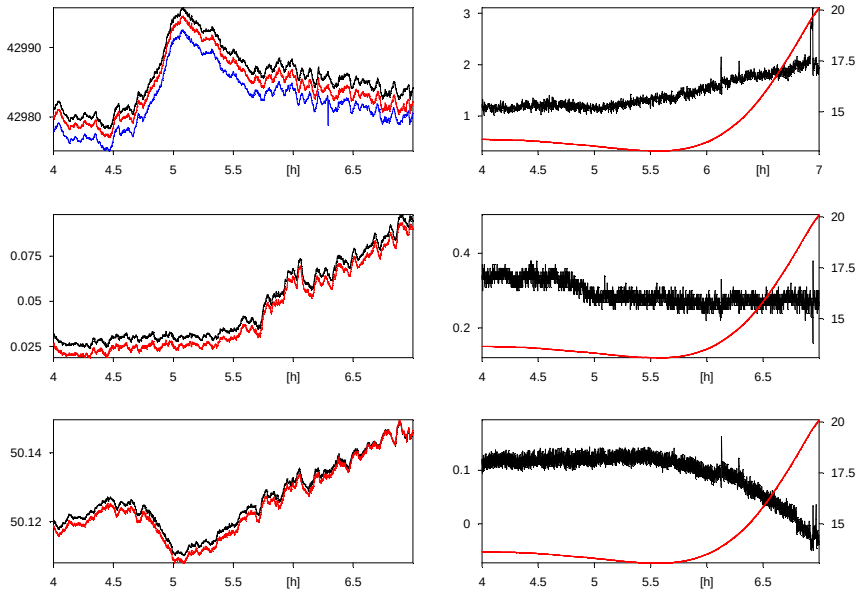

Figure 4 –On the left hand side of the top panels the field magnitude in nT calculated by components of the Magson magnetometer (black) and the observatory standard (red) as well as the results of the scalar magnetometer (blue) are plotted. The left middle panel shows the declination and the bottom panel the inclination measured by the Magson magnetometer (black) and observatory variometer (red) in degree. On the right hand side the difference between Magson and observatory magnetometers of the field magnitude in nT and the angles in arc-minutes are plotted in black. The temperature in °C (right scaled) is added in red.

The temperature dependent tilting of the sensor shows the limitation of the concept which thermally controls only the sensor. Compared to an installation in a thermally controlled variometer house the mounting arrangement (in San Fernando on top of a pillar on a Plexiglas interface) is not stabilized. Sensor installations close to Earth (e.g. in holes in the ground) are therefore the preferred accommodation options.

6. CONCLUSIONS

During the workshop the magnetometer has been installed in San Fernando Observatory. The temperature of sensor and electronics has been stabilized by a computer controlled heating system. Two hours are needed for warming up the sensor.

During this period 1 nT instabilities are visible due to temperature gradients inside the sensor. After reaching the setpoint temperature (in San Fernando setpoints are fixed to 40°C for the sensor and 50°C for the electronics) its variation is less than 0.05°C. The heater system design is fully synchronized with excitation and data acquisitions. No impact on instrument noise has been observed. The comparisons with the observatory standard shows that scale values are perfectly stabilized. A drift in Inclination (-0.02 arcmin/°C) could be observed due to temperature dependent sensor tilting.

7. ACKNOWLEDGEMENT

Nos gustaría agradecer especialmente a Manuel Catalán y a Manuel Larrán por hacer possible la comparación de medidas, así como el tiempo y esfuerzo empleado en el procesado de datos.

8. REFERENCES

Auster, H.U., Glassmeier, K.H., Magnes, W., Aydogar, O., Baumjohann, W., Constantinescu, D., Fischer, D., Fornacon, K.H., Georgescu, E., Harvey, P., Hillenmaier, O., Kroth, R., Ludlam, M., Narita, Y., Nakamura, R., Okrafka, K., Plaschke, F., Richter, I., Schwarzl, H., Stoll, B., Valavanoglou, A. & Wiedemann, M. 2008, "The THEMIS Fluxgate Magnetometer", *Space Science Reviews*, , pp. 1-30.

THE UPGRADE OF BASE ORCADAS MAGNETIC OBSERVATORY

E. Cabrera [(1)], C. W. Turbitt [(2)], J. Rasson [(3)], J. Gianibelli [(4)], J. C. Riddick [(5)]

[(1)] Argentine National Weather Service, Observatorio Central Buenos Aires, Av. de los Constituyentes 3454 (CP 1427, Buenos Aires, Argentina.
[(2)] British Geological Survey, Murchison House, West Mains Road, Edinburgh, EH9 3LA, United Kingdom, c.turbitt@bgs.ac.uk
[(3)] Institut Royal Météorologique, Centre de Physique du Globe, B-5670 Dourbes, Belgium, jr@oma.be
[(4)] Head of the Geomagnetism and Aeronomy at the UNLP, Argentina, geofisicogianibelli@yahoo.com.ar
[(5)] john_riddick@hotmail.com

SUMMARY

In January 2012 new absolute magnetometers, fluxgate variometers and recording hardware to monitor and record changes in the Earth's magnetic field have been installed at Base Orcadas Observatory, in a collaborative project between the Argentine National Weather Service (SMN), the British Geological Survey (BGS) in Edinburgh and the Institut Royal Météorologique de Belgique, Dourbes as part of the INTERMAGNET Digital Geomagnetic Observatory (INDIGO) program. This observatory is located on the Argentine Antarctic Base on the South Orkney Islands (Orcadas del Sur), with the new equipment replacing existing photographic recording equipment which was damaged by an earthquake in 2003. The equipment is designed to meet INTERMAGNET standards for data quality providing a one-minute data set which will be corrected to absolute through a program of absolute observations. The original magnetic observatory at Base Orcadas (the oldest in Antarctica) was installed by the Scottish National Antarctic Expedition in (SNAE) 1902-04 and recordings of variations in the Earth's magnetic field have continued since that time at this remote location.

1. INTRODUCTION

Base Orcadas, operated by the Argentinean Navy, is located on Laurie Island on the South Orkney Islands (latitude 60° 44´ 17"S, longitude 44° 44´ 26" W, altitude 4 m, Figures 1a,b). The Antarctic base was originally set up in 1903 by the Scottish National Antarctic (Scotia) Expedition (SNAE), led by William Spiers Bruce (Mossman et.al. 1906, Schott and Rasson 2007, Moneta 1951). This expedition established an overwintering base on Laurie Island and built accommodation from which they carried out a program of meteorological and magnetic measurements. The house, which provided living accommodation for four staff was called Omond House (Figure 2) named after Robert Trail Omond who was the first Superintendent of Ben Nevis Observatory, in Scotland. Also, as a major part of the expeditions scientific program was the study and recording of the Earth's magnetic field. A second canvas covered wooden shelter was built by the *Scotia's* carpenter and named Copeland House after Professor Ralph Copeland the then Astronomer Royal for Scotland who had given one of the expedition members, Robert Mossman, training in making measurements of the Earth's magnetic field.

Using Omond House as a base and Copeland House as a magnetic observatory, in 1903 a program of meteorological observing and magnetic measurements were begun, with this program continuing to the present day. Details of the work carried out by the SNAE and details of the many problems, both political and practical, are fully described in the excellent papers by Keighren (2005) and Swinney (2007).

In 1904 Bruce and most of the SNAE members left Laurie Island to return home to Scotland leaving Mossman to train Argentinean scientists who would continue the scientific program. Since then this work has been supported by Argentina which makes Base Orcadas the longest continuously manned base in the whole of Antarctica. As the base is in a unique location the data and results generated by the

many scientific programs carried out there are of immense value to the scientific community worldwide and it is essential that this work continues. Unfortunately in August 2003 a magnitude 7.5 earthquake, in the sea, 190 km east of the base, damaged the instruments in the magnetic recording hut. Although no major structural damage was caused to the base infrastructure by the earthquake, unfortunately the violent ground movements damaged the suspension of the declinometer which resulted in a loss of record from this instrument.

Today, the scientific community demand that the data output from magnetic observatories is digital. Ideally in an internationally recognized format, conforming to either INTERMAGNET or IAGA standards. Currently, Base Orcadas is generating data from hand scaled photographic recordings which do not conform to these standards. Because of this and as it is essential that this long data set continues the observatory was regarded as an ideal site at which to install the INDIGO hardware. This hopefully will allow Argentina to continue to provide data from this important site in a form that is readily useable by the research community.

The upgraded hardware consists of a non-suspended DMI three component fluxgate magnetometer recording variations in three orthogonal components (horizontal (H), declination (D) and the vertical (Z) components) every 5 seconds and a GEM proton magnetometer measuring total field (F) every 10 seconds. The outputs of these instruments are digitized and logged using a low-powered (battery backed) digitizer and a USB memory stick with timing control from a GPS receiver giving an accuracy better than ±1 second/day.

2. SITE LAYOUT AND INSTRUMENTS

At Base Orcadas two wooden huts, Figure 3, have been built to replace the original 1903, Copeland House, the position of these huts within the base can be seen in Figures 1a,b. One hut is the Absolute House in which BMZ and QHM magnetometers were used to determine the absolute values of Z (BMZ) and H and D, (QHM). During the 2012 visit a D/I fluxgate theodolite was installed in the absolute building replacing the obsolete QHM and BMZ instruments.

The second larger building, where temperature is controlled throughout the year, housed the photographic La Cour variometers and also a small photographic darkroom where the photographic records were processed. These instruments have been removed and replaced by the three component fluxgate and the GEM proton magnetometer. The power supplies, digitizer and data logger have been installed in the now unused photographic darkroom with a cable data transmission link installed to connect the Variometer House to the main office building. In the main office the data are decoded, displayed and logged on a PC running the INDIGO Watch software package.

3. INSTALLATION

In January 2012 a team of engineers from SNM travelled to Base Orcadas to install the new INDIGO hardware and organize an absolute observing program. Their first task was to remove the existing photographic variometers and organize the installation of the INDIGO DMI fluxgate, GEM GSM 90 proton, GPS time receiver along with the control and recording hardware in the Variometer House. In order that the operation of this equipment could be monitored remotely a trench was excavated and a multicore cable was installed between the Variometer House and the Main Office, 100m distant (Figure 4). This link is used to transmit the data from the INDIGO hardware to a PC in the office running INDIGO Watch software which allows staff to continuously monitor the operation of the variometers and also provide a backup recording facility if problems are experienced with the data logger in the Variometer House or bad weather makes it difficult to visit and check that the equipment is operating correctly.

The above work took 10 days to complete and continuous recordings started in early February 2012. The next task was to set up the absolute observing program and to measure the site differences between the GEM proton in the Variometer House and the D/I absolute observing pillar in the Absolute House.

The site difference measurements were made on 2 separate days with continuous recordings being made over a 16 hour period by Geometrics 856 proton mounted on the D/I observing pillar. The results of these measurements were subtracted from the simultaneous measurements made by the INDIGO proton in the Variometer House. These tests established a site difference of 4 nT between the proton in the Variometer House and the D/I observing position. Unfortunately it will not be possible to leave this second proton magnetometer on the Base to check this site difference every few months but this site difference will be remeasured on the next service visit.

Prior to this installation a QHM and BMZ were used to make absolute observations of the magnetic field. In February 2012 these instruments were removed and a Rukca D/I theodolite with Institut Royal Météorologique, Belgium electronics is now used to measure the absolute values of declination (D) and inclination (I). The calculation of the horizontal (H) and vertical (Z) intensities and baselines are calculated using the total field (F) measured in the Variometer House, corrected for site difference as described above.

All this work was successfully completed by 7 February 2012 when continuous recordings of the fluxgate and proton began and a regular absolute observing program was also started. From this date analog recording stopped and Base Orcadas became a fully digital magnetic observatory.

4. FUTURE PROGRAM OF WORK

Following on from this successful installation to ensure continued reliable operation of the new digital system at Base Orcadas the staff will carry out the following work program:

Regular visual checks on the operation of the INDIGO equipment.

Data files of variometer data will be transmitted daily to SMN in Argentina and to the INTERMAGNET GIN in Edinburgh.

A regular program of absolute observing will start. This program specifies that overwintering base staff make 3 absolute observations every day throughout the year.

A bulletin containing plots of the daily magnetograms and fluxgate baselines derived from the absolute observing program will be generated every month.

Annually the staff from SMN will carry out a service, calibration and maintenance visit, typically this will include:

Checks on the scale values of the fluxgate variometers.

Using astronomical observations, remeasure the declination fixed mark bearing.

Remeasure the total field site difference between the D/I observing position and the proton magnetometer in the Variometer House.

5. CONCLUSIONS

The installation of this new hardware is a significant event in the long history of Base Orcadas. The original base was set up by a Scottish expedition in 1903 with the observing program carried out by a joint Scottish/ Argentinean team of scientists making this the longest continually operational base in Antarctica. In 2012 the base was again re-equipped as part of a joint INTERMAGNET program and it is hoped that this co-operation will continue to ensure the successful operation of Base Orcadas long into the 21st century.

6. ACKNOWLEDGEMENTS

We would like to acknowledge and thank the following people, Ted Harris (BGS) and Lic. Mateo Virgilio Hernandez (Trade and Imports Office SMN) for all their help in shipping and organizing the export and import of the INDIGO hardware. Roberto Orlando Guzman, Principal Warrant Officer of the Air Force, Argentina for his help in installing the equipment in Base Orcadas and his excellent work in carrying out the absolute observing program. The staff at Base Orcadas and Esteban Hernandez, Gerardo Cifuentes Nava and the staff of UNAM Mexico for their assistance in providing the D/I theodolite. CWT contributes by permission of the Executive Director, British Geological Survey (NERC).

7. REFERENCES

Keighren, I.M. (2005) Of poles, pressmen, and the newspaper public: reporting the Scottish National Antarctic Expedition, 1902-1904. *Scottish Geographical Journal*, **121(2),** pp 203-218.

Moneta J.M., (1951). Cuatro Años en las Orcadas del Sur. *Peuser : Buenos Aires.*

Mossman, R.C., Harvey Pirie, J.H, Rudmose Brown, R.N., "The Voyage of the Scotia" 1902, reprinted 2002, *Mercat Press, Edinburgh, 2002*, **ISBN I 84183 044 5.**

Schott, J.J., Rasson, J.L., (2007). Magnetic Observatories in Antarctica, Encyclopedia of Geomagnetism and Paleomagnetism, *Encyclopedia of Earth Sciences Series*, *David Gubbins & Emilio Herrero-Bervera (Eds.)*, **ISBN: 978-1-4020-3992-8,** 1020p.

Swinney, G.N. (2007) The Scottish National Antarctic Expedition (1902-04) and the Founding of Base Orcadas, *Scottish Geographical Journal*, **Vol 123,** No 1 pp 48-67, March 2007.

Figure 1a –Base Orcadas looking south-east from Cerro Mossman the magnetic recording hut and absolute hut are the two black huts in the foreground.

Figure 1b –Base Orcadas looking north east from Cerro Mossman, the remains of Omond House can be seen beside the red building at the bottom of the picture and the magnetic recording huts at the top left of the picture.

Figure 2 –The remains of Omond House in 2010

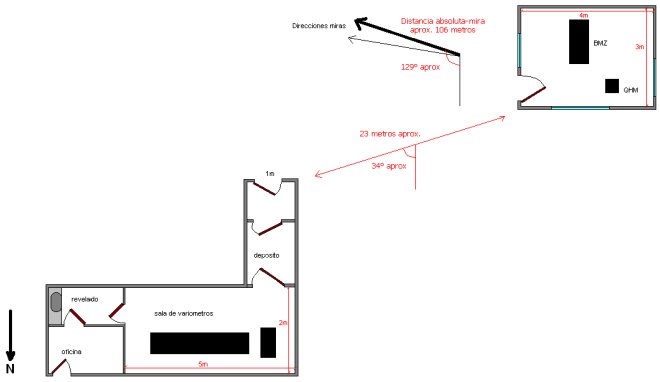

Figure 3 –The Variometer and Absolute Houses

Figure 4 –The Variometer House and data cable to the Main Office.

TOWARDS THE REINSTALLATION OF MADAGASCAR MAGNETIC OBSERVATORY

A. Chambodut [(1)], G. Rambolamanana [(2)], M. Rambolamanana [(2)], IOGA Technical Team [(2)], L.M. Razafindranaivo [(2)], F.N. Ranaivo-Nomenjanahar [(2)], M. Menvielle [(3,4)]

[(1)] Université de Strasbourg, EOST, Département des Observatoires Magnétiques; IPGS, CNRS-INSU UMR 7516, Strasbourg, France, aude@unistra.fr
[(2)] Université d'Antananarivo, IOGA, Antananarivo, Madagascar.
[(3)] Université de Versailles St-Quentin; LATMOS-IPSL, CNRS-INSU UMR 8190, Guyancourt, France.
[(4)] Université de Paris-Sud, Département des Sciences de la Terre, Orsay, France.

SUMMARY

The magnetic observatory of Madagascar (IAGA code: TAN) opened in 1889. Operated by the geomagnetic department of the Institut et Observatoire Géophysique d'Antananarivo (I.O.G.A.), formerly Tananarive observatory, in close cooperation with Ecole et Observatoire des Sciences de la Terre (E.O.S.T.), it joined the INTERMAGNET Program in 1993. After several periods of major failures due to hard climatic conditions, an EOST-IOGA meeting was organised in order to fully assess the situation of the observatory embedded in the growing urbanization. A new site was thus defined and, thanks to IOGA team, construction work was undertaken. A gradual relocation of the observatory will be undertaken over the period 2012-2014.

1. LONG STANDING MAGNETIC OBSERVATORY

The magnetic observatory of Madagascar (IAGA code: TAN) opened in 1889 (Figure 1), near the present site of the Antananarivo University. It was the second magnetic observatory that started operating in the Southern hemisphere. The institution simply called the "Observatory" to which the magnetic observatory was a part of, was the first scientific research center of Madagascar. Headed by the French Jesuit Fathers, the "Observatory", named at that time the Royal Observatory of Madagascar, was the reference for the Earth and environmental sciences at Madagascar.

Figure 1 –Historical buildings of the Malagasy Observatory (early XXth century).

On 1rst January 1967, the "Observatory" was sold by the Jesuits to the Malagasy state for a symbolic Franc. Since then, the "Observatory" is under supervision of the University of Madagascar. Since this date, the TAN observatory is part of the geomagnetic

department of the Institut et Observatoire Geophysique d'Antananarivo (I.O.G.A.); it joined the INTERMAGNET program in 1993 (Figure 2). The TAN Observatory is currently operated in close cooperation with Ecole et Observatoire des Sciences de la Terre (E.O.S.T.).

2. HISTORICAL SITE OF THE MAGNETIC OBSERVATORY

Since its foundation, the TAN magnetic observatory was located on the Ambohidempona hill, close to the university campus. In 2008, a huge lightning destroyed the entire acquisition chain (from sensors/instruments to computers).

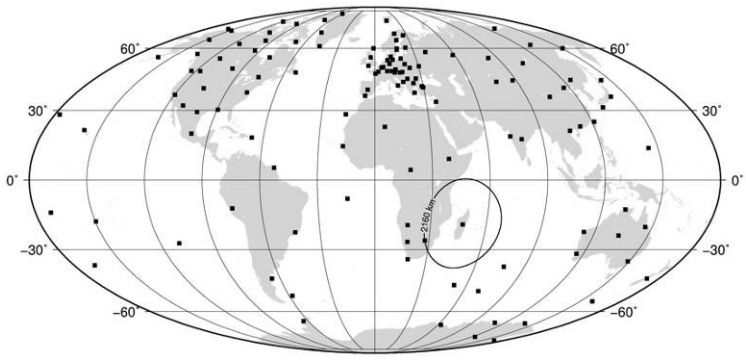

Figure 2 –Position of the TAN magnetic observatory in the INTERMAGNET network.

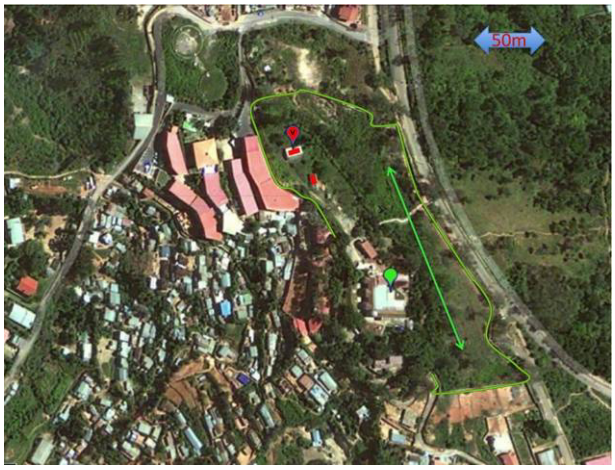

Figure 3 –Historical site of the TAN magnetic observatory nearby the University. Red: Variometer house ("V") and absolute measurements' hut; Green arrow: main electric power line; Green curve: wall of the IOGA institute that underline the "protected area" around the observatory.

In 2011, a French mission in Antananarivo was organized as part of the collaboration between IOGA and EOST, in order to fully assess the situation of the observatory. It appeared impossible to maintain the magnetic observatory at its historical location mainly because of the growing urbanization (Figure 3).

3. DATA

Records began in 1889 and have continued with interruptions until 2008. We present below the magnetic data series from 1962 onwards (Figure 4) and two examples of magnetograms for a quiet and a disturbed day (Figure 5).

4. NEW SITE FOR THE MAGNETIC OBSERVATORY

IOGA proposed to move the TAN magnetic observatory at a place contiguous to a seismological station, located at approximately 60 kilometers from the historical site. After a joined inspection of the site, it was decided to move the observatory to that place because of the following characteristics:

- site belonging to IOGA,
- reduced anthropogenic disturbances (no roads, no electric power lines, ...),
- security ensured (against malicious acts: guarding 24h/24h, against floods: position on a hill - Figure 6; against lightning: nearby ligthning rod and no direct connection to the electrical network, ...).

Magnetic survey over the areas where the magnetic observatory would be implanted, were performed before construction. Construction of the variometer cave was completed in late 2011 in order to apprehend its behaviour during the full monsoon season.

The soil on site is composed by laterite, above a bedrock of granite at approximately 3 or 4 meters deep. The obtained magnetic anomaly map shows a weak crustal magnetic field (Figure 7) with a localized stronger anomaly that, after investigation, appeared to be due to a small clay building in the Northern part of the place (bottom of the figure). The Variometer vault was planned to occupy the South West part of this area (upper right corner of the present figure) with a weaker crustal magnetic anomaly field.

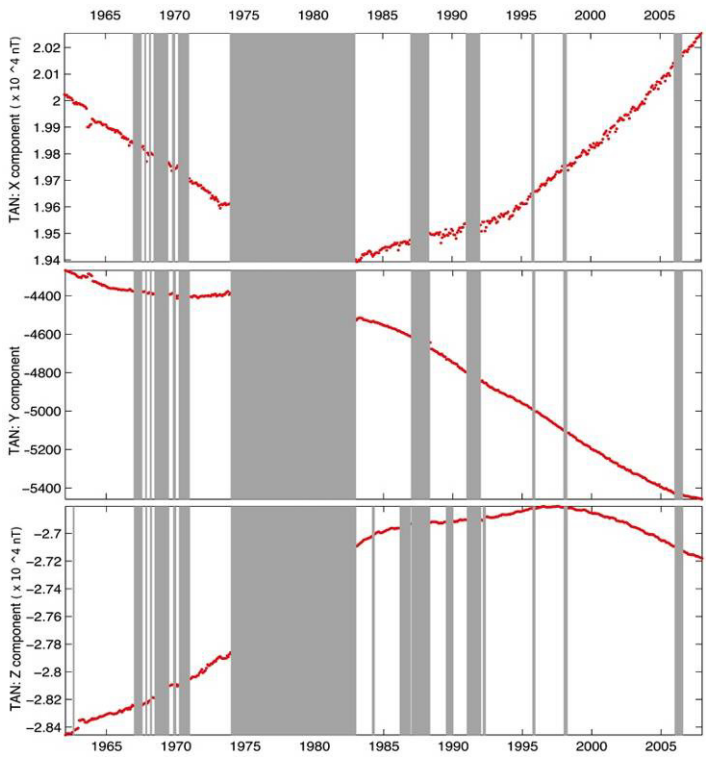

Figure 4 –Monthly means values of X, Y and Z components at TAN magnetic observatory (from BCMT database).

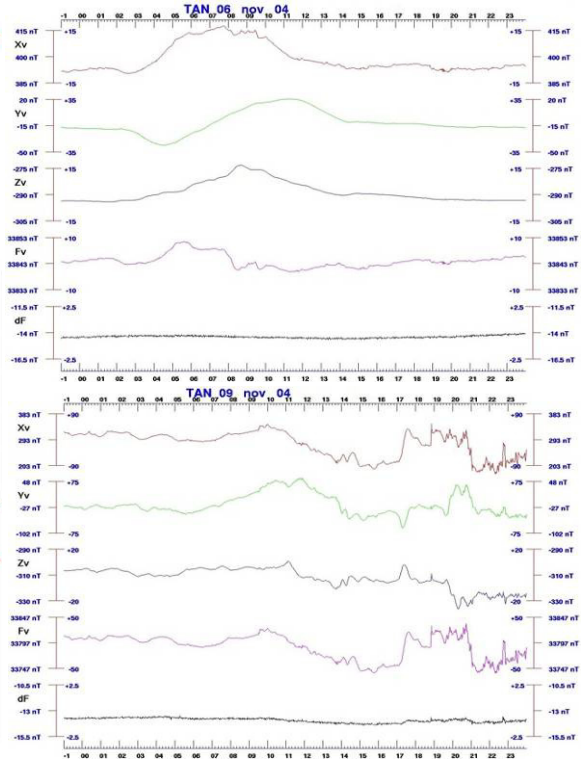

Figure 5 –Minute Values of the variometer three components and of the intensity of the magnetic field at the TAN observatory during a quiet day (left, 06 November 2004) and a moderately disturbed day (right, 09 November 2004).

Figure 6 –New site of the magnetic observatory in the Malagasy countryside.

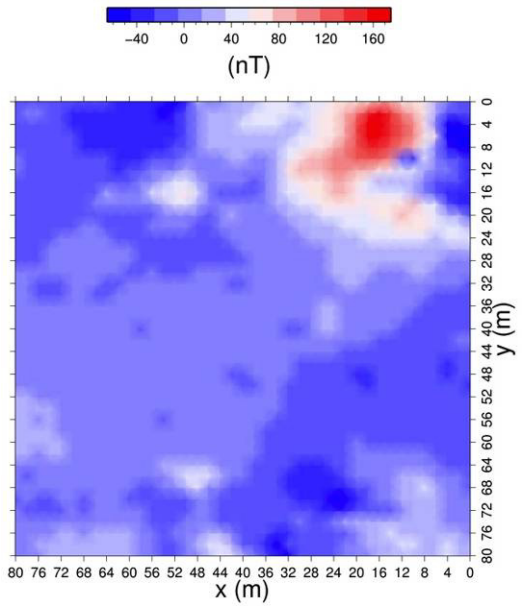

Figure 7 –Magnetic survey on the new site of the magnetic observatory before any construction

IOGA has undertaken the construction of buildings. Roof and walls of the cave were designed with the strong local rock (granite) in order to: blend into the landscape, reduce costs and allow easy repairing if needed in the future. The magnetic observatory will be gradually installed over the period 2012-2014 thanks to the cooperation between IOGA and EOST teams. Up to now, the future variometer cave is still under testing. It has to fully prove its resistance and suitability for variometer installation. In the near future, a small open hut will be designed for performing absolute measurements and another magnetic survey (the second one after construction and installation) will be achieved.

Figure 8 –First phase of the construction of the variometer vault, global view towards the South.

Figure 9 –Reimplantation of the magnetic observatory, construction of the variometer vault.

ANTROPOGENIC NOISEIN SPANISH OBSERVATORIES

J. J. Curto [(1)], S. Marsal [(1)], J.M. Torta [(1)], M. Catalán [(2)], P. Covisa [(3)]

[(1)] Observatori de l'Ebre, Roquetes, Spain, jjcurto@obsebre.es
[(2)] Real Instituto yObservatorio de la Armada, San Fernando, Spain, mcatalan@roa.es
[(3)] Observatorio Geofísico de Toledo (IGN), Toledo, Spain, pcovisa@fomento.es

SUMMARY

Although geomagnetic observatories are intended to measure natural magnetic fields, very often their records are polluted by "artificial" fields, mainly caused by the action of men and their technology. With the progressive advance of the civilization, observatories had to move away to remote places in an exodus which has not finished yet because new settlements are taking place where it was a virgin area. Roads, but especially electrified railway lines and power lines, are the dominant sources of noise. Here we will summarize the experience of the staff of the Spanish observatories dealing with anthropogenic noise and some of the remedies applied.

1. INTRODUCTION

Anthropogenic noise is a widespread problem in geomagnetic observatories *(Wienert, 1970)*. In the past, the movement of magnetic rocks or iron materials were the more common of the primitive offenders in the ancient observatories, but with the extension of the electrical network, new and very bothering offenders acting in the distance appeared*(Dupouy, 1950).*At present, in countries with DC electrified railways, the dense net of railway lines makes it very difficult to find a quiet place.Some efforts have been done to evaluate the extent of these disturbances *(Jankowski and Sucksdorff, 1996; Lowes, 2009; Pirjola, 2011).*

Figure 1 –Magnetic observatories in Spain.Livingston, not showed in this map, in Antarctica, is also maintained by Spanish Agencies.

This paper deals with the problemsencountered in the Spanish observatories in relation to noise.Due to artificial disturbances, in Spain someobservatories had to move (blue circles in fig. 1),while others had to be closed (red circles in fig. 1)**.**Following, authors' experiencesdealing with such noise will be summarized, with some more detail for what concerns Ebro and Livingston Island Observatories.

2. NOISE IN THE SPANISH OBSERVATORIES

Toledo (TOL) was founded in 1934 by the Instituto Geográfico Nacional (IGN). It was located in the centre of Spain, near Toledo city. After many years of clean magnetograms, magnetic disturbances arrived in1965 with the railway electrification (fig. 2 left). Telluric currents and rapid variations were affected, but mean hourly values werenot (at least not dramatically), and the observatory remained there for a time. Finally in 1982, the observatory was moved to San Pablo de los Montes (SPT).

Tenerife (TEN),in the Canary Islands, was founded in 1954 by the IGN, too. A radio repeater installed very close to the station spoiled the magnetic records since 1991 and they had to move to Güímar (GUI) in 1993. New instrumentation was deployed at that time. In

addition, it has to be noted that the whole island has a volcanic origin, so that magnetic gradients are important and the movement of rocks might be able to produce changes in the magnetic field measurements.

San Fernando (SFS), located in the South of Spain, in the Cadiz Bay, is the oldest Observatory in Spain. Founded in 1879 by the Spanish Navy, itwas devoted to measure the magnetic field and to create magnetic maps, essentially for navigation. It had no problems of noise until 1978, when the electrification of the railway occurred. In 1990 the observatorywas moved to Puerto Real, but this place was still too close to the railway and finally, in 2004, it was installed in La Barca de la Florida. To check if this place was completely safe from noise a simple algorithm using a b-spline filterwasdesigned.Although the noise has a very low level (fig. 2 right), it is clearly present and has a direct correspondence with train circulation. The SFS observatory staff are worried because the mean level of this noise is increasing withtime.Modern trains with more powerful engines producemore intense currents circulating through the catenaries and, obviously, more intense currents are leaked into the earth.

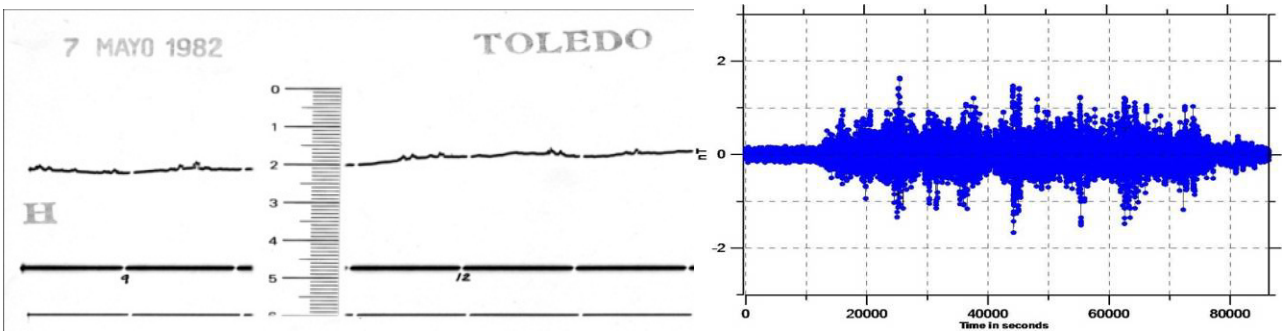

Figure 2 –Disturbed magnetogram in Toledo with spikes in the H componet (left) andthe level of noise in the Z component,in the SFS3/09/2011 (right).

Ebro (EBR) observatory, devoted to Solar-Terrestrial Physics,was founded in 1904 by the Society of Jesus in Roquetes (northeast of Spain).The original location of the magnetic observatory is still in use. As regard the noise, in the long life of this observatory we can distinguish 4 different periods.A 1st period ofquietnessstarting with its foundation, which was broken by the electrification of the railway lines in 1973 (beginning of the 2nd period). Then, plenty of noise appeared in all components of the magnetograms, but especially in the Z component. Hourly mean values were still acceptable but minute values and rapid magnetic variations were compromised (*Sanclement, 1974)*.In 1996, the majority of trains were derived to a new line several kilometres away (3rd period). The magnitude of the spikes was reduced, and the Z component was less disturbed (at least compared with the H component) due to the change in the geometry of the railway circuit. The spikes were still clear on the magnetograms (fig.3 left) and, of course, they correlate very well with arrivals and departures in Tortosa station. In fact, Ebro records could be used to verify delays in train arrivals!As some spikes were higher than 5 nT, it was decided to remove them. An algorithm to make this task was designed (Curto et al. 2009). It was based on a combined process of filtering and thresholding. The system detected where a spike was and removed the wrong datum from the corresponding file.

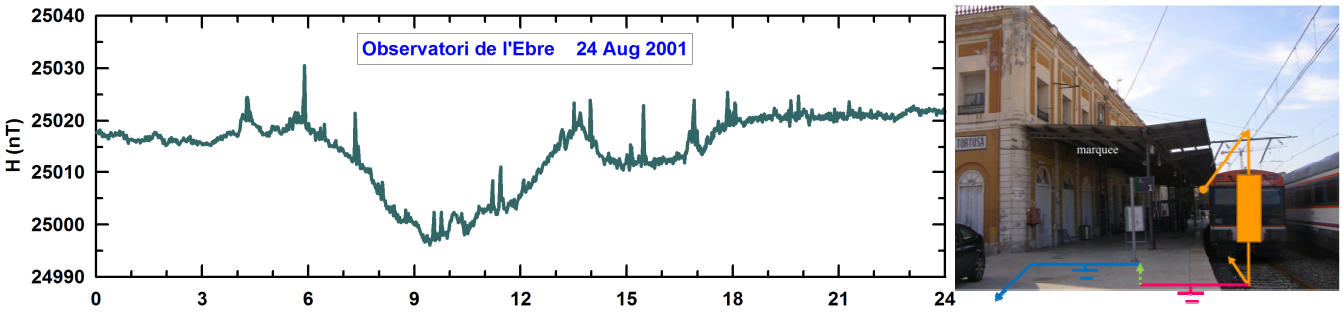

Figure 3 –Noise at EBR in the H component during the 3rd period (left) and marquee in the railway station of Tortosa(right)

Finally, in 2011 (4th period), some works in Tortosa station definitively removed the last source of noise. It seems that in Tortosastation, the earth connection of a marquee (fig. 3 right) was linked to the general water pipe of the city. This connection acted as a bridge for leakage currents which used those pipes as a gigantic antenna, producing magnetic fields far away from the noise source.By then, and additionally to the main base magnetometers, an alternative set of variometers were set in a remote place, in Horta de St. Joan. This place is far away from the railway lines (more than 20 km, following the IAGA recommendation). Magnetometers are housed in a pair of

hermitages hidden in the forest and far enough from the next village. The variometer was installed in a natural cave that goes inside the mountain providing thermal stability.

Livingston Island (LIV), founded bythe Ebro Observatory staff in 1995, was supposed to be a magnetically clean settlement, so a magnetic observatory was deployedin a quiet bay, not far away from the Spanish Antarctic Base.A fully equipped system with a proton vector magnetometer was firstly installed (fig. 4 left), while a fluxgate magnetometer was set up in a second stage. Taking advantage of this situation, they couldcompare their outputs.

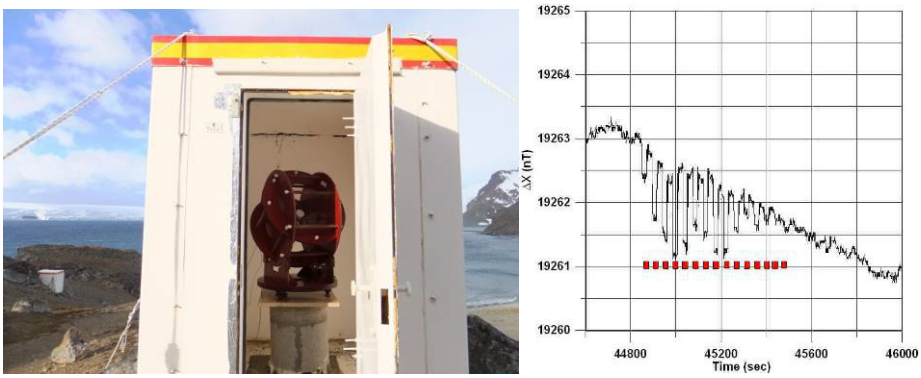

Figure 4 –Proton vector magnetometer in Livinston Island (left) and diferences betwen magnetometers showing interferences (right).

Periodic noise as trains of pulses showed upin the differences (fig. 4 right). Though it took time to figure out the source of that noise, it wasfound to be the electromagnetic waves generated bya radio emitter communicating this remote place with Ebro, which is used to get the magnetic data if satellite transmission fails. Thefluxgate magnetometer was then identified to be the instrumentsensitive to noise.

3. SOME EXPERIENCES ONFIGHTING AGAINST ELECTROMAGNETIC NOISE

Besides the related experiences of observatory relocations, we have attempted to fight against the electromagnetic noise in some occasions with some success. In particular, to avoid the above mentioned noise at LIV a laboratory test was designed at Ebro pavilions. Different points of the system were scanned by applying electric fields on it with different powersand frequencies (fig. 5 left). Even very small fields were able to produce noise. Alternate Currents being rectified in the electronic circuits created Direct Currents that were confused by the system as natural signals. The system reacted at very low electric fields (0.1 mV/m) and was especiallysensitive to radiations in frequencies from 10 to 12 MHz (fig. 5 right). Several parts of the sensors and the power supply acted as receiving antennas, introducing the noise in the electronics, where it was magnified. Filtering, shielding and earthing were remedies applied to remove that noise.

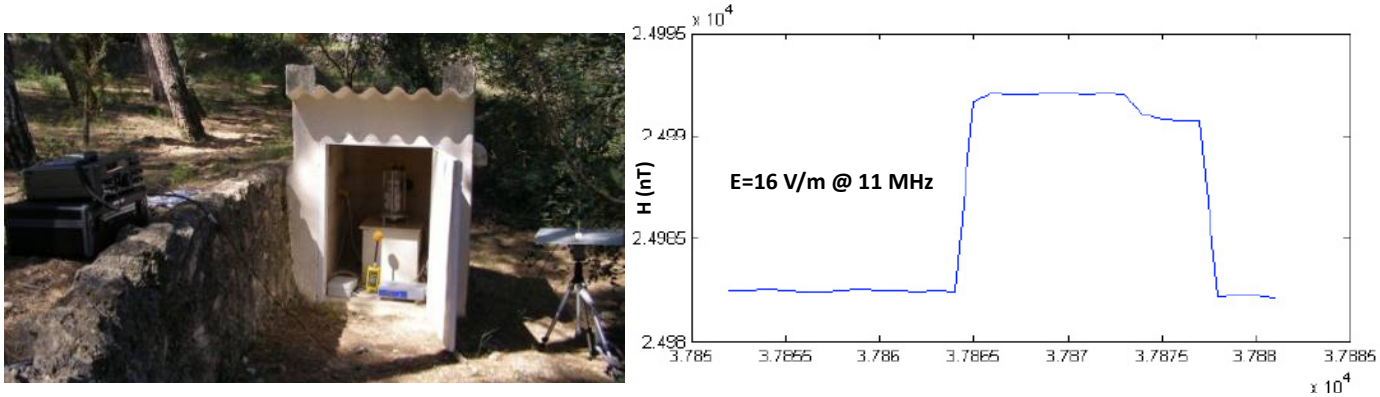

Figure 5 –Interference test performed on the flugate magnetometer at Ebro (left) andsome test results (right).

A second source of noise was detected at Ebro Observatory, where the old ionospheric sounder injected it (harmonics of the 50 Hz) in the mains, which disturbed proton precession magnetometers. This noise could be finally removed with a separator tranformer and a mainsfilter. The last episode of noise in Ebro Observatory came from itsnew ionospheric sounder. The data logger of the fluxgate variometer was renewed and thus we could have a sample rate of 1second. Figure 6showsthe interference produced by this ionospheric sounder on the horizontal (H) component of the magnetic field measured with the fluxgate magnetometer. The pattern, which had gone

unnoticed so far in the minute means, was observed to appear on a 5-minute basis in the 1-second recordings. The interferences were only noticeable when the sounder transmitted at frequencies above 6.25 MHz. Tests confirmed that the noise being radiated was electromagnetically coupled with the magnetometer by means of an ill-shielded cable joining the sensor with its electronics. After improving the insulation, the noise was reduced to about 25 % of the original amplitude.

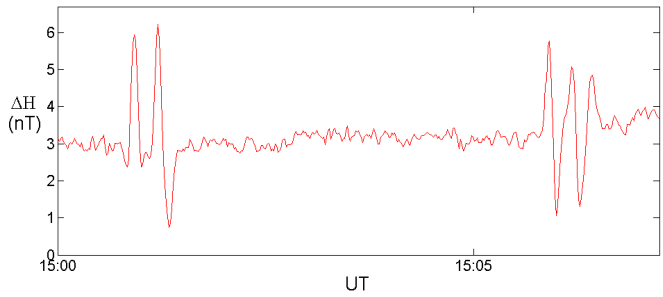

Figure 6 –Interference produced by an ionospheric sounder on the horizontal (H) component of the magnetic field measured with a fluxgate magnetometer at Ebro Observatory.

4. CONCLUSIONS

Suitable areas for magnetic observatories are in recession. Anthropogenic noise, especially that generated by industrial electric currents, is the more threatening danger for magnetic observatories. Train electrification has pushed away most of the Spanish observatories. Thus, in Spain, as in many other countries, observatories are pilgrims of an exodus not yet finished. Electromagnetic waves from radio emitters are another source of noise that has to be taken into account. Much effort and precautions have to be applied in the new designs of magnetic instruments to avoid the omnipresent anthropogenic noise.

5. REFERENCES

Curto, J.J., Marsal, S., Torta, J.M., Sanclement, E.,(2009): "Removing spikes from magnetic disturbances caused by trains at Ebro observatory",*Proceedings of theXIII IAGA Workshop on Geomagnetic Observatory Instruments, Data acquisition and Processing*, 60-66.

Dupouy, G. (1950) : "Perturbation du champ magnétique terrestre et des courrants telluriques par les chemins de fer electrifiés", *Annales de Géophysique*, V6., 18-50.

Jankowski, J. and C. Sucksdorff (1996): "Guide for magnetic measurements and observatory practice", *IAGA publications*, Warsaw.

Lowes, F. (2009): "DC railways and the magnetic fields they produce—the geomagnetic context". *Earth Planets Space*, **61**, i–xv.

Pirjola, R. (2011): "Modelling the magnetic field caused by a dc-electrified railway with linearly changing leakage currents", *Earth Planets Space*, 63, 991-998.

Sanclement, E. (1974): "Perturbación del campo geomagnético debida a la electrificación de las líneas férreas", *Proceedings de la I Asamblea Nacional de Geodesia y Geofísica*, p. 787-815, Madrid.

Wienert, K.A.(1970): "Notes on geomagnetic obervatory and survey practice", Ed. UNESCO, Brussels.

ON THE THUNDERSTORM OF 10 JULY 2011 AT MAGNETIC OBSERVATORY BUDKOV

P. Hejda [(1)], J. Horáček [(1)], M. Vlk [(1)], T. Bayer [(1)]

[(1)] Institute of Geophysics of the ASCR, 14131 Prague, Czech Republic, ph@ig.cas.cz

SUMMARY

The region around Geomagnetic Observatory Budkov suffers from strong thunderstorms. Strong lightning strikes caused severe damage to electric components and the power supply system on 10 July 2011. All magnetometers with the exception of the GDAS were damaged and put out of order. Also all three GDAS components recorded jumps in their values. It was initially supposed that the electric circuits were damaged or that the sensor slightly moved in consequence of the quake caused by the thunder and a falling tree. This hypothesis had to be modified after the jumps had been observed in the data of other variometers and lightning-induced remanent magnetization was indicated as a probable cause of this event.

1. INTRODUCTION

The region around Geomagnetic Observatory Budkov suffers from strong thunderstorms. For example, in 1994 the newly installed digital magnetometer CANMOS was, in spite of the installed lightning protection modules, severely injured by lightning. Since then all the data links were replaced by optical cables and the same security measures were adopted in installing the second digital system, GDAS. Frequent outages of the mains voltage during storms were solved by sufficient battery capacity.

The observatory is equipped with two digital systems. CANMOS, installed in 1992 in co-operation with the Geomagnetic Observatory of the Geological Survey of Canada, consists of a triaxial Narod S-100 ring-core magnetometer, an ELSEC 820 PPM magnetometer and a control unit based on MS-DOS operating system. The main parts of the GDAS system are a DMI suspended fluxgate magnetometer, an Overhauser proton magnetometer and a Pentium-type embedded PC with a QNX4 operating system and SDAS data acquisition software, developed by the British Geological Survey. Absolute measurements are carried out with the DI magnetometer (fluxgate sensor mounted on a non-magnetic theodolite Zeiss 010B). The second back-up is an analogue Bobrov variometer. The layout of the huts with the systems and the absolute house are shown in Fig. 1.

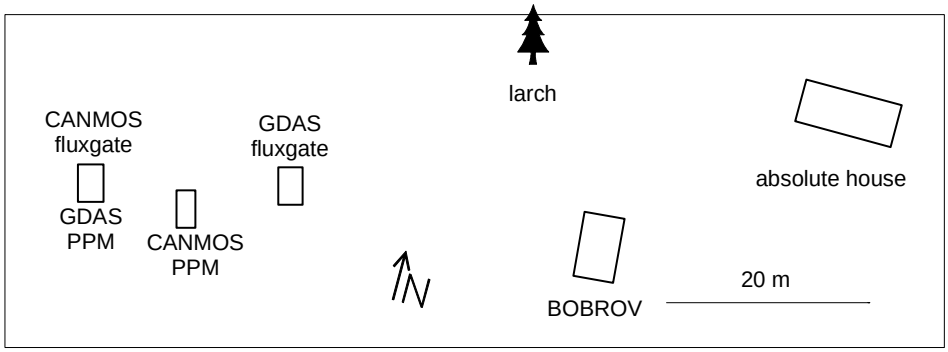

Figure 1 –Layout of the part of observatory area showing huts with variometers and absolute house.

2. THUNDERSTORM FROM 10 JULY 2011

An extremely strong storm occurred on 10 July 2011 (day number 191), when lightning struck a larch in the observatory precinct. The top of the larch broke away and the trunk was split. Most electric and electronic components were damaged. Fortunately, the GDAS

magnetometer kept working. It was later found that all three components recorded jumps: ~ 5.2 nT in D, -1.6 nT in H and 0.7 nT in Z. The time series of 1 Hz data in Fig. 2 shows that the jump occurred within one second. The spikes were caused by lightning. They provide evidence of the frequency of strikes.

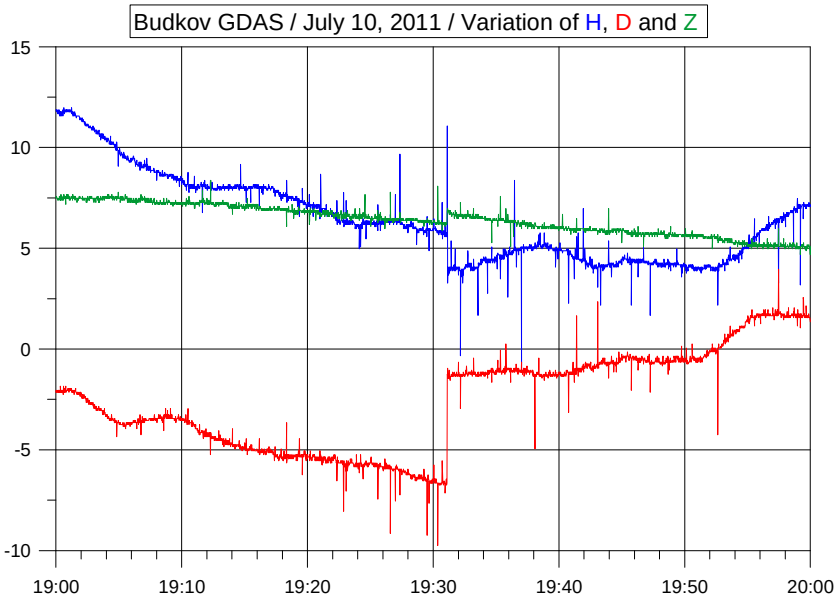

Figure 2 –Variation of the magnetic field recorded by the 3D GDAS fluxgate sensor. Sampling rate is 1 Hz. Values were shifted to zero daily mean.

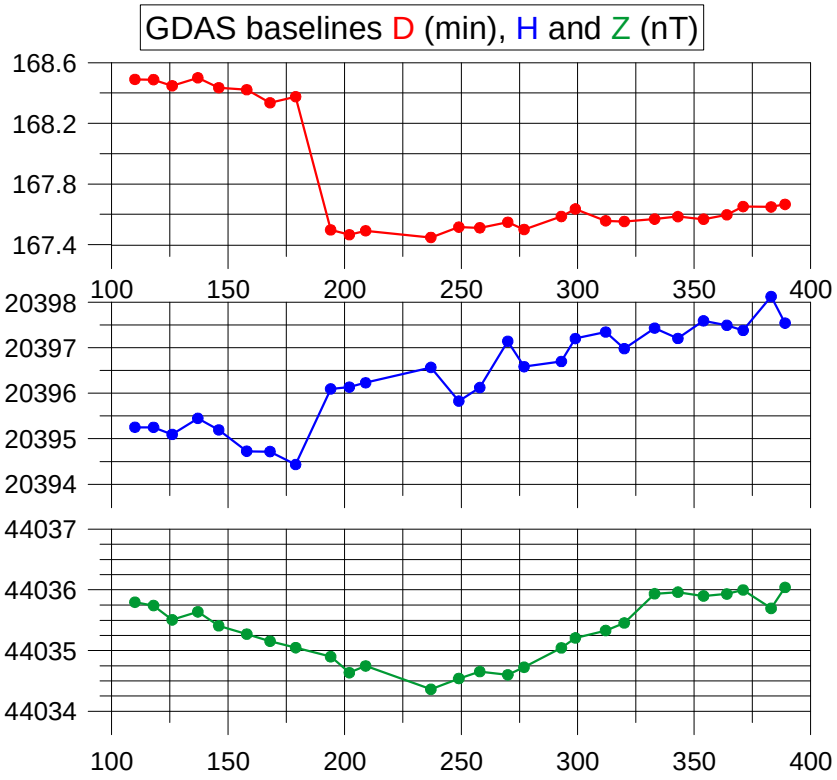

Figure 3 –GDAS baselines. Abscissa shows the sequence number of the day in year 2011; 10 July corresponds to day 191.

The absolute measurements (Fig. 3) carried out in the subsequent period showed that the jumps of the baselines are in good agreement with the jumps in the variation data. The D baseline is very stable. The annual range was 0.2 minutes of arc, which is about 1 nT. The jump caused by lightning was -0.9 minutes of arc = -5.3 nT. The H component is noisier, with a typical scatter of 0.5 nT. The jump observed after the lightning strike was 1.5 nT. The jump in Z (if any) is on the level of the noise. The D baseline indicates that the changed values are stable. There is no visible tendency towards recovery of the initial state.

Based on the results of the GDAS vector sensor, our initial explanation was that the electric circuits had been damaged or that the sensor had slightly moved and turned in consequence of the quake caused by thunder and the falling tree. However, a more detailed examination after the damaged magnetometers had been put into operation again revealed jumps in all of them. The changes are summed up in Fig. 4. The Y-sensor of the CANMOS fluxgate was unstable and the jump could not been estimated. As the influence of the Y-component on the total field is negligible, the total field can be computed from the X and Z components. The result is -3.4 nT which is in very good agreement with the -3.5 nT obtained by the Overhauser PPM placed in the same hut. The jumps of the total field computed from the 3 components recorded by the GDAS fluxgate is -0.1 nT.

The results provide strong evidence that the jumps cannot be ascribed just to faults of instruments caused by lightning. The probable cause of the changes will be discussed in the next section.

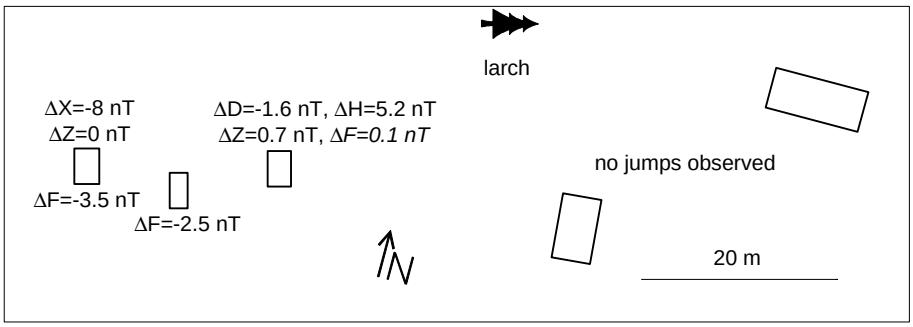

Figure 4 –Jumps of the geomagnetic field observed after the lightning strike. For corresponding magnetometers cf. Fig. 1. The change of the total field printed in italics was computed from the 3 components recorded by the GDAS fluxgate.

3. LIGHTNING-INDUCED REMANENT MAGNETIZATION

Natural remanent magnetization (NRM) of rocks is a subject of intensive study in palaeomagnetism. It is aimed at obtaining information about the geomagnetic field in the past. The components of NRM obtained at the time of rock formation are called primary and later components are called secondary. Secondary magnetization bears many forms that differ in physical and chemical principles and also in time scale. Viscous magnetization is the gradual change of magnetization with time in an applied magnetic field. Lightning-induced remanent magnetization (LIRM) lies on the opposite edge of the time spectrum. It has been recognized as a significant mechanism for sudden overprinting of natural remanence (Graham, 1961).

Lightning is the only natural way of creating magnetic fields larger than the remanence coertivity of fine ferromagnetic particles present in rocks. Verrier and Rochette (2002) explored the surroundings of a tree struck by lightning and came to conclusion that a current of peak intensity of about 100 kA produced a field of 50 mT at a distance of several decimetres. The currents involved in lightning strikes are dominantly directed upward and most lightning flashes include three or four separate upward current pulses.

An instructive example of an anomaly originated from LIRM at Magnetic Observatory Yatsugatake was given by Shimizu et al. (2007). A survey of the magnetic total intensity in the observatory area was carried out in 1975, 1982 and 2005. A magnetic anomaly in the form of a thin patch-pair appeared in the central part of the observatory between 1975 and 1982. The anomalous region was about 30 m long and the amplitude of the anomaly was as much as 80 nT at 2 m above ground level. The lightning which struck the observatory area in July 1981 was earmarked as the probable cause of the anomaly. Modelling confirmed that the anomaly can be explained by magnetization acquired from horizontal lightning electric current in the ground. The repeated survey in 2005 confirmed that the LIRM is stable. A very small effect of viscous remanent magnetization was observed shortly after the event. The surface layer of the area is a tick loam layer composed of Pleistocene volcanic ash.

There are two reasons, why we must abandon the idea of quantitative confirmation that the observed jumps were caused by LIRM. Firstly, a high-precision survey of the magnetic field was not done prior to the lightning strike. Secondly, the jump of ~ 3 nT in magnetic total intensity is too small to leave a well-marked footprint. The dominant bedrock in the observatory area is migmatite which has low susceptibility. Such background is in general less susceptible than volcanic ash at the Yatsugatake Observatory.

The good agreement between the jumps in the CANMOS 3D fluxgate and GDAS PPM records made in the same hut provides strong evidence that the source of the jumps was outside the instruments. Lightning-induced remanent magnetization is a reasonable explanation. Doubters can point out that the larch, which was evidently struck by lightning, is closer to the absolute house than to the CANMOS hut. Nevertheless, according to Shimizu et al. (2007) the vertical lightning electric current can “bend” beneath the surface and run horizontally

to become the subsurface source of remanent magnetization. Moreover, the lightning consists of multiple individual strokes that can spread out over a larger area.

The observatory area is located at the crossing of three soil types: modal cambisol (especially in the eastern part), dystric cambisol, mainly afforested and gley soils in the valley and slopes of the Libotyně Creek. The observatory area is located at the place of change-over fully terrestrial and semihydromorphic soils although significant hydromorphism is not observed. If the electric current followed a preferential water flow potentially influenced by root structure, it could be a good argument for variometer distortion. Unfortunately, we have no soil hydrological data from this event.

4. CONCLUSIONS

The jumps in the recorded geomagnetic field were at first observed in all three components of the GDAS variometer. It was initially supposed that the electric circuits were damaged or that the sensor slightly moved or skipped in consequence of the quake caused by thunder and the falling tree. After the jumps had been observed in the data of other variometers, it became clear that another explanation of the jumps had to be sought. Lightning-induced remanent magnetization was indicated as a probable cause of this event. Nevertheless, we cannot exclude the possibility that the effect was dual: skip of the GDAS variometer and lightning-induced remananet magnetization.

The absolute house was hopefully not affected by any jump in the geomagnetic field. This is supported by two arguments: Firstly, the jumps in the baselines correspond well with the jumps in the variometer data, and, secondly, the difference between Budkov and the closest observatory Fürstenfeldbruck does not show any jump, see Fig. 5. This fact is important from the point of view of the long term stability of observatory measurements.

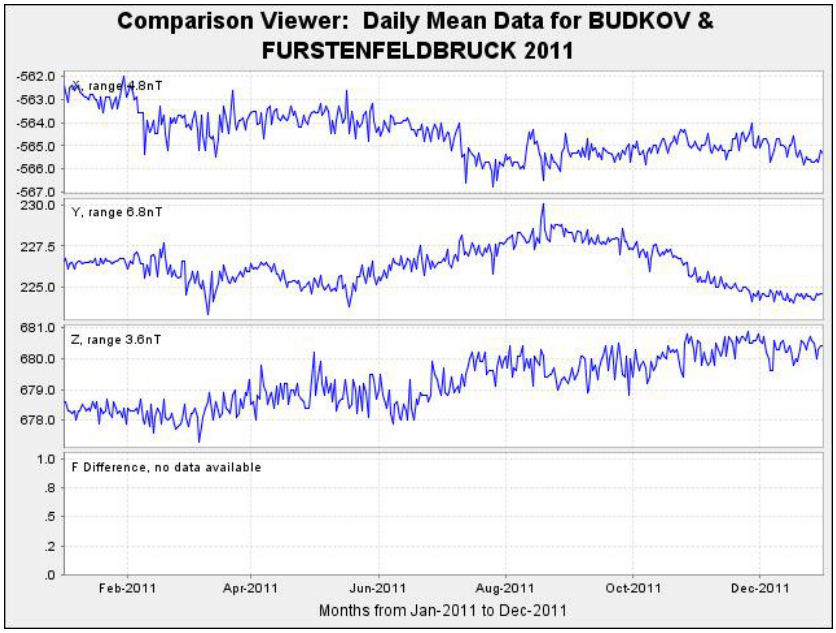

Figure 5 –Difference between Budkov and Furstenfeldbruck observatories, daily mean data.

5. ACKNOWLEDGEMENTS

The operation of the Observatory is supported by the Grant LM2010008 of the Ministry of Education, Youth and Sport of the Czech Republic.

6. REFERENCES

Graham, K.W.T. (1961): "The re-magnetization of a surface outcrop by lightning currents". Geophys. J. Roy. Astron. Soc., **6**, 85-102.

Shimizu, H, T.Koyama and H. Udata (2007): "A geomagnetic total intensity anomaly originated from lightning-induced isothermal remanent magnetization: case of the Yatsugatake Magnetic Observatory, central Japan". Earth Planets Space**, 59**, 141-149.

Verrier, V, and P. Rochette (2002): "Estimating peak currents at ground lightning impacts using remanent magnetization". Geophys. Res. Lett., **29**, 1867, doi:10.1029/2002GL015207

DALAT, VIETNAM: THE REOPENING OF A GEOMAGNETIC OBSERVATORY

B. Heumez [(1)], X. Lalanne [(1)], A. Peltier [(1)], A. Chulliat [(1)], H. Duyen Chau [(2)]

[(1)] Institut de Physique du Globe de Paris, France, heumez@ipgp.fr
[(2)] Institute of Geophysics, Vietnam Academy of Science and Technology, Vietnam

SUMMARY

The Dalat geomagnetic observatory, Vietnam, was reinstalled in April 2011 and joined the INTERMAGNET global network in September 2012. It is run in collaboration between the Institute of Geophysics, Vietnam Academy of Science and Technology, and the Institut de Physique du Globe de Paris. The new observatory is located in the South East of Vietnam, at about 1000 km to the South of the Phu Thuy geomagnetic observatory, which was the first Vietnamese observatory to get the INTERMAGNET magnetic observatory (IMO) status in 1996. One-second and one-minute variation data have been provided on a continuous basis since April 2011. Absolute measurements began at the same time and have been used to calculate quasi-definitive data following the IPGP method. Due to its location, far away from the closest IMO and close to the geomagnetic dip-equator, the Dalat geomagnetic observatory will be particularly useful for global geomagnetic field modeling and the study of the equatorial electrojet.

1. INTRODUCTION

The Dalat geomagnetic observatory (IAGA code DLT, latitude 11.940°N, longitude 108.480°E, elevation 1583 meters), Vietnam, was first opened in 1981. In April 2011, new equipment was installed and training was delivered to observers for absolute measurements by the Institut de physique du globe de Paris, in collaboration with the Institute of Geophysics, Vietnam Academy of Science and Technology (IGP VAST). The Dalat observatory is situated in the south of Vietnam, at 1040Km to the South of Phu Thuy (PHU), a geomagnetic observatory. It produces vector data sampled every second, and was the first Vietnamese observatory to join INTERMAGNET in 1996. The Dalat observatory gained official INTERMAGNET magnetic observatory (IMO) status in October 2012 and is now transmitting 1second real time and quasi-definitive data via the Paris Geomagnetic Information Node (GIN) to the scientific community.

Dalat represents a useful addition to the global network of geomagnetic observatories. It is far enough from the nearest observatory, Phu Thuy, to bring useful measurements for global geomagnetic modeling. The latitudinal distribution of the Dalat and Phu Thuy observatories, of dip-latitudes 4.0°N and 13.2°N, respectively, is particularly well suited to studying the equatorial electrojet, which flows along the geomagnetic dip-equator.

This extended abstract presents the particularities of the observatory site and the instrumental setup. After more than a year of recording, the quality of the variation data and baseline are evaluated based upon the INTERMAGNET criteria.

2. OBSERVATORY SITE AND INSTRUMENTS

The Dalat geomagnetic observatory is installed in the premises of the IG VAST, situated on the hilltop in the outskirts of Dalat. It is surrounded by small houses and fields of flowers, the main production of the area. It includes two buildings dedicated to magnetic measurements. In the first building, we find the variation room at one end, containing the continuously recording vector magnetometer mounted on a stable pillar. A few meters away, a scalar magnetometer is fixed on the wall in a thermally controlled environment. A different room, at the other end of the building, is used as the absolute room, containing the equipment for absolute measurements. A second building few meters away from the first one is used as the control room where computers, back up batteries, and Internet connection for data transmission are connected.

The three components of the Earth's magnetic field are measured by a homocentric (measuring the three components at the same point) IPGP VM391 tri-axis fluxgate magnetometer. This instrument produces 1 Hz data using a method described in Chulliat et al. (2009). One minute values are then produced using the standard INTERMAGNET Gaussian digital filter. The modulus of the magnetic field is

measured every five second by a Geomag SM90R Overhauser-type scalar magnetometer. Vector and scalar data are acquired by an IPGP ENO3 data logger, which is based on a PC system, and transmitted to the Paris Geomagnetic Information Node (GIN) via Internet. In order to compensate the small instrument drift, temperature variations and slow pillar movement, a minimum of one absolute measurement per week is made using a Bartington Mag01H single-axis fluxgate magnetometer mounted on a Zeiss 010A amagnetic theodolite. The magnetic field difference between the absolute pillar and the variation pillar is measured by an additional scalar magnetometer to compensate a local field gradient.

The observatory suffers from frequent thunder strikes in the area. This caused a two-week long loss of data in August 2011 after the electronic of the acquisition system was damaged. A thunder detection system has been installed along with a fiber optic connection between buildings to protect the equipment. During the installation, in April 2011, two observers were trained for absolute measurement and data entry (Figure 1). In order to facilitate the work of the observer and reduce the duration of the measurements, the lighting in the measurement room was improved.

Figure 1 –Training session at the Dalat geomagnetic observatory, April 2011.

3. QUALITY OF THE DATA

Variation data and absolute measurements are available from April 2011. In order to assess the quality of the data, two aspects are evaluated. First, the variation data by looking at the continuity of the data and the scalar residual, that is, the difference between the field modulus directly measured by the scalar magnetometer and the modulus calculated from the vector measurement after correction of the drift by the baseline curve. Secondly, the quality of the baselines is evaluated, that is, the calibration curves used to correct the slow drift in time of the vector magnetometer.

A. VARIATION DATA

The continuity of the recordings are at the upmost importance for the study of the geomagnetic secular variation and the geomagnetic jerks. Except from a 2-week cutout in 2011 due to a electronic damage following a thunder storm, there were no malfunction of the acquisition and very few data gaps since the opening of the observatory. The continuity of the variation data improved considerably from 2011 to 2012. The percentage of missing 1-minute values went from 20.2% on H, E and Z and 2.9% on F in 2011 to 1.1% on all components up to now.

As seen on Figure 2, the scalar residual of hourly mean values remained less than 2nT during the last 12 months of measurements, well within INTERMAGNET's requirements of 5nT accuracy on definitive data.

Figure 3 shows a typical 1-second data, 24 hour magnetogram displaying vector and scalar data along with ΔF (Fs-Fv, where Fs is the modulus measured by the scalar magnetometer and Fv is the modulus recalculated from the vector components). Typical perturbations are caused by relatively frequent flashes of lightning (in the form of 2 or 3 second large spikes on all components, not seen in Figure 3), occasional errors in the scalar acquisition (Figure 3(a), in the form of a 1-second spike on the F component) and a daily 1 nT shift of unknown origin and lasting several hours (Figure 3(b)). Tests to determine if the 1 nT shifts in the data (mostly visible in E component) were caused by human activity or by a dysfunction of the solar panel power source were inconclusive. Human disturbances, possibly caused by the security guard leaving his motorbike nearby the magnetometer room for example, were first suspected, but this hypothesis was ruled out by observing these steps during days when none of the observatory staff was working. During a future travel to Dalat, it is

planned to record the magnetic field with a spare vector magnetometer to rule out equipment malfunction. The Dalat observatory is on top of a hill surrounded by greenhouses (Figure 4), an inefficient ground connection of a nearby electricity apparatus (like the greenhouses lighting system or a large power pump to water the growing flowers/vegetables) may produce ground currents causing these small ΔF steps.

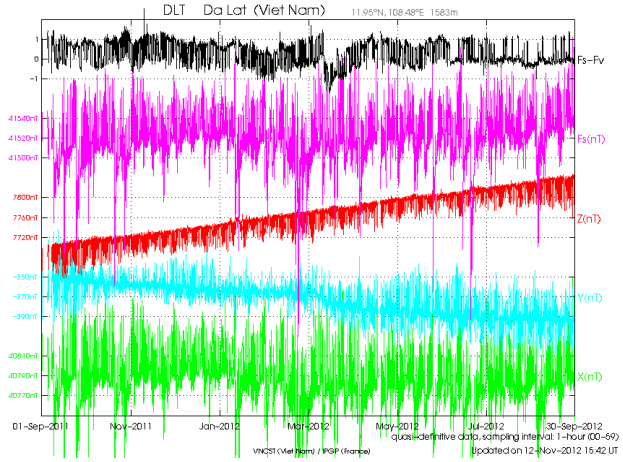

Figure 2 –Quasi-definitive data showing the three components of the vector magnetometer, the modulus values Fs from scalar magnetometer and the scalar residuals of hourly mean values for the past 12 months.

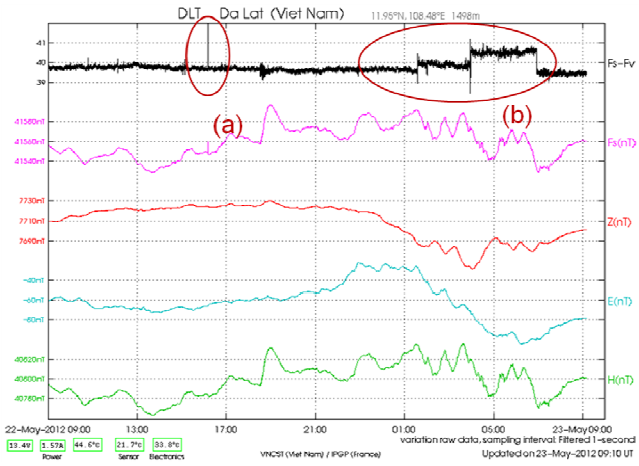

Figure 3 –Variation data recorded at Dalat observatory on May 22, 2012. H, E and Z (sampled every second) are the three components of the vector magnetometer, approximately oriented in the North, East and downward vertical directions. Fs (sampled every five seconds) is the measured scalar field. Fv is the scalar field calculated from the vector components.

Figure 4 –Aerial view of the Dalat magnetic observatory.

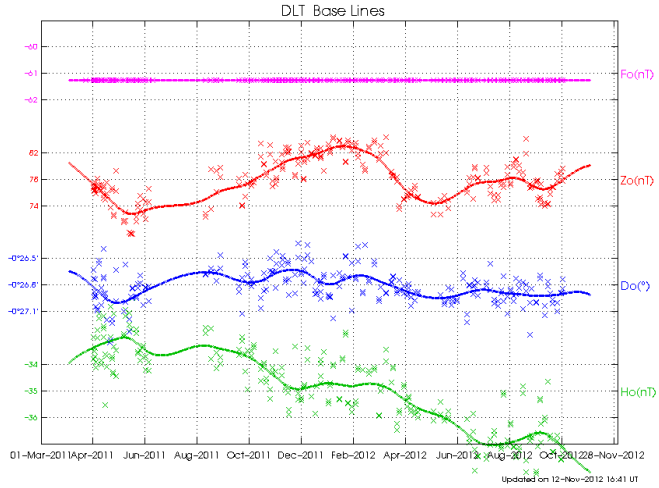

Figure 5 –Baseline of the DLT observatory since the beginning of the measurements in spring 2011 , plotted on October 2012. The baseline values are calculated by spline smoothing.

B. BASELINE

Figure 5 shows the baselines for Dalat observatory obtained for the H (horizontal), D (declination), Z (downward vertical) and F residuals (difference between variation and absolute pillars) components by fitting a spline curve to the correction values deduced from the absolute measurements (see the method described in Peltier and Chulliat, 2010). There was an improvement in the frequency and quality of the absolute measurements over time. 66 double absolute measurements were made in 2011 and so far 71 in 2012 by the local observers, each one represented by a coloured cross. For each component, the quality of the absolute measurements can be assessed by calculating the standard deviation of the differences between the measurements and the baseline curves. The obtained standard deviations are 0.58 nT for H, 9.54 arcsec for D, 1.4 nT for Z and 0 nT for F, being a constant value, which are within INTERMAGNET requirements. These

variations are expected to decrease with time as local observers improve absolute measurement accuracy. Calculated baseline curves have amplitudes of about 5 and 10 nT for H and Z, respectively, and 0.4 arcmin for the declination.

4. DISCUSSION

There is a need for constant and regular support, training and encouragement to the local observers stationed in Dalat to provide reliable data and measures to ensure that INTERMAGNET requirements are followed. The Dalat observatory is now producing quality data for the geomagnetic community.

It currently delivers the following data:

- Real-time 1-second data (every 10 sec) using Earthworm based real-time system on IPGP data platform "Magis" (Truong et al., 2009)
- Real-time 1-minute data on the Bureau Central de Magnétisme Terrestre (BCMT) website (www.bcmt.fr)
- 1-second data and derived means to the BCMT and INTERMAGNET (www.intermagnet.org)
- Quasi-definitive data (every month, see Peltier and Chulliat, 2010) to the BCMT and INTERMAGNET

From now, definitive data will be prepared within a couple of months after the end of the year. After a final cross-check by specialists from other institutions participating in INTERMAGNET, definitive data will be retrievable from the websites of INTERMAGNET and of the Bureau Central de Magnétisme Terrestre (BCMT) and will be published on a DVD together with the definitive data from the whole INTERMAGNET network. A report on the data processing and the events happening every year will be published in the regular BCMT yearbook.

5. CONCLUSION

Due to its geographic location, the value of DLT data for the scientific community data is important. After more than a year of variation data and absolute measurements, the magnetic data quality of DLT is now up to the INTERMAGNET standards. Quasi-definitive data are already produced every month. The observatory has been fully accepted in the INTERMAGNET network in September 2012. The Dalat observatory, given its geographical location, will be very useful in the future, for internal as well as external field studies.

6. ACKNOWLEDGEMENTS

The authors would like to acknowledge the local staff of the Vietnam Institute of Geophysics in Dalat and Hanoi for their cooperation and help insuring continuity in data recording and absolute measurements. On the French side, the Dalat observatory reinstallation and its operation are supported by CNRS-INSU and the IPGP. On the Vietnam side, the Dalat observatory is supported by VAST (Vietnam Academy of Science and Technology) and IGP (Institute of Geophysics).

7. REFERENCES

Chulliat, A., J. Savary, K. Telali and X. Lalanne (2009), Acquisition of 1-second data in IPGP magnetic observatories, *Proceedings of the XIIIth IAGA Workshop on Geomagnetic Observatory Instruments, Data Acquisition and Processing, June 9-18 2008, Golden, USA.*

Peltier, A. and A. Chulliat (2010), On the feasibility of promptly producing quasi-definitive magnetic observatory data, *Earth Planets Space*, 62(2), e5-e8.

Truong, F., X. Lalanne and A. Chulliat (2009), MAGIS: The information system of IPGP magnetic observatories, In: *Proceedings of the XIIIth IAGA Workshop on geomagnetic observatory instruments, data acquisition and processing*, J. J. Love (ed.), U.S. Geological Survey Open-File Report 2009-1226, 271 p..

A NEW OBSERVATORY IN WESTERN AUSTRALIA – ANALYSING THE MAGNETIC-FIELD DIFFERENCES BETWEEN THE OLD AND NEW SITES

L. Wang [(1)], P. Crosthwaite [(1)], A. Hitchman [(1)], W. Jones [(1)], A. Lewis [(1)]

[(1)] Geomagnetism Section, Geoscience Australia, Canberra, ACT 2601, Australia, geomag@ga.gov.au

SUMMARY

Gnangara geomagnetic observatory (GNA) was established near Perth, Western Australia, in 1957. The city has grown considerably over the intervening 50 years and the observatory is now close to Perth's outer suburbs. A new observatory has recently been established near Gingin (GNG), 70 km from Perth, as a successor to GNA. The two observatories will operate in parallel for approximately 12 months before GNA is closed down.

To understand the magnetic-field differences between the two sites we have analysed recorded time series in the time and frequency domains. We find that horizontal variations at both sites are nearly the same at night but are a few nT different during the day. In contrast, vertical variations are enhanced at GNA with amplitudes up to a few tens of nT greater than at GNG.

Considering electromagnetic induction within the regional geology as a likely cause of the differing vertical variations, we have used inverse modelling to derive a sub-surface electrical conductivity model consistent with the observations. The resulting model agrees broadly with the known regional geology derived from other geophysical and geological observations. We conclude that the observed vertical variation differences are largely the result of the observatories' differing proximity to major geological features in the region. We note that the new GNG observatory is less influenced by electromagnetic induction than is GNA.

1. INTRODUCTION

The first geomagnetic observatory in Western Australia was established at Watheroo (WAT), 180 km north of Perth, in 1919 by the Carnegie Institution of Washington's Department of Terrestrial Magnetism (Fleming et al., 1947). The observatory was part of a multi-disciplined program of geomagnetic, atmospheric, meteorological and solar observations carried out at Watheroo supported by a small community of scientists, tradespeople, domestic staff and their families. The observatory was transferred to the Australian Government in 1947 at which time it became the responsibility of the Bureau of Mineral Resources (BMR – now Geoscience Australia).

Watheroo's successor, Gnangara (GNA), was established just outside Perth in 1957. The two observatories ran in parallel during the International Geophysical Year of 1957-58 before WAT closed down in early 1959 (McGregor, 1979) and GNA became the sole source of geomagnetic data in southern Western Australia (see Figure 1).

The city of Perth has grown considerably since GNA was established and, while once the observatory was remote from urban activity, it is now close to Perth's outer residential and industrial suburbs. As a consequence of the increasing activity a new geomagnetic observatory has recently been built near Gingin (GNG), 70 km from Perth, as a successor to GNA, to continue the almost century-long geomagnetic monitoring in Western Australia.

GNA is an INTERMAGNET (www.intermagnet.org) observatory that supplies time series and K indices to various Australian and international data centres. To ensure a smooth observatory changeover, GNA will run in parallel with GNG for approximately 12 months during 2012 to study the differences and similarities between the magnetic fields at the two observatories. This paper discusses some of the early results of this study.

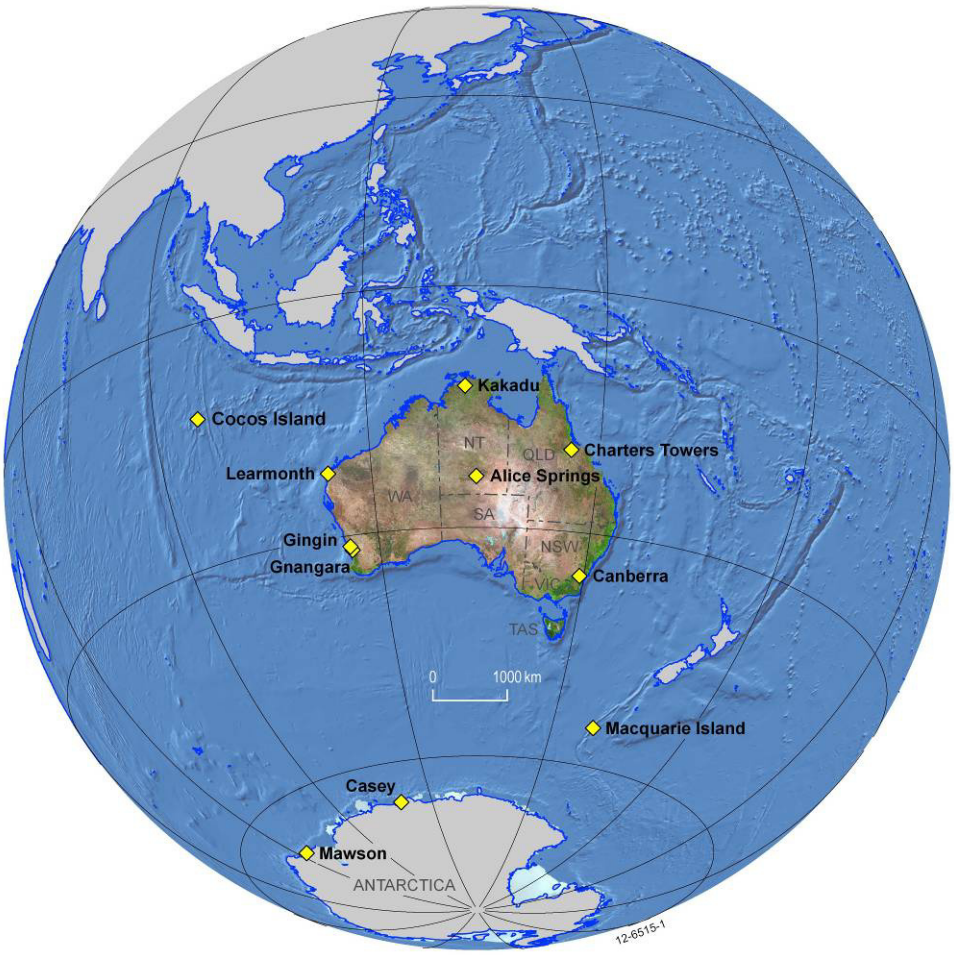

Figure 1 –Geoscience Australia operates eight geomagnetic observatories in the Australian region and three in the Antarctic region. All are INTERMAGNET observatories, with the exception of the recently established Cocos (Keeling) Islands observatory which is yet to be accredited.

2. COMPARISON IN THE TIME DOMAIN

The first approach used to investigate the differences between the magnetic variations recorded at the two observatory sites was a simple comparison of the time series measured in the horizontal north (X), horizontal east (Y) and vertical (Z) components at each site. After reviewing the available data, the time series for 30 January 2012 was selected for this analysis. On that day both quiet and active magnetic conditions are exhibited, allowing comparison of the variations under both conditions.

Difference variations were derived for each of the X, Y and Z components at the two observatories by subtracting the GNA time series from the GNG time series, point-by-point. For ease of presentation in a figure, these difference variations were then adjusted to fluctuate about zero by subtracting the resulting difference-variation mean from every point. This sequence of manipulations is represented in the following equations:

$$\begin{aligned} X(t)_{diff} &= X(t)_{GNG} - X(t)_{GNA} - \overline{X}_{diff} \\ Y(t)_{diff} &= Y(t)_{GNG} - Y(t)_{GNA} - \overline{Y}_{diff} \\ Z(t)_{diff} &= Z(t)_{GNG} - Z(t)_{GNA} - \overline{Z}_{diff} \end{aligned} \qquad (1)$$

where X(t), Y(t) and Z(t) represent the time-dependent variations in the X, Y and Z components. Figure 2 shows the difference variations obtained in this way.

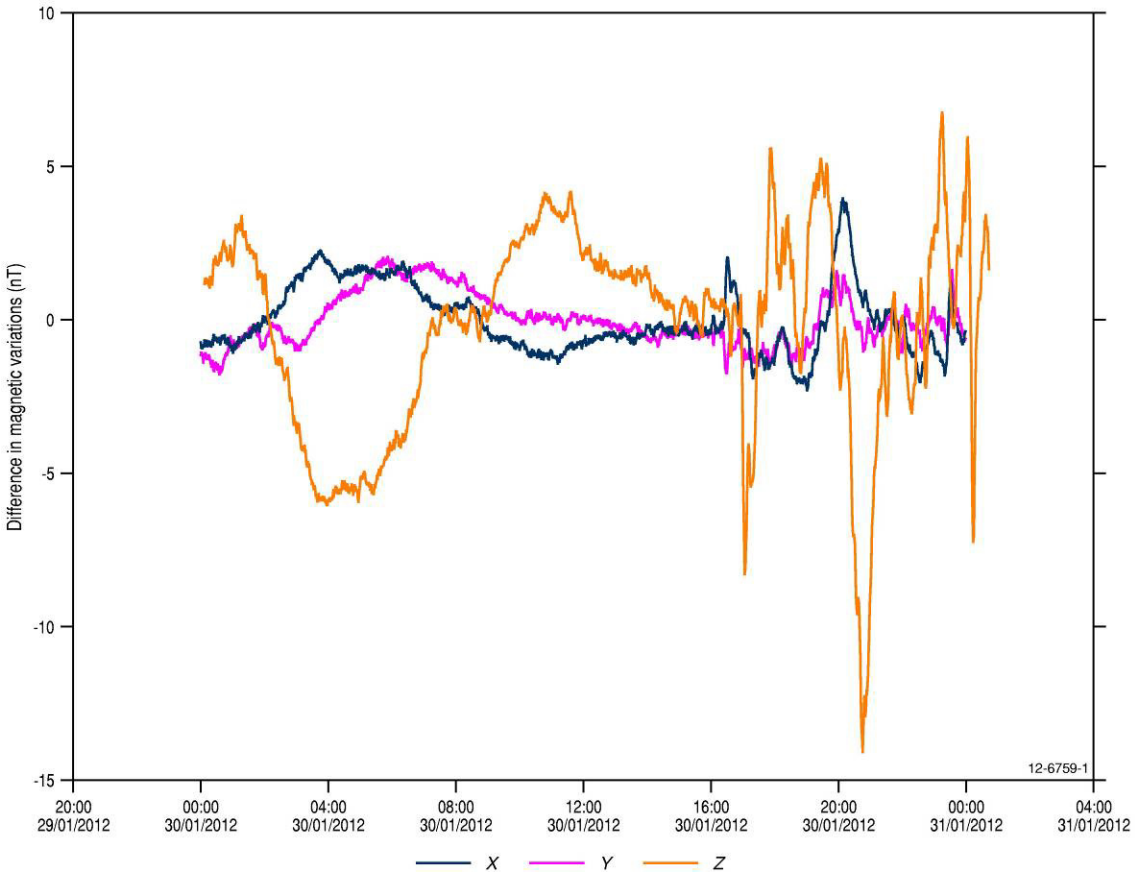

Figure 2 –Magnetic variation differences at GNA and GNG in the X, Y and Z components on 30 Jan 2012. The figure shows variation differences (GNG – GNA) with mean values subtracted (X 297.3 nT, Y 75.1 nT, Z 412.7 nT).

From Figure 2 it is evident that:

1. In both quiet and active magnetic conditions, the variations in the X, Y and Z components are not identical at GNA and GNG.
2. During the quiet period (approximately 00:00 to 15:00), the X and Y-component differences have ranges of 3.7 nT and 3.8 nT, respectively, while the Z-component difference has a range of 9.9 nT.
3. During the active period (approximately 15:00 to 24:00), the X and Y-component differences have ranges of 6.2 nT and 3.3 nT, respectively, while the Z-component difference has a range of 20.3 nT.
4. Across the full day of data, during both quiet and active conditions, differences in the X and Y variations are smaller than differences between the Z variations.

These differences in the time-dependent variations have potential implications for magnetic-activity indices derived from them. In the case of K indices (Mayaud, 1980), for example, scaled over three-hour intervals from the horizontal magnetic components, while the significant differences observed in Z variations will have no impact, the smaller variation differences in X and Y (or H and D) may result in occasional and subtle differences in the measured indices.

To investigate these effects the K indices for 30 January 2012 were scaled for each observatory in the usual manner, using the H and D variations and first removing the Sq contribution. Table 1 shows the nT residuals, the associated K_H and K_D values, and the resulting K indices. In most cases the differences between the nT residuals do not result in different K_H and K_D values. The exceptions to this pattern are the differing K_H values in the 21-24 hour interval. At GNA the 8.5 nT residual results in a K_H value of 1 while at GNG the 9.6 nT residual results in a K_H value of 2. Note, however, that the differing K_H values do not affect the final K indices for the 21-24 hour interval, which are given as 3 for both observatories, obtained from the higher K_D values in the interval. However, had the K_H values been greater than the K_D values in this interval, the K_H values would have determined the final K indices, which would then have been different at each observatory. While the final K indices from GNA and GNG are identical for 30 January 2012, this brief analysis indicates the subtlety with which the differing horizontal variations at the two observatories may play into their derivation.

Table 1 – K index comparison at GNA and GNG for 30 January 2012.

		00-03		03-06		06-09		09-12		12-15		15-18		18-21		21-24	
		nT	**K**	**nT**	**K**	**nT**	**K**	**nT**	**K**	**nT**	**K**	**nT**	**K**	**nT**	**K**	**nT**	**K**
GNA	**H**	2	0	2.3	0	3.8	0	2.8	0	4.8	1	21.1	3	25.1	3	8.5	1
	D	3.9	0	2.5	0	2.9	0	2.1	0	3.5	0	29.5	3	53.8	4	32.2	3
	K		**0**		**0**		**0**		**0**		**1**		**3**		**4**		**3**
GNG	**H**	2	0	2	0	4.2	0	3.1	0	4.7	1	22.6	3	24.5	3	9.6	2
	D	4.1	0	2.9	0	2.7	0	2.2	0	3.6	0	29.4	3	56.3	4	33.1	3
	K		**0**		**0**		**0**		**0**		**1**		**3**		**4**		**3**

3. COMPARISON IN THE FREQUENCY DOMAIN

The second approach uses frequency-domain analysis to investigate the amplitude and phase relationships between the horizontal time series measured at the two observatories. Using the Bounded Influence Remote Reference Processing (BIRRP) method (Chave and Thomson, 2004), X and Y time series from GNA and GNG for a 31-day (44640 minutes) period were Fourier transformed so that the time-dependent X(t) was transformed into the frequency-dependent X(f), and Y(t) into Y(f). Frequency-dependent transfer functions, $T(f)_{xx}$, $T(f)_{xy}$, $T(f)_{yx}$ and $T(f)_{yy}$, were then computed using the relationships described in (2). T_{xx} describes how closely the X variations at GNA and GNG are related in the frequency domain and T_{yy} describes how closely the Y variations are related. T_{xy} and T_{yx} describe the extent to which there is "cross-pollination" of the X and Y variations at the two observatories. The BIRRP analysis produces T_{xy} and T_{yx} values that are very close to zero (within ±0.1), indicating that cross-pollination is not significant, so T_{xy} and T_{yx} are not analysed further here. Figure 3 shows plots of the phase and amplitude of the T_{xx} and T_{yy} transfer functions for periods from 240 s to 98304 s (27 hours).

$$X_{GNG} = T_{xx} X_{GNA} + T_{xy} Y_{GNA}$$
$$Y_{GNG} = T_{yx} X_{GNA} + T_{yy} Y_{GNA} \qquad (2)$$

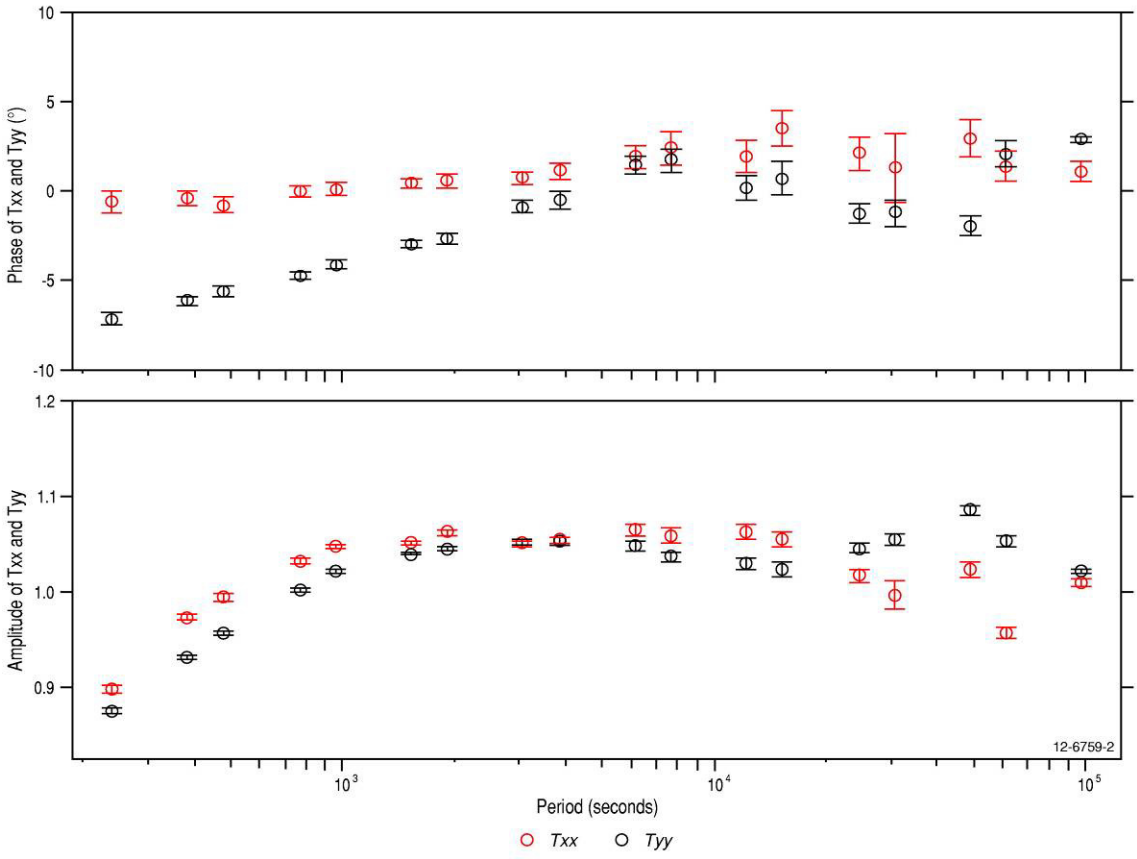

Figure 3 –The phase and amplitude of the T_{xx} and T_{yy} transfer functions in the period range 240 s to 98304 s (27 hours) are shown with their associated error bars.

In Figure 3 we see:

1. The phase of T_{xx}, shown as the red circles in the upper panel, is close to 0° over the period range in the figure, indicating that magnetic activity in the X component at those periods tends to occur essentially simultaneously at GNA and GNG.
2. The amplitude of T_{xx}, the red circles in the lower panel, is close to 1 for periods greater than 10^3 s (16 minutes) indicating that the amplitude of magnetic activity in the X component is very similar at the two observatories. For periods less than 10^3 s the amplitude values between 0.9 and 1.0 indicate that magnetic activity in X at these shorter periods tends to be marginally more subdued at GNG than at GNA.
3. Phase angles in T_{yy}, black circles in the upper panel, from -7° at 240 s to near zero at 3840 s (about 1 hour) suggests that at those periods Y variations tend to occur marginally earlier at GNA than GNG, perhaps implying some sort of westerly propagation.
4. The amplitude of T_{yy}, black circles in the lower panel, shows a similar pattern to T_{xx} and indicates that Y variations at the two obsevatories have similar amplitudes for periods greater than 10^3 s and are slightly more subdued at GNG than at GNA at shorter periods.

4. INDUCTION EFFECTS IN THE VERTICAL COMPONENT

A probable explanation for the enhanced Z fluctuations evident in Figure 2 is electromagnetic induction (EMI) in the local geology caused by deviations from a layered electrical conductivity structure (see, for example, Parkinson, 1959). These deviations may represent, for example, 3D conductivity structures in Earth's crust, the nearby ocean-coast boundary, and the contrast between the continental and oceanic geology. Electromagnetically induced contributions to Z variations tend to be most pronounced at shorter periods (Parkinson, 1959).

Equations (3) represent the relationships between variations in the horizontal and vertical components at each observatory site. All terms are frequency dependent. The transfer functions T describe the EMI effect of the local geology through which the X and Y variations influence the Z variations. They are complex numbers having both real and imaginary (or quadrature) parts.

$$\begin{aligned} Z_{GNG} &= T_{zx} X_{GNG} + T_{zy} Y_{GNG} \\ Z_{GNA} &= T_{zx} X_{GNA} + T_{zy} Y_{GNA} \end{aligned} \qquad (3)$$

Figure 4 plots the real and imaginary parts of each transfer function at each observatory. It shows:

1. At periods less than 10^4 s, at GNA (left panels, red circles), the real component of T_{zx} and T_{zy} are consistently larger than at GNG (right panels). This evidence indicates that the induced component of Z variations at GNA is stronger than at GNG. That is, the time-series data have greater short-period Z fluctuations at GNA than at GNG.
2. The amplitude of transfer function T_{zy} (lower panels) is larger than T_{zx} (upper panels) at each site for periods less than 10^4 s, T_{zx} being close to zero. This evidence suggests that variations in the Y component of the horizontal field are the main contributor, via EMI, to anomalous Z variations. Geological structures in which the EMI takes place tend to be perpendicular to the direction of the inducing magnetic field. This tendency suggests that in this case N-S oriented structures are key, such as the ocean-coast boundary and continental-seafloor geology. This scenario is investigated in the following section.

5. NUMERICAL MODELLING

We have used inverse modelling to derive a two-dimensional sub-surface electrical conductivity structure that is consistent with the T_{zy} data described in the previous section. The model approximates the two observatory positions as lying on an E-W profile (when in fact GNG lies to the NW of GNA). Data from GNG have been projected onto the profile. The model represents the geology by a series of 2D cells with approximate dimensions 2.0×1.25 km (width×depth). Cells in the starting model had a uniform electrical resistivity of 100 ohm.m. The inversion process adjusts the resistivity of each cell through a series of model increments. An unconstrained Occam 2D inversion method (Constable et al., 1987) was used.

Figure 5 shows the result of this modelling with the approximate observatory positions superimposed. A noteworthy feature is a significant electrical discontinuity in the vicinity of GNA with resistive structures to the east and conductive structures to the west, shown in the model as being continuous to a depth of 10-15 km. The model can be interpreted in simple geological terms as showing up to 10 km of conductive sediment (0.01 ohm.m) on the left overlying the basement and a resistive basement outcrop on the right.

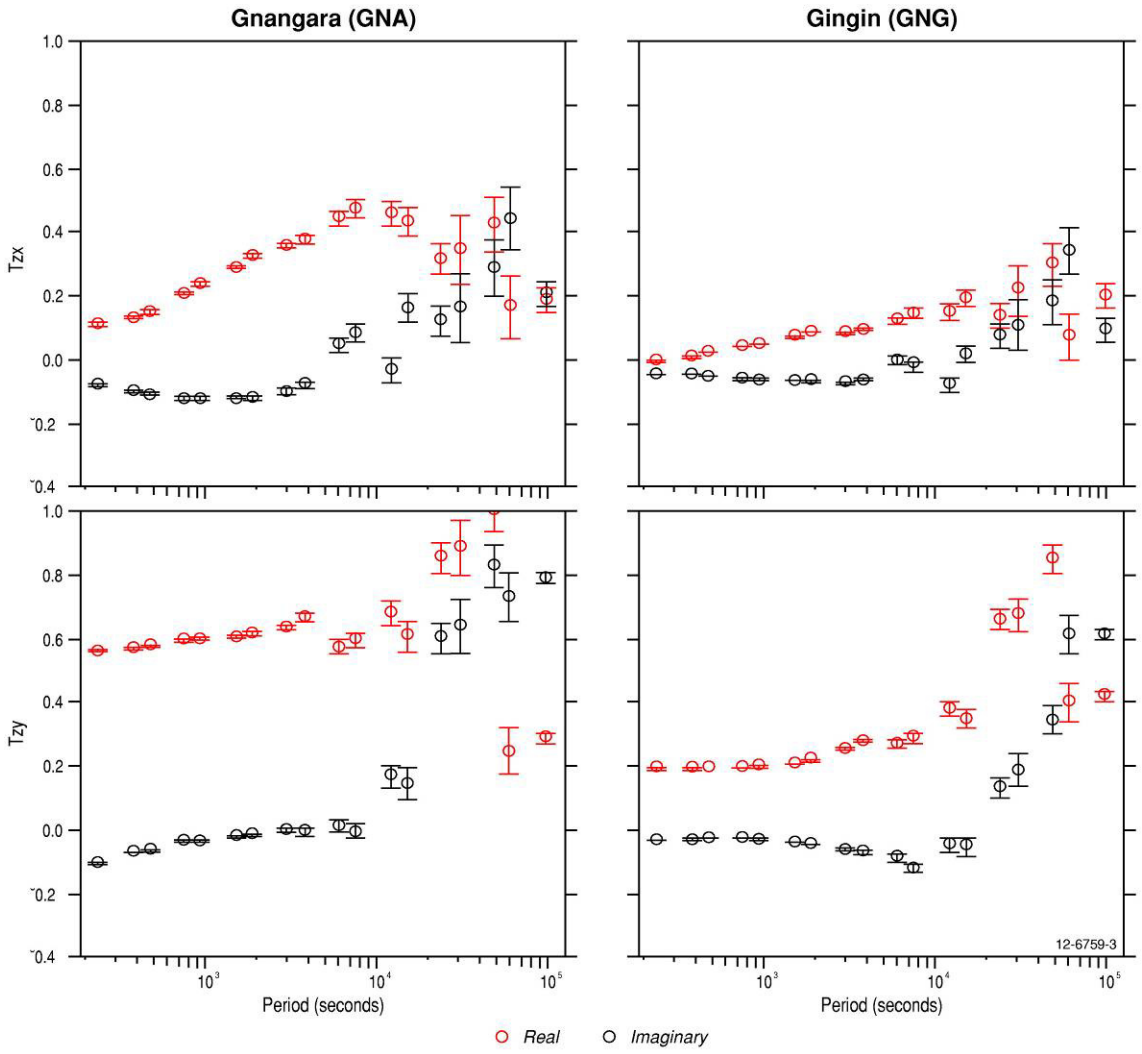

Figure 4 –Real and imaginary parts of the T_{zx} znd T_{zy} transfer functions and their associated error bars for GNA and GNG.

Figure 6 shows the observatory locations on a map of sediment thickness derived from other geophysical and geological methods (FrOG Tech, 2005). The deep blue area near GNG represents a sediment thickness of 11 km. To the right of GNA is the Yilgarn Block. It is evident from the map that GNG is located on a conductive layer (sediment) which is about 50 km away from the conductive-to-resistive (sediment-to-basement) boundary while GNA is closer to the boundary.

Figure 7 shows the model fit to the original T_{zy} data. The close correlation of the observed and modelled data demonstrates that, at short periods, the 2D model of a N-S trending discontinuity with thick conductive sediments adjoining more resistive basement adequately represents the conductivity structure in the vicinity of GNA and GNG. Based on the evidence, data from the new GNG observatory may be expected to be less influenced by EMI than at GNA.

6. CONCLUSIONS

We have used time-domain, frequency-domain and inverse modelling methods to conduct an initial investigation into the similarities and differences between temporal magnetic-field variations recorded at the Gnangara and Gingin geomagnetic observatory sites. We find there are minor differences between the horizontal-component variations but more-significant differences between the vertical-component variations. We conclude that the observed vertical-component differences are consistent with electromagnetic induction effects that are stronger at Gnangara than at Gingin. We note that, despite being minor, the measured differences in the horizontal components may occasionally result in K indices obtained from the new Gingin site being different from those from Gnangara.

7. ACKNOWLEDGEMENTS

This paper is published with the permission of the CEO, Geoscience Australia.

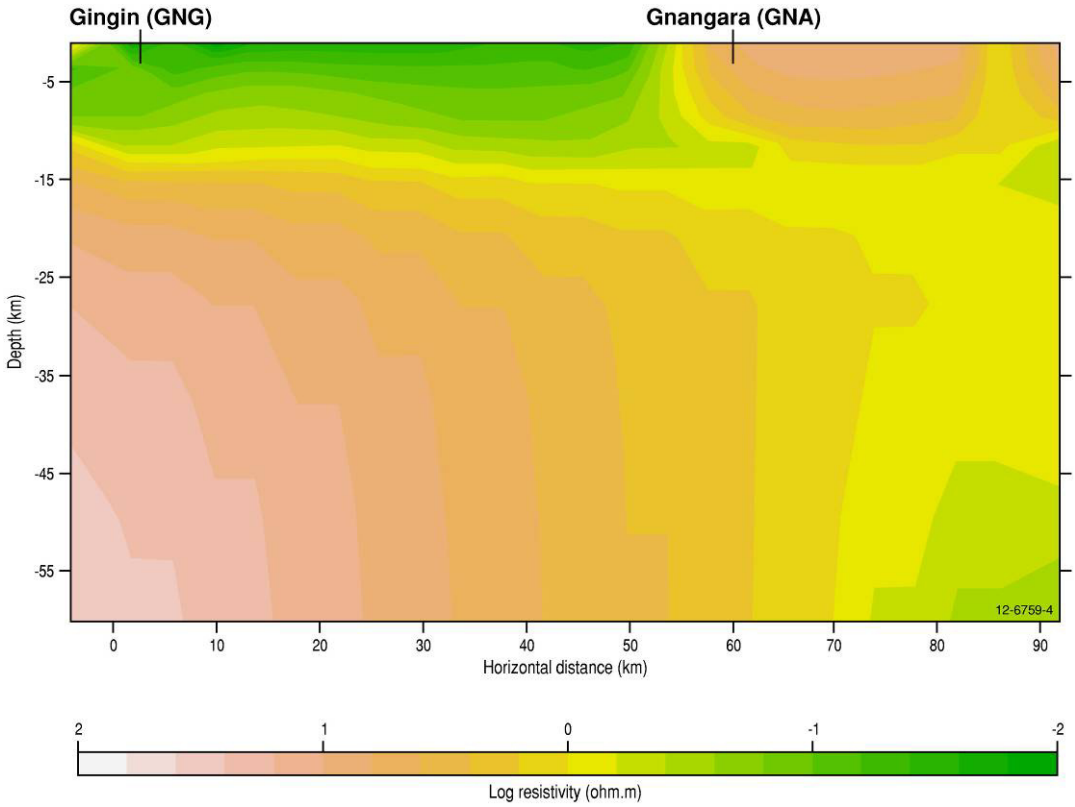

Figure 5 –2D electrical conductivity model inverted from Tzy data using Occam 2D inversion.

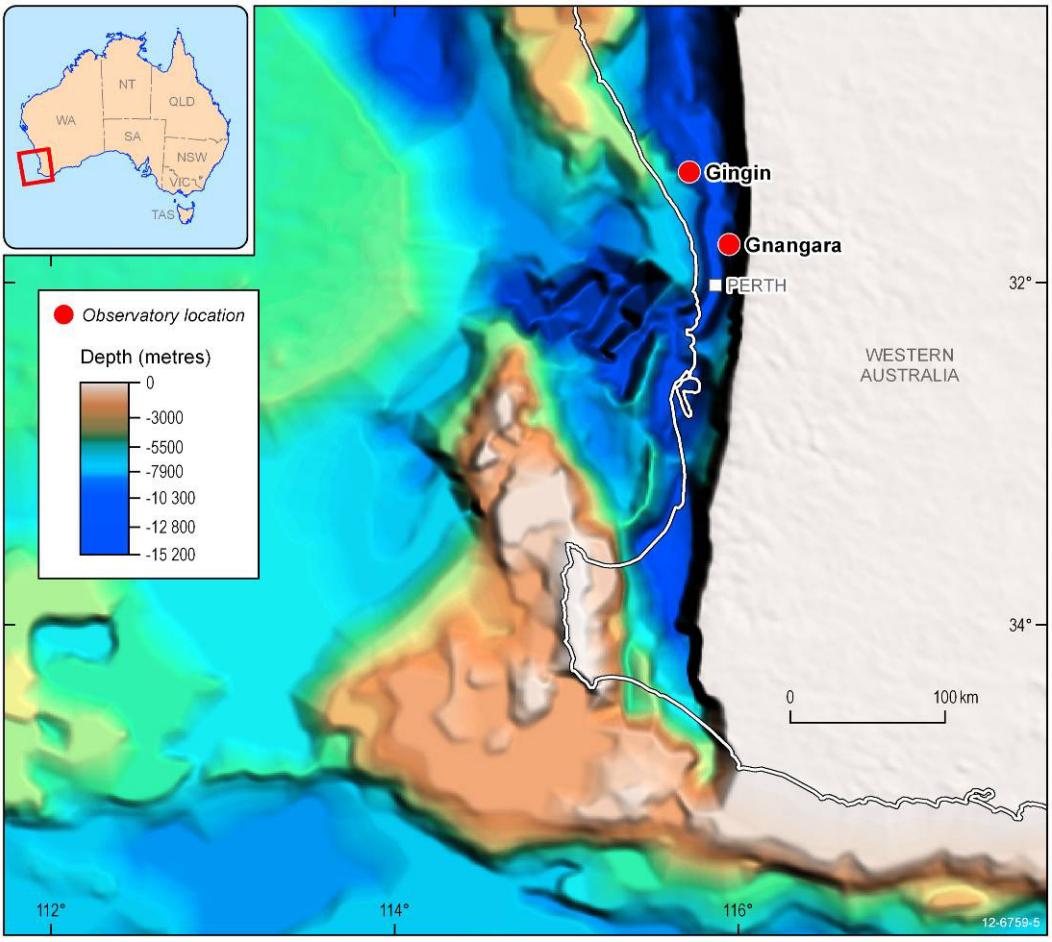

Figure 6 –Gnangara (GNA) and Gingin (GNG) observatory locations on a depth to basement map (courtesy FrOG Tech, www.frogtech.com.au) in Western Australia. The coastline is shown as a white line.

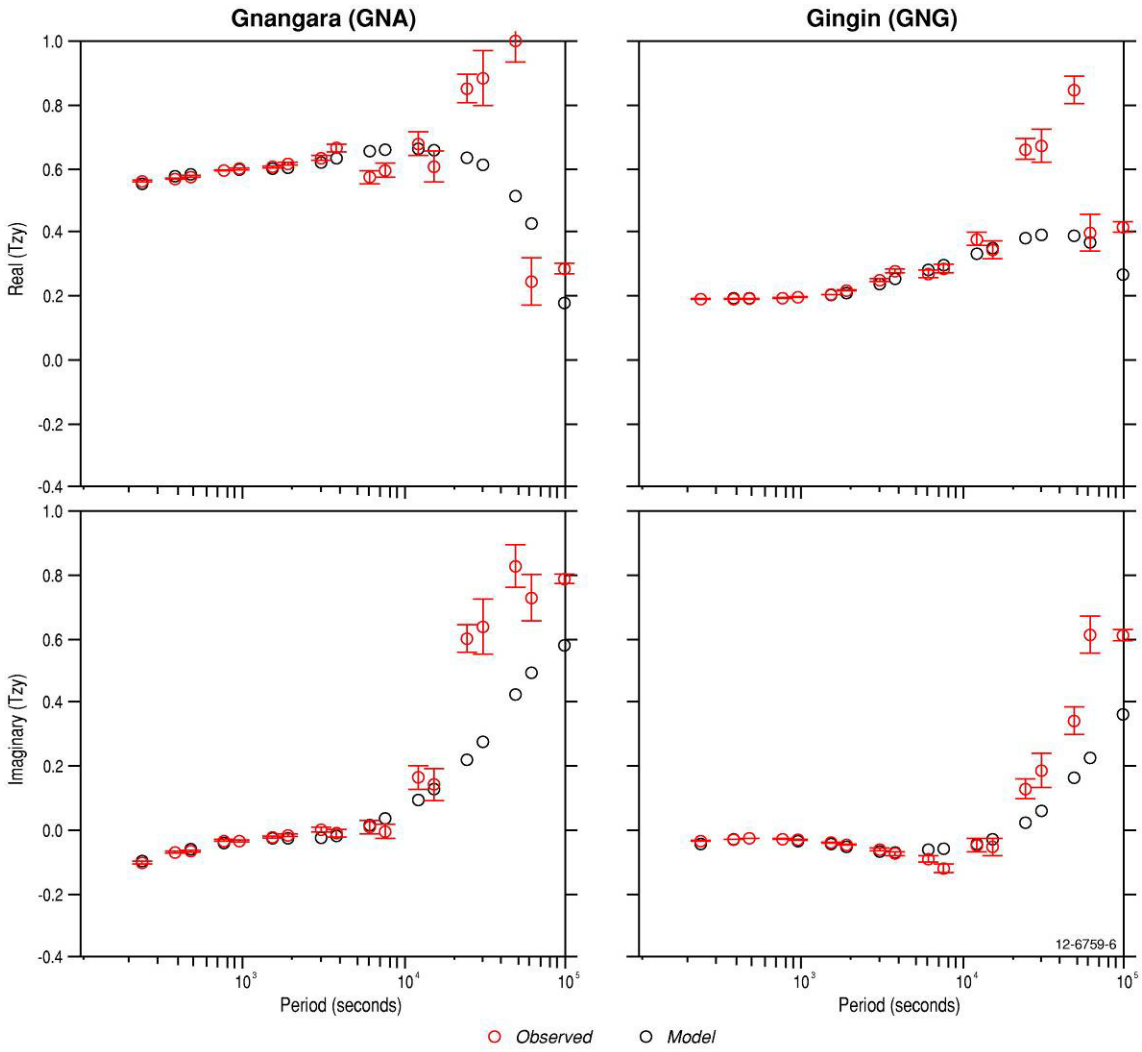

Figure 7 –The fit of the observed and modelled real and imaginary components of the T_{zy} transfer function.

8. REFERENCES

Chave, A.D. and D.J. Thomson (2004): "Bounded influence estimation of magnetotelluric response functions". *Geophysical Journal International*, **157**, 988-1006.

Constable, S. C., R. L. Parker and C. G. Constable (1987): "Occam's inversion - A practical algorithm for generating smooth models from electromagnetic sounding data". *Geophysics*, **52**, 3, 289-300.

Fleming, J.A., H.F. Johnson, S.E. Forbush, A.G. McNish and W.E. Scott (1947): "Magnetic results from Watheroo Observatory, Western Australia 1919-1935". *Carnegie Institution of Washington, Researches of the Department of Terrestrial Magnetism*, **VII-A**.

FrOG Tech (2005): "The OZ SEEBASE™ Project: A new view of Australia's Phanerozoic basins". *PESA News*, **77**, 12-13.

Mayaud, P.N. (1980): "Derivation, Meaning and Use of Geomagnetic Indices". *American Geophysical Union monograph*, **22**.

McGregor, P.M. (1979): "Australian magnetic observatories". *BMR Journal of Australian Geology and Geophysics*, **4**, 361-371.

Parkinson, W.D. (1959): "Directions of rapid geomagnetic fluctuations". *Geophysical Journal of the Royal Astronomical Society*, **2**, 1-14.

GEOMAGNETIC FIELD OBSERVATIONS AT TERRA NOVA BAY (ANTARCTICA)

S. Lepidi [(1)], M. Pietrolungo [(1)], L. Cafarella [(2)], L. Santarelli [(1)]

[(1)] Istituto Nazionale di Geofisica e Vulcanologia, Via dell'Arcivescovado 8, 67100 L'Aquila, Italy, stefania.lepidi@ingv.it

[(2)] Istituto Nazionale di Geofisica e Vulcanologia, Via di Vigna Murata 605, 00143 Roma, Italy, lili.cafarella@ingv.it

SUMMARY

During the 1986-87 austral summer a geomagnetic observatory was installed at the Italian Antarctic Base Mario Zucchelli Station (TNB, geographic coordinates: 74.7S, 164.1E; corrected geomagnetic coord.: 80.0S, 307.7E; magnetic local time MLT=UT-8). In the first years, measurements of the geomagnetic field variations were carried out only during summer expeditions. Since 1991 the recording was implemented with an automatic acquisition system operating through the year. In this work we present the most relevant results obtained from TNB observations coming from more than twenty years of observations, also including a comparison with measurements taken at other Antarctic stations.

1. INTRODUCTION

Geomagnetic field measurements at high latitudes are important to understand dynamical processes of the energy transfer from Solar Wind (SW) to magnetosphere and to characterize several geomagnetic phenomena at high latitude and their relation with the SW and the Inteplanetary Magnetic Field (IMF). Local field lines at TNB are close to the magnetopause: indeed, it is usually in the polar cap and around local geomagnetic noon approaches the cusp, which separates sunward, closed field lines from tailward, open lines. Moreover, the location of TNB with respect to other Antarctic observatories is particularly interesting (Figure 1): it is located at the same geomagnetic latitude as two INTERMAGNET observatories, Scott Base (SBA) and Dumont D'Urville (DRV), as well as the recently installed magnetometer at Talos Dome (TLD); the displacement along a geomagnetic parallel allows to study the azimuthal propagation of geomagnetic pulsations. Also the relative position of TNB and the French-Italian observatory Dome C (DMC) is peculiar, in that they are approximately located at the same geographic latitude, but at different geomagnetic latitude, in that DMC is very deep in the polar cap, close to the geomagnetic pole.

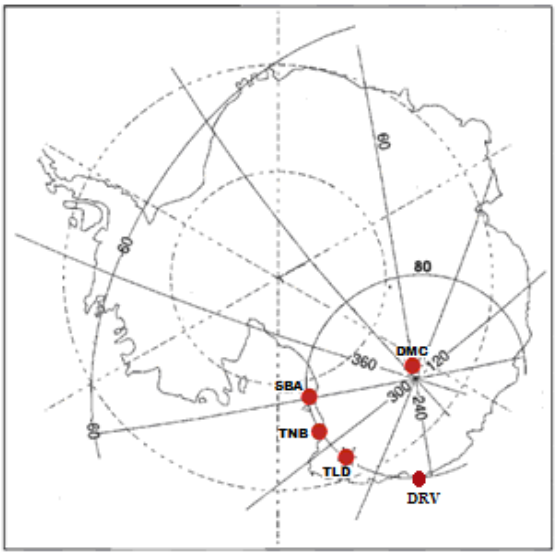

Figure 1 –TNB and the other Antarctic stations used for a comparison in the geographic(dashed) and corrected (solid) geomagnetic coordinate systems. Note that TNB, SBA, DRV and TLD are along the 80°S geomagnetic parallel, while DMC is almost at the geomagnetic pole.

2. EXPERIMENTAL RESULTS

Based on TNB observations, several studies of the geomagnetic field variations were conducted (Cafarella et al., 2009 and references therein), including secular variation, daily variation and geomagnetic pulsations. The availability of long series of data (Figure 1a) has allowed to study long term geomagnetic field variations, such as the secular variation (Bloxham and Gubbins, 1985). In Figure 2b the geomagnetic field trend of the H and Z components, the declination D and the total field intensity F is shown; the yearly data values are average values computed over local summer period, when absolute measurements are regularly performed; for a comparison, the corresponding values from the International Geomagnetic Reference Field (IGRF; McMillan and Maus, 2005) are also shown; it can be seen the good agreement between the measured long term variation and the variation expected from the global model; in particular, F shows a quite steady decrease of about 50 nT/Y (Rajaram et al., 2002).

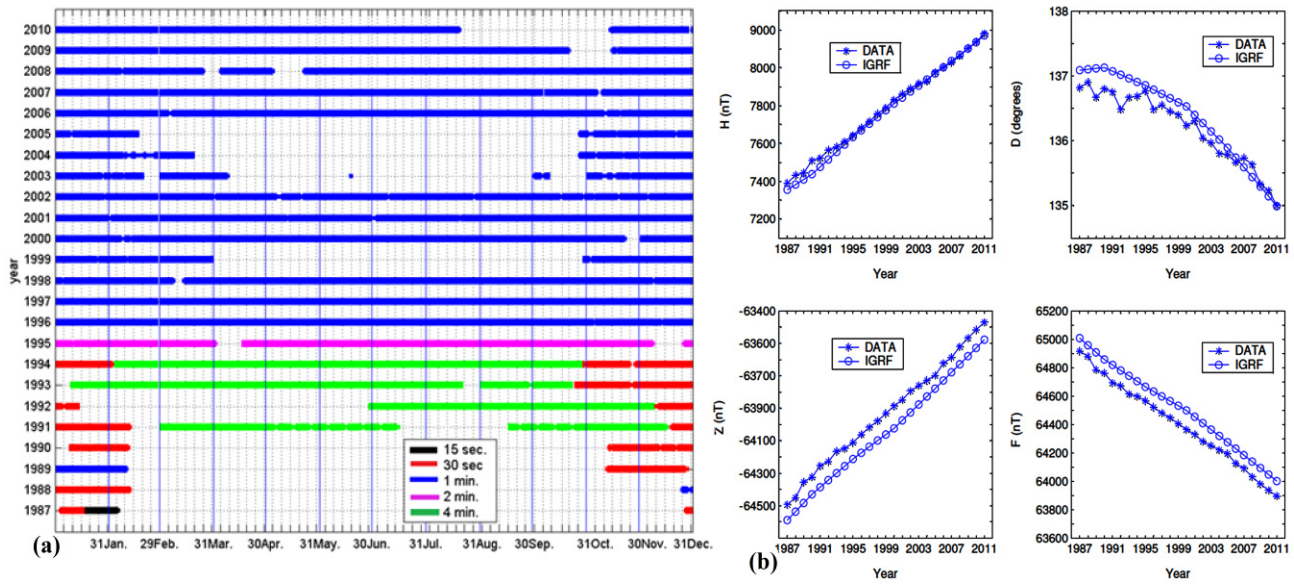

Figure 2 –(a) TNB Data availability (1987- 2010), with data sampling rate; (b) Geomagnetic field trend, together with corresponding IGRF values.

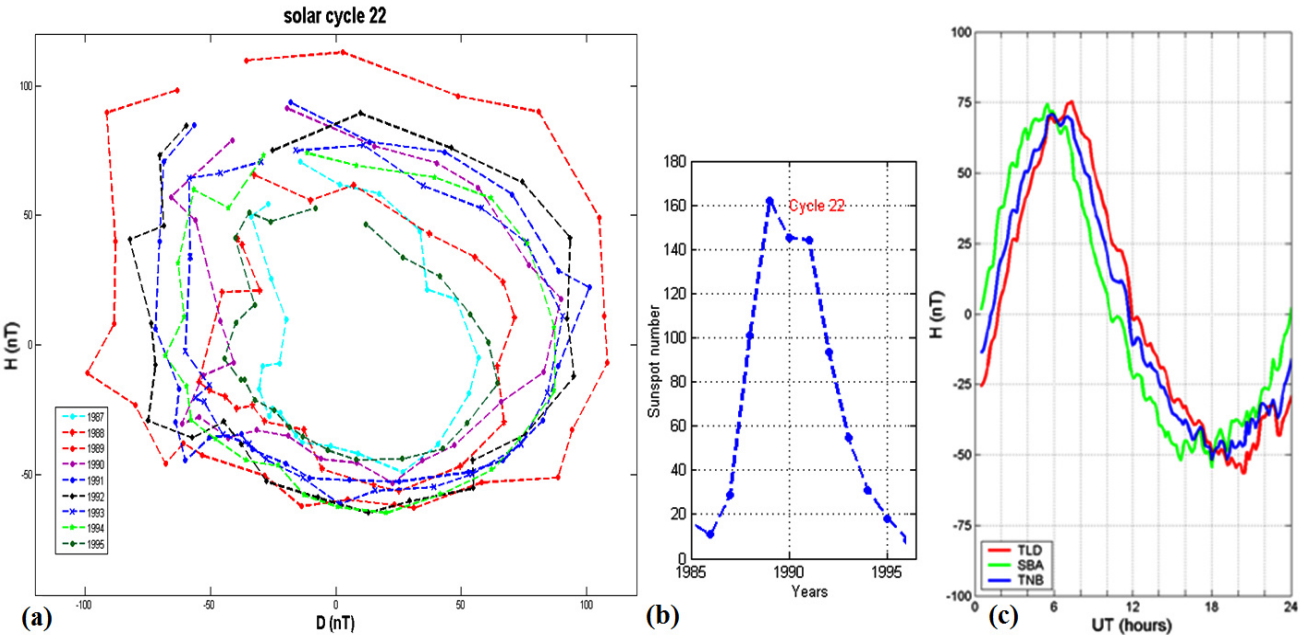

Figure 3 –(a) TNB daily variation hodograms for solar cycle 22 (1987-1995) and (b) corresponding sunspot number; (c) daily variation a three stations.

Daily variation (Matsushita and Xu, 1982) was extensively studied at TNB and other polar geomagnetic observatories (Cafarella et al., 1998, 2007; Lepidi et al., 2003; Santarelli et al., 2007a; Pietrolungo et al., 2008; Lepidi et al., 2011a); it was found that its amplitude strongly depends on solar cycle, season, magnetospheric activity and interplanetary parameters; moreover, both its shape and amplitude show relevant changes approaching the polar cusp. In Figure 3a (adapted from Cafarella et al., 2009) the daily variation is represented by hodograms in the horizontal plane; in each plot the 24 values are median hourly values, computed over austral summer season from hourly

data, after removing the average level; the curves are covered in counterclockwise direction. This odogram representation allows to easily compare different years; the dependence on solar activity clearly emerges: the smallest and largest excursions correspond to miminum and maximun sunspot numbers (Figure 3b), respectively. In Figure 3c the daily variation at TNB, SBA and TLD, averaged over about 2 months (Jan-Mar, 2008) is shown. The diurnal variation is very similar at the three stations, with a clear time shift, corresponding to the Magnetic Local Time (MLT) difference: SBA is leading about 1-hr with respect to TNB and 2-hrs with respect to TLD (Table 1).

Table 1 – Stations with Geographic and Corrected Geomagnetic coordinates and time (UT) of the magnetic local noon

Station	Geogr.Coord.		Corr.Geom.Coord.		MLT noon (UT)
TNB	74.7S	164.1E	80.0S	306.7E	20:13
SBA	77.8S	166.8E	79.9S	326.1E	19:03
TLD	72.8S	159.0E	80.4S	292.4E	21:06
DRV	66.7S	140.0E	80.4S	236.0E	00:54
DMC	75.1S	123.4E	89.0S	54.3E	13:01

Another reasearch field widely investigated from TNB data regards low frequency magnetic pulsations, mostly Pc5 pulsations (Santarelli et al., 2007b; Lepidi et al., 2007, 2011b and references therein), which are geomagnetic field variations of external origin with f=2-7 mHz. From a comparison between the observations at different stations it has been possible to investigate the spatial extent and the propagation of the observed waves. In Figure 4 some examples of pulsations simultaneously observed at TNB and at another Antarctic observatory are shown; in figure 4a (adapted from Santarelli et al., 2007b) it can be seen that the wave activity is very similar at TNB and SBA, but around 17 UT SBA, which is closer to its MLT noon, observes the signal in advance (and with larger amplitude), while the contrary happens around 21 UT, when TNB is closer to its MLT noon. Also the wave packets in Figure 4b,c are very similar at the two stations and in both cases TNB, which is closer to its MLT noon, observes the signal in advance (and with larger amplitude) with respect to the other station. These observations are consistent with a wave propagation in the antisunward direction, away from the noon region.

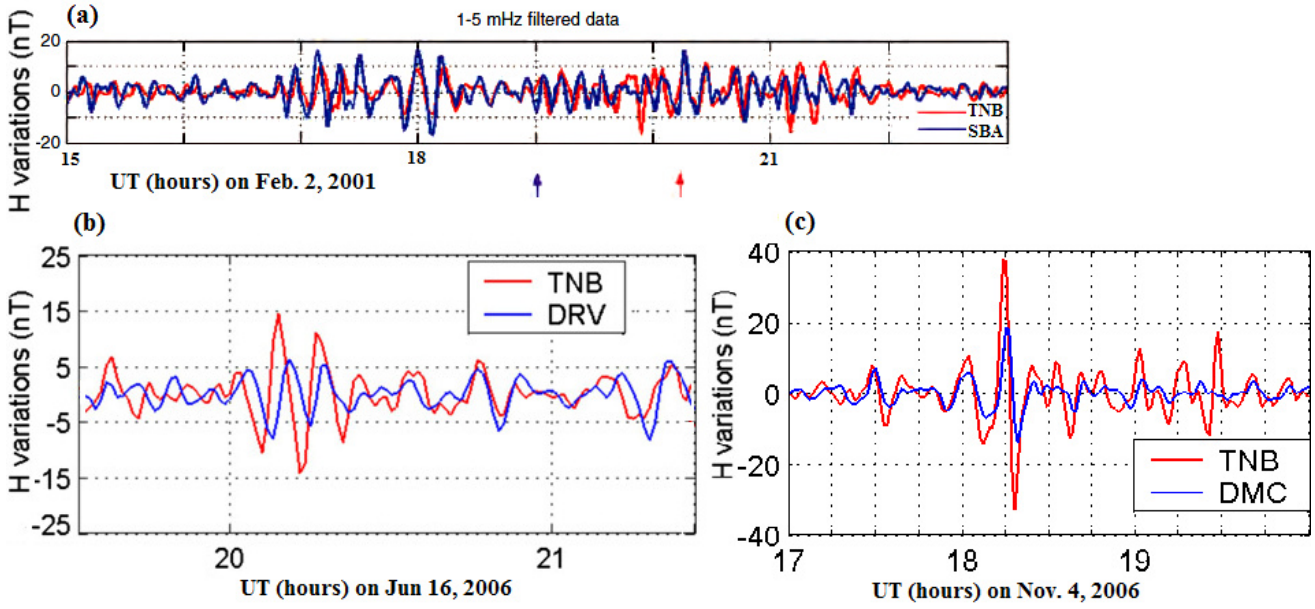

Figure 4 –Pulsation events (a) at TNB and SBA, red and blue arrows indicate 12 MLT at the two stations; (b) at TNB and DRV; (c) at TNB and DMC.

From a statistical analysis of coherent pulsations between couple of stations, with TNB as the reference, it has been possible to infer the preferential propagation direction of low frequency pulsations. In Figure 5 a schematic sketch of the observed average propagation direction between couple of stations is drawn; the subsolar point is at the bottom, so for the stations along the 80°S geomagnetic parallel, also MLT noon is at the bottom. The figure refers to eight different hours during the day for which the statistical propagation direction clearly emerges. The black arrows connecting the position of two stations indicate the dominant propagaton direction for low frequency (about 1-5 mHz) pulsations; the purple arrows indicate that the propagation direction clearly emerges only for the lowest frequencies (up to 2-2.5 mHz). The results show that along the 80°S magnetic parallel, and also between this parallel and the geomagnetic pole, they propagate in the antisunward direction in the dayside hemisphere (particularly evident in the 19 and 21 UT schetches), indicating a generation mechanism related to the Kelvin-Helmholtz instability (Atkinson and Watanabe, 1966); conversely, in the nightside hemisphere

(particularly evident in the 07 and 09 UT schetches), the propagation is in the opposite direction, indicating a generation mechanism related to the dynamics of the magnetotail (Chen and Kivelson, 1991).

Figure 5 –Schetch of the average propagation direction of Pc5 pulsations at different hours inferred from a comparison between couple of stations, with TNB as the reference. TNB, SBA and DRV are along the 80°S, while DMC is almost at the geomagnetic pole. The subsolar point is at the bottom.

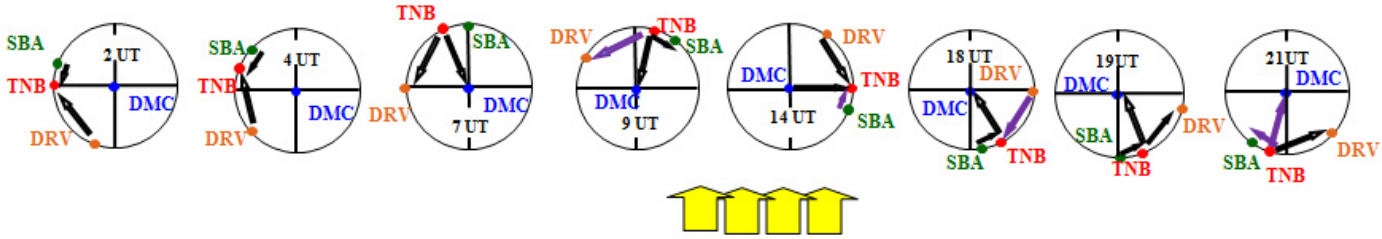

3. REFERENCES

Atkinson, G. and T.Watanabe (1966): "Surface waves in the magnetospheric boundary as a possible origin of long period geomagnetic micropulsations". *Earth Planet. Sci. Lett.*, 1, 89–91.

Bloxham, J. and D. Gubbins (1985): "The secular variation of the Earth's magnetic field". *Nature*, 317, 777.

Cafarella, L., A. Meloni and P. Palangio (1998): "Solar cycle 22 control on daily geomagnetic variation at Terra Nova Bay (Antarctica)". *Annali di Geofisica*, 41, 805–811.

Cafarella, L., D. Di Mauro, S. Lepidi, A. Meloni, M. Pietrolungo, L. Santarelli and J.J. Schott (2007): "Daily variation at Concordia station (Antarctica) and its dependence on IMF conditions". *Ann. Geophysicae*, 25, 2045-2051.

Cafarella, L., S. Lepidi, A. Meloni and L. Santarelli (2009): "Twenty years of geomagnetic observations at Mario Zucchelli Station (Antarctica)". *Annals of Geophysics*, 52, 1-14.

Chen, S.H. and M.G. Kivelson (1991): "On ultralow frequency waves in the lobes of the Earths magnetotail". *J. Geophys. Res.*, 96, 15711–15723.

Lepidi S., L. Cafarella, P. Francia, A. Meloni, P. Palangio and J.J. Schott (2003): "Low frequency geomagnetic field variations at Dome C (Antarctica)". *Ann. Geophysicae*, 21, 923-932.

Lepidi S., L. Cafarella and L. Santarelli (2007): "Low Frequency Geomagnetic Field Fluctuations at cap and low latitude During October 29-31, 2003". *Annals of Geophysics*, 50, 249-257.

Lepidi, S., L. Cafarella , M. Pietrolungo and D. Di Mauro (2011a) "Daily variation characteristics at polar geomagnetic observatories". *Adv. Space Res.*, 48, 521-528.

Lepidi, S., L. Cafarella , M. Pietrolungo and L. Santarelli (2011b): "Azimuthal propagation of Pc5 geomagnetic field pulsations in the southern polar cap". *Adv. Space Res.*, 47, 966-977.

Matsushita, S. and W. Xu (1982): "Equivalent ionospheric current system representing solar daily variations of the polar geomagnetic field". *J. Geophys. Res.*, 87, 8241-8254.

McMillan, S. and S. Maus (2005): "International Geomagnetic Reference Field the 10th generation". *Earth Panets Space*, 57, 12, 1135-1140.

Rajaram, G., T. Arun, A. Dhar and G. Patil (2002): "Rapid decrease in total magnetic field F at Antarctic stations – its relationship to core-mantle features". *Antarctic Science*, 14, 61-68.

Santarelli, L., L. Cafarella, S. Lepidi, D. Di Mauro, A. Meloni and P. Palangio (2007a): "Fourteen years of geomagnetic daily variation at Mario Zucchelli Station (Antarctica)". *Annals of Geophysics*, 50, 225-232.

Santarelli, L., S. Lepidi and L. Cafarella (2007b): "Propagation of low frequency geomagnetic field fluctuations in Antarctica: comparison between two polar cap stations". *Ann. Geophysicae*, 25, 2405-2412.

Pietrolungo, M., S. Lepidi, L. Cafarella, L. Santarelli and D. Di Mauro (2008): "Daily variation at three Antarctic geomagnetic observatories within the polar cap". *Ann. Geophysicae*, 26, 2179-2190.

GEOPHYSICAL COMPLEX OF ISTP RAS SB FOR MONITORING OF ELECTROMAGNETIC FIELDS AT HIGH AND MIDDLE LATITUDES

Y. Lipko [(1)], R. Rakhmatulin [(1)], A. Potapov [(1)], A. Pashinin [(1)]

[(1)] Institute of Solar-Terrestrial Physics RAS SB, 126 Lermontov str., Irkutsk, 664033, Russia, lipko@iszf.irk.ru

SUMMARY

The Institute of Solar-Terrestrial Physics RAS SB (Russia, Irkutsk) has got a hardware-software complex for monitoring of electromagnetic fields at high and middle latitudes. This complex includes the following observation stations:

1. Magnetic Observatory "Irkutsk", founded in 1886, is dedicated to experimental investigation into the Earth's magnetic field by continuous three-component registration of both absolute values and variations of the geomagnetic field in the frequency range between 0 and 5 Hz.

2. Norilsk Complex Magneto-ionospheric Station is situated on the north of Krasnoyarsk region, and it has worked since 1962. At this station, there is a vast complex of geophysical instruments for absolute and variational observations of the Earth's magnetic field.

3. Baikal Magneto-Telluric Observatory "Uzur" located on island Olkhon (lake Baikal, 350 km from Irkutsk) has worked since 1962. Continuous twenty-four-hour all-the-year-round observations of low-frequency horizontal electric fields (telluric current, 0.001–10.0 Hz frequency range) and three-component measurements of magnetic components of geomagnetic pulsations (induction nanoteslameter, 0.001–10.0 Hz frequency range), are performed at this station.

In this report, some scientific results, obtained from observational materials at these observatories, are presented.

1. INTRODUCTION

All observations of the Earth's variable electromagnetic field have been performed in one subdivision of the Institute of Solar-Terrestrial Physics named Joint Geomagnetic Observatory since 1996.

Such unification made it possible to focus the efforts of the Institute's scientific and technical personnel, being engaged in experimental research into the Earth's variable electromagnetic field, on solving concrete tasks arising repeatedly when organized a geomagnetic experiment.

An immediate task of the observatory is continuous twenty-four-hour all-the-year-round monitoring of the Earth's variable electromagnetic field over various frequency ranges at ISTP observatories and presentation of the data on the website of the Institute to solve fundamental and applied problems (www.iszf.irk.ru). When accomplished this main task, technical ones permanently occur and are worked out – reequipment of ISTP magnetometric observations with modern digital equipment, modernization of available equipment, creation of fast-acting information communication channels, development of application packages for data acquisition and primary processing, and so on. Besides technical problems, the personnel of the observatory solve scientific ones as well, which consist in research into the Earth's plasmasphere and magnetosphere oscillation regime during magnetosphere disturbances.

2. JOINT GEOMAGNETIC OBSERVATORY

The Joint Geomagnetic Observatory has a wide variety of geophysical instruments for observing the geomagnetic field (Fig. 1). Actually, it includes two scientific geophysical stations placed on the territory of Russia: one of them on the territory of Buryatia at the Sayan Solar Observatory of ISTP RAS SB, and another at the Norilsk Complex Magneto-Ionospheric Station of ISTP RAS SB (the north of Krasnoyarsk region).

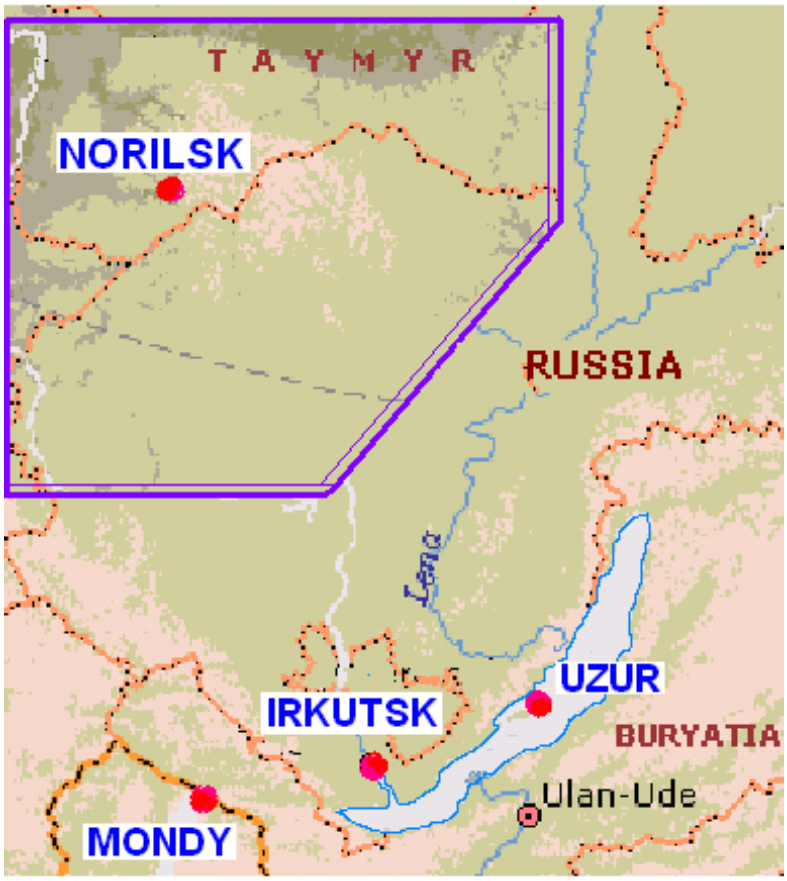

Figure 1 –The map of the Siberian region, Russia, with geomagnetic observatories of ISTP RAS SB.

The observatory is continuous twenty-four-hour all-the-year-round monitoring of the Earth's variable electromagnetic field over various frequency ranges at ISTP observatories

3. THE "IRKUTSK" MAGNETIC OBSERVATORY (MO)

The "Irkutsk" Magnetic Observatory (MO) is intended for the experimental research into the geomagnetic field through the continuous three-component record of both its absolute values and variations in the frequency range from 0 to 5 Hz. This observatory is equipped with standard and unique magnetometric instruments that provide for obtaining data on the geomagnetic field on a level with world standards. These instruments include a high-class flux-gate declinometer-inclinometer MAG-001, made in Bartington's firm, with theodolite from Ceyss's firm to measure GF declination and inclination, a proton magnetometer POS-1 to measure a full GF vector, and a three-component flux-gate magnetometer Lemi-018 to record variations of GF H, D, Z components.

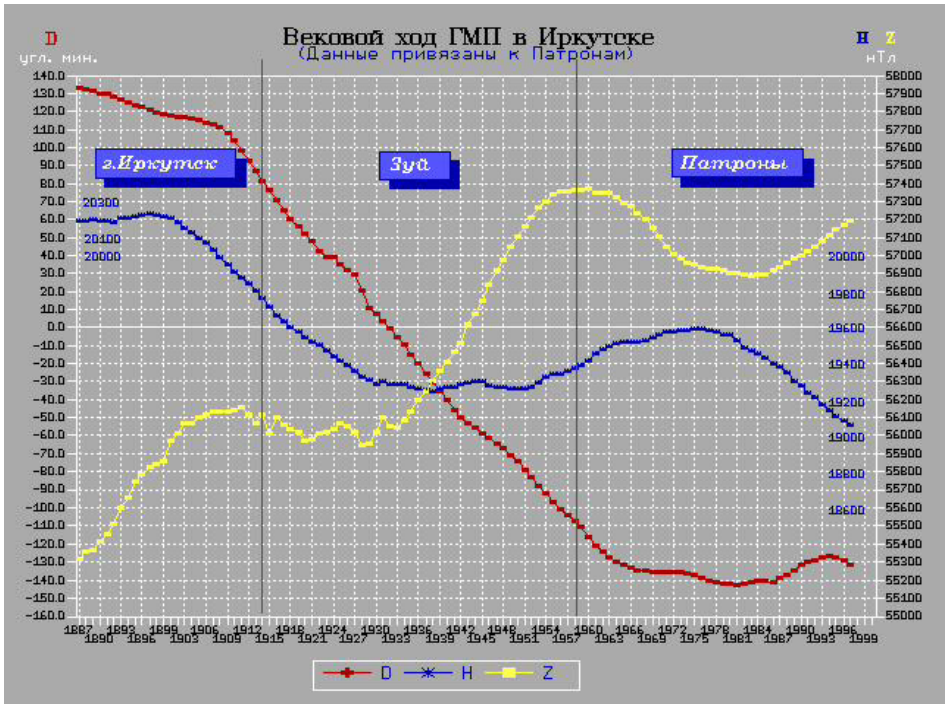

Figure 2 –Secular course of the geomagnetic field according to observations at the "Irkutsk" magnetic observatory (1887–2000).

In the observatory archives, a continuous series of observations has been contained since 1887. Nechaev S.A., the chief magnetologist of the observatory, reconstructed the secular course of the main geomagnetic field components based on observations at the "Irkutsk" observatory for 1887–2000 (Fig.2). The complexity of this procedure lies in the fact that the observatory has changed its location three times since establishment, and experimental data had to be combined considering this fact.

Since 1996, the "Irkutsk" magnetic observatory has been included into the world network of Magnetic observatories "Intermagnet".

4. OBSERVATORY SAYAN SOLAR «MONDY»

Observatory Observatory Sayan Solar «MONDY» is located at the Sayan mountains in the Republic of Buryatia on the frontier with Mongolia at 350 km from Irkutsk. At this observatory, a digital station operates of geomagnetic pulsation registration with the three-component induction nanoteslameter. Data sampling frequency is 30 Hz. Observations at this point are interesting, because nearby there is a seismic station of the Institute of the Earth's Crust RAS SB that makes it possible to carry out complex experiments on an investigation into earthquake responses in the Earth electromagnetic field.

5. THE BAIKAL MAGNETO-TELLURIC OBSERVATORY "UZUR"

The Baikal Magneto-Telluric Observatory "Uzur" (BMTO) is situated on Olkhon Island of Lake Baikal at 350 km from Irkutsk. Observatory performs continuous twenty-four-hour all-the-year-round observations of low-frequency horizontal electric fields (telluric currents, 0.001–10.0 Hz frequency range), three-component measurements of magnetic components of geomagnetic pulsations (inductive nanoteslameter, 0.001–10.0 Hz frequency range). Besides, based on special programs there is carried out:

measurement of the vertical component of geomagnetic pulsation electric field (a vertical measuring line in Baikal);

record of electromagnetic radiation in the frequency range from 10 to 300 Hz (a measuring 15-meter ring, vertical component);

observations of VLF radiations, the atmospheric electric field, and other parameters using equipment being brought.

High-accuracy calibration of sensitive magnetometric equipment is regularly carried out. Continuous observations of geomagnetic pulsations have been practised since 1967. There are observational data for 26 years, whereas for previous 5 years – fragmentary recording materials. In the data archive, there are unique materials of synchronous recordings of six components (three magnetic and three electric ones) of the low-frequency electromagnetic field carried on during special experiments on ice of Lake Baikal. This unique experiment was organized to test the hypothesis of a possibility to represent Pc3 pulsation field as a nonuniform plane wave realized by a superposition of magnetic and electric modes. The experiment disclosed that the vertical component of marine currents over a range of Pc3 pulsations is of the order of 10 % from horizontal components (Buzevich, 1981). By this is meant that ignoring electric mode in the Pc3 pulsation field is unjustified.

6. THE NORILSK COMPLEX MAGNETO-IONOSPHERIC STATION

The station is placed on the north of Krasnoyarsk region and has operated since 1962. This station has got a vast complex of geophysical equipment including a digital digisonde, a station of oblique sounding, an LFM sonde, a riometeric station, a station of cosmic rays, and fundamental and variation observations of the geomagnetic field (declinometer-inclinometer Bartington, three-component flux-gate magnetometer Lemi-018, proton magnetometer POS-1). Recording of geomagnetic pulsations is making by the induction nanoteslameter Lemi-30.

Such a vast base of experimental facilities allows us to carried out original experiments on research into variety of magneto-ionospheric relations. For one example of such a complex experiment, we cite results of experimental studies of relation between shortperiod variations of the Doppler frequency shift of a radio signal reflected from the ionosphere (DFS) and geomagnetic pulsations.

Studying interrelation between these geophysical phenomena is of indubitable interest. From the standpoint of fundamental investigations this is necessary for investigating influence of hydromantic waves on the structure and dynamics of the high-latitude ionosphere. Variations of characteristics of HF radio waves, in particular, of the Doppler spectrum, during observations of geomagnetic pulsations are of practical interest.

Unfortunately, a clear-cut idea is still absent both of the morphology and of physical nature of relations between ionosphere parameter variations and geomagnetic pulsations. The purpose of our research was to determine regularities of variation of HF radio-wave propagation characteristics during observations of geomagnetic pulsations of different types. For this purpose, a special experiment on synchronous record of DFS variations and geomagnetic pulsations was organized at the Norilsk station. The spectral analysis of many occurrences of synchronous registration of these two phenomena disclosed that in a period of Pc5 pulsation observation the DFS variation spectral component corresponding to the Pc5 frequency abruptly increases (Lipko, 2001). This agreement between time series, geomagnetic pulsation spectra, and DFS variations recorded synchronously suggests that hydromagnetic waves of the Pc5 range when interacted with the ionosphere F2 layer make a basic contribution to short-period DFS variations.

7. REFERENCES

Buzevich, A.V., Potapov A.S. (1981) “Direction analysis of Pc3 on Baikal”. *Investigations on Geomagnetism, Aeronomy, and Solar Physics*, **53**, 99–103.

Lipko Yu.V., Rakhmatulin R.A., Vugmeister B.O. (2001) “Ionosphere manifestations of geomagnetic pulsations at high latitudes”. *Geomagnetism and Aeronom*, **3**, 332–336.

A NEW GEOMAGNETIC OBSERVATORY IN CROATIA

I. Mandic[(1)], A. Csontos [(2)], B. Heilig [(3)]

[(1)] Department of Geophysics, Faculty of Science, University of Zagreb, Horvatovac 95, Croatia, mandici@gfz.hr
[(2)] Eötvös University, Budapest, Hungary
[(3)] Geological and Geophysical Institute of Hungary, Budapest, Hungary

SUMMARY

Almost a decade ago we started to renew the research and monitoring of geomagnetic activity in Croatia. The purpose of these measurements was to obtain insight into the structure of the local field and to determine the best location for an observatory. A location for the future observatory in Lonjsko Polje was found, and by October 2011 the construction of the observatory buildings was completed. Since February 2012, the total field measurements have been continuously performed and from May 2012 real-time variation data has been collected. The observatory is not yet fully established, but we anticipate it to be fully operational by the end of summer 2012.

1. INTRODUCTION

In 2003 V. Vujnović and colleagues from the Department of Geophysics, Faculty of Science, made the first measurements of total field intensity over the central northern part of Croatia (Vujnović *et al*. 2004). The following analysis of the Croatian geomagnetic field was conducted by calculating the declination, inclination, horizontal and total intensity using the global geomagnetic Comprehensive Model CM4 (Sabaka *et al*. 2004) for the entire Croatian territory (Verbanac and Korte 2006). These results were used to understand the structure of local field and to find a suitable location for a new geomagnetic observatory. The new Croatian observatory requires an area with a low field gradient to avoid magnetic anomalies (Jankowski and Sucksdorff 1996). After additional surveys and research (Verbanac and Vujić 2012) a location for the future observatory in Lonjsko Polje was determined.

2. ABOUT THE OBSERVATORY

The first geomagnetic observatory in Croatia is located in the area of the Nature Park Lonjsko Polje (central northern part of Croatia, Fig. 1). After several years of exhaustive surveys (Verbanac and Vujić 2012) this location was chosen because it is an area without magnetic anomalies, with a low field gradient and far enough from civilization noise. The location is on a flat pasture-ground (dimension of 600x500 m^2) more than 800 m from the main road (a small low-traffic non-asphalted road passes by one end of a pasture), more than 1 km from a village, 65 km from Zagreb and 90 km from DC load railway, 8 km from AC load railway and 9 km from highway, 55 km from the nearest airport.

Our observatory is comprised of several huts (Fig. 2) which are made from non-magnetic materials. The whole observatory's power supply is from the solar cells positioned on the roof of the control house (C). This is the only object which is allowed to have relatively small amounts of magnetic materials due to 90 m distance from other objects that are hosting magnetometer electronics and their sensors. Further, in C house we have a system for the data acquisition that is connected with magnetometers in other objects. The data are transmitted daily to Department of Geophysics in Zagreb.

The observatory owns several instruments, two proton magnetometers (GEM Systems, Canada), for measurement of the total intensity (*F*), Zeiss based 010A nonmagnetic theodolite (MinGeo, Hungary) with DI fluxgate magnetometer, Model G (Danish Meteorological Institute) for measurements of the absolute values of declination (*D*) and inclination (*I*), and the dIdD magnetometer (GEM Systems, Canada) that measures the relative changes in inclination (*dI*), declination (*dD*) and the total intensity (*F*).

Continuous recordings are performed by the dIdD in the variometer (V) house and the proton magnetometer in the OP hut (Fig. 2). To achieve relatively stable temperature conditions, the dIdD is enclosed by wooden box with 0.5 m thick styrofoam walls (Fig. 3). The future

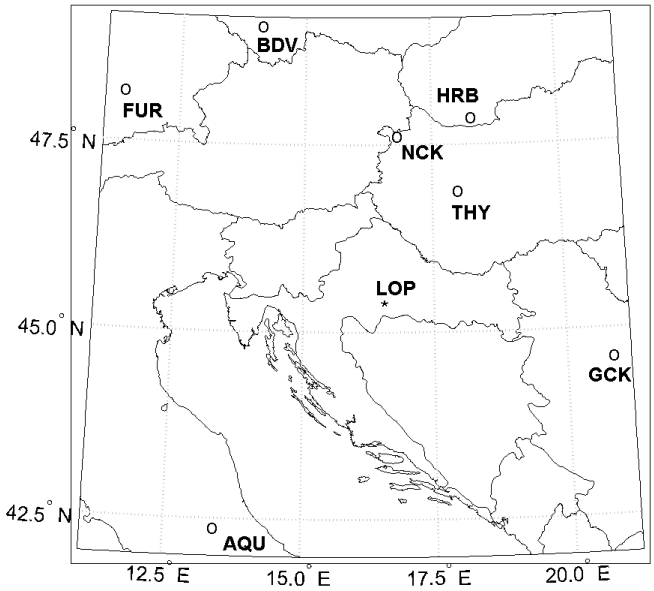

Figure 1 –Positions of the observatory in Lonjsko Polje (LOP – not official IAGA three letter code) and surrounding INTERMAGNET observatories L'Aquila(AQU), Budkov(BDV), Fürstenfeldbruck (FUR), Grocka (GCK), Hurbanovo (HRB), Nagycenk (NCK) and Tihany (THY). (Taken and modified from Verbanac and Vujić 2102.)

Figure 2 –Four objects that constitute Lonjsko Polje observatory: OP hut, control house, absolute house and variometer house.

Figure 3 –Left: The dIdD inside the insulation box; Right: The fluxgate theodolite on the absolute pillar.

DI flux measurements will be carried out on the absolute (A) pillar (Fig. 3) with coordinates: 45° 24' 29'' N, 16° 39' 33'' E and 95 m altitude above sea level. This pillar presents the observatory reference. In order to determine offset in the total field intensity between the A and V pillar the second proton magnetometer is used. Preliminary results shows that the differences in the total field intensity between the V and A pillar is around 2.1 nT and between the V pillar and the OP hut is about 4.4 nT, i.e. 2.3 nT difference between the A pillar and the OP hut. The distances between the V, A pillar and OP hut are more than 25 m, where the northernmost point of measurement is the V pillar

and OP is the southernmost. This result indicates that the observatory is located on very homogenous and the low field gradient terrain (Jankowski and Sucksdorff 1996).

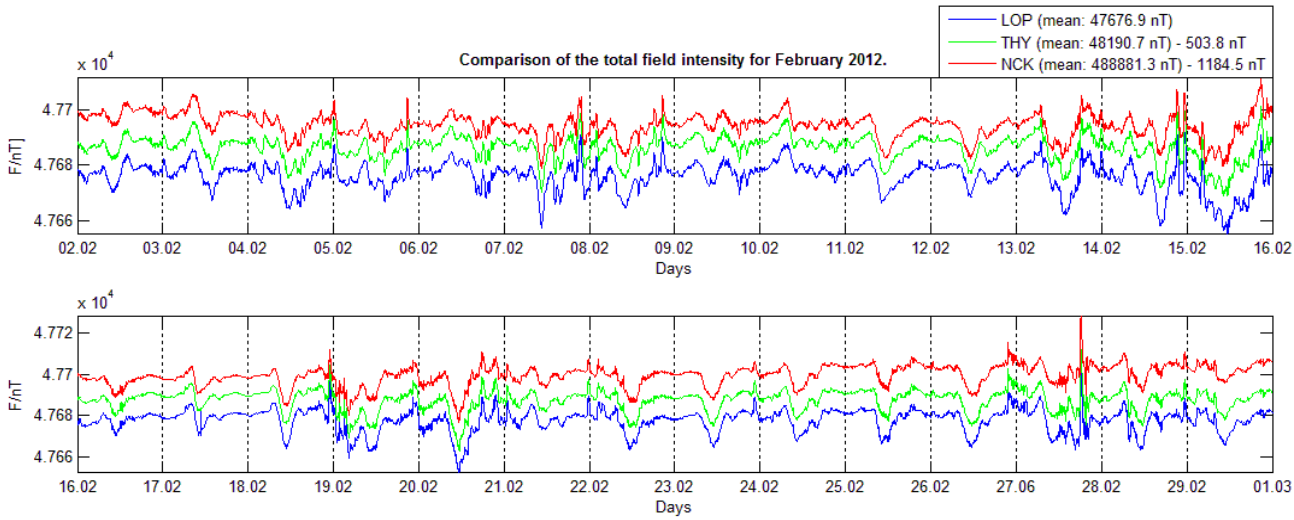

Figure 4 –LOP, THY and NCK magnetograms of the total field intensity. In curved brackets are shown mean values for period within 02 February and 01 March 2012. On the right side of the legend are displayed subtracted values from THY and NCK means so that we have 20 nT shift between recordings.

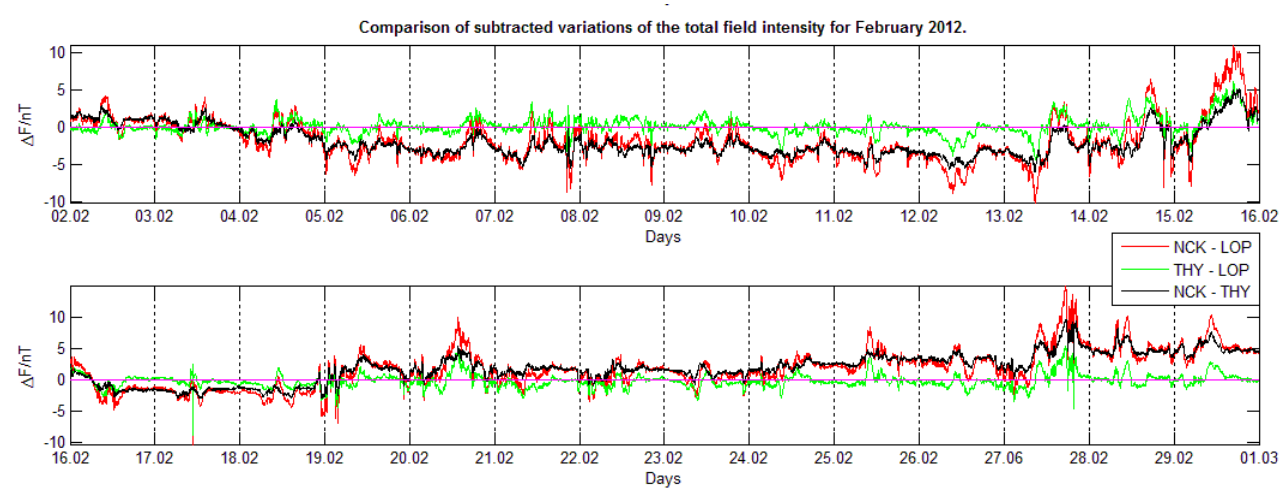

Figure 5 –Comparison of subtracted variations of the total field intensity shown on Fig. 3. Null value is denoted with magenta.

3. THE FIRST DATA

After the completion of construction works in October 2011 the observatory was ready for furnishing and installation of instruments. Due to the remote location of the observatory, the only possible source of power supply was through the solar panels and batteries. In order to examine possible interference produced by DC current from the power supply the proton magnetometer was placed in the variometer house to perform test measurements. Figure 4 shows minute mean data obtained using the Gaussian low-pass filter (St-Louis 2011) for February 2012 and they are compared with the total field intensity (preliminary data) from two closest surrounding observatories Tihany (THY) and Nagycenk (NCK). Comparison of subtracted variations of the total field (Fig. 5) reveals that the similarity between THY and LOP (not official IAGA three letter code) is better than THY and NCK although the distance among Hungarian observatories is almost two times shorter (Fig. 1). The only exception is 17 February, we can spot one spike in the middle of the day in LOP magnetogram (Fig. 4 and 5). This was caused by staff during the visit of the observatory. From this inspection we can say that we manage to avoid noise produced by DC current and that first data looks promising. Preparations for the dIdD installation have been completed by the beginning of May 2012. On Figure 6 are presented the first North, East and Vertical variation recordings measured in LOP, THY and NCK in the period between 06 May and 23 May 2012.

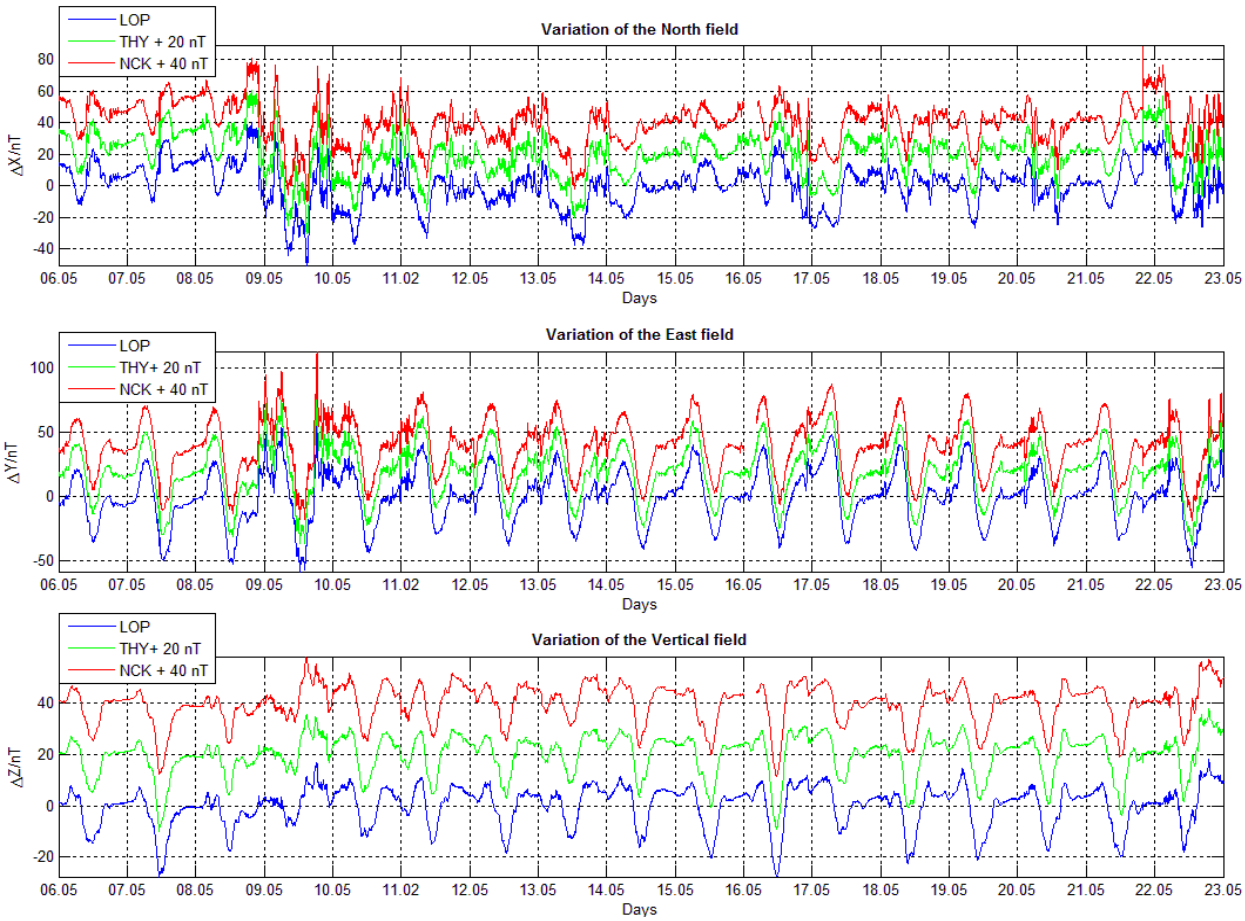

Figure 6 –LOP, THY and NCK variation recordings. Variation recordings are shifted 20nT with respect to each other.

4. CONCLUSON REMARKS

Unfortunately, due to lack of the permanent observatory staff the detailed data analysis could not be presented. There is still a lot of work to do in order to establish the observatory that will provide a long-term quality data. Geodetic measurements i.e. determination of the azimuth angle of azimuth mark will be performed in July 2012 in order to fulfill the needs for absolute DI measurements. Hopefully the observatory will be in full operation by the end of summer 2012 and we await with anticipation the first baseline results in forthcoming years.

Furthermore, we hope that in the collaboration with personnel from Tihany observatory we will host a fluxgate three axial magnetometer. The installation will be implemented in the framework of the PLASMON Project (http://plasmon.elte.hu/home.htm) thus complementing the PLASMON observatory network. In addition, this way we will have possibility to do inter-comparison of variation data provided by the dIdD and the PLASMON magnetometer.

5. ACKNOWLEDGMENTS

The results presented in this paper rely on data collected at Tihany and Nagycenk observatories. We thank Eötvös Loránd Geophysical Institute of Hungary and Geodetic and Geophysical Research Institute of the Hungarian Academy of Sciences, for supporting its operation and INTERMAGNET for promoting high standards of magnetic observatory practice (www.intermagnet.org).

6. REFERENCES

Jankowski, J. and C. Sucksdorff (1996): *Guide for Magnetic Measurements and Observatory Practice*. International Association of Geomagnetism and Aeronomy, Warszawa, Poland.

Sabaka, T., Olsen, N. and Purucker, M. (2004): Extending comprehensive models of the Earth's magnetic field with Orsted and CHAMP data. *Geophys. J. Int.*, **159**, 521-547.

St-Louis, B. (2011): *Intermagnet Tehnical Reference Manual* (Version 4.5). Online at http://www.intermagnet.org

Verbanac, G. and M. Korte (2006): The geomagnetic field in Croatia. *Geofizika*, **23**, 2, 105-117.

Verbanac, G. and E. Vujić (2012): Determination of the Croatian geomagnetic observatory location. *Acta geophysica*, **60**, 2, 337-356.

Vujnović, V., Verbanac, G., Orešković, J., Marki, A., Marić, K., Lisac, I., and Ivandić, M. (2004): Results of the preliminary geomagnetic field strength measurements in the northern part of middle Croatia. *Geofizika*, **21**, 1-13.

THE REALIZATION OF A NEW GEOMAGNETIC OBSERVATORY IN CENTRAL ITALY, REPLACING L'AQUILA GEOMAGNETIC OBSERVATORY

P. Palangio [(1)], S. Lepidi [(1)], M. Pietrolungo [(1)], F. Biasini [(1)], M. Di Persio [(1)], C. Gizzi [(1)], A. Meloni [(2)]

[(1)] Istituto Nazionale di Geofisica e Vulcanologia, Via dell'Arcivescovado 8, 67100 L'Aquila, Italy, paolo.palangio@ingv.it

[(2)] Istituto Nazionale di Geofisica e Vulcanologia, Via di Vigna Murata 605, 00143 Roma, Italy, antonio.meloni@ingv.it

SUMMARY

The geomagnetic Observatory of L'Aquila was founded by Istituto Nazionale di Geofisica e Vulcanologia (INGV) in 1958, on the occasion of the International Geophysical Year. It is the main Italian geomagnetic observatory and since 1999 is part of the Intermagnet network. In 2009 L'Aquila was struck by a strong earthquake; the town was seriously damaged, and since then many activities moved to the suburbs; close to the Geomagnetic Observatory new activities were planned. Then the necessity to find in the surroundings a new place, suitable for the installation of a Geomagnetic Observatory, arose. Several tests were made and a possible location was found in Castel Del Monte, 40km from L'Aquila; a preliminary analysis of the electromagnetic background noise and of the spatial magnetic field gradients has shown that the place can meet the requirements for a Geomagnetic Observatory. Meanwhile, in 2010, a new Geomagnetic Observatory was installed in Duronia, 130 km South-East from L'Aquila and since 2012 it is part of the Intermagnet network.

1. INTRODUCTION

INGV is in charge of geomagnetic field measurements in Italy, performed by means of geomagnetic observatories and repeat stations (Meloni et al., 2007); at the moment, it runs the geomagnetic observatory of L'Aquila (IAGA code AQU) and Duronia (DUR) in central Italy, Castello Tesino (CTS) in nortern Italy and Lampedusa (LMP) in southern Italy, providing a full coverage of the Italian latitudinal extension. L'Aquila geomagnetic observatory (geographic coordinates: 42°23'N; 13°19'E) has been the main italian magnetic observatory since 1958 (Meloni et al., 1984, 1989), providing long series of data (Figure 1), which have been widely used for scientific studies of the variations of the geomagnetic field (Francia et al., 1999, 2001; Lepidi et al., 1999, 2001, 2003) and for geomagnetic field modelings (Meloni et al., 1994; De Santis et al., 1997); after the April 6, 1999 earthquake, the necessity of moving the observatory to a new location arose, in order to give a continuity to the existing dataset.

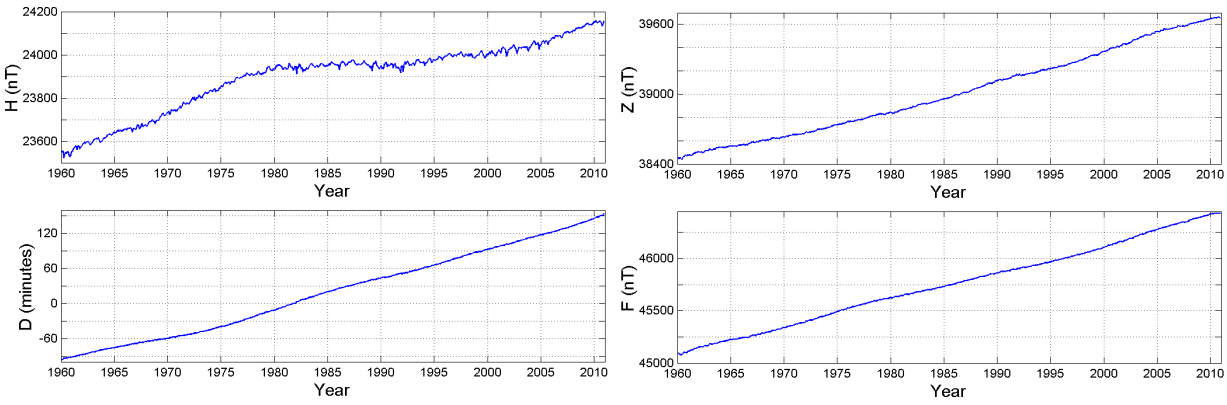

Figure 1 –Average monthly values of horizontal component H,declination D, vertical component Z and total field intensity F over 50 years.

2. TESTS FOR A NEW INSTALLATION IN CASTEL DEL MONTE

Castel Del Monte (CDM) is a small village (about 500 inhabitants) on the Apennine mountains, about 40 Km East of L'Aquila. A suitable location for a new observatory was found 3Km outside the village, at almost 1600 m altitude, where there is a quite flat piece of land of about 2 hectares, with an underlying stable bedrock. Preliminary tests have been performed to analyze the background noise level; in particluar, 1-sec variation measurements of the geomagnetic field components were recorded with a fluxgate magnetometer for a few days and were compared with simultaneous AQU data (Figure 2, left panel); it can be seen that the variations at the two stations are very similar and that the background noise level at CDM is very low. Also higher frequency variations, with a sampling rate of 125 Hz, were measured (Figure 2, right panel); the Schumann resonance at 7.8 Hz is well evident, and also in this case the background noise level is very low.

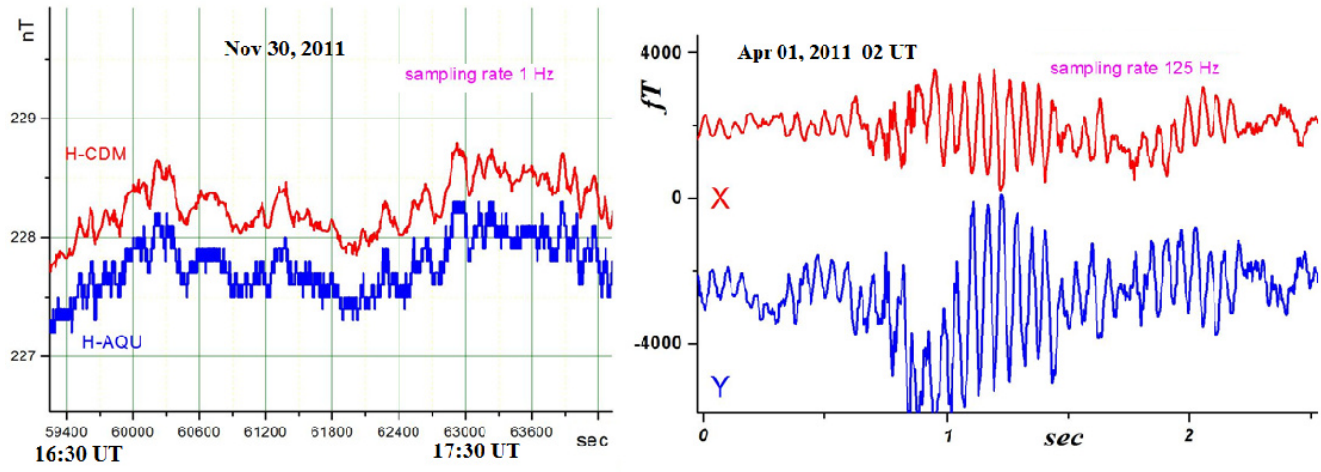

Figure 2 –Left panel: Simultaneous 1 Hz measurements of the total horizontal geomagneti field component at AQU and CDM; right panel: 125 Hz measurements of the two horizontal components at CDM.

Simultaneous absolute measurements of the declination D, the inclination I and the total magnetic field F were performed at the two sites in order to check if the differences are constant and if the values at CDM can be considered representative (Table 1).

Table 1 –Simultaneous absolute measurements (Declination, Inclination, F in nT) at CDM and AQU. Delta is the difference CDM-AQU

D(CDM)	D(AQU)	I(CDM)	I(AQU)	F(CDM)	F(AQU)	Delta D	Delta I	DeltaF
2°57'03"	2°47'35"	58°45'12"	58°42'16"	46535.20	46466.75	0°09'28"	0°02'56"	68.45
2°56'43"	2°47'16"	58°45'56"	58°42'13"	46532.85	46464.57	0°09'27"	0°03'43"	68.28
2°56'50"	2°47'20"	58°46'00"	58°42'22"	46532.73	46463.36	0°09'30"	0°03'38"	69.37
2°56'38"	2°47'00"	58°46'01"	58°42'13"	46531.89	46462.78	0°09'38"	0°03'48"	69.11

We selected an area of 80mx130m and, to check if there are any magnetic anomalies, we measured the geomagnetic field intensity F and its vertical gradient at the nodes of a square grid at distances of 10m. The results are shown in Figure 3. White squares indicate missing measurements in correspondence of a building. This building produces an evident magnetic disturbance, with vertical F gradients greater than 10 nT/m. Areas with low values of the F gradient are localized in the lower-right zone and in the upper corners. Using simultaneous AQU measurements as a reference, we computed the difference with F measured at each point of the grid (Figure 4, left panel). We then used these differences to compute their horizontal gradient, as the difference at each node of the grid with the four nearest nodes (Figure 4, right panel). It is evident that the areas in which the F difference with AQU is constant, and consequently its horizontal gradient is lower, are localized in the lower-right and upper zones of the selected area.

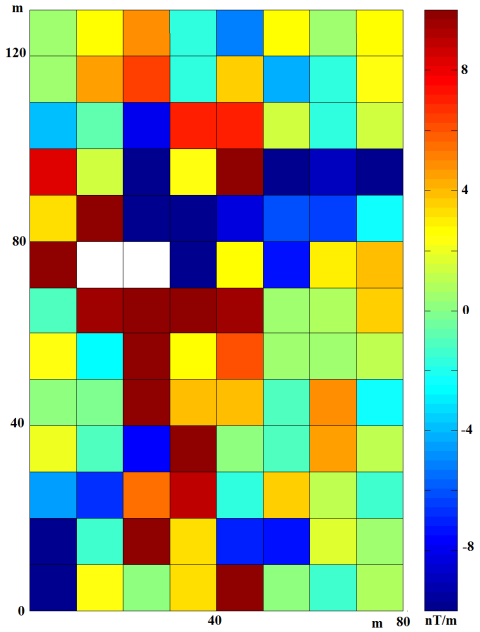

Figure 3 –Vertical gradient of F measured at each point of the grid.

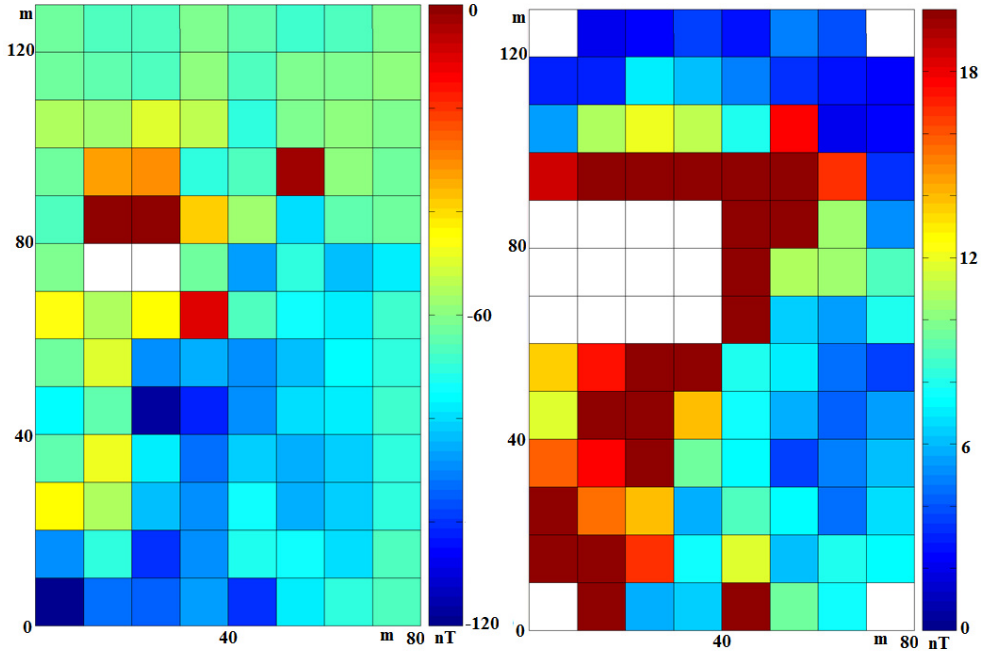

Figure 4 –Left panel: Difference between F measured at each point of the grid and the simultaneous value at AQU observatory; right panel: Horizontal gradient of the difference between F at each point of the grid and the simultaneous value at AQU.

3. DURONIA GEOMAGNETIC OBSERVATORY

Duronia observatory consists of seven little wooden buildings inside a forest: variometer, absolute measurements, automatic absolute measurements, ULF search coil, ELF search coil , VLF search coil and a wide band (1 Hz - 5 GHz) electrometers (Palangio et al., 2009). It is located in a very low noise area: the background noise level is less than 20 fT/√Hz in the frequency band 10 Hz -25 kHz. These characteristics allow to plan research activities in the field of geomagnetic sciences such as Schumann resonance (Figure 5) and Alfvén resonance. The new observatory became fully operational in June 2010, with continuous measurements of the geomagnetic field, including variation recordings and absolute measurements. In Figure 6 the difference between scalar and vectorial F and the baselines for six months are shown. The results show that the new observatory is well within the IAGA 2002 standards, with a 5 nT peak to peak baseline amplitude. In 2012 DUR was included in the Intermagnet network.

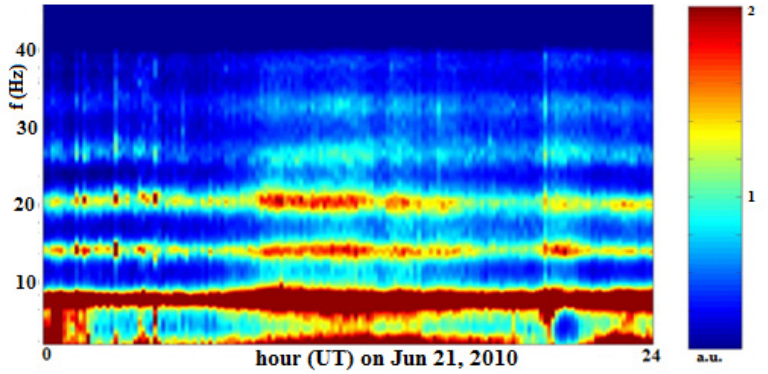

Figure 5 –Spectrogram for 1 day showing the Schumann resonance at 7.8 Hz and its harmonics

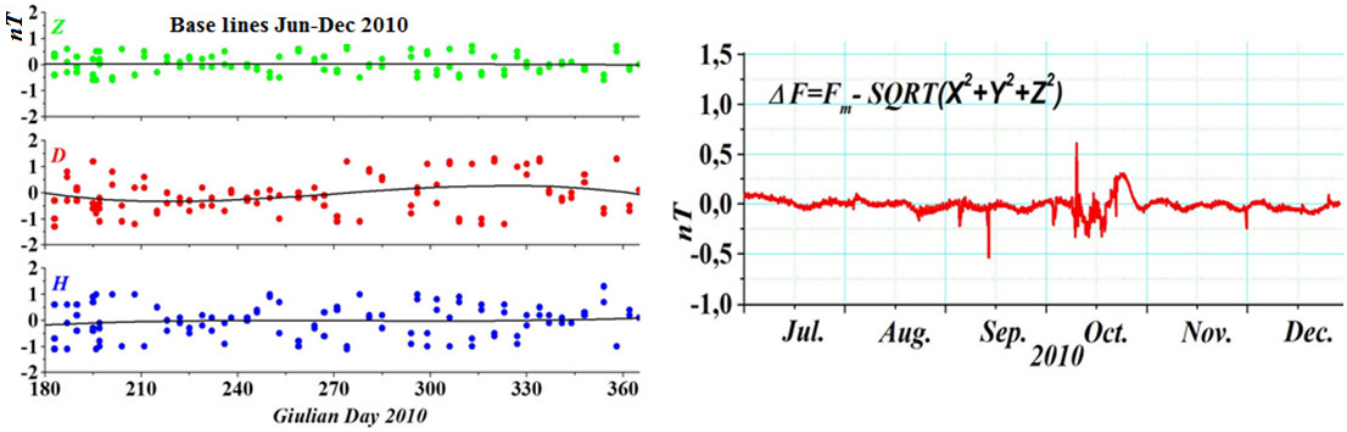

Figure 6 –Left: Baselines; right: Difference between scalar and vectorial F

4. REFERENCES

De Santis, A., M. Chiappini, G. Dominici and A. Meloni (1997): "Regional geomagnetic field modeling: the contribution of the Istituto Nazionale di Geofisica". *Annali di Geofisica*,40, 1161-1169.

Francia, P., S. Lepidi, U. Villante, P. Di Giuseppe and A. J. Lazarus (1999): "Geomagnetic response at low latitude to continuous solar wind pressure variations during northward interplanetary magnetic field". *J. Geophys. Res*., 104, 19923.

Francia, P., S. Lepidi, P. Di Giuseppe and U. Villante (2001): "Geomagnetic sudden impulses at low latitude during northward interplanetary magnetic field conditions". *J. Geophys. Res.*, 106, 21231.

Lepidi, S., P. Francia, U. Villante, L. J. Lanzerotti and A. Meloni (1999): "Polarization pattern of low frequency geomagnetic field variations (0.8-3.6 mHz) at high and low latitude". *J. Geophys. Res*., 104, 305.

Lepidi, S., P. Francia and M. De Lauretis (2001): "Local time behaviour of low frequency geomagnetic field fluctuation power at low latitude". *Annali di Geofisica*, 44, 119.

Lepidi, S. and P. Francia (2003): "Diurnal polarization pattern of ULF geomagnetic pulsations in the Pc5 band from low to polar latitudes". *J. Atmospheric and Solar-Terrestrial Physics*, 65, 1179.

Meloni A., F. Molina, P. Palangio, Q. Taccetti, and A. De Santis (1984): "Automatic Digital Recording of Geomagnetic Elements by means of a Proton Precession Magnetometer", *Geophysical Surveys*, 6, 339-350.

Meloni A. and F. Molina (1989): "Study of S variation at L'Aquila Geomagnetic Observatory", *Annales Geophysicae*, 4, 387-393

Meloni, A., O. Battelli, A. De Santis and G. Dominici (1994): "The 1990.0 magnetic repeat station survey and normal reference fields for Italy". *Annali di Geofisica*, 37, 5, 949-967.

Meloni, A., L. Cafarella, P. De Michelis, A. De Santis, D. Di Mauro, G. Dominici, S. Lepidi, P. Palangio, R. Tozzi and A. Zirizzotti (2007): "Systematic Magnetic Observations in Italy", proceedings of XII IAGA workshop on Geomagnetic Observatory instruments, data acquisition and processing, Belsk 2006, *Publs. Inst. Geophys. Pol. Acad. Sc*., C-99, 398, 209.

Palangio, P., F. Masci, M. Di Persio, C. Di Lorenzo, and E. Lampis (2009): "A new station for monitoring electromagnetic fields in Duronia (Italy)", *Annals of Geophysics*, 52, 441-452.

A CENTURY OF GEOMAGNETIC OBSERVATIONS BY IGN

J.M. Tordesillas [(1)], P. Covisa[(1)], V.M. Cabrera[(1)], I. Socias[(1)], V. Marín[(1)], J. Fernández[(1)], S. Galán[(1)]

[(1)] Instituto Geográfico Nacional, C/ General Ibáñez Ibero 3, 28003, Madrid, Spain, geomagnetismo@ign.es

SUMMARY

In 1912 the Instituto Geográfico Nacional (IGN) began the first magnetic survey of Spain in order to produce the Magnetic Map. The observatories used as reference for this work were Ebro (Society of Jesus) and San Fernando (ROA). From 1934 IGN operates their own geomagnetic observatories. The first one was stablished in Toledo, in the center of Spain, and then the number of observatories working simultaneously increased until five distributed over the Iberian Peninsula, Canary Islands and Fernando Pó in the Gulf of Guinea. At present IGN has two geomagnetic observatories regularly running on the Spanish territory: San Pablo-Toledo (SPT) and Güímar-Tenerife (GUI) that replaced Toledo observatory in 1982 and Tenerife observatory in 1993 respectively. Both of them are equipped with digital equipment and are members of Intermagnet since 1997.

As well, IGN has a network of magnetic repeat stations distributed across Spain. In some locations the series of measurements exceed 50 years. This network has been updated since 2000 and is used for the compilation of Spanish magnetic maps (IGN is in charge of this matter), and to contribute in the International Geomagnetic Reference Field and the Magnetic Network European (MagNetE).

1. INTRODUCTION

In 2012 the *Instituto Geográfico Nacional* of Spain (IGN) reaches 100 years of history in the observation of the Earth's magnetic field. In the need to have a Magnetic Map of Spain, the *Instituto Geográfico* begins to draft a report in 1905 in order to carry out a complete geomagnetic survey of Spain. For this project, two Sartorius's geomagnetic-packs were acquired, and the engineers in charge of this survey were trained at Potsdam Observatory. So, in May of 1912, the field work for the Magnetic Map started, being measured the first station in Villanueva y Geltrú, nowadays called Vilanova i la Geltrú (Barcelona). Azpiazu and Gil (1919), Cubillo (1950). In total 286 stations were measured, and the values of the magnetic components were transported to the date January 1st 1924.

Número.	ESTACIONES	Observador.	Fechas de la observación.	Valores obtenidos de la observación. D	I	H
				° ′	° ′	γ
1	Villanueva y Geltrú	Gil...	Mayo 1913..	12 46.9 W	58 3.5	23153
2	Tarragona	Fort..	Idem 1912..	12 56.0 »	57 56.6	23234
3	Mataró	Gil...	Jun. 1912..	12 30.4 »	58 14.7	23061
4	Mora de Ebro	Fort..	Idem 1912..	13 1.4 »	58 8.5	23211
5	Gerona	Gil...	Idem 1912..	13 26.1 »	58 39.3	22869
6	Caspe	Fort..	Idem 1912..	13 24.3 »	58 25.4	23038
7	Quinto	Idem.	Idem 1912..	13 31.6 »	58 42.3	22900
8	Manresa	Gil...	Julio 1912..	13 47.8 »	58 37.1	22880
9	Cervera (Lérida)	Idem.	Idem 1912..	13 23.0 »	58 37.4	22911
10	Lérida	Idem.	Idem 1912..	13 15.4 »	58 42.3	22888
11	Barbastro	Idem.	Idem 1912..	13 27.4 »	59 14.5	22640
12	Monzalbarba	Fort..	Idem 1912..	13 46.1 »	58 57.7	22781
13	Jaca	Idem.	Idem 1912..	13 50.0 »	59 44.8	22339
14	Huesca	Idem.	Idem 1912..	13 30.5 »	59 18.7	22568
15	Tafalla	Gil...	Agos. 1912..	14 18.3 »	59 56.1	22287
16	Burgueta	Idem.	Idem 1912..	14 13.0 »	60 18.1	22108
17	Alsasua	Idem.	Idem 1912..	14 35.9 »	60 20.2	22143
18	Tudela	Fort..	Idem 1912..	14 7.9 »	59 38.8	22519
19	Calahorra	Idem.	Idem 1912..	14 14.0 »	59 40.8	22364
20	Logroño	Idem.	Idem 1912..	14 33.0 »	59 54.4	22303
21	Fuenterrabía	Idem.	Idem 1912..	14 21.3 »	60 38.9	21933
22	Deva	Gil...	Sept. 1912..	14 48.1 »	60 46.8	21695
23	Bribiesca	Idem.	Idem 1912..	14 48.9 »	60 0.3	22190
24	Palencia	Idem.	Idem 1912..	15 16.6 »	59 52.6	22355
25	Medina del Campo	Idem.	Idem 1912..	15 19.8 »	59 10.1	22627
26	Vitoria	Fort..	Idem 1912..	14 23.2 »	60 11.9	22166
27	Burgos	Idem.	Idem 1912..	14 51.7 »	60 0.8	22234
28	Viana de Cega	Idem.	Idem 1912..	15 7.5 »	59 21.1	22557
29	Segovia	Gil...	Octu. 1912..	14 59.6 »	58 39.2	22935
30	Méntoles	Idem.	Idem 1912..	14 40.5 »	58 6.4	23168
31	Ortigosa	Fort..	Idem 1912..	14 54.5 »	58 58.0	22735
32	El Plantío	Idem.	Idem 1912..	14 32.4 »	58 14.9	23013
33	Moncada (Valencia)	Gil...	Nov. 1912..	13 16.3 »	56 45.1	23794
34	Denia	Idem.	Idem 1912..	13 4.1 »	55 53.4	24128
35	Játiva	Idem.	Idem 1912..	13 19.6 »	56 21.7	24005
36	Vinaroz	Fort..	Idem 1912..	12 49.3 »	57 31.9	23383
37	Castellón	Idem.	Idem 1912..	12 48.6 »	57 6.7	23579
38	Ávila	Gil...	Mayo 1913..	15 1.6 »	58 20.9	22959
39	El Escorial	Idem.	Idem 1913..	14 49.4 »	58 17.3	23021
40	Soria	Fort..	Idem 1913..	14 33.3 »	59 14.7	23089

Figure 1 –First surveys in 1912

Because IGN at that time did not owned any geomagnetic observatory, the one used as reference for this survey was Ebro Observatory (Society of Jesus) and also San Fernando Observatory (ROA) was taken into account. Although the position of these observatories was too eccentric in relation to the Iberian Peninsula, its quality was the very best because of being free of potential disturbances.

The geomagnetic survey allowed making the Spanish Magnetic Map of 1924 that was composed of three charts: one of declinations, other of inclinations, and the third of horizontal intensities.

Figure 2 –Declinations chart of the "Mapa Magnético de España" of 1924

2. IGN OBSERVATORIES

The *Instituto Geográfico Nacional*, considering the need of increasing the number of Geomagnetic Observatories and also to locate one in the center of the Iberian Peninsula, starts to manage their own Observatories since 1934. The first of them was located in Toledo and was working since 1934 to 1981. The electrification of the railway that arrives to the city make necessary to relocate it in San Pablo de los Montes. Payo and Gómez-Menor (1998).

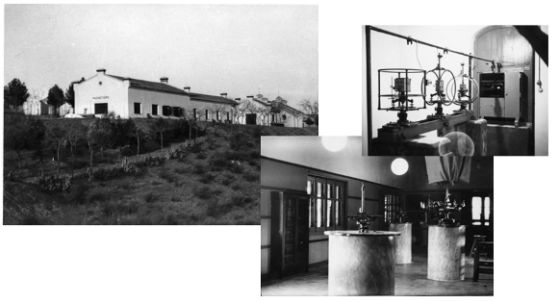

Figure 3 –Toledo Geomagnetic Observatory (1934-1981)

Because of the First International Geophysical Year, the Instituto Geográfico opens new Geomagnetic Observatories in Almería, Logroño, Fernando Pó island in Gulf of Guinea, and Tenerife in Canary Islands, reaching the number of five observatories working simultaneously (IGN, 2005).

Figure 4 –Location of IGN Geomagnetic Observatories

Eventually and due to different reasons, these Observatories have been closed, and only Tenerife Observatory was relocated in Güímar in 1993.

IGN has at present two working Geomagnetic Observatories in Spain: San Pablo-Toledo (SPT) and Güímar-Tenerife (GUI). Both of them are equipped with digital instruments and are Intermagnet members since 1997. They send real-time data to Paris GIN in IAGA-2002 format using HTTP protocol. SPT also produces Quasi-Definitive Data, submited to Paris GIN once a month. (www.intermagnet.org) (IGN- Servicio de Geomagnetismo, 2011).

Figure 5 –SPT and GUI Geomagnetic Observatories at present

The *Archivo Nacional de Datos Geofísicos y Geodésicos* it is nowadays located at Toledo Geophysical Observatory. All data produced by the different Geophysical Observatories that IGN had got along its history is being collected in this Archive. These geomagnetic, seismic and other relevant data is being catalogued and stored in controlled conditions of humidity and temperature, being available to the scientific community.

Figure 6 –Archivo Nacional de Datos Geofísicos y Geodésicos

4. IGN REPEAT STATIONS NETWORK

IGN also has at present a repeat stations network distributed around Spain. The survey of this network is made alternatively every other year the north half and the south half of the Iberian Peninsula and Balearic Islands, resulting that every two years the network is completely surveyed. This network has been updated since year 2000 and nowadays has 45 repeat stations and 10 of them have been

surveyed along last 50 years. Four of these stations are variometric, or first order stations, and allow increase quality in the survey of the network. The reference Observatory for this network is San Pablo de los Montes, although Ebro and San Fernando Observatories are also used.

Figure 7 –IGN Repeat Stations Network

The information of this network joined to previous geomagnetic surveys, are used to do the compilation of Spanish Magnetic Maps, matter in charge of IGN. Following IAGA suggestions, IGN publish since 1970 the charts of all magnetic elements every 10 years, except the declination chart that is published every 5 years (IGN-Servicio de Geomagnetismo, 2006).

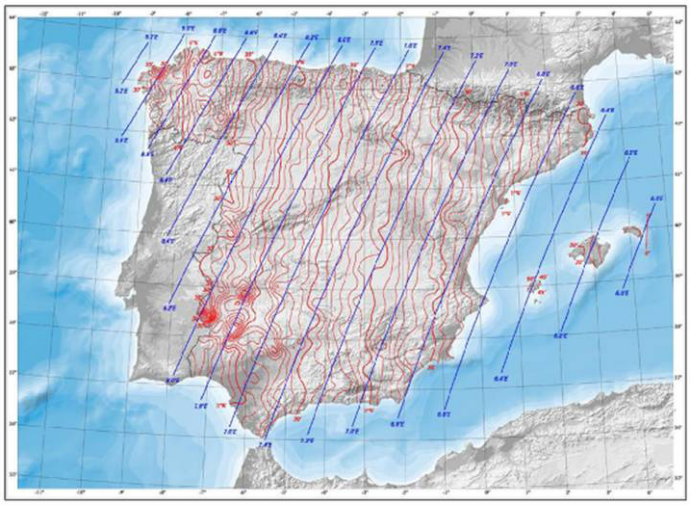

Figure 8 –Declination Map of Spain, 2005

With data obtained in this repeat station network, IGN take part in some international projects like International Geomagnetic Reference Field (IGRF) and Magnetic Network European (MagNetE). More data can be seen at IGN web site: http://www.ign.es/

4. REFERENCES

Azpiazu, U. and R. Gil (1919): "Magnetismo Terrestre. Su estudio en España". *Instituto Geográfico y Estadístico, Madrid.*

Cubillo, J. (1950): "Carta Nacional de Declinaciones Magnéticas". *Instituto Geográfico y Catastral, Madrid.*

IGN (2005): "Catálogo Inventario de Magnetómetros Españoles". *Instituto Geográfico Nacional, Madrid.*

IGN, Servicio de Geomagnetismo (2006): “Mapa geomagnético de España, Epoca 2005.0”. *Instituto Geográfico Nacional, Madrid.*

IGN, Servicio de Geomagnetismo (2011): “Anuarios de Geomagnetismo, Año 2009”. *Instituto Geográfico Nacional, Madrid.*

Payo, G. and R. Gómez-Menor (1998): “Historia del Observatorio Geofísico de Toledo”. *Instituto Geográfico Nacional, Madrid.*

GEOMAGNETIC OBSERVATIONS AND MODELLING AT VALENTIA OBSERVATORY, IRELAND: CURRENT STATUS

S. Varghese [(1)], K. Lambkin [(1)], P. Kotze [(2)], M. Crean [(1)]

[(1)] Valentia Geophysical and Meteorological Observatory, Irish Meteorological Service, Caherciveen, Co. Kerry, Ireland. Email: saji.varghese@met.ie
[(2)] SANSA Space Science, Hermanus Magnetic Observatory, South Africa.

SUMMARY

Valentia Geophysical and Meteorological Observatory, the only magnetic observatory in Ireland is located at the south-western extreme of the island of Ireland on the Iveragh peninsula in County Kerry, approximately 1 km south-west of the town of Caherciveen. Magnetic records for the observatory dates back to 1888 and has shown a change in declination from 22 degrees west of True North in 1900 to less than 6 degrees in 2012. The observatory also completes a national repeat station survey of the Island of Ireland every two years. Apart from the regular absolute and variaometer measurements, geomagnetic modelling is also a priority. The Irish secular variation regional model was recently updated. Regional field models are derived to describe the geomagnetic field across a limited region of the Earth's surface primarily because they provide a far better representation in comparison to global models like the IGRF. Polynomial models are among the most frequently used empirical models for curve fitting and to determine the parameters that have a profound effect on a particular response function. Following this technique, the secular variation model was developed based on a main field model of Ireland using repeat station and satellite data. The results of the new Irish model and an analysis of recent trends in magnetic observations are presented.

1. INTRODUCTION

Valentia Geophysical and Meteorological Observatory, the only magnetic observatory in Ireland is located at the south-western extreme of the island of Ireland on the Iveragh peninsula in County Kerry, approximately 1 km south-west of the town of Caherciveen. The Observatory is part of the Irish Meteorological Service (Met Éireann). The Geomagnetic program at Valentia focuses on monitoring, surveying and modeling the earth's magnetic field across Ireland. It is the only such program on the island of Ireland and has produced one of the longest continuous geomagnetic records in the world. Magnetic records for the observatory dates back to 1888. Details of historical measurements at Valentia observatory are well documented in publications (e.g. Sabine,1870; Rucker and Thorpe, 1890; Walker, 1919; McWilliams and Byrne, 1960). Measurements show a change in declination from 22 degrees west of True North in 1900 to less than 6 degrees in 2012.

Apart from regular absolute and variometer measurements, the observatory also carries out a national repeat station survey of the Island of Ireland every two years, provides different magnetic measurement products to different stakeholders and agencies. Providing compass verfication for aviation industry is another item in the geomagnetic program.

2. CURRENT MEASUREMENTS

Two independent absolute huts are maintained on site at the station. Both use a theodilote mounted DI-fluxgate magnetometer (DI-flux), one with a GEM Systems GSM-19 Overhauser magnetometer and the other a GSM-90. Absolute magnetic measurements are made three times weekly for baseline determination. Measurements are made at precise times and the values obtained are compared with simultaneous instantaneous values from the variometers. From these comparisons baseline values for the variometers are determined so that the true value of the elements of the magnetic field can be derived from the variometer data for any time.

Variometer readings are made by three component Fluxgate Variometers DMI Model FGE ver.G (suspended version), with MinGeo data acquisition. The outputs from the fluxgate magnetometers are connected to data loggers which convert the analogue outputs from the magnetometers to digital data and store them. Data is regularly quality controlled and processed. This includes baseline adjustments, scale

factor corrections and so on. Data is appropriately format for forwarding to the World Data Centres, catering to special requests from indistry and for magnetic yearbook publications.

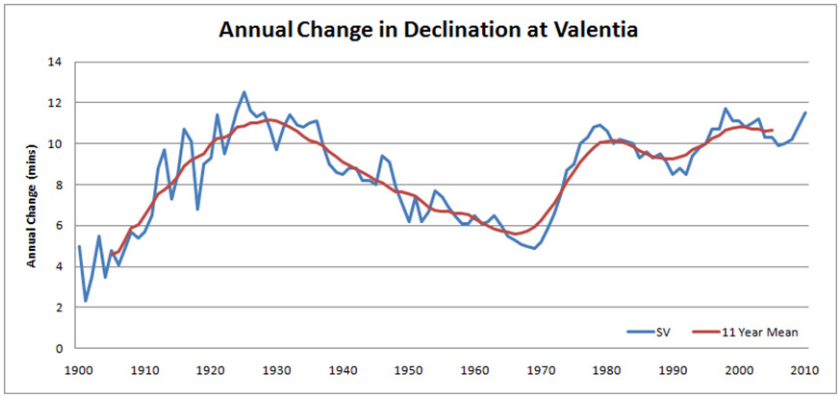

Figure 1 –Secular variation and 11 year mean of declination (minutes) at Valentia Obserbvatory.

Several national and international agencies rely on measured and modeled data from Valentia Observatory. The main users of Irish geomagnetic products are:

1. The Ordinance Survey of Ireland: magnetic declination data for inclusion in Discovery series maps.
2. The Irish Aviation Authority (IAA): magnetic variation data in order to comply with international aeronautical standards.
3. Oil/Gas exploration companies: geomagnetic data for the orientation of drill heads.
4. Irish Air Corps, Shannon Aerospace, Dublin Aerospace and regional airports: geomagnetic data and compass calibration services in compliance with ICAO safety regulations.
5. National and international research communities: data is used extensively by third level organizations and various geoscientific institutes.

3. REPEAT STATION SURVEY

The current Irish national magnetic repeat station survey programme managed by Valentia Observatory is based on a station network established in 1959. However magnetic surveys on the island date back to 1870, reducing to epoch 1842.5 (Sabine, 1870). Over the last five decades revisiting Irish repeat stations has been irregular. In 2001 a plan was implemented to reduce the frequency of subsequent surveys. The survey in 2005 saw a four year period between visits and the 2008 survey saw a period of three years. The 2010 survey has reduced the measurement period to our desired frequency of two years. Our most recent survey of 2012 maintains this frequency.

Recently we scrutinised all Irish repeat stations for their quality. Some stations have been closed as a result of advancing towns or new motorways, while some new stations have been established. Our 2012 survey represents our finalised updated network which we hope to visit biennially for the foreseeable future.

The network consists of 19 repeat stations spaced approximately 80km apart. Measurements are made using a DMI Di-Fluxgate Magnetometer (Model G) attached to a Zeiss 010B theodolite along with a Gem GSM-19 Overhauser magnetometer. As the only geomagnetic observatory in Ireland, Valentia data is used for the data reduction process. In parallel to updating the physical locations of the stations, our repeat station metadata records were also updated. Aging station location maps, some decades old, have been replaced with satellite imaging and GPS coordinates. Fixed mark photos have been retaken and digitally archived. The fixed mark angles have been recalculated using modern techniques. Site anomaly surveys have been conducted with the aim of providing a digital benchmark of the surrounding for future use.

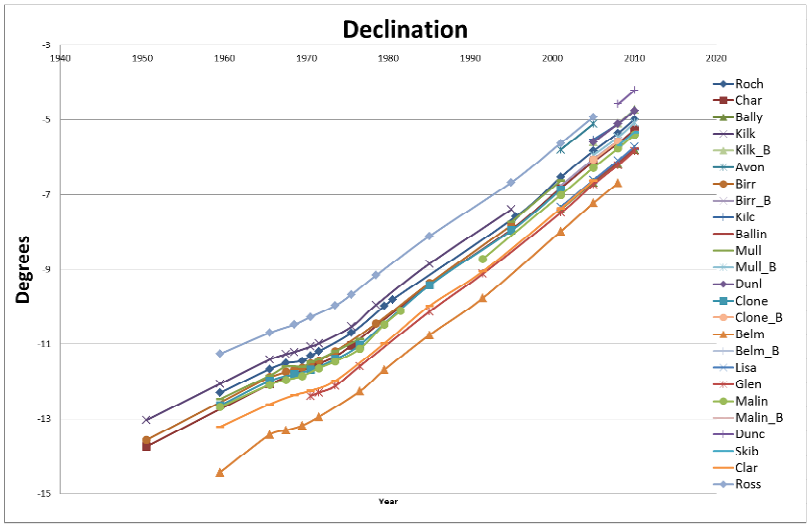

Figure 2 –Yearly variation of declination at different repeat stations in Ireland.

4. GEOMAGNETIC MODELLING

It is well known that secular change is a comparatively local phenomenon and that it does not proceed in a regular and uniform pattern all over the Earth, giving rise to regions where the field changes more rapidly than elsewhere. Regional field models are derived to describe the geomagnetic field across a limited region of the Earth's surface primarily because they provide a far better representation. Polynomial models are among the most frequently used empirical models for curve fitting and to determine the parameters that have a profound effect on a particular response function. This type of modelling is popular as polynomial models have a simple form, have well known and understood properties, have moderate flexibility of shapes, and they are computationally easy to use. However, polynomial models also have limitations such as weak extrapolation properties. Polynomials may provide good fits within the range of data, but they will frequently deteriorate rapidly outside the range of the data, like most regional field models. Different methods to model the geomagnetic field on a regional scale were reviewed by *Haines* (1990). In geomagnetism polynomials have been applied with great success to derive regional models of secular variation (*Shu et.al.,* 1996).

Since secular variation is derived as a time derivative of the geomagnetic field, one can model the main field and then differentiate the corresponding field model to get a secular variation model, or one can numerically differentiate the main field data and then fit a secular variation model directly. The latter derivative–fit approach has been applied in the derivation of a secular variation model for Ireland based on repeat station observations for the period 2008 - 2010. First central differences from repeat station observations, divided by their respective time intervals in years, are used as input data to every secular variation model. Polynomials have been used extensively to model ground magnetic field measurements to derive secular variation models for southern Africa (*Kotzé*, 2003). Here,we have selected a two-dimensional polynomial presentation based on *Xu et al*., 1992.

Secular variation model for all 7 geomagnetic field components X,Y, Z, D, I, H, and F from 14 repeat stations for the period 2008-2010 were subsequently derived. The least-squares routine used to fit the data is the stepwise regression procedure described by *Efroymson (*1960) that has the ability of both entering and removing variables at given levels of statistical significance. Various degrees were evaluated for the polynomial fits, and it turned out eventually that degree 2 was the best solution for all components, given the small regional area under consideration.

***Table 1*: Root-Mean-Square values for the differences between observation and modelled values**

Component:	X(nT/y)	Y(nT/y)	Z(nT/y)	D(min/y)	I(min/y)	H(nT/y)	F(nT/y)
RMS:	2.5	1.3	1.9	0.23	0.22	2.5	1.2

A weakness of the secular variation model for Ireland is the fact that it is based solely on repeat station data gathered over Ireland, with no secular variation data available over the surrounding sea areas.

For the main field model of Ireland and the surrounding sea areas we had at our disposal repeat station observations at epoch 2010.0, as well as vector CHAMP satellite data. CHAMP satellite vector measurements (X,Y, and Z) in the NEC coordinate system, obtained during quiet night times (20h00 – 04h00 LT) were subsequently selected between 47- 58 degrees North, and between 2 degrees East and 19 degrees West during January 2010, reduced to 1 January 2010. A total of 4602 data points, amounting to a total of 13806 vector

observations could be identified at an average satellite altitude of 300 km. Spherical harmonics were subsequently used to downward continue the data to ground level. For this purpose we assumed the repeat station measurements as 'ground truth' and adjusted the satellite data to match these measurements. Our database then consists of both the CHAMP satellite data reduced to ground level as well as the repeat station data for 2010, giving a total of 4615 three-component vector data points.

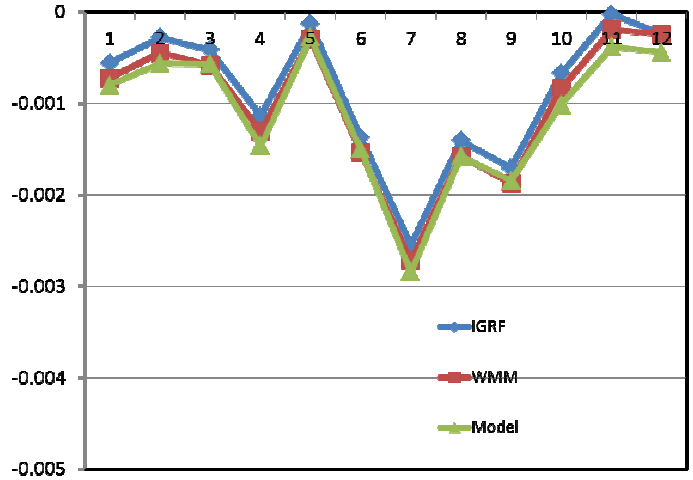

Figure 3 –Difference (nT) in declination values (measured – predicted) for IGRF, WMM and present model for different stations.

Due to the rectangular shape of the area identified for the derivation of the field models it turned out that harmonic polynomials were the best to fit observations. In order to improve the secular variation model, it will be important to include data from field surveys conducted over the United Kingdom as well as parts of Western Europe.

5. CONCLUSION AND FUTURE WORK

Valentia Observatory has one of the longest measurement record in the world. It continues to provide high quality observatory and repeat station magnetic data for the scientific community and other users. It is envisaged that further improvement will be made in the regional model by making use of the most recent repeat station data in collaboration with SANSA Space Science in Hermanus, South Africa.

6. REFERENCES

Efroymson, M.A.(1960): "Multiple regression analysis". *Mathematical Methods for Digital Computers*, edited by A. Ralston, and H.S. Wilf, John Wiley, New York, 191-203.

Haines, G. V. (1990): "Regional magnetic field modelling - A review".*Journal of Geomagnetism and Geoelectricity*, **42**,1001-1018.

Kotzé, P.B. (2003): "The time-varying geomagnetic field of Southern Africa". *Earth Planets and Space*, **55**, 111-116.

McWilliams, J. and Byrne, J. (1960): "A magnetic survey of Ireland for Epoch 1959.5". *Dept. Transport and Power*, Meteorological Service, Dublin

Rucker, A.W. and Thorpe, T.E. (1890): "A magnetic survey of the British Isles for the Epoch January 1, 1886". *Phil. Trans. Roy. Soc. London*, **181A**, 53-328.

Sabine, E. (1870): "Contributions to terrestrial magnetism No. XII. The magnetic survey of British Isles, reduced to Epoch 1842.5"- *Phil. Trans. Roy. Soc. London*, **160**, 265-275.

Shu, Y., C. An, V.P. Golovkov, N.M., Rotanova, and T. N. Bondar, (1996): "Analysis of geomagnetic secular variations in eastern Asia during the last 30 years". *Geomagn. Aeronomy*, **35**, 871-875.

Walker, G.W. (1919): "The magnetic re-survey of the British Isles for the Epoch January 1,1915". *Phil. Trans.Roy. Soc. London*, **219A**, 1-72

Xu, Y., Y. Wang, and Z. (1992): "An analysis and the models of the geomagnetic secular variation in China for 1950-1985". *Acta Geophys. Sin.*, **35**, 740-747.

EMMA FOR NEAR REAL TIME MONITORING OF THE PLASMASPHERE

B. Heilig [(1)], J. Lichtenberger [(2)], M. Vellante [(3)], J. Reda [(4)], T. Raita [(5)], P. Sutcliffe [(6)], M. Váczyová [(7)], D. Herak [(8)], M. Neska [(4)], L. Merényi [(2)], A. Csontos [(2)], P. Kovács [(2)], M. Srbecky [(7)], I. Mandic [(8)]

[(1)] Geological and Geophysical Institute of Hungary, H-1143 Stefánia út 14, Budapest, Hungary, heilig.balazs@mfgi.com,
[(2)] Eötvös University, Budapest, Hungary
[(3)] University of L'Aquila, L'Aquila, Italy,
[(4)] Belsk Geophysical Observatory of Institute of Geophysics of PAS, Warsaw, Poland,
[(5)] Sodankylä Geophysical Observatory of University of Oulu, Sodankylä, Finland,
[(6)] South African National Space Agency, Hermanus, South-Africa,
[(7)] Slovak Academy of Sciences, Bratislava, Slovak Republic,
[(8)] Department of Geophysics, Faculty of Science, University of Zagreb, Zagreb, Croatia

SUMMARY

Nowcast and forecast of space weather need near real time measurements of the terrestrial plasma environment and models that are suitable to describe the evolution of the system. PLASMON, a global collaboration of 11 institutions funded by the EU (FP7-SPACE) aims at near real-time monitoring the state of the plasmasphere. The near real time monitoring is based on continuous ground observations. One pillar is the observation of eigen-resonances of geomagnetic field lines. From the detected resonant frequency the density along the field line can be inferred. Having a meridional chain of magnetometers the whole dayside plasmasphere as well as the plasma trough can be monitored. Ground data (together with VLF whistler based electron density measurement) will be fed into a data assimilative model. To meet the needs of PLASMON, a new European quasi-Meridional Magnetometer Array (EMMA) was established. EMMA is the unification and extension of three pre-existing magnetometer networks (IMAGE, MM100 and SEGMA). At the same time, measurements in the Southern hemisphere will be carried out by SANSA in South Africa and Namibia. The paper discusses the requirements for the instrumentation which make the recorded data suitable to archive the addressed scientific goals and some preliminary results are shown.

1. INTRODUCTION

The plasmasphere is a torus-shape region around the Earth filled with cold plasma. The plasmasphere is filled up from the ionosphere along the magnetic field lines through ambipolar diffusion. In quiet periods the plasmaspheric and ionospheric plasma is in diffusive equilibrium, however, during geomagnetic storms the plasmasphere is depleted by the enhanced solar wind driven convection electric field. The refilling process after an SSC lasts several days. The PLASMON FP7-Space project (A new, ground based data-assimilative model of the Earth's Plasmasphere – a critical contribution to Radiation Belt modeling for Space Weather purposes, http://plasmon.elte.hu) addresses near-real time monitoring of the evolution of the plasmaspheric density based on ground VLF and ULF wave observations. Near real time plasma densities inferred from ground measurements will be fed into a data assimilative model of the plasmasphere, which in turn is the input of another model predicting the relativistic electron precipitation from the radiation belts.

EMMA was established as the unification of three pre-existing European magnetometer networks IMAGE, MM100 (Heilig et al., 2010) and SEGMA (Vellante et al., 2004). EMMA was also extended by 5 new stations (BRZ, SZC, ZAG, VYH, LOP) and currently consists of 25 stations ranging from North Finland to Italy (Fig 1.). PLASMON will also utilise ultra low frequency (ULF) wave measurements recorded at the network of SANSA (South Africa) (not shown). The monitoring of the plasmaspheric mass density will be carried out by means of observations of field line resonances (FLRs). From the detected resonance frequency the equatorial plasma mass densities can be inferred. The PLASMON inversion code solves the MHD wave equations in a realistic magnetic field (Tsyganenko model) topology. In this paper we discuss the requirements for the instrumentation. First results of the project are also presented.

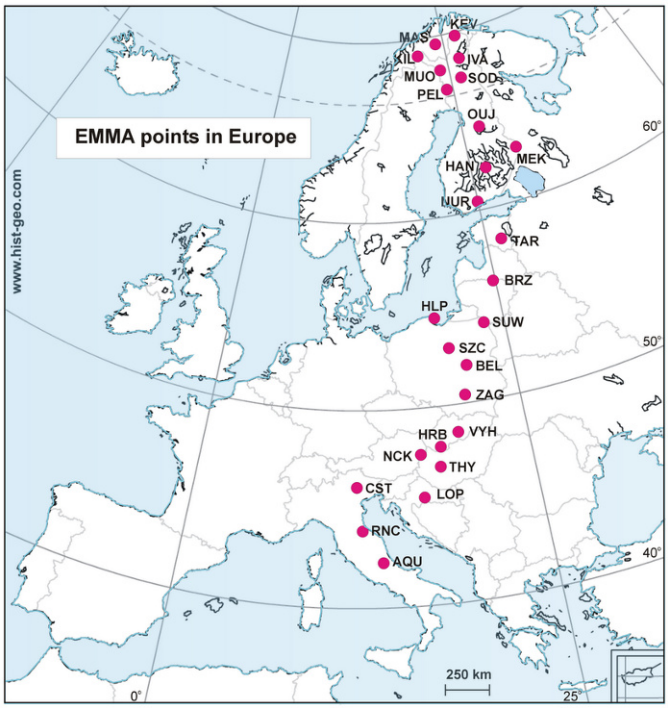

Figure 1 –EMMA stations, 2012

2. INSTRUMENTATION

The application of the phase-gradient method to detect FLRs requires low noise geomagnetic data with high timing accuracy. Also the magnetometer site should be appropriate for ULF measurements. First we summarize these requirements briefly. The magnetometer should have a very low noise level, below 10 pT at 1 Hz, and the amplitude response of the magnetometer at the analogue output should be flat from DC to several Hz. The long term stability, temperature sensitivity, which are so important for observatory applications are less important for ULF wave monitoring. Requirements for the Data Acquisition System (DAQ) are also strict. The resolution of the data should be as fine as 1 pT. The sampling rate, in accordance with the cutoff of the analogue filter has to be 10 Hz or higher, preferably over 100 Hz (two times the mains frequency). Timing accuracy is also crucial, as discussed later. To make the near real-time monitoring possible data are transmitted through the internet.

We found that there are only a few magnetometers available on the market that fulfill our strict noise requirements. These are the Ukranian LEMI-025, GEOMAG-02D and the Canadian NAROD (temporarily, sensors not available for this model) fluxgate magnetometers. The CHIMAG magnetometer developed by IWF ÖAW (Austria) and UCLA (USA) that runs at three of the SEGMA sites also fulfills both the noise criterion and has proper filter response. MM100 magnetometers were upgraded by altering the filter cutoff frequency according to the above requirements.

Since none of the models could produce high resolution real-time data, new DAQs were developed by Geological and Geophysical Institute of Hungary (MFGI), and IGFPAS. And the existing DAQs were modified by University of L'Aquila and FMI. At the same time, LEMI developed a new low-noise analogue model (LEMI-035) for PLASMON that has a cutoff at about 10 Hz. MFGI's DAQ is based on a 23-bit AD converter of LAWSON Labs. The resolution is 1 pT at a data rate 1 Hz. The raw sampling rate was chosen 128 Hz. Figure 2 (a) shows the amplitude response and the time delay of LEMI-035 with the new DAQ (raw data). Raw samples are filtered by two digital Gaussian filters subsequently.The first filter has a flat response up to 3 Hz (16 Hz data product), while the second filter used to produce the 2 Hz data cuts off at 0.25 Hz. The time delay of the whole system (magnetometer and DAQ) is ~32 ms in the frequency range we are interested in (Figure 2 (a) and (b)). This delay corresponds to approximately four samples (31.25 ms) of the raw data, and hence could be easily corrected for by a simple shift of the filter. However, since this small delay causes only 2° phase delay in a 200 mHz signal (and even less at lower frequencies) we decided not to correct the data for this delay. The delay will be added to the time labels, instead. The other reason for not correcting the data is that a known time delay (supposing linear phase delay) can easily be corrected for during data processing whenever needed. Since PLASMON makes use also of existing networks (IMAGE) running magnetometers that are not PLASMON compatible, the development of a process for the correction for timing inaccuracy is not avoidable, anyway.

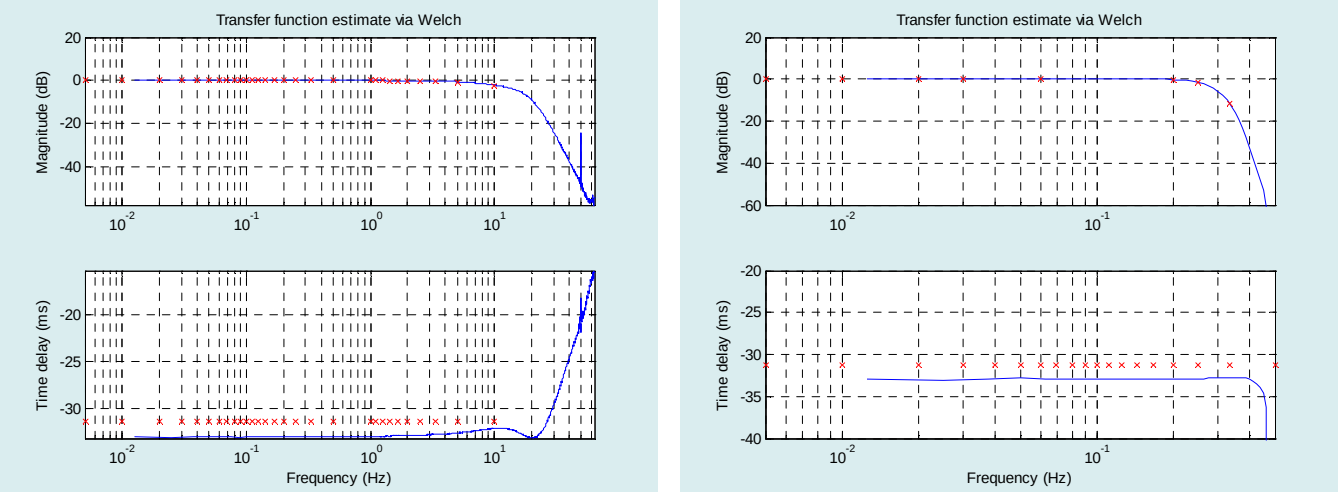

Figure 2 –Amplitude response and time delay of (a) the raw data sampled at 128 Hz (b) 1 Hz data product. Blue lines/ red crosses represent the results of filter response analysis when a step function / sine wave was used as driver signal

IGFPAS installed the magnetometers, data loggers, supply units, and batteries in plastic PVC tubes about 100 meters from the buildings supplying the 230V voltage (Figure 3). The tubes were burried about 2m deep. The magnetometers were equipped with 3Hz analog low-pass filters. The data logger samples the signal with a frequency of 12.5 kHz. 1 Hz samples are generated by digital filters. Every 2 minutes data are transmitted to an industrial computer via ftp protocol using powerline ethernet adapters. The industrial computer and the switch are placed in a building. The data are sent from the field station to Belsk Observatory using the GSM modem.

As an extension of the existing networks IGFPAS installed two stations in Poland (SCZ and ZAG) and one in Lithuania near Birzai. MFGI installed a station at Vyhne (Slovakia) and another is currently being installed at the new Croatian observatory at Lonsko Polje.

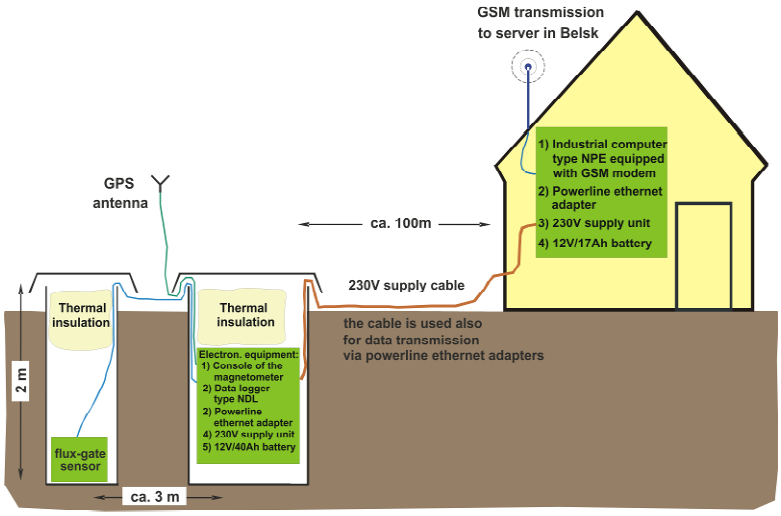

Figure 3 –Scheme of geomagnetic field station in Birzai (Lithuania

3. PRELIMINARY RESULTS OF PLASMA DENSITY MONITORING

In this section we present a few examples for the first results of the project. First, the plasma mass density measurements made during a geomagnetically disturbed period is presented. Figure 4 presents the equatorial plasma mass densities inferred through the phase-gradient technique (Waters et al., 1991) from FLR observations at the Nagycenk-Tihany pair between 2-30 November, 2004 as blue crosses. Red symbols depict electron densities deduced from VLF whistler observations. An SSC occurred on 7 Nov, 2004 (DoY 312) which was followed by another one two days later. The mass density of the plasmasphere increased after the first SSC, possibly due to the appearance of heavier ions (mostly oxygen) or to the uplifting of the F layer via the ExB drift. Later, starting from 9 Nov (DoY 314), the plasmasphere became depleted by the increased convection electric field, as a consequence of the enhanced solar wind speed. During the recovery phase of the storm (to 19 Nov, DoY 324) the flux tube along the local field line was gradually refilled from the topside ionosphere through ambipolar diffusion. Later on, the geomagnetic field became disturbed again causing a depletion. In the meantime, the temporal evolution of the electron density followed a same pattern. From the four simultaneous observations of plasma mass and electron densities,

all from the recovery phase of the storm, the average ion mass was estimated to be in the range of 1.4-2 amu/particle meaning that the overwhelming majority of the particles were hydrogen. The contribution of oxygen was not more than a few per cent. Since the VLF and ULF density measurements have not yet been intercalibrated, the results do not enable us to draw any further conclusions on the ion composition. However, this problem is also adressed by the project.

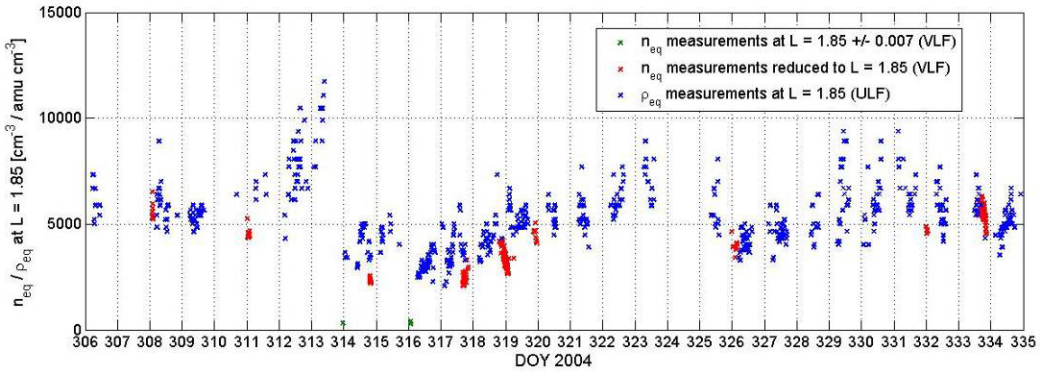

.

Figure 4 –Equatorial pasma mass / electron densities inferred from ULF FLR / VLF whistler observations at L = 1.85

Figure 5 presents the radial density gradient in the plasmasphere as inferred from VLF observations (Tihany), as well as from ULF observations (MM100 stations). The two methods yielded again consequent results. The radial density gradient of the plasmasphere increased during the main phase of the storm, and decreased gradually as the flux tube was re-filled during the storm's recovery phase.

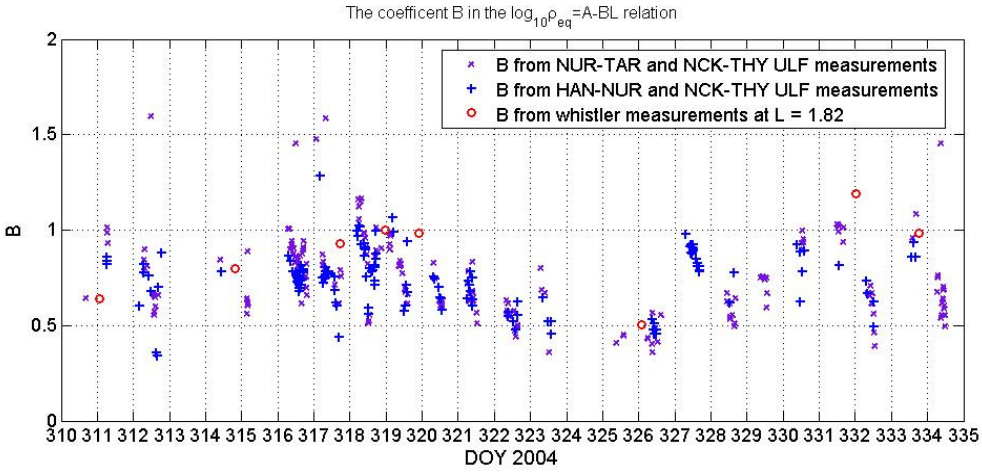

Figure 5 – Equatorial radial pasma mass / electron densitiy gradient inferred from ULF FLR / VLF whistler observations

Further studies of the dynamic behaviour of the plasmasphere will lead us to a better understanding of the solar wind-magnetosphere-plasmasphere coupling. PLASMON will build an unprecedented real-time monitoring system and develop a data assimilative model of the plasmasphere to help scientist to get closer to this goal.

4. ACKNOWLEDGEMENT

The research leading to these results has received funding from the European Union Seventh Framework Programme (FP7/2007-2013) under grant agreement no 263218.

5. REFERENCES

Heilig, B., S. Lotz, J., Verő, P. Sutcliffe, J. Reda, K. Pajunpää, and T. Raita (2010): "Empirically modelled Pc3 activity based on solar wind parameters.". *Annales Geophysicae*, **28**, 1703-1722.

Vellante, M., Lühr, H., Zhang, T. L., Wesztergom, V., Villante, U., Lauretis, M. D., Piancatelli, A., Rother, M., Schwiegenschuh, K., Koren,W., and Magnes,W.. (2004): " Ground/satellite signatures of field line resonance: A test of theoretical predictions ". *J. Geophys. Res.*, **109**, 213, A06 210, doi:10.1029/2004JA010392.

Waters, C. L., Menk, F. W., and Fraser, B. J. (1991) The resonance structure of low latitude Pc3 geomagnetic pulsations, *Geophys. Res. Lett.*, **18**, 2293-2296.

NEW OBSERVATIONS FROM REMOTE EQUATORIAL STATIONS IN THE SOUTHERNMOST PARTS OF INDIA

P. Chandrasekhar[(1)], K. Arora [(1)] , N. Nagarajan [(1)]

[(1)] CSIR-NGRI, Hyderabad-500007, India, phaninelapatla@gmail.com, karora_ngri@yahoo.co.uk, nandini_ngri@yahoo.com

SUMMARY

The southern parts of India provide a unique geographical locale to investigate the influence of latitudinal and longitudinal variability of ionospheric phenomena in records of magnetic variations, close to the dip Equator. Additionally, this region also represents significant variation in tectonic setting with the Andaman-Sumatra subduction zone in the east, the aseismic Chagos-Laccadive Ridge to the west and the continental margin of Peninsular India in between. First attempt at recording magnetic variation data concurrently at the Andaman-Nicobar Islands and KanyaKumari at the southern tip of the Peninsula was made in 2010, overcoming acute logistic hurdles. Three months of concurrent data for year 2011 from threesites have been obtained and are presented here. The data represents the first observations from a region of sparse geophysical data and has the potential to contribute to fundamental studies on ionospheric variability as well as electromagnetic induction effects of distinct geotectonic regimes. The induced component of the observations would be analysed to estimate electrical conductance distribution generated by the different subsurface structures.

1. INTRODUCTION

Studies based on the longitudinal and latitudinal behavior of the geomagnetic field based on ground measurements in the region of the dip Equator are limited. Several reasons contribute to this fact, the primary one being that large parts of thiszoneare covered by ocean. Such observations made on medium to long term basis would provide crucial information on subtle changes in ground measurements in equatorial regions, leading to understanding of variability in ionospheric and magnetospheric phenomena (Fambitakoye and Mayaud, 1976; Rastogi, 1973). Taking advantage of the unique locale of the Indian Peninsula and adjoining Andaman-Nicobar islands, remote measurement sites were established at Port Blair (PBR, dip :2.9^0 , 92^0 42.536'E) and Nicobar (CBY, dip : -1.66^0 , 93^0 55.585'E) and KanyaKumari (VEN, 0.076^0, 77^0 10.977'E) as indicated in Figure 1.The Hyderabad [HYB] magnetic observatory (dip: 10.18^0, 78^0 3'E) is an INTERMAGNET OBSERVATORY (IMO) at the CSIR-National Geophysical Research Institute, Hyderabad.

Executing field studies and remote operation of instruments in Andaman & Nicobar is a challenging task. Limited land area, strict regulation of access to remote regions, pressure on scant resources consequent to devastation by Indian Ocean Tsunami, are reasons for limited visits for recovery / trouble shooting. At CBY, the station is located at a forest check post whereas the VEN station is running in the premises of a school; the PBR station is located within the premises of office buildings. Concurrent data from these sites for a span of threemonths are presented here for the purpose of initial characterization and to obtain preliminary estimates of longitudinal variability of Equatorial Electrojet (EEJ).

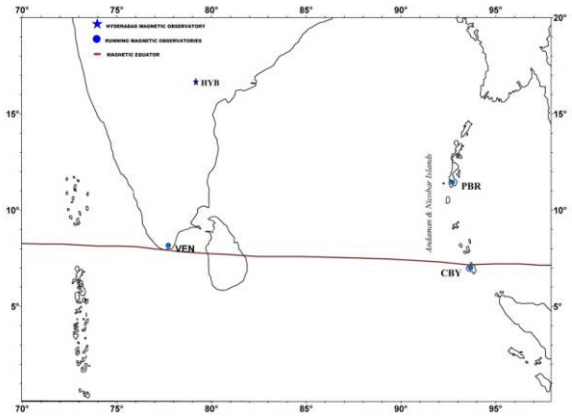

Figure 1 –Layout of the remote stations.

The observations presented here, additionally, form the basis of comparing estimated induced response of 3-d ocean and crustal conductivity structure beneath the surrounding ocean with observed induced Z-variations. Computation of induced response using 3-d ocean bathymetry grid has shown remarkable results to fully explain anomalous daily variation at coastal sites (Kuvshinov et al, 2007). Preliminary assessment of anomalous Z-variations is presented here.

2. DATA

Figures 2 to 4 show daily means of all components of the Earth's magnetic field as recorded at PBR, CBY and VEN for the duration Oct-Dec 2011.

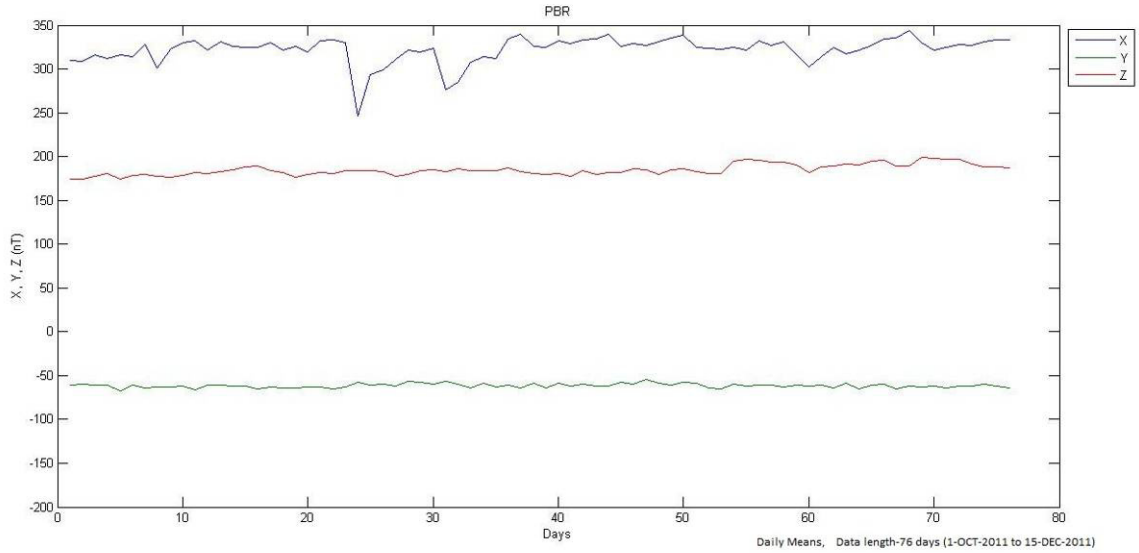

Figure 2 –Three component variation data from Port Blair (PBR).

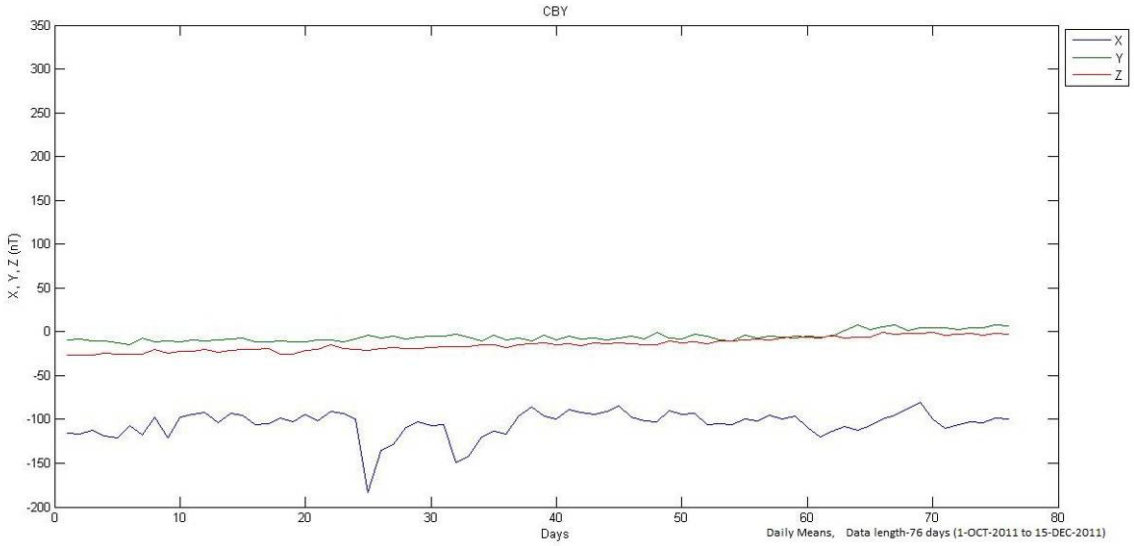

Figure 3 –Three component variation data from Campbell Bay (CBY).

At PBR, X>Z>Y in terms of amplitude. At CBY it is Y~Z>X; this station being south of dip equator, the X variation data are negative. At VEN, X~Y~Z, X being slightly positive and Y and Z near zero as this station is very close to the dip equator. Baseline data from the three stations have been infrequent due to reasons of distance and difficulty of access. Sample measurements are presented in Figure 5.

Power spectrum analysis of the minute data serves to make quantitative comparisons of the new data with that of IMO-HYB, shown in Figures 6 and 7. Significant variations at short (<4h) and long (> 4h) periods are seen. At high frequencies, VEN(X) and VEN (Z) are dominant, but corresponding CBY(X) and CBY (Z) are even stronger. At low frequencies VEN(X) and PBR (Z) are significant but CBY(X) and CBY (Z) exhibit the maximum power. A preliminary assessment of the effect of ocean induction on VEN (Z) and CBY (Z) data can be inferred. At the dip equator, Z-variations are expected to be small. However, the influence of anomalous induced effects of ocean-continent contrast (Parkinson, 1987,Manoj et al, 2006a, Maus et al, 2006 and Maus et al, 2010) and the effects of 3-d ocean bathymetry on coastal observatories (Kuvshinov et al, 2007) would explain the anomalous Z variations.

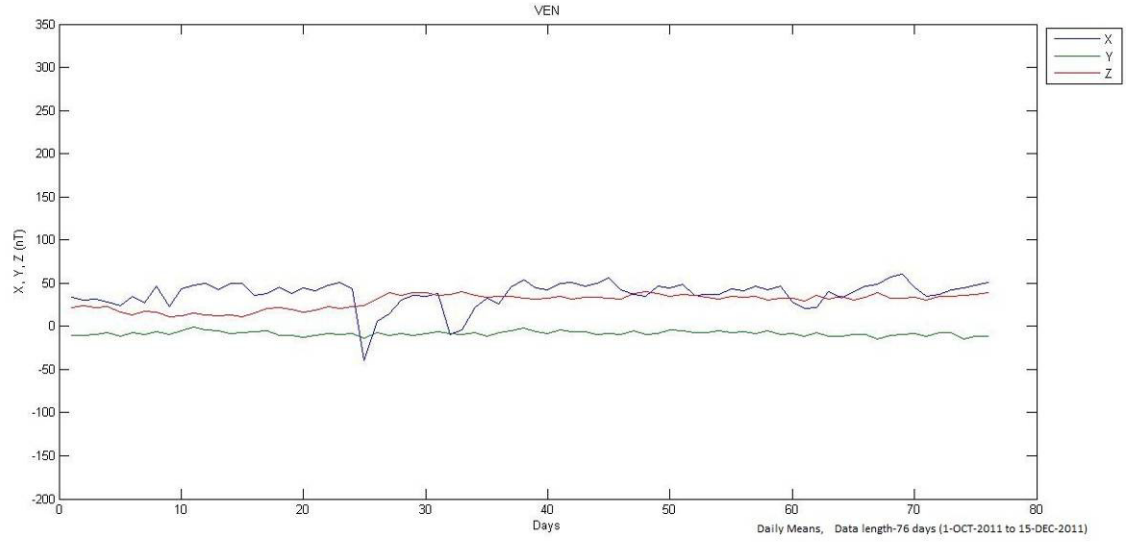

Figure 4 –Three component variation data from Vencode (VEN).

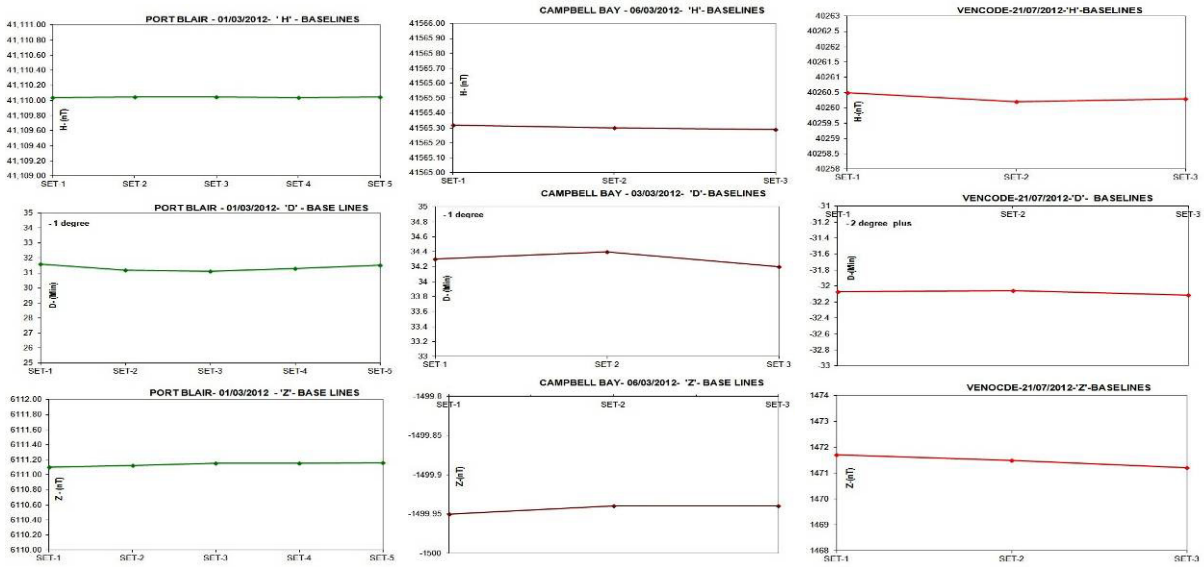

Figure 5 –Sample baseline measurements in PBR, CBY and VEN

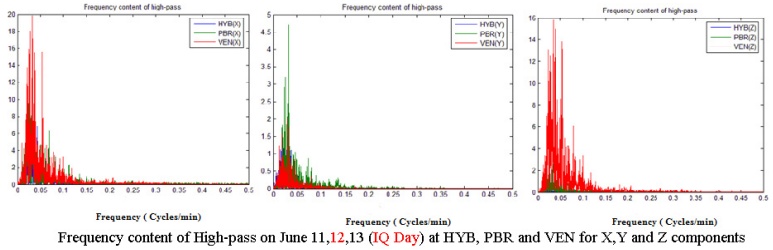

Frequency content of High-pass on June 11,12,13 (IQ Day) at HYB, PBR and VEN for X,Y and Z components

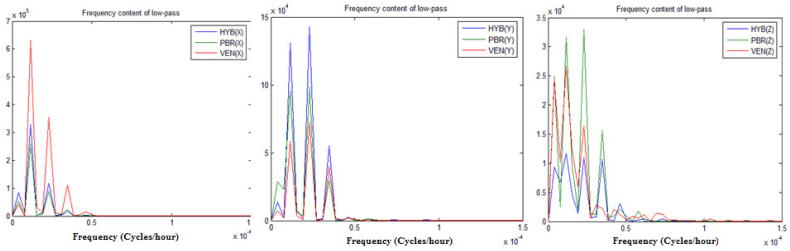

Frequency content of Low-pass on June 11,12,13 (IQ Day) at HYB, PBR and VEN for X,Y and Z components

Figure 6 –Comparison of power spectrum of PBR and VEN data with HYB

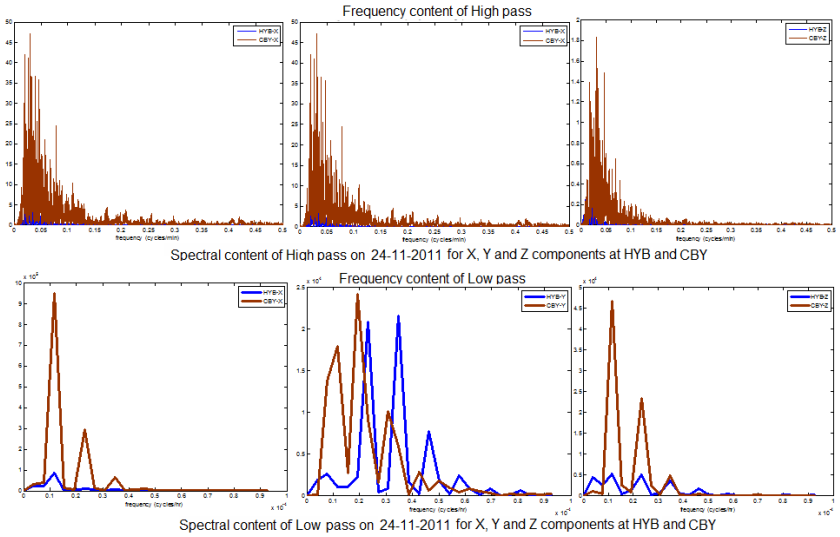

Figure 7 –Comparison of power spectrum of CBY data with HYB

The time difference of the noon time peaks is clearly recorded between CBY to the east, where the noon time maximum is one hour earlier and VEN to the west. Figure 8 shows an example for longitudinal variability in horizontal component recorded at all the stations on Nov 9th, 2011, plotting hourly averages. Thus it is possible to use this unique set of observations at the dip equator, and indifferent ocean margins, for preliminary estimates of both equatorial ionospheric variability and sub-surface electrical conductance.

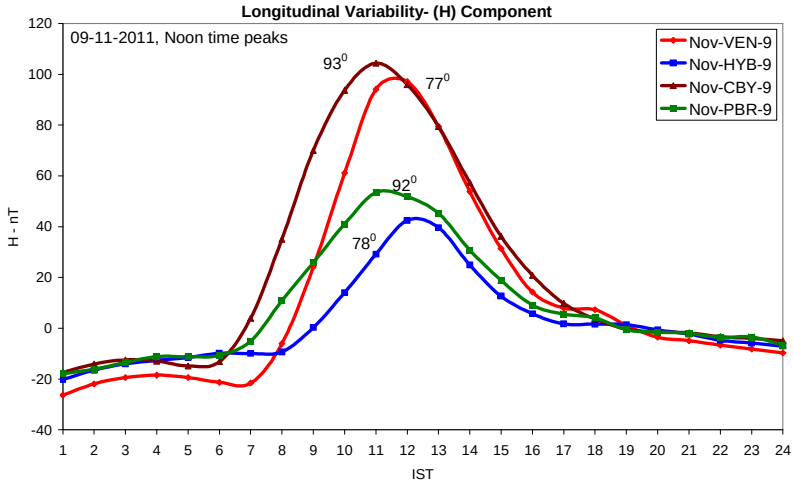

Figure 8 –Time difference in noon time maxima between PBR, CBY, HYB and VEN

3. LONGITUDINAL VARIABILITY OF THE EEJ

The Equatorial Electrojet (EEJ) is an exciting phenomenon, which needs more extensive studies. VEN and CBY are sites influenced by the EEJ and the data obtained have been used for preliminary comparisons. Figure 9 shows the hourly averages of each day of Dec 2010, from which the midnight means have been removed. Visual examination shows the strength of the daytime signal to be of an average strength of 60 nT at VEN and 100 nT at CBY.

The diurnal change at EEJ stations is sometimes obscured in such a way that the amplitudes are suppressed and variation is well below the night time level. This was described as Counter Electrojet (CEJ) by Gouin and Mayand (1967). CEJ occurs on quiet days and often on consecutive quiet days and also on disturbed days. The causative mechanisms of the CEJ have been detailed in numerous studies (Onwumechilli et.al (1973), Rastogi (1973), Sizova (2002). Tidal, auroral and interplanetary effects responsible for the CEJ formation have been modeled (Manoj et al 2008, Alken et al 2011). The equatorial field strength is further constrained by removing Sq variations $(\Delta X_{SQ+EEJ} - \Delta X_{SQ})$, where (ΔX) is the difference in X-variation over mean midnight (18:00 to 21:00 LT) level at each of the selected pair. Two electrojet pairs, **VEN-HYB=ΔX_1** and **CBY-PBR = ΔX_2**, separated by a 15^0 longitude are used here to estimate EEJ and CEJ variations for the period under study.A sample comparison for the day of 9 Nov, 2011 is shown here. On this particular day the strength of Morning CEJ as well as EEJ is more at VEN shown in Figure 10. Observations over longer periods are required to establish trends of this pattern.

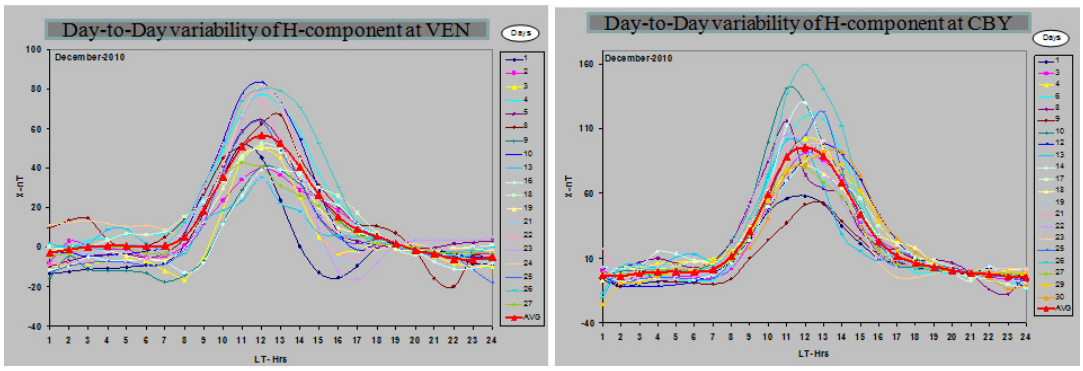

Figure 9 –Typical variability of electrojet strength at VEN and CBY, Red color line represents average– December, 2010 electrojet strength of one complete month

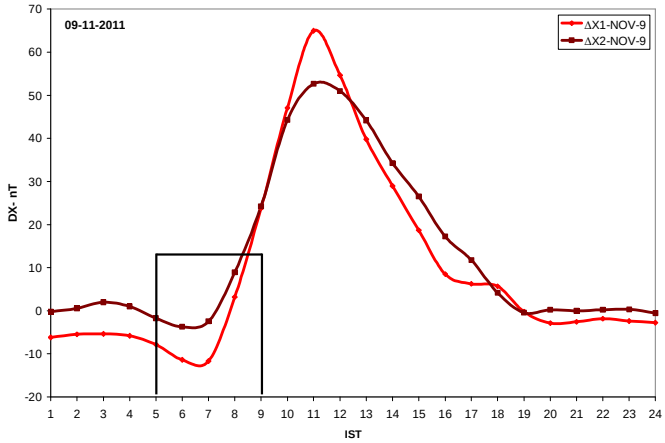

Figure 10 –A typical example for Morning CEJ as well as EEJ at electrojet stations

4. DISCUSSIONS AND INFERENCES

Magnetic variation data from remote equatorial sites are being presented in this study. These sites are in coastal and island regions of the northern Indian Ocean. The data represent the cumulative effects of ionospheric characteristics in equatorial regions, coast effect and induction of ocean waters. A few preliminary results from the comparison of 2 equatorial stations (CBY and VEN) separated by 15^0longitude are presented here. Present data indicates that the phenomenon of CEJ or any variability in EEJ could be a localized event and may not occur on the same day even at locations separated by a longitude of 2-3 hours (Alex and Mukherjee, 2001, Luhr et al, 2011, Manoj et al, 2006b).

The new set of electrojet pairs used in the present study (VEN-HYB=ΔX1 and CBY-PBR = ΔX2) formed the first set of magnetic field records across the globe, separated by 15^0 longitude. These studies present the nature of equatorial electrojet day-to-day variability and association with different interplanetary parameters. Short period disturbances on the earth's magnetic field at the electrojet stations play a key role in understanding dynamics of the ionosphere. These studies at equatorial electrojet stations will provide opportunity to understand the correlations between geomagnetic variations and solar–terrestrial environment.

5. ACKNOWLEDGEMENTS

The authors are thankful toProf. MrinalSen, Director, CSIR-NGRI permission to publish this work. We thank Dr.P.B.V.SubbaRao (IIG, Bombay) for lending magnetometers for the period of observations, our colleagues Mr. S.R. Sannasi, Mr. K. Chandrasekhar Rao, Ms. L. Manjula and Mr. Ankit Singh for their assistance in data acquisition and baseline measurements. These observations are possible with the co-operation of Bethany Navajeevan High School, Vencode and Assistant Commissioner, Nicobar Administration, in permitting the observations on their land at Vencode and Campbell Bay. This work is carried out with financial assistance from 11^{th}Five year plan to the *Supra-Institutional Project*as well as GENIAS project of CSIR-NGRI.

6. REFERENCES

Alex S and Mukherjee S (2001) ; Local time dependence of the equatorial counter electrojet effect in a narrow longitudinal belt; *Earth Planets Space*.53 1151–1161.

Alken P, Maus S, Richmond A, Maute A (2011) ; The ionospheric gravity and diamagnetic current systems; J.Geophys. Res. 116,

Fambitakoye, O., and P. N. Mayaud (1976); Equatorial electrojet and regular daily variation SR — II. The centre of the equatorial electrojet, J. Atmos. Terr. Phys., 38, 19 – 26, doi:10.1016/0021-9169(76)90189-6.

Gouin P and Mayaud P N (1967) ; Apropos de existens possible d'un counter electrojet aux latitudes equatorials; *Ann. Gephys*. 23 41-50.

Kuvshinov, A., and Manoj, C., and Olsen, N. and Sabaka, T. (2007); On induction effects of geomagnetic daily variations from equatorial electrojet and solar quiet sources at low and middle latitudes. J. Geophys. Res., 112, B10102, doi:10.1029/2007JB004955.

Luhr H, Rother M, Hausler K, Fejer B and Alken P (2011) ; Direct comparison of non migrating tidal signatures in the electrojet, vertical plasma drift and equatorial ionization anomaly; *J. Atmos. Terr. Phys.*Doi: 10.1016/j.jastp.2011.07.009.

Manoj, C., Kuvshinov, A. V., Maus, S., and H.Lühr, (2006a), Ocean circulation generated magnetic signals, Earth, Planets and Space, 62, Issue 10 pp 729-735.

Manoj C, Luhr H, Maus S and NandiniNagarajan (2006b) ; Evidence for short spatial correlation lengths of the noontime equatorial electrojet inferred from a comparison of satellite and ground magnetic data; *Journal of Geophysical Research*. 111 A11312,doi: 10.1029/2006JA011855.

Manoj C., S Maus, H Lühr, P Alken (2008). Penetration charecterstics of the interplanetary electric field to the day time equatorial ionosphere, J. Geophys. Res Volume 113 Pages

A12310.

Maus, S. M., Rother, M., Hemant, K., Stolle, C., Lühr, H., Kuvshinov, A., and N. Olsen (2006), Earth's lithospheric magnetic field determined to spherical harmonic degree 90 from CHAMP satellite measurements, Geophys. J. Int., 165, 319-330. , 429-437.

Maus, S.; Manoj, C.; Rauberg, J.; Michaelis, I.; Lühr, H.(2010); NOAA/NGDC candidate models for the 11th generation International Geomagnetic Reference Field and the concurrent release of the 6th generation POMME magnetic model, Earth Planets and Space, 62, 2010. Pp.729-735.

Onwumechilli C A, Kawasaki A K and Akasofu S (1973); Relationship between the equatorial electrojet and the polar magnetic variations ;*Planet. Space Sci*. 21 1–16.

Parkinson W D (1987) ; Introduction to Geomagnetism, Elsevier Science Ltd.

Rastogi R G (1973) ; Counter equatorial electrojet in the Indian zone; *Planet.Spase Sci*. 21 1355-1365.

Sizova L Z (2002) ; The field-aligned currents effect on equatorial geomagnetic field variations; *Adv. Space Res*. 30, 2247-2252.

A NEW MEASUREMENT METHOD FOR MAGNETIC REPEAT STATIONS

X. Lalanne[(1)], A. Peltier[(1)], A. Chulliat[(1)], A. Telali[(1)], B. Heumez[(1)]

[(1)] Institut de Physique du Globe de Paris, lalanne@ipgp.fr

SUMMARY

The relevance of traditional magnetic repeat station networks to geomagnetic modeling has been increasingly challenged during the last decade, as the Ørsted and CHAMP satellites provided data of unprecedented precision and spatial resolution. Yet magnetic repeat networks organized on a national or regional basis can still be viewed as relatively inexpensive safety nets in case satellite data are not available. Here we present a new method for magnetic repeat measurements, where repeat stations are located on airports, azimuth sightings are determined using GNSS geodetic receivers and magnetic measurements are performed at night (around 0200 local time). This method aims at improving the measurement precision while keeping the cost low, by facilitating the measurement execution. It was first implemented in metropolitan France during the summer 2012. Its full evaluation will be made in 2013, after a first reoccupation of the new French repeat network.

1. INTRODUCTION

Magnetic repeat stations are precisely located points at the Earth's surface, where the three components of the geomagnetic field are regularly measured to the highest possible accuracy, in order to determine the geomagnetic secular variation (Newitt et al., 1996). The role of magnetic repeat stations is to complement magnetic observatories, by providing data in areas where the installation of a full observatory would be too costly and/or impossible due to the lack of infrastructure and local manpower. For this reason, many countries have set up magnetic repeat station networks in order to regularly update geomagnetic charts on their territory. In France, a national repeat station network was set up in 1947, expanded and upgraded in 1965 and reoccupied every five years until 2007 (Chulliat, 2012).

The advent of magnetic satellites such as Ørsted and CHAMP has challenged this traditional approach. High-precision, vector satellite data make it possible to calculate geomagnetic secular variation models of unprecedented spatial resolution without using repeat station measurements. For example, the latest International Geomagnetic Reference Field model (Finlay et al., 2010) provides the average secular variation between 2005 and 2010 up to spherical harmonic degree 13. Some research models actually provide the time-varying secular variation up to degree 13 over the entire decade (e.g., Lesur et al., 2010). Within the *Bureau Central de Magnétisme Terrestre*, the French organization in charge of ground magnetic measurements, a decision was made to continue repeat station measurements as a "safety net" in case no high-precision satellite data are available for an extended period of time in the future, but using a smaller network and an improved measurement method in order to reduce the overall cost of each measurement campaign. The key ideas of the new method are to implement stations on airports, use the Global Navigation Satellite System (GNSS) for precise azimuth measurements and perform magnetic measurements at night, when ionospheric disturbances are minimal.

Here we present the new method and how it was implemented in metropolitan France over the summer 2012. A full evaluation of the method will be made in 2013, after a second measurement campaign, by comparing the obtained secular variation with the secular variation provided by the IGRF model and, if available, the first models derived from the upcoming ESA Swarm satellite mission (Friis-Christensen et al., 2006).

2. NEW METHOD: KEY IDEAS

Implementing stations on airports

French magnetic repeat stations setup between 1947 and 1965 were materialized by a survey marker buried or semi-buried in the soil, sometimes along roads in colocation with stations of the French Reference Leveling Network, and more often in fields under an agreement with local owners (often farmers). Fifty years later, the leveling network is no more maintained as it was largely replaced by a GNSS network, some roads have been enlarged and some private properties have changed owner. As a result, keeping survey markers intact from one survey to the next becomes more difficult. In addition, some prominent features used as azimuth marks (e.g., church steeples,

lighthouses, telecommunication antennas, etc.) have been modified during building maintenance operations or have become invisible due to vegetation growth. For all these reasons, it was decided to start a new network from scratch and two objectives were assigned to the stations of the new network: the sustainability of the site (public premise versus private property) and its magnetic cleanliness along an extended period of time.

Airports satisfy very well these two requirements, provided some precautions are taken. For the first requirement, it is necessary to select airports belonging to a public authority and having no risk of being closed in a foreseeable future. This is the case for all airports that were selected for the new repeat station network. Regarding the second requirement, the positioning of the measurement mark on the airstrip axis offers a good guarantee of stability of the magnetic environment. In France the runway is generally made of several layers of compacted limestone gravel and a final layer of bituminous concrete which are largely nonmagnetic. Secondly, the runway is about 45 m wide and, as no obstacle over an angle of 5° is allowed from the edge of the airstrip, there is very low risk that a significant building is erected at a distance less than 100 meters from the magnetic station. In addition to their favorable magnetic properties, airports offer a perfect line of sight along the runway to install the azimuth target.

Finally, it is worth noting that, as aeronautical charts are referenced to the magnetic North, airport authorities are interested in accurate magnetic declination measurement on their premises.

Performing night-time measurements

Our experience on airborne or marine surveys shows that precise removal of the diurnal variation can't be achieved when the distance to the reference station is greater than 200 km. Some groups install a 3-axis variometer in the vicinity of the magnetic repeat station, but the installation of such an equipment is not easy and relatively time consuming, as it is needed to ensure a good enough mechanical and thermal stability. For these reasons, we decided to operate at times when the diurnal variation is minimum, between 2 and 4 LT (i.e., between 4 and 6 a.m. in French summer time). This time slot also has the advantage of minimizing the interferences with airport operations.

Operating by night in a steel-free environment is not easy and some devices have to be built for this purpose. The most important is the theodolite lighting device. We developed a dedicated system for the Zeiss 010 theodolite (Figure 1a), as light paths are specific for each type of theodolite. It consists of a small PC board of FR4 equipped with 3 white LED and feed in D.C through a nonmagnetic coaxial cable. The second lighting device is the azimuth target. We made a 20 cm square surface with black and white sectors backlighted by white LEDs (Figure 1b). Schematics and pictures for both systems are available on demand.

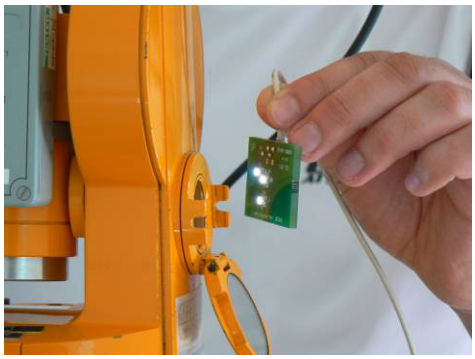

Figure 1a –The lighting device for Zeiss 010.

Figure 1b –The illuminated azimuth marker.

Using GNSS

Operating at night means that the use of prominent features as azimuth marks is no more possible, since these features cannot be easily illuminated. Star sighting requires considerable training to be performed to the required level of accuracy, and is weather dependent. By contrast, determining the azimuth using GNSS is easier and this is the method we chose.

The GNSS method consists in setting up GNSS geodetic receivers (Trimble NetR9 in our experiment) at the two ends of a 420 m baseline defined by the theodolite and the target, and recording the GNSS signal phase observables at 1Hz frequency. The acquisition lasts about 5 hours. We used the Ashtech Solution software for the data post processing that determines the precise positions of the two receivers, from which we calculated the azimuth of the baseline defined by the two receivers. Figure 2 shows the azimuth calculated at each epoch of the acquisition (example of Lyon airport). The determination of geodetic azimuth by GNSS reaches an accuracy range of 1- 5 arc-second, well below the requested accuracy of 20 arc-second obtained by Sun or star sighting. As was observed in the Cannes airport, where the measurement session had to be interrupted due to an emergency sanitary flight, the requested accuracy is even reached for short acquisition duration (3 hours).

Thanks to the short length of the baseline and the field environment, the accuracy of the GNSS measurements is quite good. On the airport runways, there is no more interfering obstructions (as buildings, trees…), which leads to an increased number of satellites seen by the receiver, an increased strength of satellite geometry, fewer satellite signal multi-paths and less corruption of GNSS measurements.

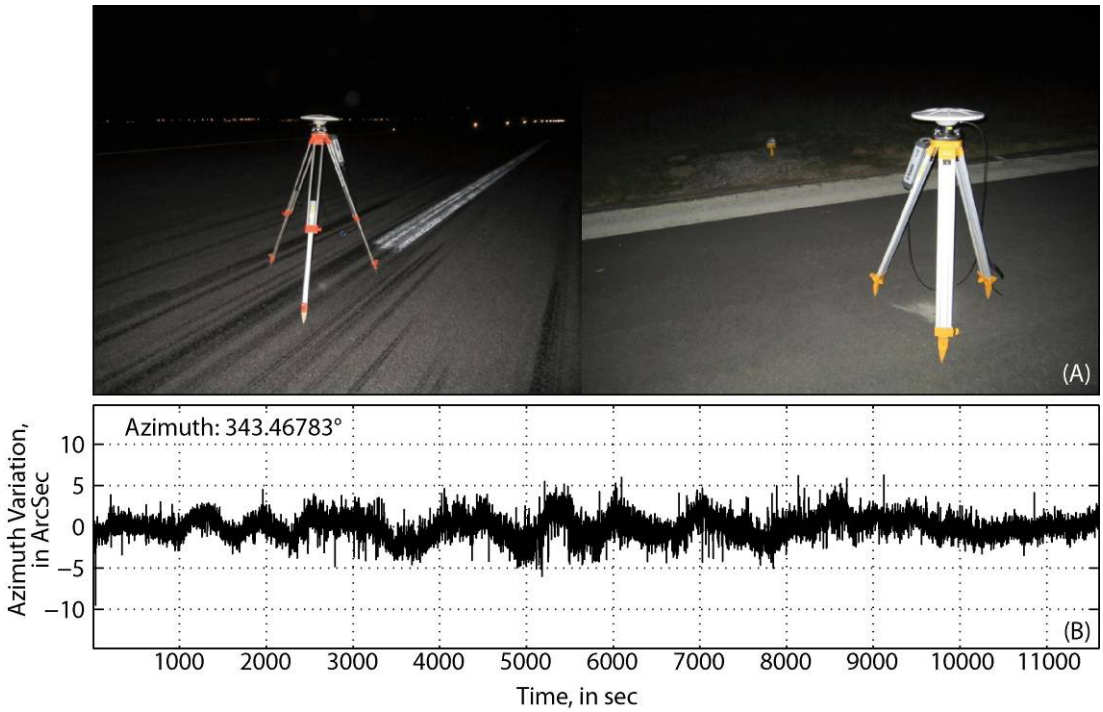

Figure 2 – (A) GNSS receivers set up on the runway of the Lyon-Bron airport. (B) Azimuth variation recorded in the same airport.

3. NEW METHOD: OPERATION WORKFLOW DURING THE 2012 SURVEY

The new French repeat stations network is made of eleven stations covering the territory of metropolitan France (Figure 3). This distribution of stations is thought to be sufficient to guarantee a precision of the secular variation over France similar to that obtained from satellite measurements. This will be checked after the 2013 measurement campaign.

Operations on airports require several months of preparation and cannot be improvised or easily re-scheduled. Even if the airports we selected are closed at night, they can be used for landing by an aircraft in distress or for a sanitary flight. In the first case, the airport authorities have to issue a NOTAM to inform all flight that such runway will be unusable in any case during this specific night. In the second case, a 1-hour pre-alert is common and sufficient to remove all equipment's from the runway. Of course safety and security regulations must me strictly observed. Operators must wear fluorescent yellow safety vest to enhance their visibility when working on airport grounds, the car must be equipped with an orange flashing light and the operators must dispose a VHF radio or cell phones. Operator's IDs and car documents must be provided to airport authorities several days in advance.

The installation and first occupation of the new repeat station network was organized in three 5-day sessions mobilizing 2 operators each. One airport was occupied every night and a distance between 450 and 600 km was travelled by car every day.

A typical installation and measurement session happens as follows. The 2-person team arrives on the airport at 5 p.m. (French summer time), so that a daylight visual reconnaissance of the runway is possible, in order to locate a flat section of 420 m - the distance between 7 runway lighting markers - for the azimuth sighting. Only a few minutes are available, inserted between the aeronautical operations. The team comes back at the airport closing time in order to deploy the GNSS geodetic equipment. On the runway central axis, at the place identified during the afternoon reconnaissance, a quick magnetic check is done with a scalar magnetometer. Then a 10 mm hole is drilled and a steel free marker is placed (see Figure 2a). A steel-free tripod is installed vertically and a geodetic GNSS antenna is precisely centered with respect to the ground marker. The same operation is done at a distance of 420 m for the azimuth mark, but generally not on the runway central axis – as the magnetic environment is not sensitive – but on the runway at 1 m distance from a lighting aid for easy recovering in the future. Both receivers are switched on for a 1-Hz sampling rate recording, until the beginning of the magnetic measurements.

A few hours later, after taking some rest at a nearby hotel, the team comes back to the airport at 3:30 a.m. for the magnetic measurement. The antenna of the GNSS receiver on the runway axis tripod is replaced by the DI-Flux theodolite precisely centered on the ground marker and the second antenna is replaced by the azimuth backlighted target.

A scalar magnetometer is set up for continuous recording a few meters away from the theodolite. A seat and a table are placed for the operator who notes the observations on a logbook. Great care is taken for keeping magnetic and lighting devices at a safe distance from the theodolite.

Generally a set of 8 complete observations can be performed before 6 a.m. Then, 15 minutes are sufficient to remove all the equipments before the runway is inspected and the air operations restart (around 6 a.m.)

No onsite data check is performed, because the team has to take some rest before travelling to the next station, and also because operations on an airport must be scheduled several days in advance and therefore no additional measurement and/or change in the experimental setup could be made on the same day anyway. In case of instrument malfunction or measurement errors at a given site, a new campaign for this site has to be organized later. However, the measurements made each day are sent by email to a second team in the IPGP offices, in order to detect a possible malfunction of the DI-flux or the scalar magnetometer.

Subsequent reoccupations of the new repeat station network will be easier. Before reoccupying each station, we will ask to the airport authorities to check for the presence of the ground marker. If the ground marker is still there, no new GNSS geodetic measurement will be necessary.

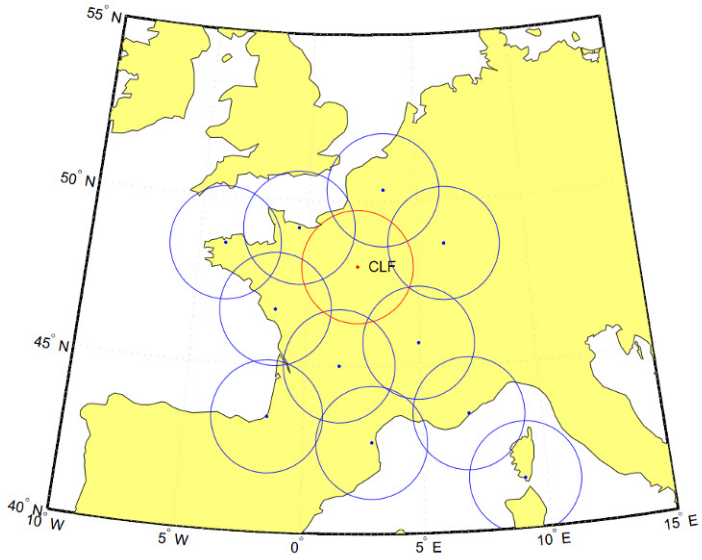

Figure 3 –Map of the new repeat station network for metropolitan France. Circles centered on each station and of radius 1.7° are shown.

4. REFERENCES

Chulliat, A., ed. (2012): *Réseau magnétique de répétition de la France - French magnetic repeat station network 2007*. Bulletin No 28, Bureau Central de Magnétisme Terrestre, Paris.

Finlay, C. C., S. Maus, C. D. Beggan, T. N. Bondar, A. Chambodut, T. A. Chernova, A. Chulliat, V. P. Golovkov, B. Hamilton, M. Hamoudi, R. Holme, G. Hulot, W. Kuang, B. Langlais, V. Lesur, F. J. Lowes, H. Lühr, S. Macmillan, M. Mandea, S. McLean, C. Manoj, M. Menvielle, I. Michaelis, N. Olsen, J. Rauberg, M. Rother, T. J. Sabaka, A. Tangborn, L. Toffner-Clausen, E. Thébault, A. W. P. Thomson, I. Wardinski, Z. Wei and T. I. Zvereva (2010): "International Geomagnetic Reference Field: the eleventh generation". *Geophys. J. Int.*, **183**, 1216-1230, doi:10.1111/j.1365-246X.2010.04804.x.

Friis-Christensen, E., H. Lühr and G. Hulot (2006): "Swarm: A constellation to study the Earth's magnetic field". *Earth Planets Space*, **58**, 351–358.

Lesur, V., I. Wardinski, M. Hamoudi and M. Rother (2010): "The second generation of the GFZ Reference Internal Magnetic Model: GRIMM-2". *Earth Planets Space*, **62**, 765-773.

Newitt, L.R., C.E. Barton and J. Bitterly (1996): *IAGA Guide for Magnetic Repeat Station Surveys*. International Association of Geomagnetism and Aeronomy.

MONITORING AND ANALYSIS OF SPATIAL-TIME ALLOCATION OF BAIKAL RIFT ZONE INHOMEGENEITIES

Y. Lipko [(1)], R. Rakhmatulin [(1)], S. Khomutov [(1)]

[(1)] Institute of Solar-Terrestrial Physics RAS SB, 126 Lermontov str., Irkutsk, 664033, Russia, lipko@iszf.irk.ru

[(2)] Altay-Sayan Branch of Geophysical Survey of SB RAS, 3 Koptyga str., Novosibirsk, 630090, Russia, khomutov@gs.nsc.ru

SUMMARY

The Baikal rift zone (BRZ) is a unique geological and tectonic formation, and it exerts a substantial influence on the local geological profile and behavior of the constant magnetic field vector in the region of the Baikal depression. Nevertheless, since the end of the 1970s, mass magnetic measurements in the BRZ for studying the magnetic field have hardly been conducted. In the time that has elapsed since these quite uncoordinated and incomplete observations, significant spatiotemporal changes have occurred in the BRZ's natural magnetic field related to both global changes in the geomagnetic field and geotectonic processes in the Lake Baikal region.

To obtain reliable geophysical data, magnetic observations were conducted in 2009 in fracture areas on land and on the ice of Lake Baikal. According to the observation results, the presence of a large_scale magnetic anomaly in the measurement region has been established: magnetic declination D is from 5°20′ to 6°20′, whereas magnetic declination in the Irkutsk region is approximately 3°. This large_scale magnetic anomaly has a complex structure and is not shown on magnetic field distribution maps of Irkutsk oblast.

1. REVIEW OF BRZ MAGNETIC FIELD STUDIES

The BRZ is an object of large scientific and applied studies. In experimental studies on the BRZ magnetic field and its central part, Lake Baikal, three stages can be singled out.

1. Aeromagnetic survey in the 1960s, generalization of the results of which is reflected in (Anistratenko et al., 1973); Bulmasov, 1968).
2. Hydromagnetic survey of the entire Lake Baikal water area, performed in 1970 with the help of a boat mounted PM_5 proton magetometer (Valyashko et al., 1979). The complex hydromagnetic survey done in 1977 also pertains to this, performed using apparatus of the Institute of Oceanology, Russian Academy of Sciences (RAS), in separate areas of Lake Baikal, including component magnetic measurements over individual profiles, accompanied by echo_sounding measurements and seismic profiling. The results of these works are described in (Dyad'kov at al., 1999), but, unfortunately, details of this survey are omitted in the paper.
3. Nearly continuous magnetic measurements conducted in the 1980s (single observations were performed in earlier periods) in separate local BRZ areas; measurements were oriented toward tectonomagnetic problems for earthquake prediction (see, e.g., (Korostin, 1968)).

Thus, since the end of the 1970s, mass magnetic measurements in the BRZ for studying the anomalous magnetic field have hardly been conducted at all. The main probably reason for this is the relatively high cost of field work and problems with Russia's economy in those years. When experimental works were renewed, more attention was focused on seismic methods, drilling, and deepwater immersions. Efforts were also directed at developing data interpretation methods, including those obtained earlier (see, e.g., (Novoselova, 1975)). Note that the data on the BRZ magnetic field mostly contain only anomalies of the induction *F* modulus, partially augmented by variational profile measurements of the *H* and *Z* components. Changes in the total vector at constant points (except for the magnetic observatory in

Patrony (Institute of Solar and Terrestrial Physics, Siberian Branch, RAS (ISZF SO RAN) and partially at INGG SO RAN (Institute of Oil_and_Gas Geology and Geophysics) at point Enkheluk and during surveys were not conducted.

There are few scientific papers devoted primarily to analysis of the BRZ magnetic field, mainly, (Novoselova, 1978) and (Dyad'kov et al., 1999). Epov et al. (2007) used then_available aeromagnetic and hydromagnetic survey data of various degrees of detail and drew the following conclusions.

1. Fragmentation of extended anomalies into smaller ones upon switching from a large_scale survey to a more detailed survey points to a shallow location of magnetic objects.
2. Positive anomalies in the total magnetic field vector strength ΔTa with amplitudes on the order of 500–1000 nT primarily form three separate areas, which makes it possible for the authors to refute the presence of an overall extensive regional magnetic minimum in the Lake Baikal depression.
3. The structure and composition of the upper part of the magnetic basement under Lake Baikal and the near shore zone are similar. The depth of the bottom of the magnetic layer is estimated at 18 km, and its size, 10–12 km.

Dyad'kov et al. (1999) hold a somewhat different opinion on the structure of the anomalous magnetic field in the Lake Baikal region; they constructed a map of ΔTa isolines, augmenting the earlier available data with the results of profile surveys, including component ones. They believe that along the BRZ there is a zone of negative values of the magnetic field anomaly of a regional scale with amplitude up to –400 nT, and asymetrically bordered by a zone of positive anomalies, more intense in the northwest and north and less intense in the southeast and south. The negative anomaly itself is divided into three parts by regions of positive ΔTa: the Selengiskii threshold and Academic Ridge. The authors see the reason for the formation of such a regional minimum as the existence of a recess in the magnetic basement along the western and northwestern coast with a height of 3 km. Even with such low magnetization of its rocks, the height of the recess is such that it is possible to explain the occurrence of the minimum above the depression and the maximum above the uplifted block.

Thus, analysis of available publications on studying the BRZ magnetic field has shown the following. First, works on surveying the field in the BRZ have not been conducted for a long time, with the exception of single local measurements. Second, studies of the geological and tectonic structure of the BRZ, predominantly based on seismological sounding data, analysis of earthquake foci data, and data on the warm flow and local electrical exploration, including modern methods for interpreting them, do not permit reliable conclusions on the structure of the BRC and its geological development.

In connection with this, works were conducted on high-precision magnetic surveying of the total magnetic induction vector on the ice of the central part of Lake Baikal.

2. EQUIPMENT, WORK REGION, AND MEASUREMENT CONDITIONS

The complex for conducting a component magnetic survey from the ice surface included high-precision observatory class magnetometers.

- A POS-1 running overhouse magnetometer (Ural State Technical University_Ural Polytechnical Institute, Yekaterinburg) in observatory (registration for notebooks) and field (registration for a special DLPOS storage device) versions. The absolute accuracy of measuring the magnetic induction modulus $F$is around 0.5 nT, and the measurement periodicity is up to 1 s.
- A *DI* magnetometer for measuring magnetic declination and inclination on the basis of 3T2KP non-magnetic theodolite and an iron_probe sensor as a zero indicator. The instrument error of the field angular components is around 5–15 s; inclination was determined in the absolute sense; declination, in the relative sense (the azimuth of a remote reference point was necessary). A nonmagnetic stand was used to mount the magnetometer.

The magnetic survey region (north of Ol'khon Island to the Ushkan Islands) was chosen with allowance for the state of the extent to which Baikal had been studied, regions of scientific interest, possible base stations, and ice conditions.

The first profile was along Academic Ridge; the two halves were planned according to the results of the first day of measurements and lay across the first profile from the west shore to the east (Figure 1). Since *DI* measurements were more laborintensive, it was decided to perform them every 10 km, and *dZ* and *F* measurements, every 5 km.

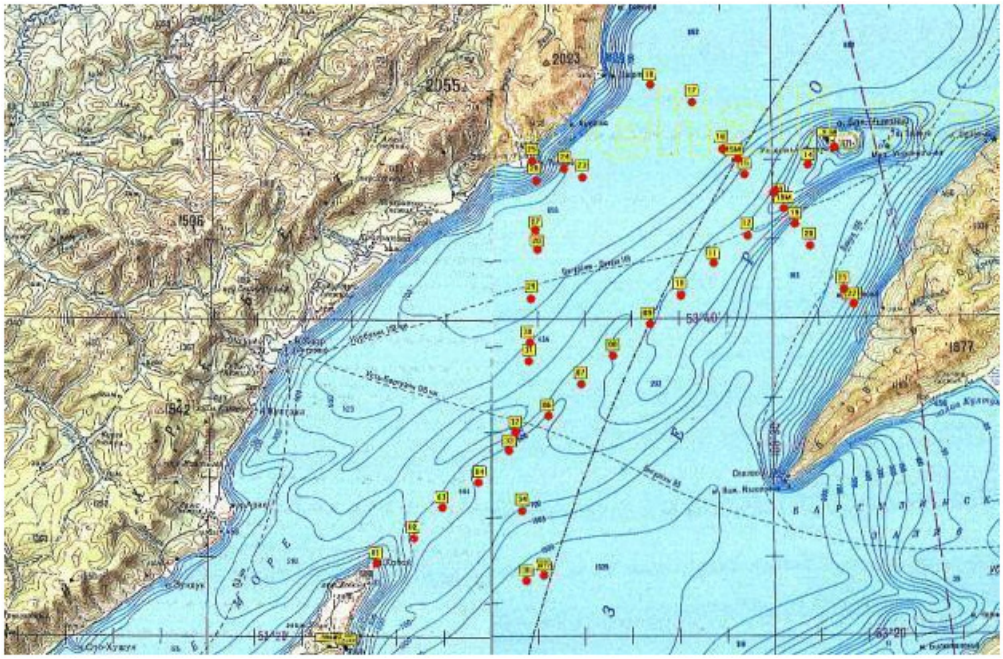

Figure 1 –Region of Lake Baikal with pickets of profile magnetic measurements.

The overall extent of the profiles was around 150 km, and there were 36 *dZ* and *F* measurement points in total; as well, the total vector (*D*, *I*, *F*) was determined at 16 points.

The survey on the ice was conducted March 6–8, 2009 (one profile per day). Meteorological conditions were acceptable: the daytime temperature was no lower than –10°; the wind was variable up to strong; sunny weather on March 6; on March 7, 8, variable cloudiness and snow. The ice conditions were favorable: secure ice more than 1 m thick, with no hummocks on the route.

There were no magnetic disturbances in the measurement period; the *K* index on March 6, 7 did not exceed 1; on March 8, it was no higher than 3.

3. RESULTS

For the first time since the 1970s, a high-precision magnetic survey of the total magnetic field vector was conducted at Lake Baikal. The following tasks were performed.

Expedition observations were carried out in March to measure the total magnetic field vector (*D*, *I*, *Z*, *F* components) and decrements of the vertical *dZ* component on the ice of Lake Baikal north of Ol'khon Island. Measurements were conducted along and transverse to the axis of Academic Ridge. Absolute measurements were performed at 16 points, and *dZ* measurements, at 36 points. The quality of field measurements on the ice surface at temperatures down to -10°C were quite acceptable for estimating the spatial field variations (anomalies with amplitudes of hundreds of nanotesla). The errors in determining declination (without allowance for possible errors in determining the reference point) were estimated at 1–1.5′; errors in inclination, 0.1–0.2. The accuracy of *F* measurements with the POS_1 are no less that 1 nT; the accuracy of *dZ* decrements, at a level of the first tens of nanotesla.

Analysis and processing of the experimental data were performed. Maps were constructed of the magnetic field component distribution in a triangle between the northern end of Ol'khon Island, Cape Rytyi, and Bol'shoi Ushkanii Island, as well as the northern part of Ol'khon Island. From the observation results, the presence of a large_scale magnetic anomaly was established in the measurement region: magnetic declination *D* is from 5°20′ to 6°20′, whereas magnetic declination in the Irkutsk region is approximately 3°. This magnetic anomaly is not shown on magnetic field distribution maps of Irkutsk oblast.

This large_scale magnetic anomaly has a complex structure. The magnetic field distribution pattern in the triangle between the northern part of Ol'khon Island, Cape Rytyi, and Bol'shoi Ushkanii Island can be represented as follows. Inclination *I* and the horizontal *H* component slowly change along Academic Ridge: *I* increases by approximately 30′, and *H* decreases by about 500 nT. For the *F* and *Z* distribution, Academic Ridge is a certain watershed decreasing to the east and increasing to the west of the ridge. The overall difference is about 400–500 nT. The *D* distribution has a complex structure with closely located anomalies with differences in extrema of more than 30′.

4. REFERENCES

Author, I. (2001): "One author's work". *Journal of Geofisica*, **19**, 23, 110-120.

Anistratenko, A. (1973), et. al, “Magnetic Survey of Lake Baikal”. *Geomagn. Aeron.*, **13**, 2, 387–388.

Bulmasov, A. (1968) “Certain Features of Geophysical Fields and the Structure of the Earth’s Crust in the Baikal Region, in Baikal’skii rift (The Baikal Rift)”, *Nauka*, 113–123.

Valyashko, G.M., Mirlin, E.G., Shreider, A.A. et al., (1979) “The Anamolous Magnetic Field of the Lake Baikal Water Area, in Geolgo-geofizicheskie i podvodnye issledovaniya oz. Baikal “. *Geological–Geophysical and Underwater Studies of Lake Baikal.* Moscow, 111–118.

Dyad’kov, P.G., Mandel’baum, M.M., Tat’kov, G.I., et al., (1999) “Features of the Development of the Seismotectonic Process and Earthquake Preparation Processes in the Central Bail Rift Zone from the Results of Tectonomagnetic Studies”. *Geol. Geofiz.*, **40**, 3, 346–359.

Korostin, P.V., (1968) “The Magnetic Field of the Baikal Region and the Experience of Its Geological Interpretation, in Baikal’skii rift (The Baikal Rift)”, *Moscow: Nauka*, 131–140.

Novoselova, M.P., (1975) “On the Features and Sources of Gravitational and Magnetic Anomalies of the Northeast Part of the Baikal Rift Zone, in Baikal’skii rift (The Baikal Rift).” *Moscow: Nauka*. 50–65

Novoselova, M.P., (1978) “A Magnetic Model of the Baikal Depression, in Seimichnost’ i glubinnoe stroenie Pribaikal’ya (Seismicity and Deep Structure of the Baikal Area)”. *Novosibirsk: Nauka.* 1978, 89–94.

Epov, M.I, Nevederova, N.N., and Sanchaa, A.M., (2007) “A Geoelectric Model of the Bagruzinsk Depression of the Baikal Rift Zone”. *Geol. Geofiz.*, **48**, 7, 811–829.

ULF MAGNETIC OBSERVATIONS: A USEFUL TOOL TO INVESTIGATE THE OCCURRENCE OF EARTHQUAKE PRECURSORS?

F. Masci [(1)]

[(1)] Istituto Nazionale di Geofisica e Vulcanologia, via dell'Arcivescovado 8, L'Aquila, Italy
fabrizio.masci@ingv.it

SUMMARY

In the last two decades many researchers investigated ULF (Ultra-Low-Frequency) magnetic data in the hope of finding pre-earthquake seismogenic signals. Several ULF stations were installed and many papers documented the observations of pre-earthquake magnetic anomalies. These claims motivate the belief that one day short-term earthquake prediction based on magnetic data may become a routine technique. Since the earthquake prediction is a very important topic of social importance, recently some researchers gave rise to a re-examination process of controversial scientific claims and they published their findings. These authors demonstrated that many presumed seismogenic signatures were normal variations driven by the geomagnetic activity. Here, some examples of presumed earthquake precursors are reported hoping to shed light on the usefulness of the ULF magnetic measurements to study the occurrence of pre-earthquake seismogenic signals.

1. INTRODUCTION

The history of ULF earthquake magnetic precursors can be summarized as follow:

i. Fraser-Smith et al. (1990) documented the occurrence of possible ULF magnetic earthquake precursory signals before the Loma Prieta 1989 earthquake. Campbell (2009) and Thomas et al. (2009a) put into question the seismogenic origin of this precursor. Fraser-Smith et al. (2011) reaffirmed the possibility that the Loma Prieta precursor may have a seismogenic origin.
ii. After Fraser-Smith et al. (1990) ULF stations were installed in order to study earthquake precursors and a huge number of papers claimed the observation of magnetic ULF earthquake-related signatures using different methods of analysis.
iii. Recent studies re-examined dubious earthquake precursors and demonstrated that many presumed precursors were normal signatures induced by the normal geomagnetic activity.

The starting points of this re-examination process are:

i. Any potential anomaly, before to be considered a reliable earthquake precursor, should be excluded as a random anomaly or as an anomaly related with other possible sources, both natural and artificial.
ii. According to the normal scientific process, further independent confirming measurements are required before such magnetic field changes can be referred to definitively as precursors.

Here, some examples of the results obtained using different methodologies which were claimed to be useful tools to investigate the occurrence of ULF magnetic seismogenic signals are reported.

2. FRACTAL ANALYSIS

Several researchers, by means of the investigation of changes in the fractal parameters (i.e. the spectral index, the fractal dimension, and the multi-fractal parameters) of the geomagnetic field components, claim the observation of pre-earthquake magnetic anomalies. Recently, Masci (2010, 2012c) demonstrated that these changes in the fractal parameters were actually signals induced by the normal geomagnetic activity. As example, in Figure 1 is reported the fractal dimension changes of the geomagnetic field Z component during the period of the Sumatra 2004-2005 earthquakes. Saroso et al. (2009) claimed that the fractal dimension is affected by the seismic activity. ΣKp index time-series has been superimposed onto the original view. The figure shows that there is a strong correlation between the fractal dimension and the geomagnetic ΣKp index time-series. Thus, the fractal dimension variations are undoubtedly induced by the normal geomagnetic activity and nothing can be related to the preparation process of Sumatra earthquakes. See Masci (2010) for details.

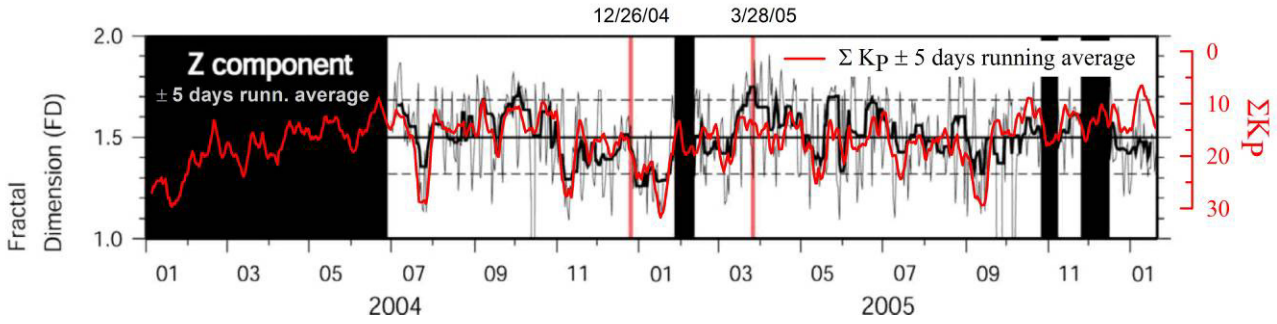

Figure 1 –Fractal dimension time-series of the geomagnetic field Z component as reported by Saroso et al. (2009) compared with the ΣKp index.

3. POLARIZATION RATIO

Many researchers consider the investigation of the magnetic field polarization ratio as a key parameter that allows us to distinguish the normal ULF geomagnetic field pulsations from other signals such as possible seismogenic emissions. The magnetic polarization ratio is defined as the ratio between the integrated (in a fixed range of frequency) power of the vertical component Z and one of the horizontal components H and D. Thomas et al. (2009b) and Masci (2011a, 2012a, 2012b) showed that presumed seismogenic magnetic pre-earthquake polarization ratio variations were actually normal signals induced by the solar-terrestrial interaction.

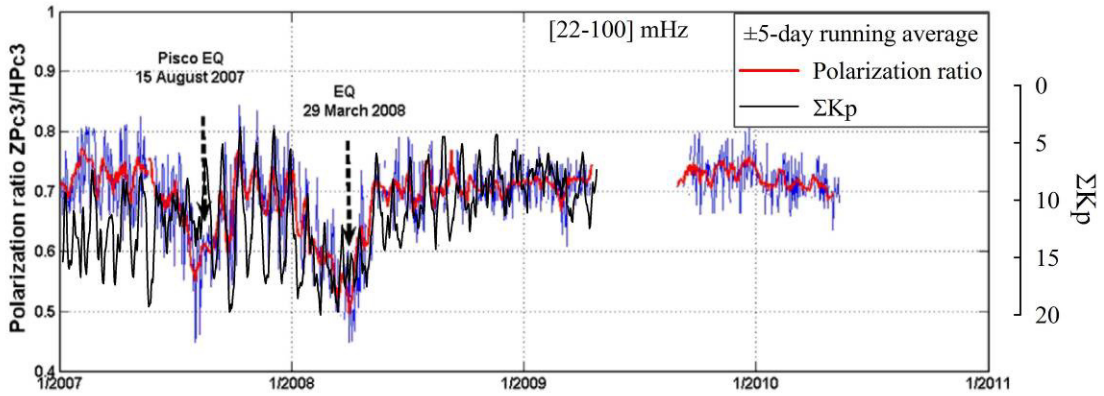

Figure 2 –Polarization ratio Z/H during the period of the 2007-2008 Peru earthquakes compared with the ΣKp index.EQ: Earthquake.

Figure 2 shows the polarization ratio analysis during the period of two Peru earthquakes as reported by Takla et al. (2012). The authors claimed that the polarization ratio decreases which occurred before the two earthquakes are undoubtedly earthquake-related signatures. Conversely, Figure 2 shows a close inverse correlation between the polarization ratio Z/H and ΣKp index time-series which has been superimposed onto the original view. Thus, the two polarization ratio decreases were undoubtedly induced by changes of the geomagnetic activity level.

4. PRINCIPAL COMPONENT ANALYSIS

Figure 3 shows the increases (see the envelope curve) of the third Principal Component Analysis eigenvalue λ_3 of the geomagnetic field H component before the IZU swarm 2000. Hayakawa (2011), by drawing the envelope curves connecting λ_3 peaks, claims that the λ_3 increases were induced by the preparation process of the IZU earthquakes, as well as correlated with the effect of Earth's tides. However, by drawing the envelope curves connecting the peaks of the global geomagnetic Ap index, we can see that there is an inverse correlation between the envelope curves of λ_3 and Ap. The inverse correspondence is evident in the majority of the periods delimited by vertical dotted green lines; this correspondence fails only during some periods. Obviously, the choice of the peaks used to draw the envelope curves could influence their shape. Therefore, we do not expect that a strict inverse correspondence always exists between λ_3 and Ap. However, the inverse correspondence between the envelope curves of λ_3 and Ap in the majority of the periods suggests us a possible relation between λ_3 and the global geomagnetic activity (see Masci, 2011b for details). In summary, connecting the λ_3 increases with the earthquakes occurrence is an oversimplified assumption.

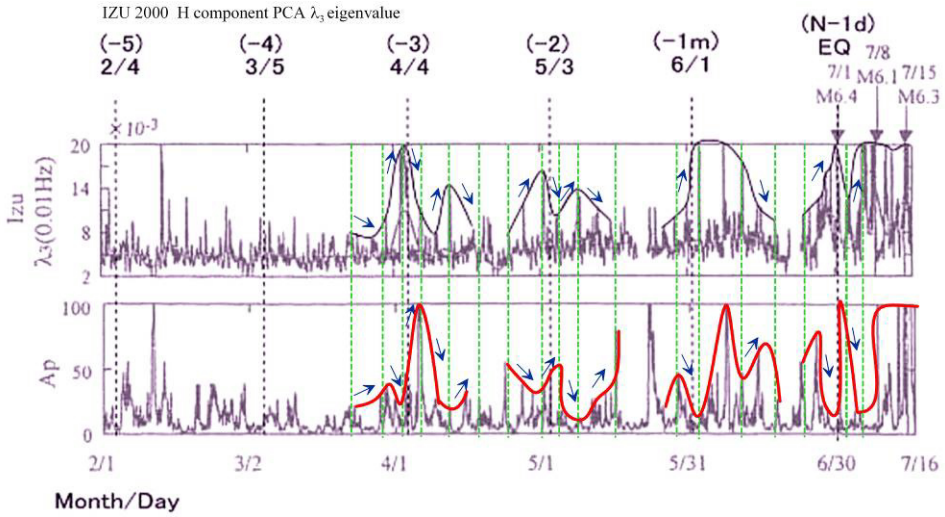

Figure 3 –Third PCA eigenvalue λ_3 increases before the IZU swarm 2000 compared with the Ap index time-series.EQ: Earthquake.

5. RATIO BETWEEN CONJUGATE STATIONS

Takla et al. (2011) claim the observation of Pc 3 anomalous variations possibly associated with two Mw5.7 earthquakes occurred respectively on 31 October and 1 November 2002 in the Molise region, Italy. The authors compare geomagnetic field data from the stations of L'Aquila (LAQ) and Hermanus (HER), which is the almost conjugate point of L'Aquila. According to the authors, in conjugate stations the Pc 3 pulsations have the same amplitude, therefore the anomalous increase of the LAQ/HER ratio during October 2002 (see Figure 4) is related to the Pc 3 amplitude increase at LAQ station caused by the preparation process of the Molise earthquakes.

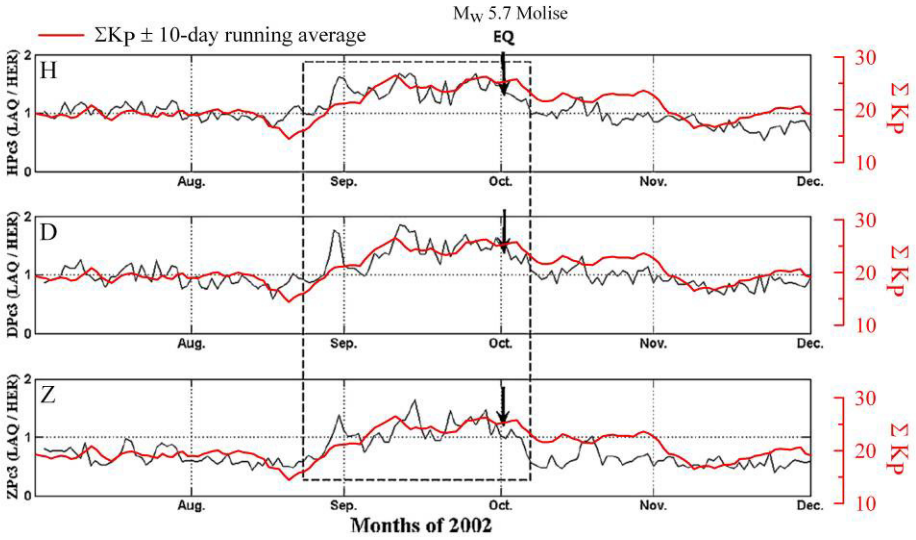

Figure 4 –Pc 3 amplitude ratios between the conjugate stations LAQ and HER during the period August-November 2002 compared with the ΣKp ±10-day running average.

As the matter of fact, Figure 4 shows that the Pc3 LAQ/HER ratio is close related to the long-term variation of the geomagnetic index ΣKp (see the ΣKp ±10-day running average). This suggests that the Pc3 ratio increase which occurs during October 2002 could be induced by the long-term increase of the normal geomagnetic activity. Namely, in conjugate stations the amplitudes of Pc3 pulsations are not always equal even if they may be of the same order of magnitude. As a consequence, we should not expect that in conjugate stations the Pc 3 amplitude ratio is always almost constant. Bearing in mind these considerations, we can suppose that the increase of LAQ/HER ratio during October 2002 may be related to a residual signal caused by the different amplitude of Pc 3 in the two conjugate stations. In conclusion, the Pc 3 ratio increase during October 2002 seems to be induced by the raise of the global geomagnetic activity. Therefore, this increase cannot be undoubtedly associated with the preparation process of the Molise earthquakes.

6. CONCLUSIONS

All the methodologies here reviewed do not show strong evidence of correlation between the presumed precursors and the subsequent earthquakes. In contrast, the authors which have investigated the reliability of presumed ULF precursors have shown that there is a close

correspondence between these precursors and the normal global geomagnetic activity level. Therefore, previously reported associations with the preparation process of the earthquakes occurrence are not correct. In my opinion, the authors documented the observation of pre-earthquake anomalous signals without properly investigate the influence of other possible ULF sources, as well as the geomagnetic activity which is the main source of ULF signals. In summary, the methodologies which were used in investigating ULF seismo-magnetic signals show some problems of fundamental importance. In addition, I would like to emphasize that, a single analysis by itself cannot establish if an anomaly is a seismogenic signal, or is just a chance event induced by other sources, either natural or artificial. Consequently, a more careful approach should be adopted before claiming that any ULF pre-earthquake anomalous observation is a precursory signal so as not to create illusions of a future development of short-term earthquake prediction capabilities based on ULF magnetic precursors. At present, questions of fundamental importance should be: The ULF magnetic earthquake precursors are fact or fiction? Additional scientific and economical efforts in this field of research are justified?

7. REFERENCES

Campbell, W. H. (2009): "Natural magnetic disturbance fields, not precursors, preceding the Loma Prieta earthquake", *J. Geophys. Res.*, 114, A05307, doi:10.1029/2008JA013932.

Fraser-Smith, A. C., A. Bernardi, P.R. McGill, M.E. Ladd, R.A Helliwel and O.G. Villard Jr. (1990): "Low frequency magnetic field measurements near the epicenter of the Loma-Prieta earthquake", *Geophys. Res. Lett.*, *17*, 9, 1465-1468, doi:10.1029/GL017i009p01465.

Fraser-Smith, A. C., P:R. McGill and A. Bernardi (2011): "Comment on "Natural magnetic disturbance fields, not precursors, preceding the Loma Prieta earthquake" by Wallace H. Campbell", *J. Geophys. Res.*, 116, A08228, doi:10.1029/2010JA016379.

Hayakawa, M. (2011): "On the fluctuation spectra of seismo-electromagnetic phenomena", *Nat. Hazards Earth Syst. Sci.*, 11, 301–308, doi:10.5194/nhess-11-301-2011.

Masci, F. (2010): "On claimed ULF seismogenic fractal signatures in the geomagnetic field", *J. Geophys. Res.*, A10236, doi:10.1029/2010JA015311.

Masci, F. (2011a): "On the seismogenic increase of the ratio of the ULF geomagnetic field components", *Phys. Earth Planet. Inter.*, doi:10.1016/j.pepi.2011.05.001.

Masci, F. (2011b): "On the recent reaffirmation of ULF magnetic earthquakes precursors", *Nat. Hazards Earth Syst. Sci.*, 11, 2193–2198, doi:10.5194/nhess-11-2193-2011.

Masci, F. (2012a): "Comment on "Ultra Low Frequency (ULF) European multi station magnetic field analysis before and during the 2009 earthquake at L'Aquila regarding regional geotechnical information" by Prattes et al. (2011)", *Nat. Hazards Earth Syst. Sci.*, doi:10.5194/nhess-12-1717-2012.

Masci, F. (2012b): "On the ULF magnetic ratio increase before the 2008 Iwate-Miyagi Nairiku earthquake by Hirano and Hattori (2011)", *J. Asian Earth Sci.*, 56, 258-262, doi:10.1016/j.jseaes.2012.05.020.

Masci, F. (2012c): "On the multi-fractal characteristics of the ULF geomagnetic field before the 1993 Guam earthquake", *Nat. Hazards Earth Syst. Sci.*, under review.

Saroso, S., K. Hattori , H. Ishikawa, Y. Ida, R. Shirogane, M. Hayakawa, K. Yumoto, K. Shiokawa and M. Nishihash (2009): "ULF geomagnetic anomalous changes possibly associated with 2004–2005 Sumatra earthquakes", *Phys. Chem. Earth*, *34*, 343-349, doi:10.1016/j.pce.2008.10.065.

Takla, E.M., K. Yumoto, P.R. Sutcliffe, V.M. Nikiforovd and R. Marshalle (2011): "Possible association between anomalous geomagnetic variations and the Molise Earthquakes at Central Italy during 2002", *Phys. Earth Planet. Inter.*, 185, 29-35, doi:10.1016/j.pepi.2010.12.003.

Takla E.M., K. Yumoto, J. Ishitsuka, D. Rosales, S. Dutra, T. Uozumi and S. Abe (2012): "Geomagnetic variations possibly associated with the Pisco earthquake on 15 August 2007, Peru", *Tectonophysics*, 524–525, 29–36. doi:10.1016/j.tecto.2011.12.008.

Thomas, J. N., J. J. Love, M. J. S. Johnston (2009a): "On the reported magnetic precursor of the 1989 Loma Prieta earthquakes", *Phys. Earth Planet. Inter.*, 173, 207–215, doi:10.1016/j.pepi.2008.11.014.

Thomas, J. N., J. J. Love , M. J. S. Johnston and K. Yumoto (2009b): "On the reported magnetic precursor of the 1993 Guam earthquake", *Geophys. Res. Lett.*, 36, L16301, doi:10.1029/2009GL039020.

MAGNETIC FIELD OBSERVATIONS CLOSE TO THE EPICENTER OF THE 2009 L'AQUILA EARTHQUAKE

F. Masci [(1)], M. Di Persio[(1)], C. Gizzi[(1)]

[(1)] Istituto Nazionale di Geofisica e Vulcanologia, via dell'Arcivescovado 8, L'Aquila, Italy fabrizio.masci@ingv.it

SUMMARY

On 6 April 2009 a seismic sequence culminated with the Mw6.3 main shock which heavily damaged the town of L'Aquila.

Here, we report the analysis of ULF magnetic field data from the Geomagnetic Observatory of L'Aquila during the period 2008-2009. Magnetic data are investigated by means of conventional techniques of polarization ratio and fractal analysis. In addition, total geomagnetic field data from the INGV Central Italy tectonomagnetic network were also investigated using the simple inter-station differentiation method. Our study does not show any anomalous signal that could be undoubtedly related to the seismic activity.

1. INTRODUCTION

The characteristics of the L'Aquila 2008-2009 seismic sequence are that the earthquakes were shallow and very close to the INGV Geomagnetic Observatory of L'Aquila. The epicentre of the main shock was only 6 km further from the observatory. These characteristics could justify the observation of possible seismogenic electromagnetic signals also providing an opportunity for a careful investigation of the reliability of the methodologies adopted in previous studies which have documented the observation of magnetic earthquake precursors. After April 2009, many papers retrospectively claimed the observation of pre-seismic electromagnetic signals up to several hundreds of kilometres from the epicentral area (see the references by Masci and Di Persio, 2012). On the contrary, other studies (e.g. Biagi et al., 2010; Villante et al., 2009) based on magnetic observations from the L'Aquila area did not found any electromagnetic precursory signal. Here are reported the results of the analysis of magnetic data from the INGV (Italian Istituto Nazionale di Geofisica e Vulcanologia) Geomagnetic Observatory of L'Aquila and from the Central Italy tectonomagnetic network.

2. ULF ANALYSIS

ULF Magnetic data (1 Hz sampling rate) from the Geomagnetic Observatory of L'Aquila are analyzed in the range of frequency [3–100] mHz by investigating the changes in the magnetic polarization ratio and the variations of the fractal characteristics of the geomagnetic field components (see Hayakawa et al., 1996, 1999). The time window [22:00–02:00] UT (LT=UT+1) has been chosen to minimize the background noise level. Figure 1 shows the geomagnetic field polarization ratio during the period 2008–2009 in four frequency bands. The lack of data in December 2008 is due to instrumental problems. The figure does not show any clear anomalous polarization ratio change that could be reasonably related to L'Aquila earthquakes. However, a slight increase of the polarization ratio can be seen in the lower frequencies between the last months of 2008 and the beginning of 2009 just before the 6 April main shock. Further analyses, not reported here, using geomagnetic data from previous years showed that this increase is related to an annual modulation of the polarization ratio, thus this increase cannot be explained in term of seismogenic emissions. In addition, magnetic data are also analyzed by mean of the "improved polarization analysis" proposed by Ida et al. (2008). Also in this case, there are no seismogenic signatures which could be related to the L'Aquila earthquake.

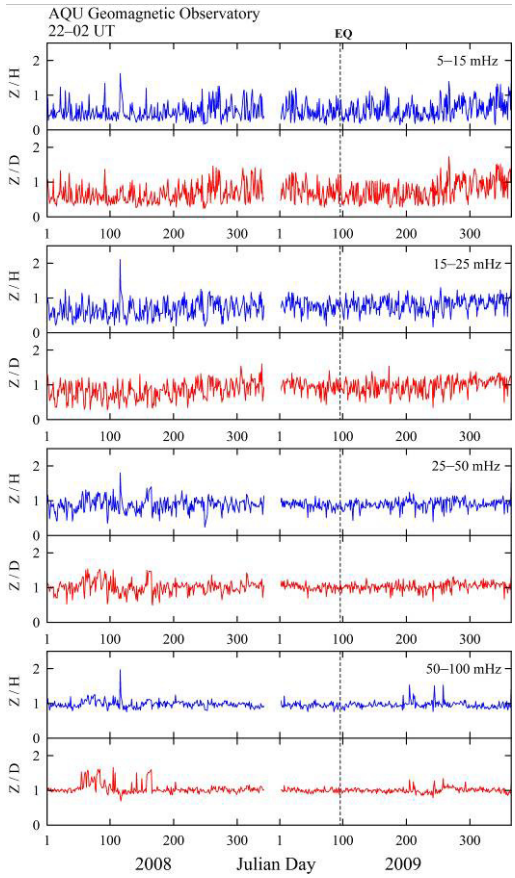

Figure 1 –Polarization ratio during 2008–2009 in four bands of frequency.EQ: Earthquake.

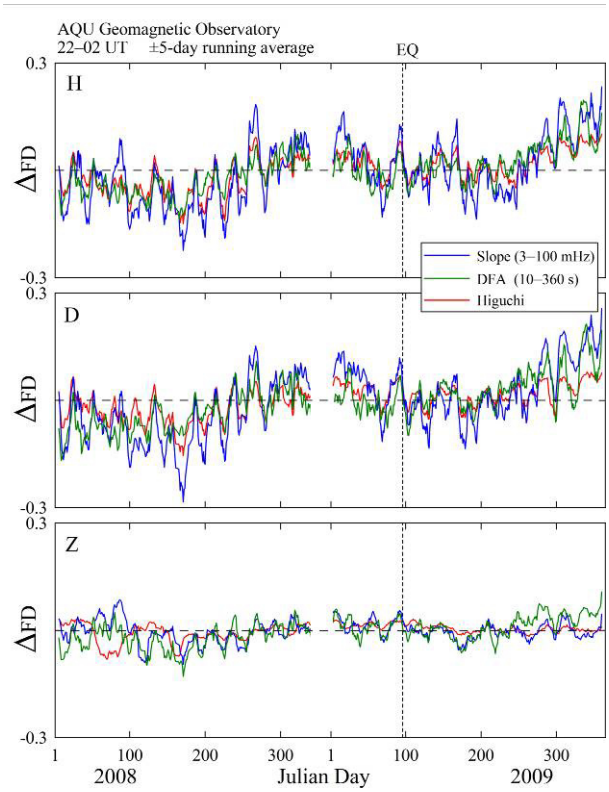

Figure 2 –Variation of the geomagnetic field fractal dimension with respect to the 2008–2009 average value. EQ: Earthquake.

The fractal dimension of the geomagnetic field components was calculated using the Slope, the Higuchi, and the DFA methods. In Figure 2 we report the FD variation (ΔFD) of the AQU geomagnetic field components with respect to the average value calculated in the period 2008–2009 (see Masci and Di Persio, 2012 for details). ΔFD is shown as ±5-day running average. The three methods provide similar results; ΔFD shows a ≈27-day modulation superimposed to a longer-term behaviour. This modulation is more evident in the horizontal components H and D of the geomagnetic field than in the vertical component Z, the latter being the component less influenced by magnetospheric and ionospheric disturbances. This characteristic suggests that the fractal dimension changes have mainly a magnetospheric origin caused by solar-terrestrial interaction. In summary, the fractal analysis does not show anomalies that could be related to the seismic activity. However, if we take into account the fractal dimension temporal evolution in the same manner as it has been done in previous studies, we note an increase of ΔFD which starts about the middle of March 2009. Later, just after the main shock, the fractal dimension decreases. All the components of the geomagnetic field show this behaviour. The FD increase which occurs just before the earthquake is more evident in Figure 3b where the Higuchi fractal dimension of the geomagnetic field H component, the temporal evolution of global geomagnetic index ΣKp, and the seismic activity (Ml) during the period July 2008–July 2009 are shown. We can also note that the ΔFD increase corresponds to the rise in the seismic activity during March 2009. As a matter of fact, Figure 3b shows that the ±5-day running average time-series of the Higuchi fractal dimension and ΣKp have a negative correlation during the entire period of time. In addition, the figure also shows that the FD increase which occurs before the main shock is closely related to a decrease in the geomagnetic activity. Thus, the possible correlation to the seismicity is not supported by the analysis. In summary, the simultaneous increase of FD and seismic activity is a coincidence. As expected (see Masci, 2011a), a similar correspondence also exists between the geomagnetic activity and the polarization ratio. Figure 3a shows this correspondence in the frequency band [5–15] mHz for the H component of the geomagnetic field.

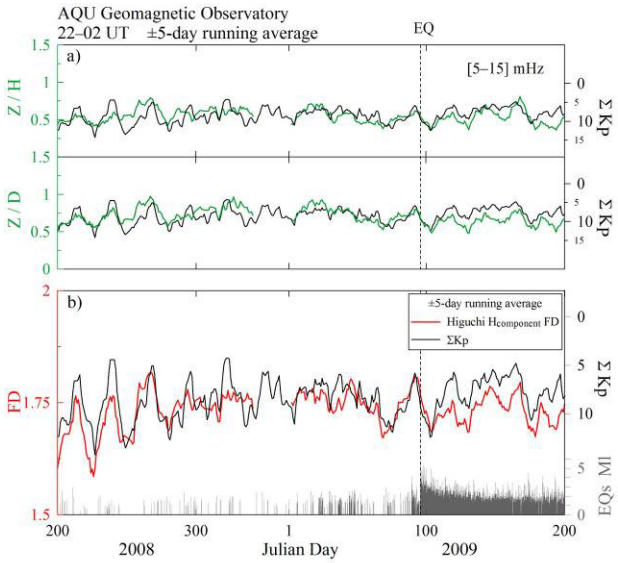

Figure 3 –(a) Polarization ratio in the frequency band [5–15] mHz and (b) Higuchi fractal dimension of the geomagnetic field H component compared with the ΣKp time-series. The seismicity (Ml) of the L'Aquila area is reported as well. EQ: Earthquake.

3. TOTAL GEOMAGNETIC FIELD ANALYSIS

Several tectonomagnetic networks of total field magnetometers are in operation around the world. A well-known tectonomagnetic network is located along the San Andreas Fault in California. Even if the observations of co-seismic magnetic anomalies (up to few nT) are quite frequent, pre-seismic changes of the total geomagnetic field are uncommon. Johnston et al. (2006) maintain that during 25 years of observations along the San Andreas Fault (about 150 M>5.0 earthquakes) a clear 1nT pre-earthquake magnetic anomaly has only been observed once. The simplest method to isolate anomalous changes in the total magnetic field is calculating the differences of synchronously sampled measurements from pairs of stations located some kilometres apart. The differentiation procedure should remove the contributions from other sources, which are external (e.g. electric currents in the ionosphere and magnetosphere) and internal to the Earth (e.g. secular trend of internal origin due to the Earth's core electric currents). Any remaining signal could be attributed to local magnetization changes in the Earth's crust and to the tectonic activity.

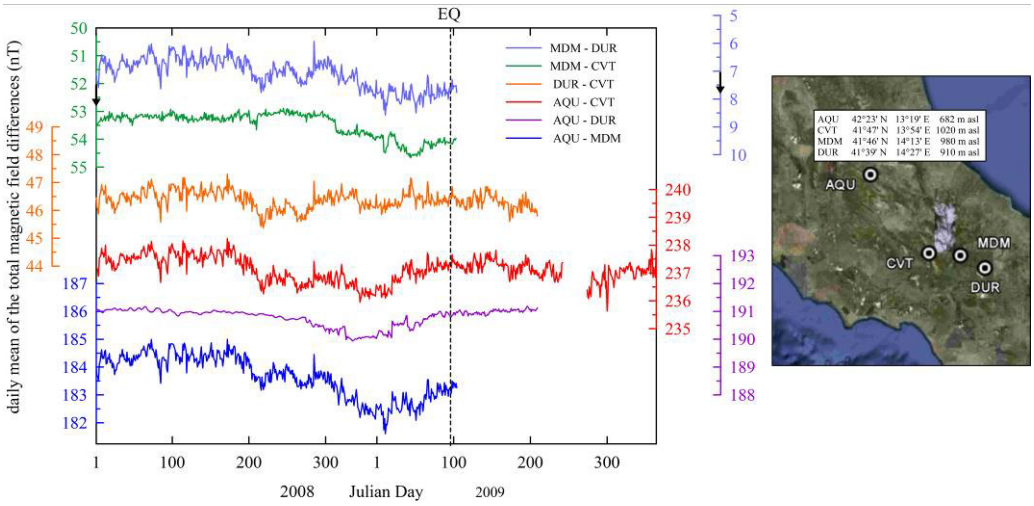

Figure 4 –Daily means of the total magnetic field differences between pairs of stations of the INGV tectonomagnetic network. The location in Central Italy of the network stations is shown in the right part of the figure.EQ: Earthquake.

During the last two decades, a time-synchronized network of total field magnetometers has been in operation in Central Italy along the Apennine chain (see Masci et al., 2007 for details). In Figure 4 the daily mean of the differences between pairs of stations are reported. The figure does not show any magnetic anomaly that can be identified as precursor of the 6 April earthquake. In addition, also the expected co-seismic offset is not present. As the matter of fact, a long-term behaviour in the AQU-DUR time-series can be noted. More precisely, we see a slow decrease between the middle of 2008 and the beginning of 2009. Later, AQU-DUR increases during the period just before the main shock. This could suggest the possible presence of a local effect in the AQU data which could be considered a long-term seismogenic

signature of 6 April earthquake. However, all the differences seem to show the same long-term behaviour, thus the behaviour of the AQU-DUR difference cannot be reasonably associated to the preparation process of the L'Aquila earthquakes.

4. CONCLUSIONS

Our study does not show anomalous signals that could be specifically related to the seismic activity. On the contrary, by means of the ΣKp index time-series we have found that during 2008-2009 the fractal dimension, as well the polarization ratio, show a close inverse correlation with the global geomagnetic activity. This correlation is also evident just before the 6 April main shock. In addition, total geomagnetic field analysis of the Central Italy tectonomagnetic network shows that no seismogenic pre-earthquake and co-seismic signals have been observed. In conclusion, within the limits of our analyses no earthquake-related signal can be identified. Our results support the conclusions of several studies (e.g. Masci, 2010, 2011a, 2011b, 2012a, 2012b, 2012c; Thomas, 2009) which have demonstrated the lack of any evident pre-earthquake seismogenic signatures in the fractal dimension, as well as in the polarization ratio, of the geomagnetic field for earthquakes which occurred at different latitudes, and having magnitudes that range between 4 and 9.

5. REFERENCES

Biagi, P. F, L. Castellana, T. Maggipinto, D. Loiacono, L. Schiavulli, T. Ligonzo, M. Fiore, E. Suciu, A. Ermini (2010): "*Brief communication* "A pre seismic radio anomaly revealed in the area where the Abruzzo earthquake (M=6.3) occurred on 6 April 2009", *Nat. Hazards Earth Syst. Sci.*,10, 215–216, doi:10.5194/nhess-10-215-2010

Hayakawa, M., R. Kawate, O. A. Molchanov,K. Yumoto (1996): "Results of ultra-low frequency magnetic field measurements during the Guam earthquake of 8 August 1993", *Geophys. Res. Lett.*, 23 (3), 241–244, doi:10.1029/95GL02863.

Hayakawa, M., T. Ito, N. Smirnova (1999): "Fractal analysis of ULF geomagnetic data associated with the Guam earthquake on August 8, 1993", *Geophys. Res. Lett.*, 26, 2797–2800, doi:10.1029/1999GL005367.

Ida, Y., D. Yang, Q. Li, H. Sun, M. Hayakawa (2008): "Detection of ULF electromagnetic emissions as a precursor to an earthquake in China with an improved polarization analysis", *Nat. Hazards Earth Syst. Sci.*,8, 775–777. doi:10.5194/nhess-8-775-2008.

Johnston, M.J.S., Y. Sasai, G. D. Egbert, R. J. Muller (2006):" Seismomagnetic effects from the long-awaited 28 September 2004 M 6.0 Parkfield earthquake", *Bull. Seismol. Soc. Am.*, 96 (4B), S206–S220. doi:10.1785/0120050810.

Masci, F. (2010): "On claimed ULF seismogenic fractal signatures in the geomagnetic field", *J. Geophys. Res.*, A10236, doi:10.1029/2010JA015311.

Masci, F. (2011a): "On the seismogenic increase of the ratio of the ULF geomagnetic field components", *Phys. Earth Planet. Inter.*, doi:10.1016/j.pepi.2011.05.001.

Masci, F. (2011b): "On the recent reaffirmation of ULF magnetic earthquakes precursors", *Nat. Hazards Earth Syst. Sci.*, 11, 2193–2198, doi:10.5194/nhess-11-2193-2011.

Masci, F. (2012a): "Comment on "Ultra Low Frequency (ULF) European multi station magnetic field analysis before and during the 2009 earthquake at L'Aquila regarding regional geotechnical information" by Prattes et al. (2011)", *Nat. Hazards Earth Syst. Sci.*, doi:10.5194/nhess-12-1717-2012.

Masci, F. (2012b): "On the ULF magnetic ratio increase before the 2008 Iwate-Miyagi Nairiku earthquake by Hirano and Hattori (2011)", *J. Asian Earth Sci.*, 56, 258-262, doi:10.1016/j.jseaes.2012.05.020.

Masci, F. (2012c): "On the multi-fractal characteristics of the ULF geomagnetic field before the 1993 Guam earthquake", *Nat. Hazards Earth Syst. Sci.*, under review.

Masci, F., P. Palangio, M. Di Persio, C. Di Lorenzo (2007): "The development of the INGV tectonomagnetic network in the frame of the MEM Project", *Nat. Hazards Earth Syst. Sci.*, 7, 473–478, doi:10.5194/nhess-7-473-2007.

Masci, F., M. Di Persio (2012): Retrospective investigation of geomagnetic field time-series during the 2009 L'Aquila seismic sequence, *Tectonophysics*, 530-531, 310-317, doi:10.1016/j.tecto.2012.01.008.

Thomas, J. N., J. J. Love , M. J. S. Johnston and K. Yumoto (2009): "On the reported magnetic precursor of the 1993 Guam earthquake", *Geophys. Res. Lett.*, 36, L16301, doi:10.1029/2009GL039020.

Villante, U., M. De Lauretis, C. De Paulis, P. Francia, A. Piancatelli, E. Pietropaolo, M. Vellante, A. Meloni, P. Palangio, K. Schwingenschuh, G. Prattes, W. Magnes, W., P. Nenovski (2010): "The 6 April 2009 earthquake at L'Aquila: a preliminary analysis of magnetic field measurements", *Nat. Hazards Earth Syst. Sci.*,10, 203–214, doi:10.5194/nhess-10-203-2010..

IMPROVING OLD MAGNETIC DATA PRODUCT BY USING COMPREHENSIVE MODELS

M. Catalán [(1)], M. Larrán [(1)], N. Fernández [(1)]

[(1)] Royal Observatory of the Spanish Navy, San Fernando 11100, Spain, mcatalan@roa.es

SUMMARY

Most of the knowledge concerning the secular variation of the geomagnetic field comes from magnetic observatories or from networks of repeat stations. The first are able to monitor short and long wavelength components of the geomagnetic field spectra (commonly from 1 minute to several years), while the second are only able to monitor the longest features, usually known as secular variation. Anyway to monitor the temporal variation of the geomagnetic field's components it is completely necessary to have available a variometer recording to extract the external fields contribution. Sometimes this instrument fail or is not available, although a continuous absolute observation serie of the different components of the Earth's magnetic field is mantained. In this paper we analyze this situation and if it could be benefitted by the use of the so-called comprehensive models. Finally we applied our conclusions to a real situation which has to do with vertical component at San Fernando observatory, which was inoperative from 1964 to 1968.

1. INTRODUCTION

The Earth's geomagnetic field is a dynamic concept which covers periods ranging from a fraction of a second to millions of years. High frequency domain is related to what are known as external contributions mainly caused by the influence of the sun.

The so-called 'main field' generated in the Earth's outer core justifies more tha 90 per cent of our magnetic field. The main field varies slowly in time and can be describied by mathematical models, such as the International Geomagnetic Reference Field (IGRF), which was originally updated every 5 yr (Finlay et al., 2011). This situation has been modified and improved by the availability of unprecedented high quality data from the latest satellite missions, making a higher rate of more new version releases possible. Traditionally, one of the most important tasks undertaken by magnetic observatories was to determine the annual rate of change or secular variation (SV) of the main field.

The Earth's magnetic field (EMF) is caused by sources in the Earth's core, ionosphere, magnetosphere, lithosphere and from coupling currents between the ionosphere and the magnetosphere. Comprehensive models merge and model all them together (Sabaka et al. 2004). Its latest version called CM4 was designed using POGO, Magsat, Oersted and CHAMP measurements, as well as observatory data to account for magnetic sources and their temporal variations from 1960 to 2002. The CM4 is not only more accurate than IGRF models to estimate core field during its period of validation, moreover, it provides a proper estimate of external field contributions anywhere in the world, which was very valuable for marine data far from magnetic observatories (Quesnel et al., 2009).

San Fernando magnetic observatory (SFS) kicked off in 1891. From then onward it has been able to track the temporal evolution of different components of the EMF, but due to anthropogenic growing influence, it had to moved, and have occupied two more different sites during the following periods: 1991-2005, and from 2005 onward.

To monitor the temporal variation of the EMF's components it is completely necessary to have available a variometer recording to extract the external fields contribution. Sometimes the variometer register fail, or is not available, although a continuous absolute observation serie of the different components of the EMF's is mantained. In this paper we analyze this situation, and if it could be benefitted by the use of the so-called comprehensive model CM4.

2. METHODOLOGY

It is well-known that when we performed an absolute observation, this measurement reflects several contributions. A large amount (nearly a 95%) comes from the core field, but external fields affects our data too. One way to minimize its influence consist in performing the observation at nightime when the regular magnetic daily variation impact is minimal.

The ionospheric and magnetospheric contribution mainly characterize the so-called external fields. The former are in the order of 10-50 nT, depending upon component, latitude, season, solar activity and hour of the day, whilst the later have magnitudes of 10-50 nT near the Earth during magnetically quiet periods, but can increase to several hundred nT during disturbed times (Sabaka et al., 2002).

We may think that even to derive yearly averages the use of abolute observations should be enough. We have taken advantage of the CM4 facility, which provide the magnetospheric and ionospheric fields except during large storms and substorms. We have displayed at Figure 1 the ionospheric and magnetospheric contribution to vertical component at near-Earth from year 2000 to 2010 at SFS. Ionospheric temporal evolution shows a strong harmonic behaviour which can not be discerned from the magnetospherics. In any case their influence does not average when we considered a long or medium tamporal range of years.

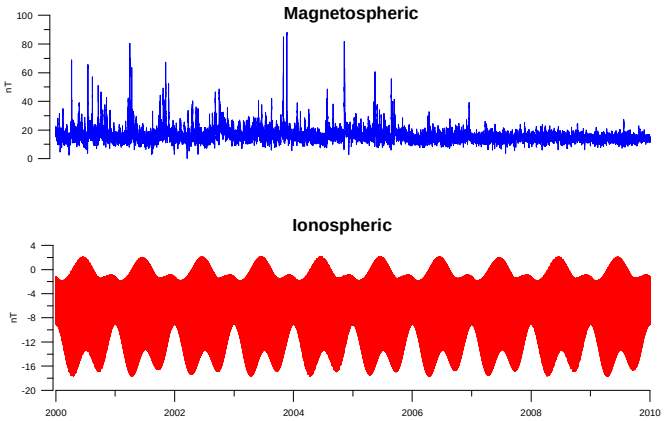

Figure 1 –Magnetospheric (upper plot) and Ionospheric (lower plot) magnetic evolution on SFS from year 2000 to 2010.

Our aim is to test if by using absolute observations only we could inferred SV values, and in any case which limitations could have this idea. We will analyze this procedure along several years on two magnetic observatories: San Fernando (SFS) and Toledo (TOL). This will serve to test the behaviour of our approach on a near-the-coast and on a continental magnetic observatory.We proposed the following methodology:

a) We will obtain the so-called $H_{OBSERVED}$ and $Z_{OBSERVED}$ value, which is the value of either horizontal or vertical component derived after the absolute observation.
b) We will extract the external fields contribution from the $H_{OBSERVED}$ or $Z_{OBSERVED}$ deriving the so-called H_{CORE} or Z_{CORE}.
c) We will compare this results [a) and b)] against the value obtained after extracting the external fields contribution using the CM4 model (H_{CM4} or Z_{CM4}).

To obtain b) we must set a procedure to identify the value of the external fields contribution. First we should set a ground or reference level. We have selected the first five hours of the day where the external fields are minima (Figure 2). We have obtained a plot where every dot resembles the evolution of this average along the period of time we were checking (Figure 3). It shows a linear drift, which has to do not only with the SV, but with the evolution of the magnetosphere, and ionosphere status too. Besides this plot helps us to recognize disturbed days as the averages of magnetic activity makes them to be out of the general cluster.

These disturbed days were disregarded, deriving a continuous plot after applying a moving average on the time serie for every magnetic component: Horizontal (H) and Vertical (Z). This curve allows us to set a ground to identify the external fields contribution at least in its short wavelength (daily contribution).

Arbitrarily we set two thereshold criteria on the absolute observations serie: a) We will not use absolute observations obtained after midday. b) We will not use absolute observations derived on officially disturbed days.

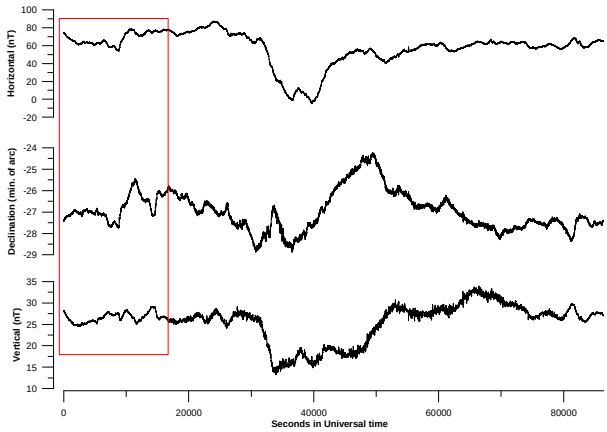

Figure 2 –This plot shows the raw register of the variometer at SFS magnetic observatory. Horizontal component (upper plot), Declination (mid plot), and Vertical (lower plot). A red square highligt the fraction of day used to set a reference for every component.

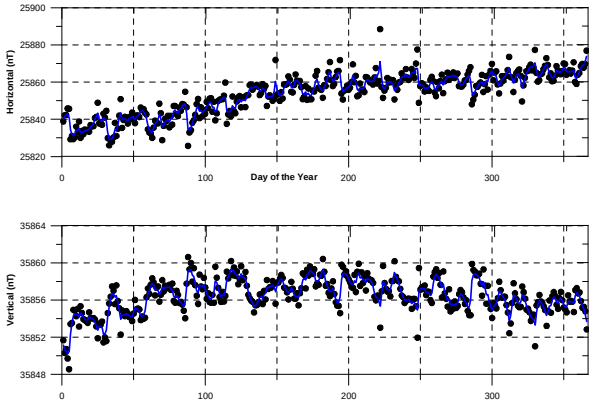

Figure 3 –Evolution of the Horizontal and Vertical components averages (3-day running average) at calm periods along a whole year period at Toledo Observatory for 2008.In blue a filtered version of the averages.

Figure 4 shows the result obtained for the Z-component at TOL for 2006-2009 period. In blue we show the absolute observations results after extracting the real external field contribution (Z_{CORE}), while in red we plot the Z absolute observations once corrected by using the CM4 model (Z_{CM4}), and in black the absolute observations without being corrected by external fields contribution ($Z_{OBSERVED}$). Z_{CORE} delineates quite well the evolution of the inner magnetic field (SV). $Z_{OBSERVED}$ shows fluctuations and a shift with respect to the previous two plots. It seems clear that using $Z_{OBSERVED}$ there will be no possibility to recover the SV. This limitations does not come from the fluctuations at the register but from the offset which affects the whole register.

Concerning the Z_{CM4} the amplitude of the fluctuations slightly decrease if we compare them against those present at $Z_{OBSERVED}$, as it benefitted by the use of the CM4 model predictions for magnetospheric and ionospheric contributions. Table 1 shows the average value obtained for this component along 2006.5, 2007.5 and 2008.5 years. The difference between Z_{CM4} and official annual means are below or equal to 3 nT, on similar terms to those values derived after the Z_{CORE}.

Table 1 – Average value obtained for Z-component for 2006.5, 2007.5 and 2008.5 years.

Year	**$Z_{OBSERVED}$**	**mean Z (*)**	**Z_{CM4}**	**Z_{CORE}**
2006.5	35839	35844	35847	35847
2007.5	35843	35850	35852	35853
2008.5	35850	35854	35857	35856

(*) Values obtained from Observatory yearbooks.

Similar results were obtained for the H-component at TOL observatory (Figure 5). Table 2 shows the average value obtained for this component along 2006.5, 2007.5 and 2008.5 years. The difference between H_{CM4} and official annual means are below or equal to 1 nT , although better results were obtained with H_{CORE}.

Table 2 – Average value obtained for H-component for 2006.5, 2007.5 and 2008.5 years.

Year	$H_{OBSERVED}$	mean H (*)	H_{CM4}	H_{CORE}
2006.5	25790	25793	25791	25793
2007.5	25822	25823	25822	25823
2008.5	25852	25852	25852	25853

(*) Values obtained from Observatory yearbooks.

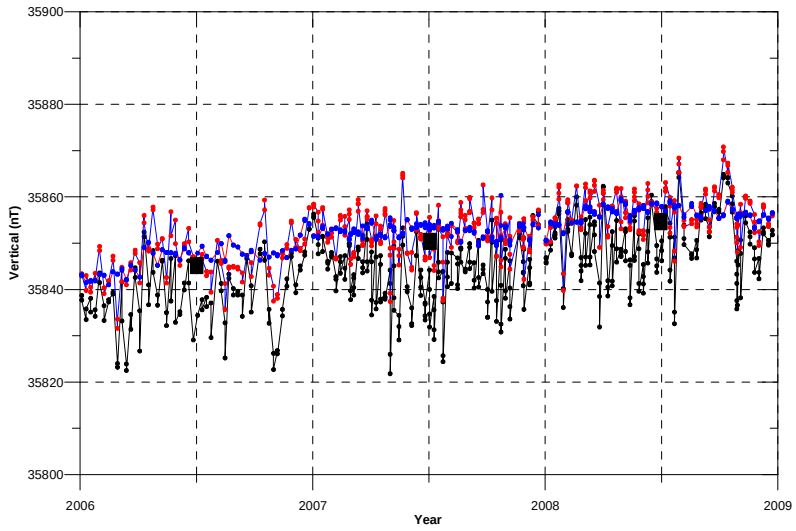

Figure 4 –Results obtained for Z-component at TOL for 2006-2008 years. In black dots it is $Z_{OBSERVED}$, in red we plot Z_{CM4}, and in blue it is plotted Z_{CORE}. Black squares mark the official yearly value obtained from TOL magnetic observatory's yearbook.

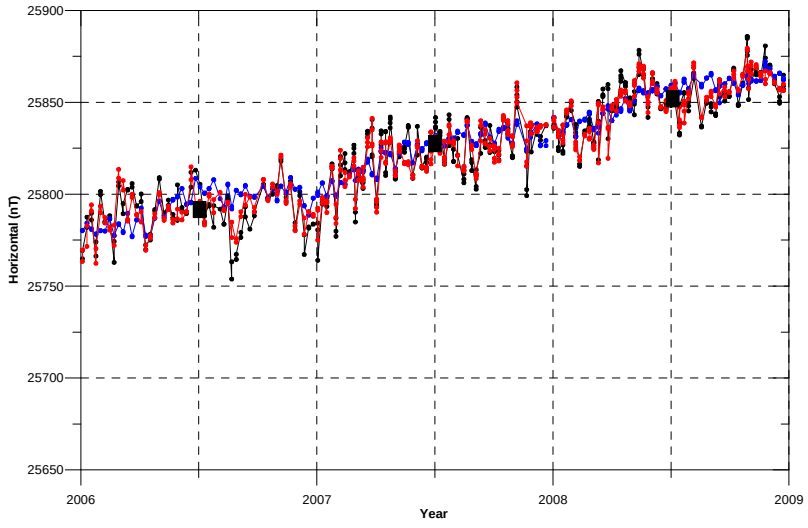

Figure 5 –Results obtained for H-component at TOL for 2006-2008 years. In black dots it is $H_{OBSERVED}$, in red we plot H_{CM4}, and in blue it is plotted H_{CORE}. Black squares mark the official yearly average value obtained from TOL magnetic observatory's yearbook.

3. PRACTICAL CASE

We have applied this method on the H component for SFS magnetic observatory on the period which goes from 1960 to 1968, using the absolute observations serie. To obtain the so-called H_{CORE}, we have followed a similar procedure than that applied on TOL magnetic observatory, that is: a) we have digitized the H component values from tables at SFS yearbooks, b) we have determined the reference level selecting the first five hours of the day where the external fields contribution is minima, c) we considered that any depart at the H variometer register from this ground reflected external fields contribution. Figure 6 shows our results where we compared them against H average yearly values H taken from SFS yearbooks.

From 1964 to 1968 the vertical variometer component was inoperative at SFS. While absolute observation sessions were still performed during all those years. This situation offers the opportunity to recover yearly averages after applying the previous method on the Z component.

As we lacked real vertical variometer data from 1964 to 1968 we have only derived Z_{CM4} values and plot them at Figure 7, (small blue squares for period 1964-1968 are yearly average values derived after the Z_{CM4}). Black squares plotted on 1968-1971 period represent real yearly average obtained from SFS yearbooks. These yearly averages describe a smooth linear transition which connects with those yearly averages derived from SFS yearbooks for 1968-1970 period.

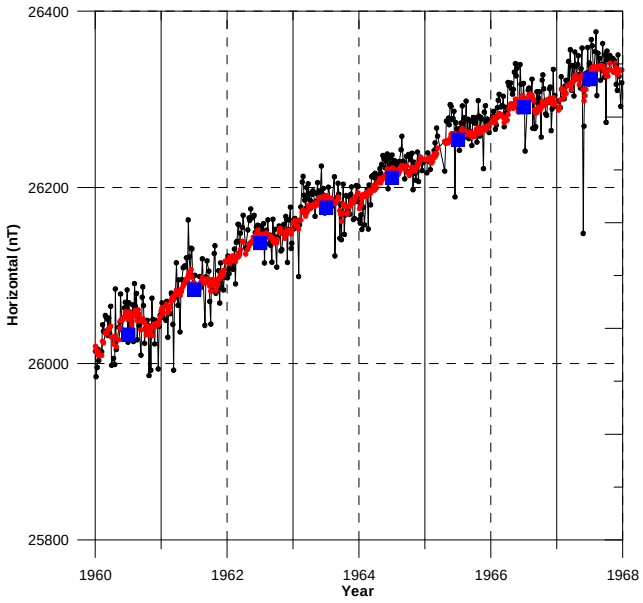

Figure 6 –H component for SFS observatory from 1960 to 1968 period. H_{CORE} is represented in re dots, while H_{CM4} is represented in black dots. Blue squares represent average taken from SFS yearbooks.

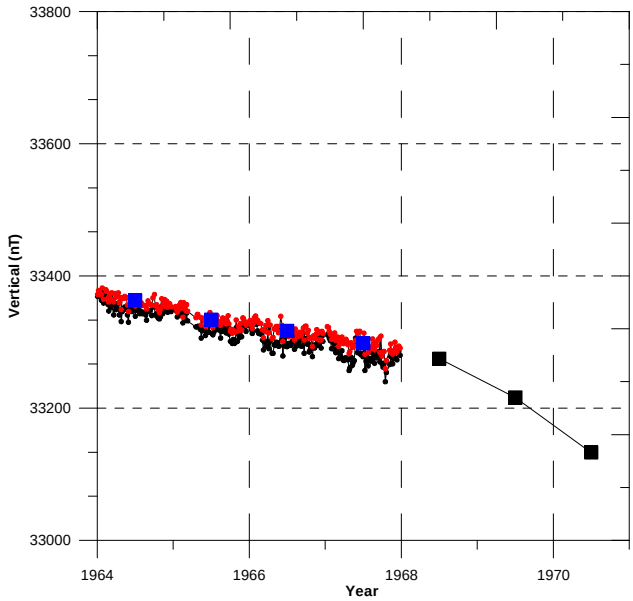

Figure 7 –Z component for SFS observatory from 1964 to 1968 period. $Z_{OBSERVED}$ is represented in black dots, while Z_{CM4} is represented in red dots. Blue squares represent yearly averages derived after Z_{CM4}. Black squares represent average for 1968.5, 1969.5 and 1970.5 taken from SFS yearbooks.

4. CONCLUSIONS

We have checked the advantage of using comprehensive models on real magnetic observatory data. We have observed their ability to recover yearly average values by applying an original method using absolute magnetic observations on SPT magnetic observatory. Our results once compared with real average values, reflected an error which was always better than 3 nT on accuracy. This method allows the

following opportunities: a) To recover SV when you keep an absolute set of observations but lacked variometer as it was presented on SFS from 1964 to 1968, b) It offers an independent source to control any misbehaviour on variometers when we digitized old magnetic records.

5 REFERENCES

Finlay, C.C., Maus, S., Beggan, C. D., Bondar, T. N., Chambodut, A., Chulliat, A., Golovkov, V. P.,Hamilton, B., Hamoudi, M., Holme, R., Hulot, G., Kuang, W., Langlais, B., Lesur, V., Lowes, F. J., Luehr,H., Macmillan, S. Mandea, M. McLean, S., C. Manoj, Menvielle, M., Michaelis, I. Olsen, N., Rauberg, J.,Rother, M., Sabaka, T. J., Tangborn, A., Toffner-Clausen, L. Thebault, E., Thomson, A. W. P., Wardinski, I.,Wei, Z., and Zvereva, T. I., 2010. "International Geomagnetic Reference Field: The Eleventh Generation", *Geophysical Journal International*,**183**, 1216-1230.

Quesnel, Y., Catalán, M. and Ishihara, T., 2009: "A new global marine magnetic anomaly data set", J. Geophys. Res., 114, B04106, doi:10.1029/2008JB006144.

Sabaka, T. J., Olsen, N., and Langel, R. A., 2002: "A comprehensive model of the quiet-time, near-Earth magnetic field: phase 3", *Geophysical Journal International*, **151**, 32–68.

Sabaka, T. J., Olsen, N., and Purucker, M. E., 2004: "Extending comprehensive models of the Earth's magnetic field with Oersted and Champ data", *Geophysical Journal International*, **159**, 521–547.

TRANSMISSION OF THE MEASUREMENT DATA FROM THE SINJI VRH GEOMAGNETIC OBSERVATORY

R. Čop [(1)], D. Deželjin[(2)]

[(1)] Higher Education Centre Sežana, Laboratory for Geomagnetism and Aeronomy, Kraška ulica 2, 6210 Sežana, Slovenia, rudi@artal.si
[(2)] Higher Education Centre Sežana, Laboratory for Geomagnetism and Aeronomy, Kraška ulica 2, 6210 Sežana, Slovenia, damir.dezeljin@dezo.org

SUMMARY

During the testing of the operation of the Sinji Vrh Geomagnetic Observatory, most time was dedicated to the magnetometers; and next to the remote transmission of the measuring data and their graphical presentation in near real time. The telemetry development was based on the practical experiences gained during the work on the existing international information systems for observing the physical parameters measured on site for the needs of the governmental institutions of the Republic of Slovenia. The observation of the change in the geomagnetic field at the Observatory, which has been simultaneously carried out by telemetry, enabled a step-by-step discovery of sources that caused such changes and an improvement in both the measuring system and telemetry. For the purpose of continual control over the measurements and the improvement of operation reliability, a parallel measuring system and telemetry as well as the storage of the measuring data on two separate servers were installed. During the process of data acquisition the measuring data were dismembered and stored in structured form. The next step was data transmission to the central server in the related database, where they were first checked and then stored and post-processed. Therefore the operating system used for data acquisition was customized for autonomous operation in real time.

Key words: data transmission, data storage, data processing, data acquisition

1. OBSERVATORY CONSTRUCTION

For formal reasons, as early as at the beginning, the construction works of the Sinji Vrh Geomagnetic Observatory located under the mountain peak Sinji Vrh above the town of Ajdovščina (Long = 13.94005° E; Lat = 45.89910° N; h = 867m) was divided into a first and second stage. Preliminary to the observatory construction we had to find a proper location for the observatory [Paliska et al. (2010)], complete drafts for the construction, thoroughly study and supplement an outline scheme and plan the construction projects, and also obtain permissions for arranging an access road and for the actual observatory construction.

After selecting the contractors and completion of the first stage of the geomagnetic observatory construction, we continued with the arrangements of relationships with our neighbors on the boundary between their plots and the observatory plot in the area of Gora. The operation of the observatory's integral parts has been gradually progressing and the measuring system and its telemetry has been upgraded. The reliability of both measuring instruments and the devices for transmission, storage and processing of measuring results has been systematically increased. The commencement of the second stage of the observatory construction was delayed until August 2011. Thanks to good weather condition these works, together with laying electricity-supply and optical cables, were completed as early as December of the same year.

The observatory is of a unique design as it is located in a nature conservation area, Nature 2000, and in the narrower area of Gora which is under environmental protection regulation. As building permission has been issued for the construction of auxiliary premises for the observation of the surroundings of the location, the observatory is scattered over the broader area of two plots. Most of the premises are linked with each other through underground high-density polyethylene tubes. The initial duct of the underground tube is next to a concrete pillar of low-voltage overhead power lines; an electrical connection cabinet is also installed on this pillar. The whole underground tubes are

more than 190 meters long. The main duct is 52 meters away from the beginning of underground tube and has also side branch of underground connection to the hut of measurements 36 meters long.

During the first stage of the construction works, a hut with the measuring pillar was built together with a hut for measurements; however, the underground connection does not lead to the hut with the measuring pillar. The hut with the measuring pillar is independent and situated on the location, which is proper for the measurements of the absolute values of geomagnetic-field elements. In the second stage two small buildings housing equipment for variable measurements, and a small building for power supply were built, which were located on the edge of a karstic funnel-shaped hole. These three buildings are permanent facilities at the observatory, while the huts are formally temporary facilities.

2. TEST RUN OF THE OBSERVATORY

The test run of the observatory was ready to start after the completion of the first stage of the construction works, which included the underground tube from the initial duct to the main duct together with a tube to the duct next to the hut for measurements, setting up the hut for measurements together with the temporary location for a sensor of 3-axis magnetometer. These construction and installation works were completed in December 2010 together with the temporary connection of the observatory to the public low voltage network.

Above the main duct, the separated hut housing equipment for telemetry was constructed; its task is to reduce interferences which cause inaccuracies of magnetometers. Besides the main duct and the duct to the hut of measurements, two additional ducts for rechargeable batteries were constructed for their temperature stabilization during the winter time when the outdoor temperatures become lower than -20°C. The measurement data from the hut for measurements are transferred to the hut for telemetry through optical fibers to provide galvanic separation between the measuring and telemetry equipment. During test period the results of inaccurate measurements are excluded by comparative verification with other observatories in neighborhood [Čop, R. et al (2011)]. Comparative verification of magnetometers on other observatories and additional measurements of variations of geomagnetic field on territory of Slovenia were done too.

All huts hosting 3-exes fluxgate magnetometers and their electronics were checked for temperature stability. After their additional 30 centimeters thick thermal isolation the temperature stability of less of ±1°C per day was reached. Before the conclusion of the observatory construction the geomagnetic properties of the surroundings of the observatory location were checked again; we checked the level of electromagnetic noise caused by spatial geological characteristics, and the impact of this electromagnetic noise on the data measured. The mean value of standard deviation of absolute values of geomagnetic field on our observatory is 1.35 nT. These results are taken from the periods of three hours after midnight UTC in the geomagnetic calm days. We carried out also reference measurements at the selected location and the results proved that the selected location of the observatory and the specification of selected instruments meet all predetermined criteria. The power supply system of the huts housing equipment for measurements was examined, to be improved and used as a model for the power supply system of telecommunications and for the rest of the observatory.

When the regular measurements of the absolute values of the geomagnetic field were established, and when the parallel system of variable measurements was partially established, the stage of the test run of the observatory was considered to be completed. On our geomagnetic observatory in 71 days at the end of autumn and in the beginning of winter we reached to make 7 cycles of absolute measurements of declination with standard deviation of 0.0081 degree and inclination with standard deviation of 0.0032 degree. Under existing conditions we measured normally once a week except in winter time when we measured two times monthly.

3. TELEMETRY

The mountain where the observatory is located is exposed to rapid weather changes. Those are more frequent during the period from November to April, when the mountain is difficult to access due to frost, strong gusts of wind and snowstorms; however, already during the test run of the observatory we became aware that the regular observation and study of variations in the geomagnetic field is very important [Kraker, P. et al. (2008)]. This was the reason for designing the remote supervision system – called the remote telemetry system – which enables the remote supervision of geomagnetic measurements and the control of the observatory.

The design of the telemetry system depended on the availability of data connection possibilities on the mountain itself. Additionally, we had to take into account the specifics of the observatory, as the absence of a fixed communication infrastructure, the unreliable and low data bandwidth of the mobile communication infrastructure (GSM/GPRS), the necessity of the low consumption of electricity because of the strong likelihood of interruptions in electricity supply, extraordinary operation circumstances such as very low temperatures, and so on. All these requirements could be met by the introduction of the autonomous operation of the system throughout a longer period, and

establishing normal working conditions through the normalization of telecommunications, power supply and other conditions. Practically we achieved 6 days of total energetic autonomy of our observatory with tree separate nests of rechargeable batteries.

In accordance with these requirements for the construction of telemetry the following guidelines were defined:

- The system for the acquisition of data obtained during geomagnetic measurements (hereinafter referred to as “the data logger”) should be resistant to interferences generated by external sources, should have low electricity consumption, and at the same time be of a small size, so that operators may easily carry it in and out off the observatory to carry out measurements on site or laboratory measurements.
- The data logger should be a standard product and as such be available and at a reasonable price.
- It should provide at least one month of autonomous work, which means local data acquisition.
- An operator should have the possibility to carry out the remote examination of data logger (e.g., if it is located at the observatory as a part of the remote telemetry system).
- The easy transmission of measurement data, locally stored in data logger, to a central data server, should be enabled.

The embedded computer PC Alix3d3, manufactured by the Swiss company PC Engines GmbH [PC Engines GmbH (2010)], complies with the guidelines for a course of development. This PC is compatible with the Intel processors, type x86. It has built in 256 Mb of RAM and a controller for using a Compact Flash memory card as solid state drive. The computer is closed in a housing with dimensions 113mm x 163mm x 30mm and it has the following connectors: 1x RS232, 2x USB, VGA and MIC output, and three programmable LED-s used as status indicators.

The initial test showed that the operation of the PC is reliable; however, it also detected aural interference during the acquisition of measurement data from two or more measuring instruments directly connected to the built in interface RS232 and one or more RS232_to_USB adapters. The noise (aural interference) has been done away with connecting each measuring instrument to its own data logger. This decision consequently added a new requirement to the specification of a data logger; a data logger should be universally applicable to all measuring instruments used at the observatory.

Each data logger uses a CF memory as primary storage. A CF card is divided into two partitions. The data logger is running Voyager Linux operational system. The operating system is installed on the first partition configured to work in read-only mode to minimize CF card memory cells degradations caused mostly by writes. The second partition is used in read-write mode and it is designed for local data storage.

The data logger’s PC is running a Python program for data acquisition, which receives measurement data from the measuring instruments in the form of a character string, which is input signal to the interface RS232. The program parse out the received data block by following a set of rules in accordance with the data format of a connected measuring instrument, so that it can be more easily interpreted, and write the data to the second partition of a CF card in organized form.

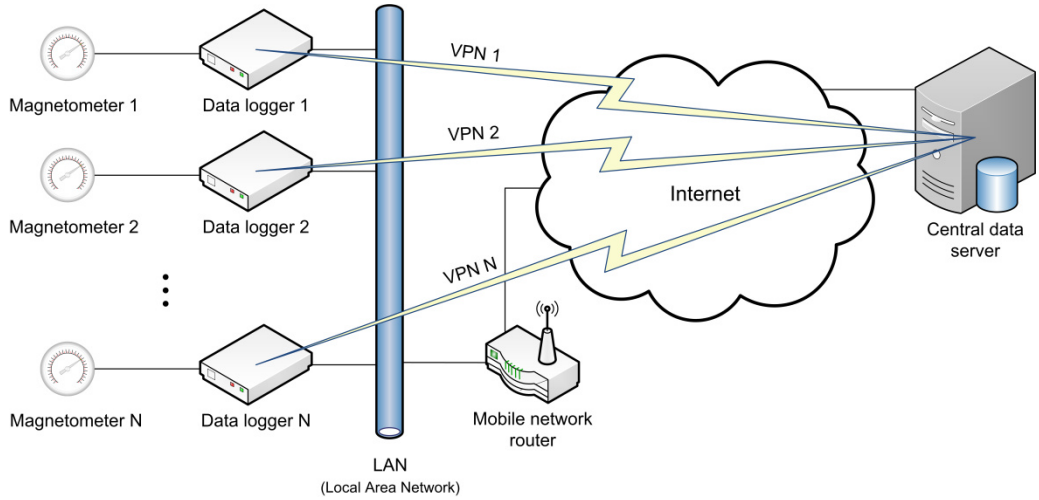

Figure 1 –Telemetry logical representation.

The PC is also running a program which is continuously checking whether the connection to the internet is working. When internet connectivity is detects by the program, it will configure a VPN (Virtual Private Network) connection to a central server. When the VPN connection is established, the data logger will switch from the logical state of connection to the state “connected” which enables the

transmission of acquired data from the data logger to the central server, and also enables the remote control of the data logger by remote operator from the central server. The VPN connection to a central server has been selected as it allows the data logger to switch into the state "connected" (that is to connect to a central server) from a remote location, irrespective of the network to which the data logger is connected to internet. For example in order to make certain measurements, an operator may take one of the data loggers out of the observatory, and bring it in the laboratory or home, or to another measuring point, connect it to the internet there and the acquired data from the data logger will be automatically transferred to the central data server.

The observatory itself is connected to internet via G2 GSM-GPRS connection with the use of the dedicated mobile network router, GSM router. After the data transmission from each data logger to the central data server, they are further automatically imported into a relational database. The imported data is later subject to data quality control and data post-processing. These processed data will be applied for drafting the graphic presentation of the geomagnetic field measurements.

4. RESULTS OF THE REMOTE TRANSMISSION OF MEASUREMENT DATA

The system for measurement data acquisition, transmission and presentation in real time enables simultaneous observation, analysis and interpretation of variations in the geomagnetic field recorded at the observatory. The important sources of additional information are both the internet and the testimony of neighbors on the mountain Gora.

The geomagnetic storm may be predicted by the comparison of data obtained by solar satellites which work as orbiting solar observatories [SOHO, ESA and NASA (2012), SDO, NASA (2012)]. The obtained data on planetary Kp-index, which are made public every tree hours on the website for observing and predicting space weather [SWPC, NOAA (2012)], serve for the first check of the measurements carried out at the observatory. The next important reason for extraordinary variations in the geomagnetic field at the observatory is change in weather condition. Significant impacts on variations in the geomagnetic field are made by the crossings of weather fronts and changes in the humidity. These effects are under detail investigation last months. We use also the data from automatic weather station in nearby village 4 km far away from observatory. The preliminary results show that the additional variation of local geomagnetic field is caused by observatory's position and karstic terrain with underground caves and underground rivers. If we wanted to fully present the correlation between local geomagnetic field and other natural phenomena we need an automatic meteorological station at observatory and hydro-meteorological station on the source of nearest river.

5. FURTHER DEVELOPMENT

In addition to the better explanation of measurement data, in the next short-term period we should provide automatic data processing in accordance with the recommendations of the international organizations IAGA [Jankowski, J., Sucksdorff, C. (1996)] and INTERMAGNET [St-Louis, B. et al. (2011)], and we should establish redundant systems for the transmission and storage of measurement data. Further, both the operation of measuring instruments and the acquisition of measurement data through the interface RS232 should be investigated to reduce the number of inaccurate parsed measurements to a minimum.

For the reliable operation of the Sinji Vrh Geomagnetic Observatory the development of procedures for the regular testing of all instruments at the observatory and for their regular maintenance should be finalized, along with the development of the most appropriate methods for the correction of errors which occur due to the cutouts of each measuring system, power supply system or telemetry.

6. REFERENCES

Paliska, D., Čop R., Fabjan D. (2010): "The Use of GIS-based Spatial Multi-criteria Evaluation in the Selection Process for the New Slovenian Geomagnetic Observatory Site". Annales Series Hisoria Nataturalis, **vol. 20, no. 1**, 1-8.

Čop, R. et al. (2011): "Preliminary Measurements of Geomagnetic-field Variations in Slovenia". Elektrotehniški vestnik, **vol. 78, n.3**, 96-101.

Kraker, P. et al. (2008): "Telemetric System for Geomagnetic Field Monitoring. International Conference on Magnetism, Geomagnetism and Biomagnetism". Zbornik MGB: Higher Education Centre Sezana, Laboratory for Geomagnetism and Aeronomy, 65-73.

PC Engines GmbH (2010): "PC Engines ALIX.3c3 / alix.3d3 system boards". Available in PDF format at: (2012-12-12) http://pcengines.ch/pdf/alix3d3.pdf.

SOHO, ESA and NASA (2012): "Solar and Heliospheric Observatory SOHO" [online]. SOHO is a joint project of international cooperetion between ESA and NASA. Available at: (2012-12-12) http://sohowww.nascom.nasa.gov/.

SDO, NASA (2012): "Solar Dynamics Observatory SDO" [online]. Goddard Space Flight Center. Available at: (2012-12-12) http://sdo.gsfc.nasa.gov/.

SWPC, NOAA (2012): "National Weather Service & National Centers for Environmental Prediction". Available at: (2012-12-12) http://www.swpc.noaa.gov/.

Jankowski, J., Sucksdorff, C. (1996): “Guide for Magnetic Measurements and Observatory Practice”. Boulder (CO, US): International Association of Geomagnetism and Aeronomy, NOAA Space Environment Center.

St-Louis, B. et al. (2011): “INTERMAGNET Technical Reference Manual Version 4.5 (2011)”. INTERMAGNET c/o British Geological Survey.

ACCURACY OF ONE-HOUR MEANS OF GEOMAGNETIC ELEMENT H HAVING MISSING DATA

P. Dolinský, F. Valach, M. Váczyová

Geomagnetic Observatory, Geophysical Institute, Slovak Academy of Sciences, Komárňanská 108, 947 01 Hurbanovo, Slovakia, dolina@geomag.sk

SUMMARY

This study deals with the production of one-hour geomagnetic elements data from incomplete one-minute data sets. We solved this problem analytically, employing some statistical properties of the data file used. The statistical properties were derived from the one-minute data of the horizontal component (H) of the geomagnetic field registered by the mid-latitude Hurbanovo Geomagnetic Observatory (HRB) in years 1997 to 2008. That means that roughly one complete cycle of the solar activity was covered with the data. The statistical properties of the subsets containing one-minute data within one-hour periods were determined with regard to the subsets averages as well as to the regression lines. We assigned quantitatively the number of data in the statistical sample which was required in order to achieve the predetermined value of accuracy. A significant effect of the geomagnetic diurnal variation to the results of the analysis emerged. This fact strikes against the commonly used recommendations about missing data based on geomagnetic indices (Dst, Kp etc.), which are rid of the diurnal variation.

1. INTRODUCTION

In the observatory practice sometimes happens that there is a data gap in the record of the geomagnetic field. The observers ponder over how big is the error if one-hour means are produced from incomplete data sets. In this study we tried to answer the question. We solved this problem analytically, employing some statistical properties of the data file used.

2. DATA USED

In the paper we used the data of Hurbanovo Geomagnetic Observatory (HRB). These were the one-minute definitive data that were available on the web page of INTERMAGNET (http://ottawa.intermagnet.org/apps/dl_data_def_e.php#). The data covered almost the whole 23rd cycle of solar activity. They spanned the period from January 1997 to December 2008. We had at disposal all in all 105170 hours of data. The north component *X* of the geomagnetic field was used in this study. We decided so because its course was similar to the course of the horizontal component *H* in which the changes of the geomagnetic activity were manifested most visibly. The value of the magnetic declination varied around two and a half arc degrees, which was small value sufficient to proxy the horizontal component with the north component for the purpose of our study. Hurbanovo Geomagnetic Observatory is a mid-latitude magnetic observatory with geographical longitude 18.19º and co-latitude 42.14º.

As shown in (Herzog , 2009), it is convenient to work with preprocessed magnetograms (daily records of geomagnetic elements, e.g., X, Y and Z) from which the one-hour linear trend (a linear fit over one-hour interval) has been removed. Also our analysis made in Section 3.1 put forward the need for such a data preprocessing. That is why we subtracted linear trends from the analyzed data in advance.

3. OUTLINE OF THE METHOD

The estimate of one exact value of the error which one makes as he calculates the one-hour value from incomplete data set is a difficult task. Therefore we combined statistical and analytical methods in order to determine inferior and superior limits of the error. We perform the analysis in two steps. The former one (Section 4) led to the establishment of the lower boundary of the error under an assumption that the one-minute values within one hour could be treated as a set of statistical data possessing no time dependence. The

analysis made in Section 5 revealed that such an assumption was justified in part. In the latter part of the analysis (Section 5) we estimated the maximum error for respective numbers of successive missing data. In doing so, we expected that there was a functional dependence of the missing data on time.

4. THE LOWER BOUND OF THE ERROR

When filling the data gaps on magnetograms, it is favorable to have knowledge about the slope or linear trend of the magnetogram for the time period in question (Herzog, 2009). In this paper, we assumed that the slope (the parameter a in the straight line $y = ax + b$), was somehow known. We obtained it from a linear least-square fit based on our complete time series. If one really needs to fill the gaps for some purpose, he can estimate the incline (slope) from the existing data round the gap or he can use magnetograms of the nearby observatory.

For the whole studied interval, we computed the variance of one-minute values around the corresponding one-hour mean value. The calculations were made for the original data and for the data rid of the one-hour linear trends. Standard deviations were 2.820 nT and 1.630 nT, respectively. The signification of the linear trend for standard deviation σ (which characterize 60 points lying on the line $y = ax + b$) grows together with the absolute value of the slope of the linear trend (a) as follows

$$\sigma \approx 173 \,.\, |a| \qquad (1)$$

where a is expressed in nT/min and σ stands for standard deviation of the set of all 60 one-minute values within the one-hour interval. More detailed description of the relation between σ and a is presented in Figure 1a, showing standard deviation of the one-minute data about their mean value (one-hour value) as a function of slope a. The standard deviation calculated from the data which are rid of the linear trends (Figure 1b) shows an unexpected result – the variance for these data is not a function of slopes a of the original un-preprocessed data set. This can be partly explained by the fact that also during quiet days, especially within summer seasons, the diurnal variation causes large values of the slope a.

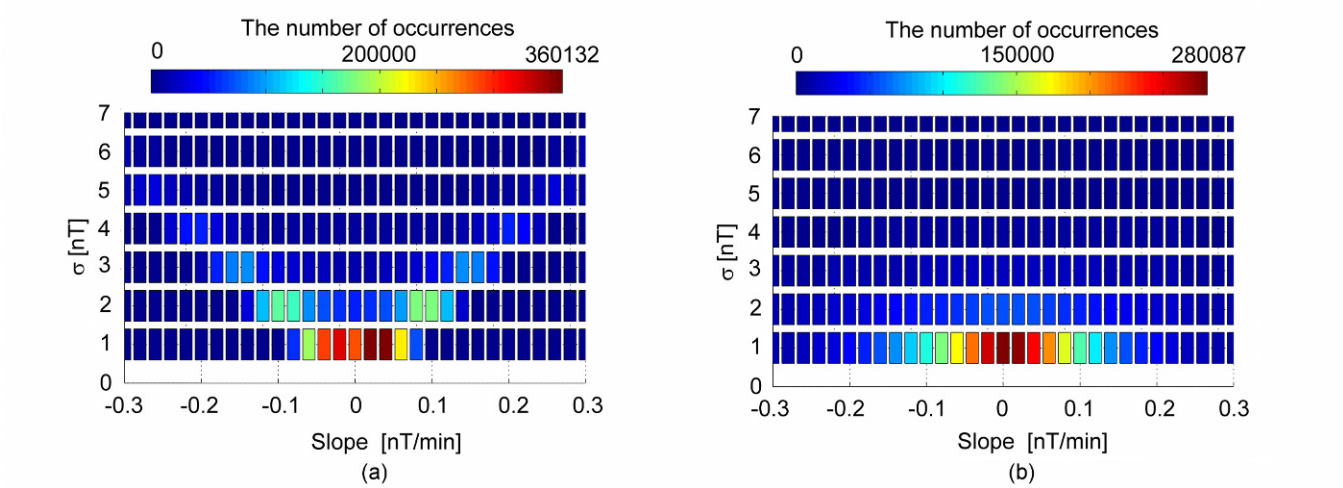

Figure 1 –Standard deviation σ as function of the slope of the regression line. (a) σ was computed for original unprocessed data. (b) σ was computed for the data that were rid of the linear trend as function of slope of the original un-preprocessed data.

In the common observatory practice, information about Kp index is pondered over as one decides on filling a data gap on the magnetogram. However, the diurnal variation is eliminated in the process of determining that index. Therefore, the using *Kp* as a guide is justified only in the cases when the diurnal variation is significantly exceeded by the transient variation. This usually happens for the geomagnetic activity

of $Kp > 5$ (Vaczyova and Valach, 2006).

The standard deviations for the statistical sets of 60 and n ($n \leq 60$) samples are $\langle\sigma_{60}\rangle = \sigma \,.\, (60)^{-½}$ and $\langle\sigma_n\rangle = \sigma \,.\, (n)^{-½}$, respectively. Providing that both of the sets are representative, we can derive a minimal error for the one-hour means computed from incomplete data sets as

$$\langle\sigma_n\rangle = \sigma \,.\, (n)^{-½} = \langle\sigma_{60}\rangle \,.\, (60 / n)^{½}, \qquad (2)$$

where σ stands for the standard deviation of the individual one-minute value around the one-hour mean, $\langle\sigma_{60}\rangle$ is the deviation of the average of the complete set, consisting of 60 one-minute data, and $\langle\sigma_n\rangle$ is the deviation of the average for the incomplete data set of the data, consisting of n one-minute data.

The variable $<\sigma_n> = \sigma \,.\, (n)^{-½}$ may be interpreted as the minimal error which we commit, computing a one-hour mean knowing only n data instead of the full set of 60 data. The course of variable $0.01<\sigma_n> = f(n)$ is drawn as the blue curve in Figure 2. Here, we used $<\sigma_{60}>$ as to be the mean value of $<\sigma_{60}>$ for the all one-hour intervals for the whole analyzed interval. Therefore the graphs in Figure 2 characterize the studied time period of the Hurbanovo data en bloc. The factor 0.01 means that approximately one per cent of the data occurs below the related boundary. The factor 0.01 was determined directly from the tabulated integral of the Gaussian distribution.

5. ESTIMATE OF THE MAXIMAL ERROR

In this part we assumed that the one-minute data within one-hour intervals remained time-dependent even though the linear trends had been removed from them. Moreover, we assumed that the gap consists of single continuous series of missing data.

We computed the Fourier spectra for all one-hour intervals of the studied period. In that way we obtained for each of the Fourier frequencies a set of representations.

$$\mathbf{X}_{(k)} = \sum_{n=1}^{N} x_{(n)} \exp\{ - 2\pi \, i \, (k\text{-}1)(n\text{-}1)/N \} \,. \qquad (3)$$

Here k is an integer from interval [1, N], $x_{(n)}$ is a value from the preprocessed data set, and $\mathbf{X}_{(k)}$ is the Fourier coefficient. The inverse Fourier transform for real variable can be written as

$$x_{(n)} = 1/N \sum_{k=1}^{N} |\mathbf{X}_{(k)}| \cos[2\pi \, (k - 1)(n - 1) / N + \varphi_k] \,, \qquad (4)$$

where φ_k are the initial phase angles.

From these sets we took a critical value $X_{k,p}$, where through the letter k we indexed the Fourier frequency and p is for the corresponding percentile which was set to 75, 90, and 99 per cent. Values $X_{k,p}$ were entered to an inverse Fourier transform. Here the initial phases φ_k were adjusted in order the contribution of each frequency to the gross amount to be maximal. That means

$$\sum_{n=1}^{N-L} |\mathbf{X}_{(k)}| \cos [2\pi \, (k - 1)(n - 1) / N + \varphi_k] \qquad (5)$$

has to be maximal for each L = 1 to 59, where L is the number of the missing data. This step was done numerically. The procedure was repeated 60 times, for k = 1 to 60 and for every length of the data gap (bottom scale in the Figure 2), or, if you like, for all possible numbers of data at disposal within the 60-minute interval (top scale in Figure 2).

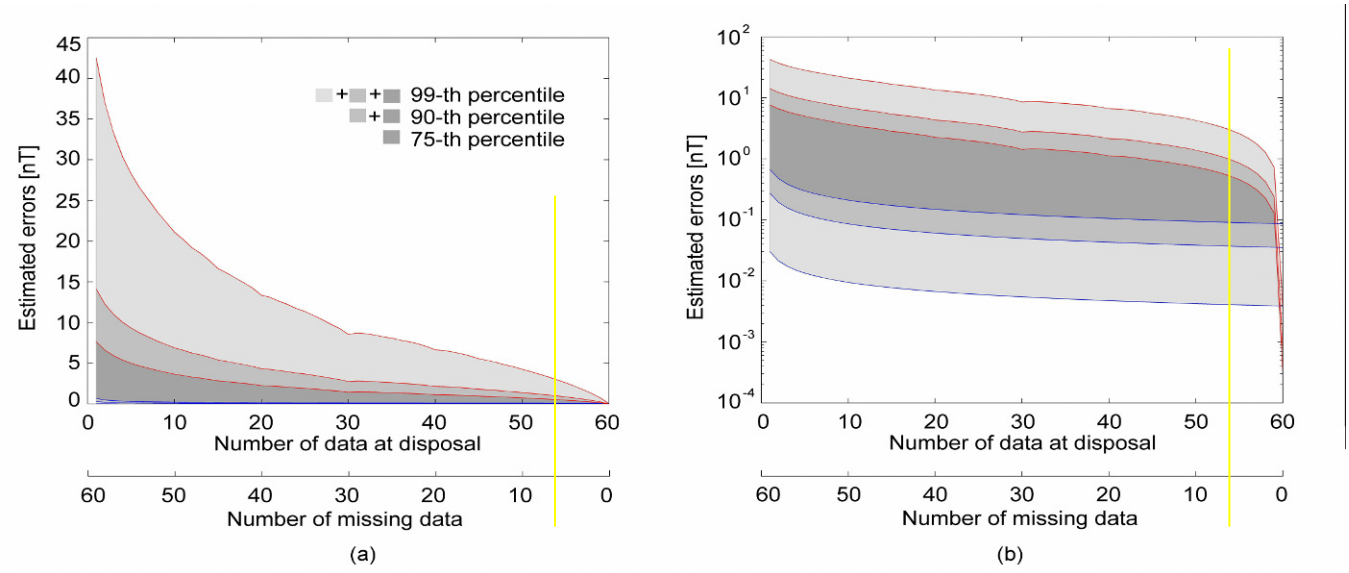

Figure 2 –The error of the produced one-hour means as function of the number of missing one-minute data. All told 99, 90 and 75 per cent of the occurrences lie beneath the red curves, and 99, 90 and 75 per cent of the occurrences lie above the blue curves, respectively. The yellow lines indi-cate 54 data at disposal, which corresponds to the 90% rule. (a) The graph drawn in normal scale. (b) The same graph in the semi-logarithmic scale.

6. RESULTS AND DISCUSSION

Based on the extensive analysis of the data base which covered nearly the whole 23rd cycle of the solar activity we came to the results presented in Figure 2a. We obtained boundaries within which the error as a function of number of available data was located. Here the error is the difference (absolute value) between the one-hour value computed from the complete set of data and that one computed from an incomplete data set. Four different grades of gray color indicate for respectively 99, 90, and 75 percentile the range of the error values. To be exact, 99, 90, and 75 per cent of the occurrences lie beneath the red curves. Likewise, 99, 90, and 75 per cent of the occurrences lie above the blue curves. The shaded out areas are then the intersection of the corresponding areas above the blue and beneath the red curves. The same graph when redrawn in a semi-logarithmic scale (Figure 2b) exhibits that the upper boundaries (red curves) are roughly of an exponential shape.

Love (2009) concluded that a 5 nT level of accuracy would be satisfied, on average, if the 90% rule were to be adopted. Similar is the result of Marsal and Curto (2009), who advised to implement a simple algorithm which rejects hourly intervals with less than 53 minutes of the data.

The graph in Figure 2 shows that 10 per cent of the missing data, which is the upper limit recommended by Mandea (2002) and Love (2009), yield the maximal deviation of about 3.2 nT for the one-hour value for the Hurbanovo Geomagnetic Observatory. The 5 nT maximal deviation, which was recommended by Newitt (2009) and Love (2009), corresponds to 13 missing one-minute data within an hour. This is satisfied for 99 per cent of the actual data. (For lesser confidence intervals one needs to abide by the graph of the corresponding percentile.)

7. CONCLUSIONS

We used an analytical approach to the analysis of the basic properties of large data base of the horizontal component of the geomagnetic field at mid-latitude Hurbanovo Geomagnetic Observatory (HRB). We found how errors characterizing the one-hour means of the geomagnetic element depended on the number of missing one-minute data (Figure 2). The result was designed to be a tool to answer the question: “The loss of how many data within an hour could we get over to be able to produce one-hour values meeting a prescribed precision?” It must be said, that the prescribed precision depends on the usage of the data.

The analysis says about the most frequent events occurring on the magnetograms. It was not treated as a case study of some selected phenomena. Approximately 1 per cent of the data occurs outside the shaded out area of the graph (Figure 2). That means that during a year only 90 cases happen for which the values of the estimated error (for 90 one-hour intervals) lie outside the gray area.

Some significant effect of the geomagnetic diurnal variation to the results of the analysis emerged, too. This fact strikes against the commonly used recommendations about missing data based on geomagnetic indices (*Dst*, *Kp*, etc.), which are rid of the diurnal variation.

8. ACKNOWLEDGMENTS

The work was supported by Scientific Grant Agency of the Ministry of Education of Slovak Republic and Academy of Sciences, project number VEGA 2/2015/11. We are grateful to Dr. Milos Revallo for the grammar correction.

9. REFERENCES

Herzog, D. C. (2009): "The effects of missing data on mean hourly values". *Proceedings of the XIIIth IAGA Workshop on Geomagnetic Instruments, Data Acquisition, and Processing*, 116-126.

Love, J. J. (2009): "Missing data and the accuracy of magnetic-observatory hour means". *Annales Geophysicae*, **27**, 3601-3610.

Mandea, M. (2002): "60, 59, 58 … How many minutes for a reliable hourly mean?". *Proceedings of the Xth IAGA Workshop on Geomagnetic Instruments, Data Acquisition, and Processing*, 112-120.

Marsal, S. and J. J. Curto (2009): " A new approach to the hourly mean computation problem when dealing with missing data ". *Earth Planets Space*, **61**, 945-956.

Newitt, L. R. (2009): "The effects of missing data on the computation of hourly mean values and ranges". *Proceedings of the XIIIth IAGA Workshop on Geomagnetic Instruments, Data Acquisition, and Processing*, 194-201.

Vaczyova, M. and F. Valach (2006): "The effect of the geomagnetic activity on the geomagnetic measurement’s accuracy". *Contributions to Geophysics and Geodesy*, **36/2**, 229-237.

MAGPY – A PYTHON BASED SOFTWARE FOR ANALYZING GEOMAGNETIC OBSERVATORY MEASUREMENTS

R. Leonhardt [(1)], J. Matzka [(2)], M. Wack [(3)]

[(1)] Conrad Observatory, Central Institute for Meteorology and Geodynamics, Hohe Warte 38, 1190 Vienna, Austria, roman.leonhardt@zamg.ac.at
[(2)] National Space Institute (DTU Space), Technical University of Denmark, Copenhagen, Denmark, jrgm@space.dtu.dk
[(3)] Department Geowissenschaften, Ludwig-Maximilians-Universität München, Theresienstr. 41, München, Deutschland, michael.wack@geophysik.uni-muenchen.de

SUMMARY

The MagPy software is a platform independent, multi-purpose software to assist geomagnetic data analysis primarily in observatory environments. It supports various common data formats of the geomagnetic community, among them instrument specific formats and general purpose formats like IAGA02, cdf and hdf5. Direct url-data access is also possible and new format conventions can be easily incorporated. Using the scriptable access of the underlying functions for import, treatment, and export of data, an automated real-time analysis of geomagnetic data is possible. Currently supported are variometer data, scalar data and absolute measurements as well as auxiliary data. For this, basic analysis features like filtering, smoothing and data fitting routines are available. Baseline stability tests, outlier detection and flagging procedures allow for a detailed examination of data quality. The package is completed by routines for coherence and spectral analysis as well as k-index calculation and variation (storm) detection making use of well established routines from the seismological community. Beside the scriptable access and command line routines, a graphical user interface based on Python WX is developed which allows, platform independent, windowed access to most routines and a direct graphical demonstration. The software has currently been tested on Linux and Windows systems.

1. INTRODUCTION

Recent international programs like the ESA Space Situational Awareness Program define a demand on high quality, near real time availability of geomagnetic data. Especially the assessment of data quality, as well as the application of basic and sophisticated analysis routines needs to be automatized in order to obtain a near real time availability. Furthermore data treatment need on the one hand be flexible enough in order to regard for current developments and increasing resolution, and on the other hand reproducible and transparent to maintain an optimal comparability within the global observatory network. In order to meet these criteria fast and flexible software routines need to be available which can be automatized, which are usable among a huge variety of different hardware systems, which ideally allows for directly accessing data via internet connections and most important which use definite algorithms and are transparent to be continuously checked and tested as well as improved by the community.

Instead of writing a specific software for analyzing data and visualization we provide a framework for an open source programming language called python (www.python.org). Thus individual routines of the MagPy Package can not only be used for analysis purposes to any desired level of complexity, but also facilitate an easy and fast development of improved functionality and stability. The open source character of the MagPy software additionally supports that all routines are comprehensive and furthermore allows for a general control of correctness and reproducibility of all obtained results.2.

2. BASIC SOFTWARE DESCRIPTION AND REQUIREMENTS

The primary aim of the MagPy software is providing a python framework especially for the analysis of time series usually encountered in geomagnetic observatories. The software is loosely related to and profited from the ObsPy package (Beyreuther et al. 2010, Megies et al. 2011) which is developed for the analysis of seismological data. MagPy is platform independent and has been tested so far on Linux 32 and 64 bit as well as on Windows 32 and 64 bit systems.

The MagPy Software is currently in a development state. For that reason it is not yet provided as installable package but has to be imported manually. The current package with core files and the format library can be downloaded in the download section of the Conrad Observatories webpage "http:\\www.conrad-observatory.at". Please look at the README for additional requirements and the current revision. This article refers to revision 69 from November 2012. In order to run the MagPy Software the following python packages should be installed: Python 2.6 or 2.7, Numpy, SciPy, Matplotlib. Optional packages are SpacePy (Morley et al., 2011), NetCDF, PythonWX. It is recommended to obtain the NASA CDF packages (http://cdf.gsfc.nasa.gov/) to use that functionality in the program. After downloading the MagPy package (MagPy.tar.gz) unzip it in a directory of your choice (e.g. /home/yourusername/magpy or C:\Programme\Magpy). The following files will be unpacked: within the directory "core" you will find the three main programs: magpy_stream, magpy_absolutes and magpy_transfer. Within the lib directory you will find available format conversion filters. In the main folder a README and the file "examples.py" will be found. A basic introduction on how to use this package will be given in the next section.

A huge number of individual functions are already implemented in the MagPy package. Usually the starting point is to load a geomagnetic time series into the working memory, apply any kind of analysis and calculation routines and finally produce a result or visualization of the performed steps. Every data set is treated as an object which contents can be accessed by specific keywords. This data stream object has two main parts: firstly a list containing the time series, hereinafter referred to as *data* and secondly a dictionary with meta information associated with the data, further referred to as *header*. The data part contains a series of predefined keys and associated formats (Table 1).

***Table 1* – List of data keys**

Data keys	Format
time, sectime	Date - Datetime object
x,y,z,f	Magnetic components (x,y,z) – contents can be specified by the 'typ' key, absolute field intensity f
dx,dy,dz,df	Uncertainties of x,y,z,f
t1,t2	Temperature (t1-sensor, t2-electronics)
var1-5	5 optional variables – float
comment	Comment – string
Flag	Used for flagging – special string
str1-4	Optional strings
typ	Defines xyz information – "XYZF", "HDZF", "IDFF"

The main keys to access data. Any different content and unit of these columns can be defined in the header dictionary.

3. SYNTAX AND APPLICATION

To access the functionality of the MagPy package you need to obtain a most basic idea on how python works. Suggested readings are the web tutorial which you can find here (http://docs.python.org/2/tutorial/). But even without that knowledge, we try to highlight the most important steps in the following: Firstly you need to provide the functions to your python installation by importing the MagPy package. For the current development version this can be done by adding the following lines to a python script:

```
(1)-import sys
(2)-sys.path.append('/home/yourusername/magpy')
(3)-from core.magpy_stream import *
(4)-from core.magpy_transfer import *
```

These four lines allow you to access all functions of the MagyPy package. Add a “core.magpy_absolutes” line for additional routines for DI measurement analysis. Please replace the path in the second line with your installation directory. Now you can access the individual functions of the program by directly referring to the functions. This works with very simple commands which can be modified by keywords. How this works is here demonstrated by a simple plot function. Firstly we read data from the WDC repository in Edinburgh by using the pmread command:

```
(5)-stream = pmRead(path_or_url='ftp://ftp.nmh.ac.uk/wdc/obsdata/hourval/single_year/2011/fur2011.wdc')
```

Hereby the hourly data file of the year 2011 from the observatory Fürstenfeldbruck provided at the WDC is downloaded (thus requiring an internet connection) and stored as a local data stream object called stream. Any further analysis can then be applied to the stream. Using starttime and endtime keywords the loaded stream can be trimmed to a more appropriate time range:

```
(6)-stream = pmRead(path_or_url='ftp://...',starttime='2011-05-01',endtime='2011-06-01')
```

I order to plot the data the pmplot function can be used. For this purpose the function is applied onto the stream object. Here automatically any relevant meta information from the header is extracted to display correct axis labels.

```
(7)-stream.pmplot(['x','y','z','f'])
```

Beside the desired columns, which are obligatory, the plotting function can be extended by many additional keywords in order to change the appearance according to personal preference (figure 1):

```
(8)-stream.pmplot(['x','y','z'],padding=10,labelcolor='0.2',bgcolor='#d5de9c',grid=True,gridcol
   or='r',confinex=True,outfile='ffb.png')
```

The colors of labels (greyscale), background and grid are manually changed, a general padding for axis limits is defined and the output is transferred to a png-file. These basic syntax rules apply for any further application. The following example makes use of this principle technic and provides a quick but cursory overview.

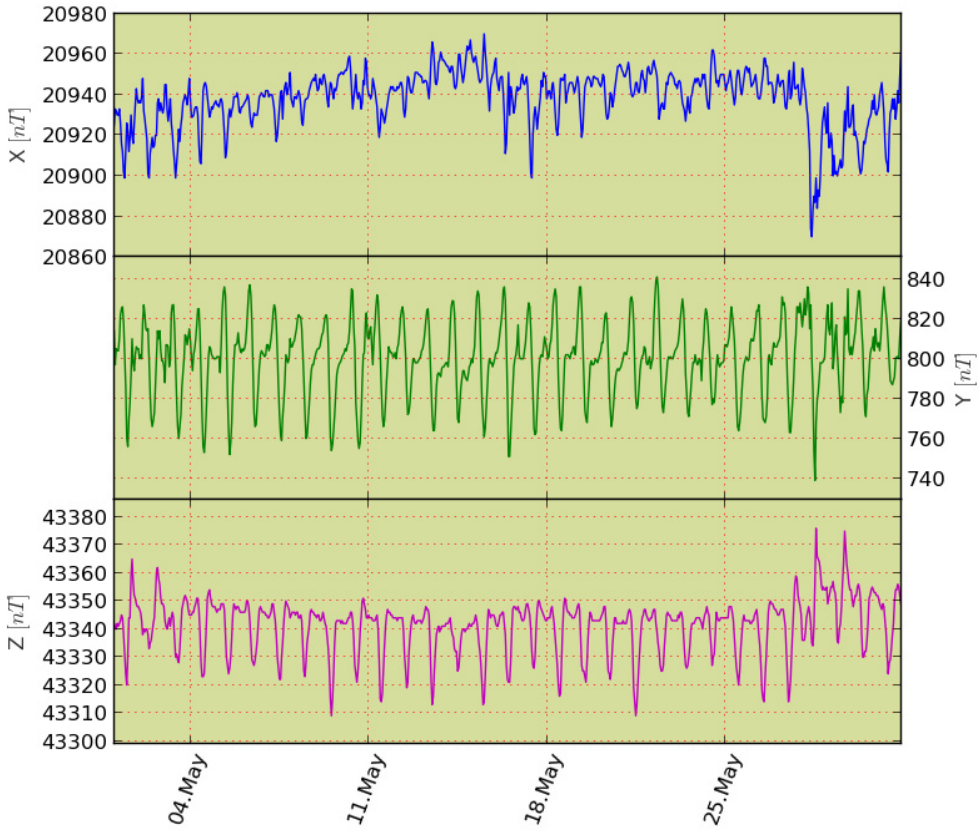

Figure 1 –Graphical output of command line (8).

4. AN EXAMPLE

In the following a short application example is briefly introduced. Here we load a daily file with second resolution e.g. from an IAGA02 type ASCII file (9). We have a quick look at the powerspectrum of the x component first (10). Then we mark any outliers/spikes

(11). Outlier detection is based on quartiles. Calculated is the interquartile range IQR, which is the difference between the first and third quartile (Q3 - Q1). The IQR is termed to be a relatively robust statistic compared to the range and standard deviation. Q1 is based on the lower 25% of data, Q3 on the upper part, after using medians to divide the data set. Using an optional threshold value outliers are then characterized by exceeding the limit defined by $L = M \pm t\ IQR$ where L denotes the limit, M is the median of the values and t is the optional threshold value. By default the threshold value is set to 4, which keeps all data except prominent spikes even during stormy conditions in a noisy environment. The outlier function accepts several optional keywords for modifying threshold, time window, and the column key. Detected outliers are not removed but flagged. In order to proceed with filtering the flagged data is not used and thus removed (12). Afterwards we filter the data using a Gaussian filter according to IAGA recommendation (Jankowski and Sucksdorff, 1996) creating a minute file (13). Finally we write the data stream to a file again (14). A log file will automatically be created providing information on the stepwise procedure, calculation durations and flagged records.

```
(9)-stream = pmRead(path_or_url=os.path.join('/home/yourusername/magpy','*.sec'))
(10)-stream.powerspectrum('x')
(11)-stream = stream.routlier(keys=['x','y','z'])
(12)-stream = stream.remove_flagged()
(13)-stream = stream.filtered(filter_type='gauss',filter_width=timedelta(minutes=1))
(14)-stream.pmwrite('/home/yourusername/magpy',filenamebegins='IAGA_',format_type='IAGA')
```

Many more functions, which would significantly exceed this extended abstract are available and can be tested. These functions include baseline analysis and correction, smoothing, derivatives, spectra, information changes (e.g. storm recognition), and also functions for merging, subtracting and adding different streams.

5. CONCLUSIONS

Although the MagPy package is not yet finished, the current development version is ready to be tested and applied on many typical observatory related issues as summarized above. The current development is using the Subversion environment (http://subversion.apache.org/ - providing version control, development access, tickets, wiki documentation). Operational test can be viewed on the webpage of the Conrad Observatory. In its present state the main functions can be assessed by script programming. The main benefit is that any kind of frequently applied analysis routine can be easily summarized in a step wise protocol thus guaranteeing perfect reproducibility and can be automatically scheduled using cron or the systems scheduler programs. Although a wide variety of functions is already available, the program is under continuous development and improvement. Any suggestion, support and error corrections are highly welcome and appreciated. The graphical front end is still under development but will be available soon at the Conrad Observatories web page.

6. REFERENCES

Beyreuther,M., Barsch,R., Krischer, L., Megies, T., Behr, Y. and Wassermann, J. (2010): ” ObsPy: A Python Toolbox for Seismology”. *Seismological Research Letters*, **81**, 530-533

Jankowski, J. and Sucksdorff, C. (1996): "IAGA Guide for Magnetic Measurements and Observatory Practice". Warsaw, pp 238

Megies, T., Beyreuther, M., Barsch, R., Krischer, L. and Wassermann, J. (2011): “ObsPy – What can it do for data centers and observatories?”. *Annals Of Geophysics*, **54**, 47-58

Morley, S. K., Koller, J., Welling, D.T., Larsen, B. A., Henderson, M. G. and Niehof, J.T. (2011): Spacepy - A Python-based library of tools for the space sciences. In *Proceedings of the 9th Python in science conference (SciPy 2010)*, Austin, TX

OBSERVATORY DATA QUALITY CONTROL – THE INSTRUMENT TO ENSURE VALUABLE RESEARCH

H.-J. Linthe [(1)], J. Reda [(2)], A. Isac [(3)], J. Matzka [(4)], C. Turbitt [(5)]

[(1)] GFZ Potsdam - Adolf Schmidt Geomagnetic Observatory, Lindenstr. 7 14823 Niemegk Germany, linthe@gfz-potsdam.de
[(2)] Institute of Geophysics, Polish Academy of Sciences, 01-452 Warsaw, Poland, jreda@igf.edu.pl
[(3)] Geological Institute of Romania, No. 1 Caransebes Str. Sector 1 RO-012271 Bucharest, Romania, margoisac@yahoo.com
[(4)] Technical University of Denmark - National Space Institute, Elektrovej 327, 2800 Kgs. Lyngby, Denmark, jrgm@space.dtu.dk
[(5)] British Geological Survey, West Mains Road Edinburgh EH93LA, UK, cwtu@bgs.ac.uk

SUMMARY

Observatory data are the foundation for international scientific research. Valuable results can be achieved only if the data are precise and faultless. High quality instruments and a high level of ability and motivation of the observatory personnel are necessary, but a rigorous process of checking is as important for data quality control. Observatory data are useful for science only if the quality can be assured through peer review prior to publication.

INTERMAGNET encourages participating observatories (IMOs) to check their definitive data before they are submitted. Furthermore, definitive data are carefully double-checked by volunteers and by the Definitive Data Subcommittee before they are published to the scientific community. This procedure is labour-intensive, but is essential to maintain a consistently high level of data quality.

Different methods of data checks are described and their efficiency is discussed with consideration to the different instrument base of an observatory. Reason will be given as to why each data check is necessary and the tools available for effective data checks are described.

1. INTRODUCTION

Since Gauss' time in the early 19th century, geomagnetic observatories have monitored the Earth's magnetic field following the same principle. As a result of limitations on instrumentation, all observatories make separate absolute measurements and variometer recordings i.e. variometer data need to be calibrated by means of absolute measurements. Final observatory data are a combination of absolute measurements and variometer recordings. Many aspects of data quality ensuring can be found in Reda et al. (2011).

2. ABSOLUTE MEASUREMENTS

Variometer recordings are periodically calibrated to the absolute level by means of manually performed absolute measurements, which estimate the variometer baselines i.e. the non-constant difference between a variometer output and the absolute field vector. Since baseline values are usually isolated spot values, the deviation of a variometer's baseline between absolute measurements is modelled by interpolation (typically polynomials or splines). Today's standard instrument set consists of a fluxgate-theodolite, used to determine the declination and the inclination of the field vector, and a scalar magnetometer for the measurement of total intensity.

The quality of the measurement results depends on the quality of the instruments and on the ability of the observer making the measurements. For all measurements, the measurement environment is critical and instruments should be operated in a controlled, magnetically clean facility. Since fluxgate-theodolite measurements are currently a manual procedure at most observatories, observer training and a well-defined practice are key to good quality absolute measurements. The biennial IAGA Workshops on Geomagnetic

Observatory Instruments, Data Acquisition and Processing, provide a means of standardising instruments and observer practice internationally through measurement comparisons at a single observatory.

3. VARIOMETER RECORDINGS

Because the Earth‘s magnetic field is a vector, a three-component variometer is required to record its time-varying intensity and direction. A number of differing variometer technologies have developed over the last 180 years; many observatories now operate triaxial fluxgate magnetometers while others operate triaxial photoelectric feedback magnetometers based on a suspended magnet. Other observatories are using vector magnetometers based on scalar magnetometers with compensation coils (for instance, the dIdD variometer).

Baseline stability and effective sampling of any baseline drift through good quality absolute measurements are important quality criteria for an observatory. Such baseline drift may be caused by temperature changes in the variometer room or by tilting of the measuring pillar supporting the instrument. Such baseline drifts can be minimized by a temperature stabilized variometer room (thermal insulation, thermoelectric temperature control) and sensor suspension.

Modern variometers record the variations of the Earth’s magnetic field in digital form and the most straight-forward quality check is a regular inspection of the plotted recordings. A simple daily magnetogram plot of all components can readily show serious problems, such as large scale instrument noise, external interference and data outages. However, a plot of ΔF (difference of F calculated from the baseline corrected vector variometer minus F continuously recorded by a scalar magnetometer) is much a more sensitive detector of instrument problems such as baseline and scale value errors, temperature drift and anthropogenic noise. This ΔF method of problem identification is only possible where an observatory is making continuous F recording by means of a separate scalar magnetometer. The parameters detectable using the ΔF method depend on the type of variometer being used e.g. because coil-compensated scalar magnetometers use a similar F magnetometer, parameters such as baseline and scale errors or temperature drift cannot be checked by additional scalar recording.

If the observatory operates more than one variometer set, the recordings should be compared with each other in order to provide additional quality information. Such comparisons can identify component-specific problems such as scale value errors or, where the variometers are not co-located, room temperature instabilities, data logger time synchronization problems and artificial noise.

4. DATA MANAGEMENT

In addition to good measurement practice, a significant amount of data processing is required to produce a definitive time-series from a set of variometer records and absolute measurements. To maintain the quality level required by scientific research, observatory data require accurate and reliable data management procedures through, inspection, correction, baseline derivation, to preparing for publication. Because the global observatory data set spans such a large period of time, practice and procedure need to be rigorous and consistent in order to ensure that this data set is homogeneous, hence observatory staff are required to be well trained and experienced. This becomes more and more important in a time of an increasing number of unmanned observatories, which are operated by a remote institute. It is currently common place that a single institute will operate a network of geographically disparate observatories with the responsibility for absolute measurements contracted to a third party. Operating such an observatory model brings new challenges in maintainging the measurement environment, training observers and meeting data quality standards.

In the frame of the International Geophysical Year, the system of World Data Centres (WDCs) was established during the 1950s. This improved the use of observatory data. During the 1970s and 1980s, the number of magnetic observatories making digital rather than analog recordings increased rapidly and the WDCs in turn adapted their data management procedures to this trend.

At the end of the 1980s a new data collection and distribution system was established initiated by the British Geological Survey (BGS), Canadian Geological Survey (CGS), the Institute of Physics of the Earth Paris (IPGP) and the United States Geological Survey (USGS). Over the subsequent years, INTERMAGNET became a global network of observatories, taking advantage of near real-time data dissemination and the quality control offered by digital data.

5. INTERMAGNET

Although INTERMAGNET was established using a limited number of magnetic observatories, it was quickly extended to include all absolute magnetic observatories capable of meeting set data quality and distribution standards:

- Near real-time distribution of Reported Data within less than 72 hours. Reported Data are unchecked variometer data, not baseline corrected or only approximately corrected.

- Supply of Definitive Data, which meet a specified data quality standard and which are comprehensively checked for their quality by INTERMAGNET.

With time, an increasing number of international observatories have attained status of an INTERMAGNET observatory (IMO). As of 1 March 2013, 133 observatories are part of the INTERMAGNET network. Besides Reported and Definitive Data, a new data product has recently been established to meet the demand by the magnetic field modelling community for good quality data, delivered more rapidly than definitive data: Quasi-Definitive Data are close to the expected Definitive Data, de-spiked and baseline adjusted, but to be delivered within three months rather than annually**.**

In the beginning Reported Data were distributed by satellite transmission, and Definitive Data were provided on CD-ROMs. Nowadays the web is the base of the data submission and distribution. Reported data and Quasi-Definitive Data are transmitted by e-mail or by a web based data delivery system to one of the 5 Geomagnetic Information Nodes (GINs) and then to the INTERMAGNET web site. Definitive Data are now available at the INTERMAGNET web page for download and on DVDs. Reported and Quasi-Definitive Data can be also downloaded from the INTERMAGNET web page.

INTERMAGNET requires that the IMOs to meet a specified data quality standard and provides support to observatories in the form of software for data processing; quality and data format checking; training for observers on request; and assists IMOs in the processing data from the raw recorded stage to the final published product.

One of the principle tools made available by INTERMAGNET for data quality inspection has been created by the BGS – the so called CD (or DVD) Data Viewer. This is not only a simple data viewer, but it is a comprehensive instrument to detect data problems. In addition to plotting 1-minute data, the application can be used to view hourly, daily, annual mean values and variometer baselines, thus providing analysis of the long-term performance of the data set. It is also possible to plot the first differences of 1-minute data and comparisons (differences) of 1-minute data against neighbouring IMOs. The plotting utility has a number of features that are tailored to monitoring the continuous, long-term nature of observatory recordings e.g. the time window can be extended to plot part of the previous day, month and year and the following one, respectively.

The functionality of the INTERMAGNET CD Data Viewer is particularly useful for an IMO preparing Definitive Data for publication. For example, being able to compare one observatory time-series against another nearby observatory can detect artificial noise generated at a distance to one of the observatories. This type of noise (where both scalar and vector instruments at an observatory see the same level of noise) will be invisible in the ΔF plot of a single observatory. In addition, the ΔF plot will not detect any perturbation affecting only the declination component as the East component generates only a very weak influence on ΔF. As stated previously, observatories operating exclusively variometers based on scalar magnetometers with compensation coils (e.g. dIdD variometers) can often only detect problems in the orthogonal components through comparison with the data of neighbouring observatories.

Plots of first differences plot using the CD Data Viewer can be especially useful in assessing the artificial noise level in a given observatory, particularly for transient interference, such as steps or spikes, at levels above the natural signal.

Baseline jumps or drifts can be found also by means of a comparison plot against data from neighbouring observatories. Baseline variations are typically low amplitude and long period so often, baseline values are assigned on a daily basis. For magnetograms plotted in time windows of 24 hours, baseline jumps between consecutive days can go undetected but if the time window is extended by some percent into the previous and the following day, baseline jumps can become evident.

It is worth noting here that special care should be taken to avoid misinterpretation. In some cases natural variations can be wrongly recognized to be artificial noise. In cases of a suspected artificial disturbance, it is necessary to look carefully at the magnetograms of neighbouring observatories, their first differences plots and at the difference plots. Short periodic natural variations such as sudden storm commencements (SSC) can manifest as irregularities in the ΔF plot due to differing sampling rates, filtering and aliasing. 1-minute vector data are routinely processed from higher frequency data samples using a Gaussian filter while the scalar data can be one minute samples following the present INTERMAGNET standards, given in St. Louis (2011).

One of INTERMAGNET's current projects is planning for the distribution of 1-second data. The first steps for data quality validation have already been undertaken in that the data quality parameters, such as the accuracy of the time stamp and noise characteristics, have been specified. Developing processes to ensure that observatory data meets these specifications and the processes involved in checking these data are the next challenge for the INTERMAGNET team.

6. MAGNETIC CLEANLINESS

It is obvious to state that a magnetically clean environment is most important for the successful operation of a magnetic observatory, but this is frequently difficult to achieve in practice. The distance from the measurement point to ferromagnetic materials and DC currents needs to be sufficient to avoid their influence. Big cities produce a high level of industrial and urban noise due to moving vehicles and electric railways. A number of long-term operated observatories have had to be moved due to expanding cities, increasing industrial activities and traffic. External noise is extremely disturbing for the successful operation of a magnetic observatory and this is normally out of the control of the observatory, however it is critical that an observatory produces no artificial noise by its own activities. Where laboratories or workshops are operated at the site of an observatory, personnel must continuously take care to ensure that variometer recordings and absolute measurements are undisturbed. The number of observatories, having such activities is small and probably further decreasing, as more and more observatories become unmanned, although it s worth noting that a disadvantage of an unmanned observatory is the loss of close supervision on activities which may be a source of artificial noise in the immediate vicinity of the observatory

Randomly occurring artificial noise can be recognized by means of the ΔF check from the vector and scalar recordings of the observatory of concern or by means of difference plots to neighbouring observatories as described in the sections 3 and 5 but noise level can be of a level that it can be seen in a plot of the first differences of a quiet day. Where there is no neighbouring observatory, a useful comparison can be that of the first differences of the same day of an observatory of nearly the same geomagnetic latitude.

Modern infrastructure, such as DC powered railway lines or electrical DC power distribution systems, often produce increasing levels of perturbation on particular magnetic observatories as demand on that infrastructure increases with time. It is, in most cases, impossible to mitigate against this noise. The economic and public significance of the operation of railway and electrical power distribution are of higher importance than the noise-free working of a magnetic observatory. In the past, many magnetic observatories have been moved to places promising (hopefully) sufficiently quiet conditions for the further long-term operation of the observatory. Such a movement is extremely expensive, time consuming and in order to achieve a significant distance from the noise source, the time series of the observatory can, in general, no longer be considered continuous. Some observatories are currently faced with this problem, or are already in planning to move, as the only open to an observatory not able to continue operating at a new location is closure, , which has also unfortunately happened in some cases.

To correct artificially disturbed observatory data series by means of mathematical modelling of the anthropogenic noise and subtracting the modelled signal from the recordings is non-trivial and is frequently not possible. Fox Maule et al. (2009a) tried to establish a useful method for the “cleaning” of the Brorfelde (BFE) time series from perturbations produced by two DC electrical power lines in the Baltic Sea. Neska et al. (2011) describe comprehensively the analysis of the effect of DC powered railway lines on Belsk (BEL) and Lviv (LVV) observatories and suggest an algorithm to correct the contaminated data. But the authors clearly state: “By the way, every trial to correct data can produce unwished secondary effects in the result. For this reason, only original data are accepted by the World Data Centers that collect the observatory data. So our reconstructed data are by no means supposed to substitute the original data.”

7. CONCLUSIONS

High quality observatory data are highly appreciated by the international geomagnetism research community. A number of observatories of exceptional position and particularly long-term time series are of extremely significant interest. Observatory data quality is not explicit– it requires experience, thoroughness and is time consuming. The production of high quality geomagnetic observatory, long-term time series is a challenge that is often not highly enough recognised by data users. Faced by staff reduction, ensuring data quality becomes more of a challenge to institutes operating observatories. Often the operation of observatories is not sufficiently acknowledged by funding organisations and agencies. The result of the painstaking work applied to observatory operation is not directly visible in a time-series alone. The routine work of observers does naturally not lend itself to the publication of scientific articles, however numbers of publications are often the criteria on the results of scientific institutes. Nevertheless, many high level scientific publications are dependent on the high quality absolute magnetic observatory data series.

8. REFERENCES

Fox Maule, C., P. Thejll., A. Neska, J. Matzka, L. W. Pedersen. and Nilsson, A. (2009a). “Analyzing and correcting for contaminating magnetic fields at the Brorfelde geomagnetic observatory due to high voltage DC power lines”. Earth Planets Space **61**, 1233–1241.

Neska, A., J. Reda, M. Neska and Y. Sumaruk (2012). “On the influence of DC railway noise on variation data from Belsk and Lviv geomagnetic observatories”. ACTA GEOPHYSICA (2012), DOI: 10.2478/s11600-012-0058-0

Reda, J., D. Fouassier, A. Isac, H.-J. Linthe, J. Matzka and C. W. Turbitt (2011). “Improvements in geomagnetic observatory data quality”. Geomagnetic Observations and Models, IAGA Special Sopron Book Series 5, 127-148.

St. Louis, B. (2011): “INTERMAGNET Technical Reference Manual Version 4.5”. http://www.intermagnet.org/TechnicalSoft_e.php

A STATISTICAL STUDY OF L.T. VARIATIONS OF K-DERIVED SECTORIAL GEOMAGNETIC ACTIVITY INDICES

M. Menvielle[(1,2)], A. Chambodut[(3)], A. Marchaudon[(4,5)], F. El-Lemdani Mazouz[(1)], C. Lathuillère[(6)]

[(1)] Université de Versailles St-Quentin; LATMOS-IPSL, CNRS-INSU UMR 8190, Guyancourt, France.
[(2)] Université de Paris-Sud, Département des Sciences de la Terre, Orsay, France.
[(3)] Université de Strasbourg, EOST, Département des Observatoires Magnétiques; IPGS, CNRS-INSU UMR 7516, Strasbourg, France, aude@unistra.fr
[(4)] Université d'Orléans; LPC2E, CNRS-INSU UMR 7328, Orléans, France.
[(5)] Université Paul Sabatier; IRAP, CNRS-INSU UMR 5277, Toulouse, France.
[(6)] Université Joseph Fourier - Grenoble 1; IPAG, CNRS-INSU UMR 5274, Grenoble, France.

SUMMARY

Solar-wind/magnetosphere interactions are not symmetrical and show a local time dependency. In order to better describe this effect, we use longitudinal and M.L.T. (Magnetic Local Time) K-derived sectorial geomagnetic activity indices. These indices are calculated on the basis of aλ regional sector geomagnetic activity indices (themselves derived from am network observatories) and thus reflect the geomagnetic activity at sub-auroral latitudes.

In this study, we present a statistical study of the variations of the longitudinal and K-derived M.L.T. sectorial activity indices, as a function of local time and seasons.

1. PLANETARY ACTIVITY

***am, an* and *as* Indices** were initially introduced by Mayaud (1968). They constitute a continuous and homogeneous series since 1959. Expressed in nT, they are derived from *K* indices scaled at observatories, located in the subauroral zones and arranged in groups (5 in Northern hemisphere and 4 in Southern).

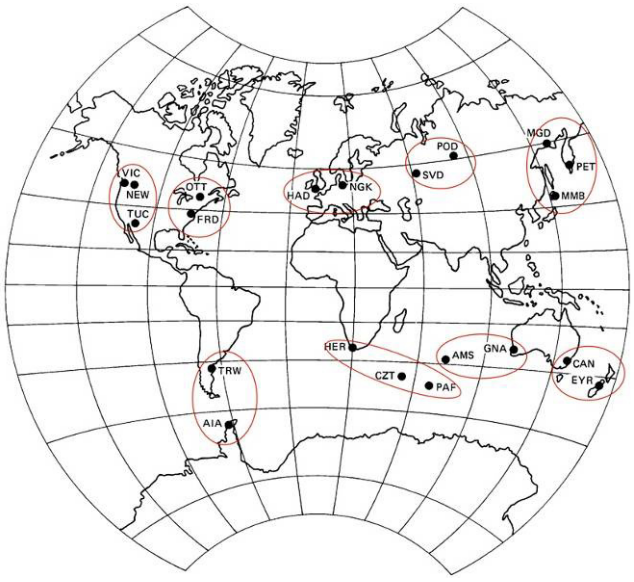

Figure 1 –Network of 22 observatories used for am indices calculation.

Each hemispheric index (*an*: Northern hemisphere, *as*: Southern hemisphere) is a weighted average of the activity at each group of the hemisphere (represented as red ovals on Figure 1). The planetary index *am*, and the hemispheric *an* and *as* indices measure the magnetic activity at subauroral latitudes (corrected geomagnetic latitudes near 50°, see grey curves in Figure 4).

am indices estimate the energy state of the magnetosphere during a three hour interval (Svalgaard, 1977); they are closely related to the magnetic energy associated with the activity of the ionospheric-magnetospheric dynamo.

The statistical analysis of *am* indices allowed to characterize the diurnal and seasonal variations of the magnetic activity.

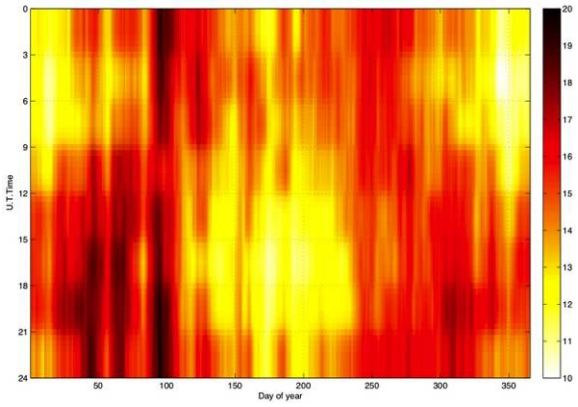

Figure 2 –am index mean variation as a function of U.T. and Day of Year. Each pixel (DoY, UT) corresponds to the average of the corresponding indices during the period 1959-2011.

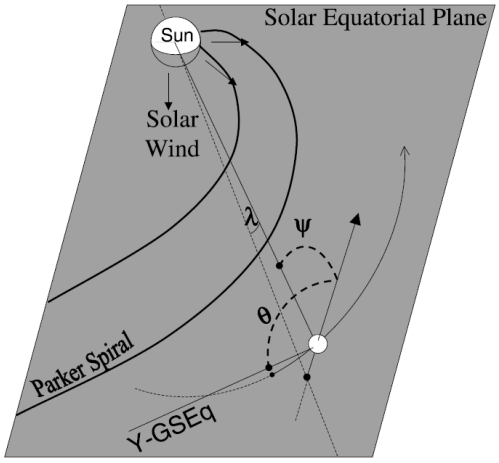

Figure 3 –Representation of ψ_m and θ angles

Figure 2 shows the well-known characteristics of the U.T./seasonal *am* variation:

- a minimum around solstices : at 06:00 U.T. for the December solstice and at 18:00 U.T. for the June solstice;
- a maximum around equinoxes in March and September.

These variations are mainly linked to the fluctuations of various parameters such as (see Figure 3) :

- the angle ψ_m between the Sun-Earth direction and the geomagnetic dipole axis

The magnetic activity is maximum whereas $\psi_m = 90°$ and the variation of ψ_m is thus responsible for a large part of the diurnal and annual ψ_m modulation (McIntosh, 1959; Crooker and Siscoe, 1986; Lyatsky *et al.*, 2001).

- the day-side reconnection probability

This probability is increasing with decreasing θ angle values. θ is the angle between the geomagnetic dipole and the perpendicular to the Sun-Earth direction in the ecliptic plan. This modulation appears as a seasonal (maximum around the 5th of October and the 5th of April) and a diurnal variation (Russell and McPherron, 1973).

2. K-DERIVED SECTORIAL INDICE

***aλ* regional indices** were proposed by Menvielle and Paris (2001). They constitute a continuous and homogeneous series since 1959. They are calculated for each group of *am* network observatories: for each group, the activity is characterized by the mean *K* indices measured in observatories of the concerned group, converted as amplitude in nT. Their time-span is thus 3 hours as for K-indices.

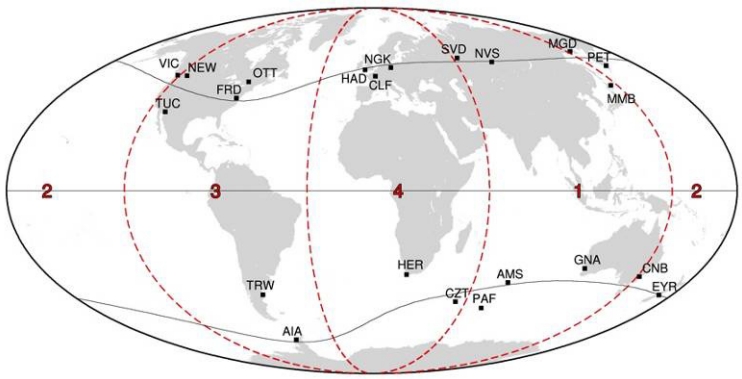

Figure 4 –Network of 22 observatories used for am indices calculation. In red, longitudinal definition and numbering of sectors used in the present study for the calculus of the K-derived longitudinal sectorial indices.

For the present study, we consider two kinds of ***K*-derived sectorial indices, Longitudinal and M.L.T. ones,** depending on how the 4 longitudinal sectors, each 90° wide, are defined: fixed with regards to the Earth' surface or to the Sun-Earth direction. For each kind of indices and each sector, three *K*-derived sectorial indices have been calculated from *aλ* indices:

- "Sectorial North" (from the $a\lambda_N$ indices at boreal latitudes),
- "Sectorial South" (from the $a\lambda_S$ indices at austral latitudes) and,
- "Sectorial" (from a mean of "North" and "South" indices).

The definition of the **K-derived Longitudinal Sectorial Indices** (four 6-hour wide sectors) is given in Figure 4. Sectors are fixed with respect to the Earth' surface.

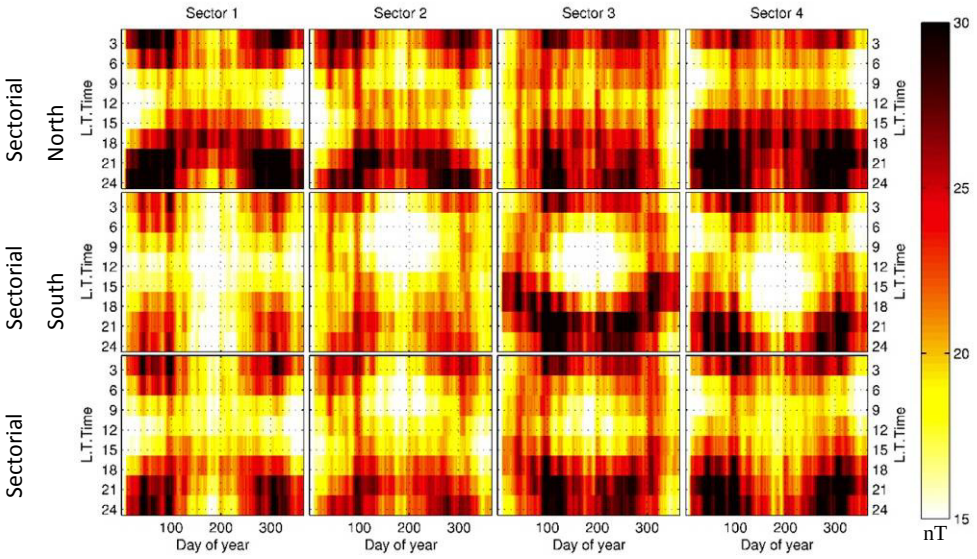

Figure 5 –Mean variation of the magnetic activity described by the the K-derived longitudinal sectorial indices as a function of Local Time and Day of Year (period: 1959-2011).

If one calculated the mean of the four sectorial indices (last row of the Figure 5) the obtained result would be similar in shape to the one directly obtained by using *am* indices (Figure 2). For each hemisphere, the magnetic activity shows in each longitudinal sector a different behaviour, which may be due to the topology of the main magnetic field. Concerning the Southern hemisphere, the maximum of energy (between 21:00 and 03:00 L.T.) is weaker in sectors *1* and *2*: again the question arises about the possible influence of the morphology of the main magnetic field. The L.T. variation of the maximum of activity is traducing the inadequacy between a geographical representation for a phenomena governed by the magnetosphere.

The **K-derived $a\sigma$ M.L.T. Sectorial Indices** (four 6-hour wide sectors) are defined such as the magnetic stations are drifting over time and are contributing successively to the four sectors: dawn: 03:00-09:00, noon: 09:00-15:00, dusk:15:00-21:00 and midnigth: 21:00-03:00 M.L.T.

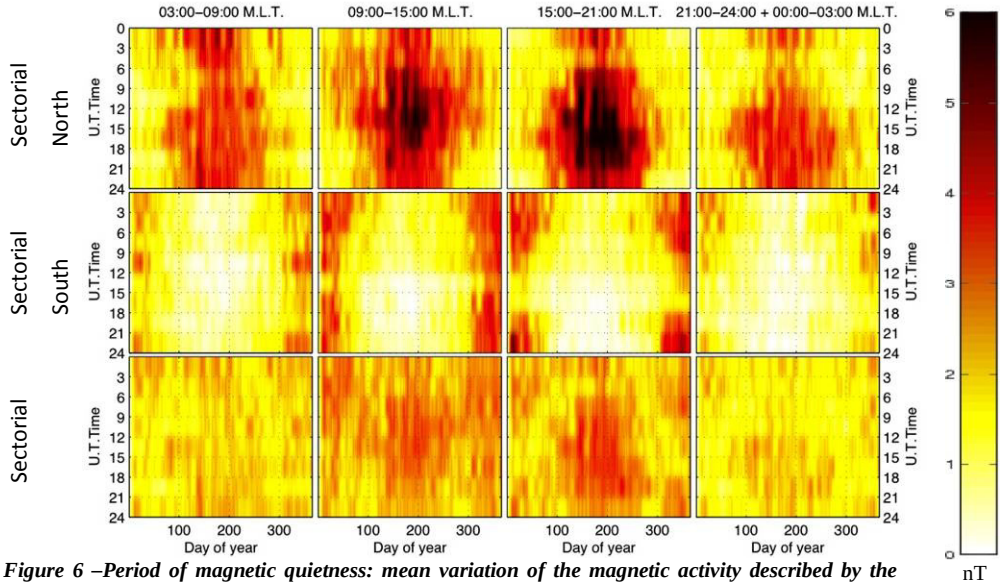

Figure 6 –Period of magnetic quietness: mean variation of the magnetic activity described by the K-derived $a\sigma$ M.L.T. sectorial indices for the 0<am<5 nT activity level (period: 1959-2011).

Onto the Figure 6 (for period of magnetic quietness), the following characteristics may be observed: a maximum energy on the day-side during summer as a response to the sunshine effect, and a maximum energy in the 09:00-15:00 M.L.T. sector localized onto the summer solstice that traduces the influence of the day-side energy transfer of the magnetosphere amplified by the solar illumination. Moreover this maximum should be uniform in U.T. (along the longitude): this is not the case here. Another phenomenon is acting here that still needs to be investigated. The geographical representation (the longitude of the limits of the M.L.T. sectors varies with UT) does not seem to be suitable here.

The figure 7 (for period of moderate magnetic activity) presents a higher activity level on the night-side and a maximum localized around noon in U.T. in the 09:00-15:00 M.L.T. sector that shows magnetospheric dynamics or internal magnetic field origin. The maxima around the summer solstice for the 15:00 - 21:00 M.L.T. sector, and around the winter solstice for the 21:00-03:00 M.L.T. sector, are well represented here.

3. PERSPECTIVES

Ionosphere influence is dominant at low magnetic activity levels (*am* < 5 nT) whereas the magnetosphere is playing a predominant role at high activity level. The transition between low and high activity levels has still to be studied in details but the sectorial indices, and in particular the K-derived $a\sigma$M.L.T. sectorial ones appear to be a reliable promising tool for space weather studies.

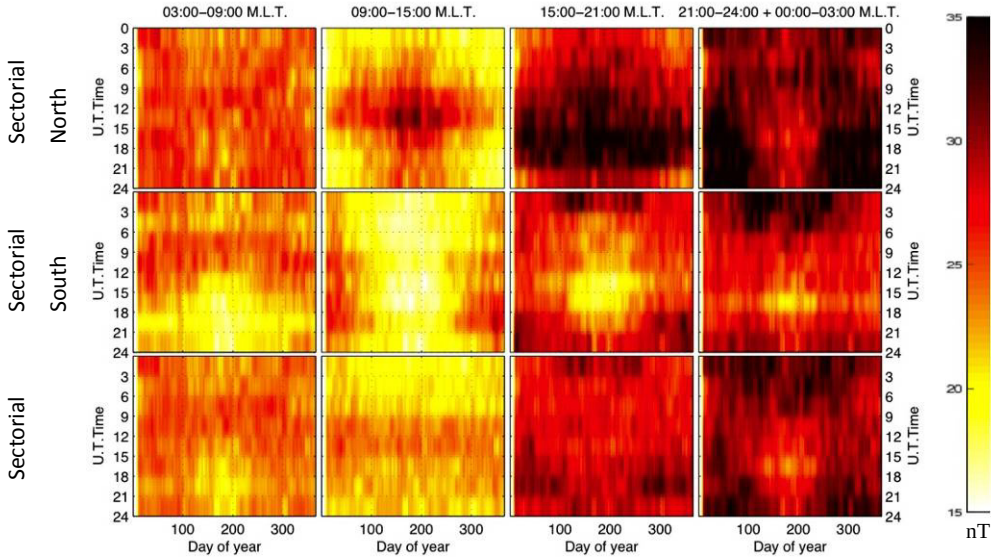

Figure 7 –Period of moderate magnetic activity: Mean variation of the magnetic activity described by the K-derived $a\sigma$M.L.T. sectorial indices for 20< am < 40 nT.

4. ACKNOWLEDGEMENTS

This work is partly supported by the ATMOP project – Advanced Thermosphere Modelling for Orbit Prediction (FP7-SPACE-2010-1/Project #261948).

5. REFERENCES

Crooker, N. U. and Siscoe, G. L. (1986) On the limits of energy transfer through dayside merging, *J. Geophys. Res.*, **91**, 13 393.

Lyatsky, W., Newell, P. T., and Hamza, A. (2001) Solar illumination as the cause of the equinoctial preference for geomagnetic activity, *Geophys. Res. Lett.*, **28**, 2353.

Mayaud, P.N. (1968) Indices Kn, Ks, Km, 1964-1967, 156 p., Centre National de la Recherche Scientifique, Paris.

Mayaud, P.N. and M. Menvielle (1980) A report on Km observatories visit, in *IAGA Bull. 32i*, p. 113, Int. Union of Geod. and Geophys.Publ. Off., Paris.

Mcintosh, D. H. (1959). On the annual variation of magnetic disturbances, *Phil. Trans. Roy. Soc. London, Ser. A*, **251**,525.

Menvielle, M. (1979) A possible geophysical meaning of K indices. *Ann. Geophys.*, **35**, 189.

Menvielle, M. and J. Paris (2001) The al longitude sector geomagnetic indices, *Contrib. Geophys. Geod.*, **31**, 315**.**

Menvielle, M., T. Iyemori, A. Marchaudon and M. Nose (2011) Geomagnetic indices, *in* Geomagnetic Observations and Models, M. Mandea, M. Korte (eds.), I*AGA Special Sopron Book Series 5*, DOI10.1007/978-90-481-9858-0_8, Springer.

Russell, C. T. and R. L. McPherron (1973) Semi-annual variation of geomagnetic activity, *J. Geophys. Res.*, **78**, 92.

Svalgaard, L. (1977) Geomagnetic activity: Dependence on solar wind parameters, *in* Skylab Workshop Monograph on Coronal Holes, edited by J. B. Zirker, chap. 9, p. 371, Columbia Univ. Press, New York.

OVERVIEW OF THE STABILITY OF BASELINE VALUES FOR 1-SEC FLUXGATE MAGNETOMETER LEMI-025 AT HERMANUS OBSERVATORY

E. Nahayo [(1)], P.B. Kotzé [(2)], E. Julies [(3)]

[(1)] South African National Space Agency (SANSA) Space Science, PO Box 32, Hermanus, South Africa, enahayo@sansa.org.za
[(2)] South African National Space Agency (SANSA) Space Science, PO Box 32, Hermanus, South Africa, pkotze@sansa.org.za
[(3)] South African National Space Agency (SANSA) Space Science, PO Box 32, Hermanus, South Africa, ejulies@sansa.org.za

SUMMARY

The South African National Space Agency (SANSA) Space Science operates 4 permanent geomagnetic observatories which are INTERMAGNET members (Hermanus, Hartebeesthoek, Tsumeb and Keetmanshoop). The FGE fluxgate magnetometer is the only vector magnetometer running at these observatories and records data at a sampling rate of 5-sec from which 1-min data is obtained. In the future, one of the requirements from these observatories is to submit real-time 1-second data to one of the INTERMAGNET Geomagnetic Information Nodes. 1-sec Fluxgate Magnetometer LEMI-025 was recently installed at Hermanus to investigate the stability of baseline values and have a hands-on experience for its successful installation at other observatories in the near future. The investigation of the stability of baseline values was conducted and the baseline values of the LEMI-025 and FGE fluxgate magnetometers were compared. The results show that the baseline values of 1-second Fluxgate Magnetometer LEMI-025 are quite stable at Hermanus observatory.

1. INTRODUCTION

The SANSA Space Science is in the process of installing 1-sec Fluxgate Magnetometer LEMI-025 (fig. 1) at its 4 INTERMAGNET observatories shown in fig. 2 (Hermanus, Hartebeesthoek, Tsumeb and Keetmanshoop). For the successful installation, 1-sec Fluxgate Magnetometer LEMI-025 was installed at Hermanus to study the baseline stability of the instrument and get a hands-on experience before installing it at other stations.

Figure 1 –The 1-sec Fluxgate Magnetometer LEMI-025. Figure adopted from the website of the Lviv Centre of Institute of Space Research (Korepanov, 2010).

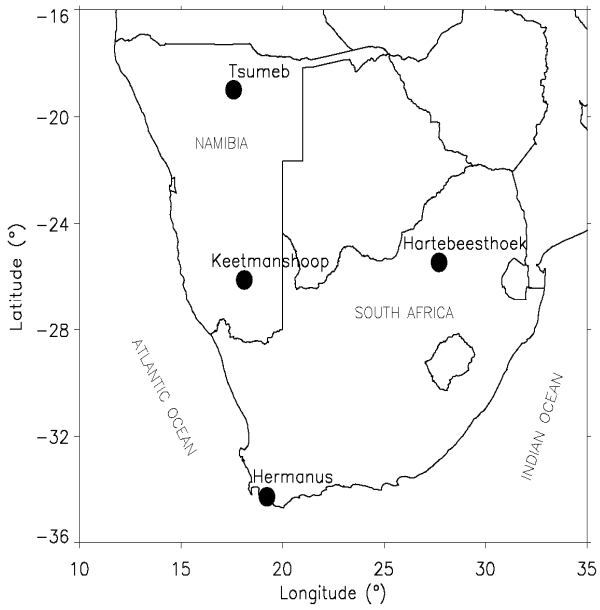

Figure 2 –The SANSA Space Science network of permanent observatories (Hermanus, Hartebeesthoek, Tsumeb and Keetmanshoop).

The absolute control at a magnetic observatory requires a series of measurements of the absolute values of the geomagnetic field using a combination of absolute instruments like a proton precession magnetometer and a Declination/Inclination Fluxgate Magnetometer. The quality of the absolute control may be judged by examining the baseline corrections to the variometer data. Furthermore, a good adopted baseline is derived from individual baseline determinations with a low scatter, and with few drifts or offsets (INTERMAGNET Operations Committee and Executive Council, 2011). The baseline drift of the Fluxgate Magnetometers is mainly due to the temperature change of the fluxgate sensor and the tilting of the sensor basement (Shimizu and Utada, 1999).

In this study, the sensor basement is considered to be solid and stable and the analysis of the temperature variation for both instruments was conducted.

2. COMPARISON OF BASELINE VALUES OF FGE AND LEMI-025 FLUXGATE MAGNETOMETERS

The same set of absolute observations was used in this comparison. The baseline values were computed on a period of nearly 4 months (3 January - 24 April 2012). The cubic spline fitting technique was used to get adopted baseline values for both instruments. Figure 3 shows the plots of baseline values for FGE and LEMI-025 Fluxgate Magnetometers.

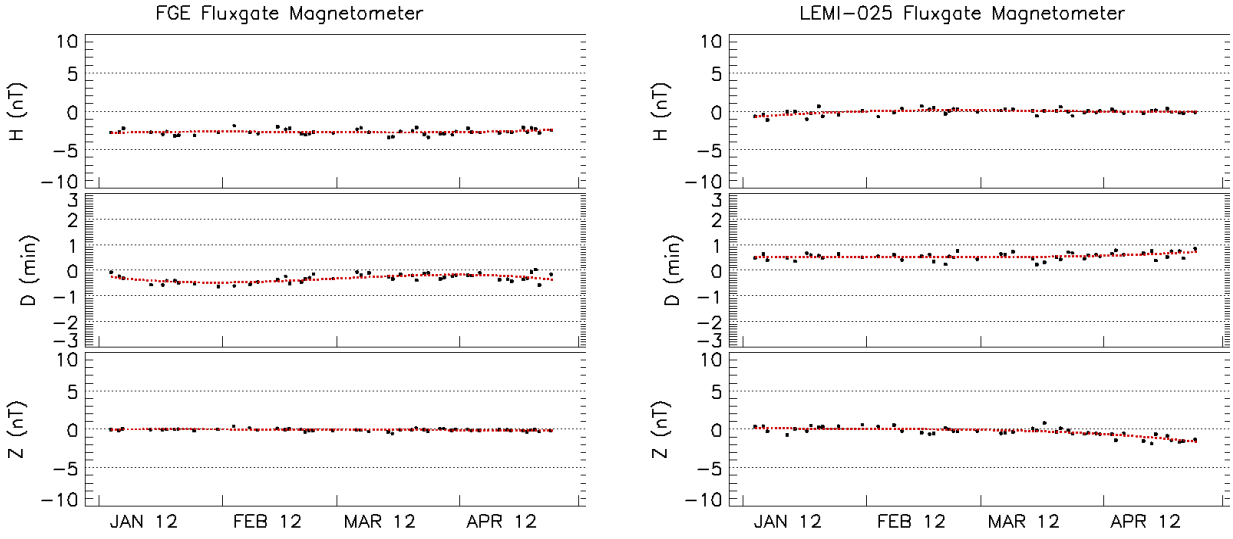

Figure 3 –The plot of the baseline values for absolute observations taken between 3 January and 24 April 2012 for FGE and LEMI-025 Fluxgate Magnetometers. The black dots represent the observed baseline values and the red fitting curve represents the adopted baseline values.

The comparison of baseline values for these 2 instruments was conducted by looking at the scatter of individual measurements (Table 1) and the difference between the adopted baseline values (fig. 4). The scatter values of individual measurements, namely, δH, δD and δZ for magnetic field components H, D and Z respectively, were calculated using the following formula:

$$\delta_C = \sqrt{\frac{\sum_{i=1}^{n}(BV_{C_i} - \overline{BV_C})^2}{n}} \qquad (1)$$

where BV_{C_i} is the individual observed baseline value, $\overline{BV_C} = \frac{1}{n}\sum_{i=1}^{n} BV_{C_i}$, n is the number of individual measurements and δ_C is the scatter value of individual measurements for the magnetic field component C.

Table 1 – The scatter values of individual measurements taken between 3 January and 24 April 2012 for FGE and LEMI-025 Fluxgate Magnetometers.

Type of instruments	δH (nT)	δD (min)	δZ (nT)
FGE Fluxgate Magnetometer	±0.37	±0.17	±0.16
LEMI-025 Fluxgate Magnetometer	±0.40	±0.14	±0.64

The technical specifications of FGE and LEMI-025 Fluxgate Magnetometers indicate that the temperature drift is less than 0.3 nT/°C and 0.2 nT/°C respectively (Korepanov, 2010; Pedersen, 2009). In an attempt to study what might be the cause of the baseline drifts, the temperature variation for both instruments was plotted in Figure 4.

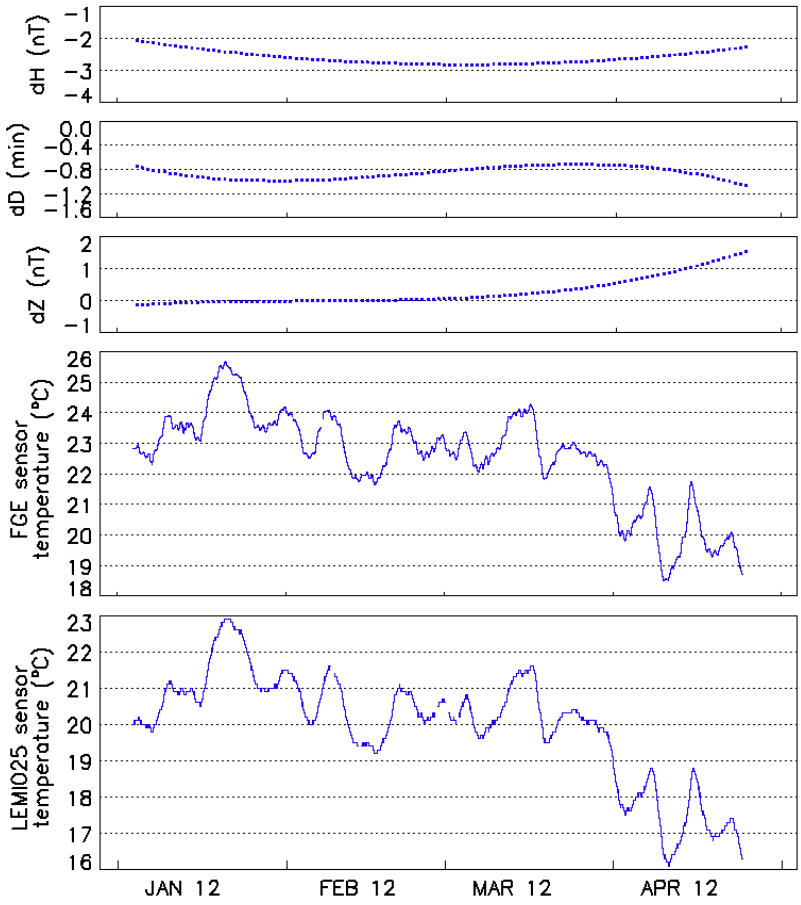

Figure 4 –The plot of the differences between the adopted baseline values of FGE and 1-sec LEMI-025 Fluxgate Magnetometers and the temperature variation of their sensors for the period 3 January - 24 April 2012.

3. DISCUSSION AND CONCLUSIONS

The investigation of the stability of baseline values for 1-sec Fluxgate Magnetometer LEMI-025 involved the calculation of the scatter value of individual measurements, the temperature variation analysis and the comparison with the long time running FGE Fluxgate Magnetometer. For both fluxgate magnetometers, the scatter values of individual measurements of the H, D and Z field components for the period of 3 January - 24 April 2012, as shown in Table 1, are less than 0.70 nT in the H and Z components and 0.20 min in the D component. The slightly large difference between the scatter values of the baseline values of these instruments is noticed in the Z component where the scatter values for FGE and LEMI-025 Fluxgate Magnetometers are 0.16 nT and 0.64 nT respectively.

Furthermore, Figure 4 shows the differences between the adopted baseline values of both instruments, they vary within the range of 0.75 nT, 0.36 min and 1.68 nT for H, D and Z components respectively. The sensor temperature variations for FGE and LEMI-025 Fluxgate Magnetometers are within the range of 7.2°C and 6.8°C respectively. Although, this investigation was conducted on a small period of time (~4 months), it can be stated that the small noticeable drift of 1-sec Fluxgate Magnetometer LEMI-025 baseline value in the Z component from the middle of March might be associated with the drop of the temperature values in March and April (temperature variation range of 5°C in less than 2 months).

It can be seen from the above analysis, that the baseline values of the 1-sec Fluxgate Magnetometer LEMI-025 are stable at Hermanus. However, their stability can be improved by keeping the temperature constant.

4. REFERENCES

Korepanov, V. (2010): "3-component 1-second observatory Magnetometer LEMI-025". *Lviv Centre of Institute for Space Research*, Available at: http://www.isr.lviv.ua/lemi025.htm.

INTERMAGNET Operations Committee and Executive Council (2011): "INTERMAGNET Technical Reference Manual". *INTERMAGNET*, Available at: http://www.intermagnet.org/TechnicalSoft_e.php.

Pedersen, L. W. (2009): "3-axis Fluxgate Magnetometer Model FGM-FGE". *Technical University of Denmark*, Available at: http://www.space.dtu.dk /English/Research/ Instruments Systems Methods/3-axis Fluxgate Magnetometer Model FGM-FGE.aspx.

Shimizu, H. and H. Utada (1999): "Ocean Hemisphere Geomagnetic Network: its instrumental design and perspective for long-term geomagnetic observations in the Pacific". *Earth Planets Space*, **51**, 917-932.

AN INSTRUMENT PERFORMANCE AND DATA QUALITY STANDARD FOR INTERMAGNET ONE-SECOND DATA EXCHANGE

C. Turbitt[(1)], J. Matzka[(2)], J. Rasson[(3)], B. St-Louis[(4)], D. Stewart[(5)]

[(1)] British Geological Survey, United Kingdom, cwtu@bgs.ac.uk
[(2)] DTU Space, Denmark, jrgm@space.dtu.dk
[(3)] Institut Royal Météorologique, Belgium, jr@oma.be
[(4)] Natural Resources Canada, Canada, stlouis@geolab.nrcan.gc.ca
[(5)] United States Geological Survey, United States, dcstewart@usgs.gov

SUMMARY

With the advent of developments in instrumentation, data acquisition and data dissemination, an increasing number of observatories are producing a filtered one-second data product in addition to traditional one-minute data, hourly means, daily means, monthly means and annual means. An INTERMAGNET survey of the user community in 2005 concluded that there is a desire for one-second data to be made available through the INTERMAGNET network and that, as is the case for one-minute data, a minimum standard of instrument performance and data quality should be set for definitive one-second data. Here, the INTERMAGNET Observatories & Standards Subcommittee introduces such a one-second data standard resulting from consultation with the scientific community and instrument developers.

1. INTRODUCTION

INTERMAGNET is a global network of over 100 absolute geomagnetic observatories formed as cooperation between international geophysical institutes. Since its inception in 1991, INTERMAGNET has made use of existing technologies to disseminate data from observatories in the network to data users in near real-time and to provide a publishing platform for final (or definitive) data sets. To ensure operational uniformity and to provide a consistent data quality across the network, the INTERMAGNET Operations Committee publishes a set of common standards (INTERMAGNET, 2011), which include definitions of file formats for data exchange as well as parameters detailing the minimum quality requirements for an observatory participating in the network.

Since 1991, the principle INTERMAGNET publication output has been an annual definitive data set comprising one-minute, three-component samples from each of the participating observatories, along with associated metadata and derived mean values. Recent developments in technology have now made it possible to manipulate and exchange data at a higher sample rate and several INTERMAGNET observatories have begun to make experimental one-second recordings, enabling monitoring of a higher frequency band of the geomagnetic spectrum. As a result of the requirements of the observatory and scientific communities, manufacturers have also begun to develop instruments capable of sampling at this higher data rate.

Based on a survey of the geomagnetic scientific community, and in consultation with observatory operators and instrument producers, INTERMAGNET has drafted a set of data quality standards intended to apply to future publication of definitive one-second data. Rather than set out the specifications of the instrument alone, the parameters described here define the overall specifications of a complete observatory system for a one-second vector data set including recording environment, magnetometer, and data processing procedure. The standard has been defined such that the general parameters of the system transfer function are specified. However, to allow a range of instrumentation and system solutions, specific parameters such as base sampling frequency and digital filter type are not explicitly defined.

2. INTERMAGNET ONE-SECOND DEFINITIVE DATA SPECIFICATIONS

The consensus of a survey of the scientific community conducted by INTERMAGNET was that, in order to ensure that one-second data acquired by the INTERMAGNET network was of sufficient quality, the minimum parameters should be: accurate time stamping (within 0.01 s); high resolution (<0.01 nT); uniformly & digitally filtered with near linear phase response. The task of the INTERMAGNET

Observatories & Standards Subcommittee has been to interpret these general requirements set by the user community into a practical data standard of use to the observatory community. The resulting specification parameters are listed in Table 1.

Table 1 – INTERMAGNET One-second Definitive Data Specifications

General Specifications	
Time-stamp accuracy	0.01 s
Phase response	±0.01 s
Maximum filter width	25 seconds
Instrument Amplitude Range	≥±4000 nT High Latitude, ≥±3000 nT Mid/Equatorial Latitude
Data resolution	1 pT
Pass band	DC to 0.2 Hz
Maximum component orthogonality error	2 mrad
Maximum Z-component verticality error	2 mrad
Pass Band Specifications [DC to 8 mHz (120 s)]	
Noise level	≤100 pT RMS
Maximum offset error	±2. 5 nT
Maximum component scaling & linearity error	0.25%
Pass Band Specifications [8 mHz (120 s) to 0.2 Hz]	
Noise level	≤10 pT/√Hz at 0.1 Hz
Maximum gain/attenuation	3 dB
Stop Band Specifications [≥ 0.5 Hz]	
Minimum attenuation in the stop band (≥ 0.5Hz)	50 dB
Auxiliary measurements:	
Compulsory full-scale scalar magnetometer measurements with a data resolution of 0.01 nT at a minimum sample period of 30 seconds. Compulsory vector magnetometer temperature measurements with a resolution of 0.1 °C at a minimum sample period of one minute.	

3. GENERAL SPECIFICATIONS

To comply with the requirements stipulated by the user community, the standards set in Table 1 specify a maximum time-stamp error for data digitally filtered to one-second samples. The time-stamp error applies to the centre point of the digital filter and is measured from the top of the UT second.

To meet the requirement for linear phase, a maximum group delay (frequency derivative of phase) is set as a limit on non-linearity. Data samples may be time-shifted to correct for latency (e.g. instrument response and filter delay) provided that the system phase response is met.

The specified minimum instrument ranges have been inherited from the INTERMAGNET one-minute specification to provide an attainable noise level for an instrument of fixed dynamic range, however it is recognised that these ranges may be exceeded by extreme geomagnetic events hence it is recommended that either a low-gain instrument is run in parallel; an offset is applied to the H-component; or the instrument range is extended (e.g. by auto-ranging).

A maximum filter width is set to minimise the time extent of the system response to a step input i.e. filter ringing.

4. PASS BAND SPECIFICATIONS [DC TO 8 mHz (120 s)]

Observatories moving from absolute one-minute recordings to absolute one-second recordings will require to monitor over not only a larger frequency band but, due to the spectrum of the natural magnetic field, also a larger dynamic range. To meet these stringent measurement requirements yet ensure that the limitations on the instrumentation are realistic, the pass band has been split into two: the existing INTERMAGNET one-minute data band (DC to 120s) and the extended band (8mHz to 0.2Hz).

In comparison with the extended band, the low frequency band (DC to 120s) has been specified a higher system noise level limit but more constraint on the absolute accuracy. The offset error specifies a maximum low frequency instrumental error, including instrument drift

and thermal drift i.e. an absolute accuracy limit. Here, there is no specification on the frequency of absolute magnetic observations, other than observations must be sufficient to achieve the specified maximum offset error under quiet geomagnetic conditions.

It is recognised that in setting a scaling & linearity limit of 0.25%, this creates an inconsistency with the maximum offset error for variations in the magnetic field over 1000nT. Such large disturbances are considered to be of sufficiently short duration and scarcity that it is reasonable to specify errors during these periods in terms of percentage accuracy at the expense of absolute accuracy. In other words, the scaling & linearity error could be considered to apply to the higher frequencies (within the DC to 0.2Hz band) and the maximum offset error to the lower frequencies without explicitly specifying a delineating frequency. The inconsistency between the two standards is deemed necessary in order to specify an achievable system calibration parameter, whilst also specifying an absolute accuracy level that applies during normal conditions i.e. where the field deviates by no more than 1000nT from quiet level between absolute observations, which is the significant proportion of the time series.

5. PASS BAND SPECIFICATIONS [8 mHz (120 s) to 0.2 Hz]

In the high frequency band of the pass band (8 mHz to 0.2 Hz), the noise level is set at a lower level to ensure sufficient resolution of low amplitude signal in this band of the natural geomagnetic spectrum. Since absolute signal amplitude is not as critical to the user community in this band as it is in the low frequency band, and to allow for instrument roll-off with sufficient attenuation in the stop band, the maximum signal gain/attenuation is specified at a less stringent 3dB in the high frequency band.

6. STOP BAND SPECIFICATIONS [≥ 0.5 Hz]

The minimum stop band attenuation parameter has been set to ensure an easily achievable roll-off in the transition band whilst reducing aliased natural geomagnetic signal in the pass band to below the specified pass-band noise levels. However, there remains the possibility that large amplitude, non-natural signals in the stop band (e.g. 50/60 Hz) could be aliased into the pass-band at frequencies other than 0.1Hz and still meet this specification, hence there is a recommendation to separately attenuate (e.g. by a notch filter) non-natural, large-amplitude signals above the Nyquist.

7. AUXILLIARY MEASUREMENTS

Another modification over the INTERMAGNET specification for one-minute data is the requirement for auxiliary measurements from an absolute scalar magnetometer and monitoring of the variometer temperature for the purpose of quality control.

8. CONCLUSIONS

The authors acknowledge that the instrument specifications, particularly the low noise level in the pass band, are not met by most of the instrumentation currently available. However, the authors have undertaken extensive consultation with instrument manufacturers to ensure that these specifications are realistic and can be achieved by manufacturers in further developments of their instruments. It is also necessary to set such ambitious specifications to ensure that future observatory data sets are well suited to the needs of the data user community.

The set of standards described here will be defined and, where possible, tested to be the minimum quality requirements for definitive one-second data to be distributed by absolute magnetic observatories via the INTERMAGNET web site and DVD. For the purpose of brevity, a full discussion on the proposed standard has not been included here, but has been documented in INTERMAGNET Discussion Document 20, a copy of which can be obtained from a member of the Observatories & Standards Subcommittee or by request from secretary@intermagnet.org.

It is important to note that, whilst INTERMAGNET encourages observatories to participate in the exchange of one-second data, the INTERMAGNET network will continue to distribute one-minute data and existing definitive one-minute standards are unaffected.

9. ACKNOWLEDGEMENTS

In reaching the set of standards listed here, the INTERMAGNET Operations Committee has sought consultation with as broad a representation of the data user community, observatory operators and instrument developers as possible. In particular, the Operations Committee is grateful to the following for their valuable input in this process: Arnaud Chulliat, Laszlo Hegymegi, Valery Korepanov, Xavier Lalanne, Andriy Marusenkov, Barry Narod, Lars William Pedersen, Jan Raagaard Petersen, Gerhard Schwarz and Tom Shanahan.

10. REFERENCES

INTERMAGNET Operations Committee. (2011): "INTERMAGNET Technical Reference Manual V4.5".*c/o Natural Resources Canada, #7 Observatory Crescent, Ottawa, Ontario Canada K1A 0Y3.*

GEOMAGNETIC OBSERVATION AT MERIDIAN STATIONS IN CHINA

X.Z. Wang[1,2], Y.T. Teng[1], D.M. Yang[1]

(1) Institute of Geophysics, China Earthquake Administration, No.5, Minzudaxue Nanlu, Haidian District, Beijing, China, 100081, wxz9288@yahoo.com.cn

(2) State Key Laboratory of Space Weather, Chinese Academy of Sciences, NO.1, Nanertiao, Zhongguancun, Haidian district, Beijing, China, 100190

SUMMARY

In this paper, we introduce the Meridian Project of China and instruments installed. As an example, we display the magnetic storm observation results taking place on Jan. 24, 2012. The results show there are clear amplitude difference along longitude for fluxgate magnetometer and search coil magnetometer.

1. INTRODUCTION

The Meridian Project, namely the Meridian Space Weather Monitoring Project, is a massive scientific research project that will survey solar-terrestrial space environment, which began to be build in 2008 and became fully operational in Dec. 2012. It consists of three parts and they are space environment monitor system, data and communication system and research forecast system respectively. The space environment monitor system is a Chinese multi-station chain along 120ºE starting from the Mohe station to China Zhongshan station and along 30ºN starting from Hangzhou station to Lhasa station. The station location is shown in figure 1 and other information is shown in table 1.

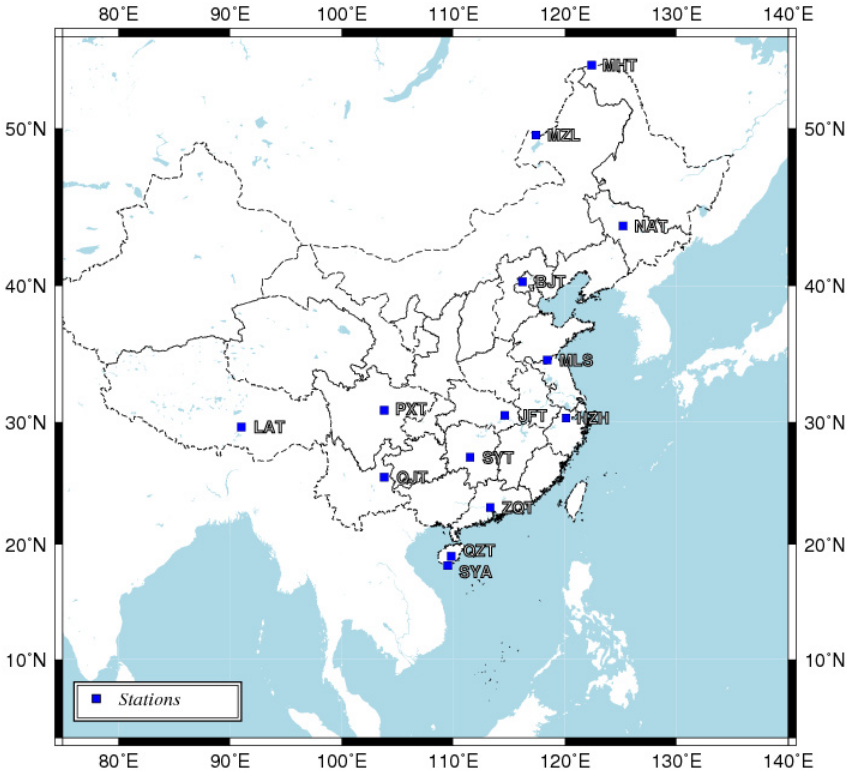

Figure 1 –Meridian Geomagnetic Stations in China.

The space environment monitor system includes various equipments, such as magnetometers, ionosondes, incoherent scattering radar, HF back-scattering radar, LIDARs, Fabry-Perotinter ferometer, interplanetary scintillation and sounding rockets and so on. And they can survey space environment in geospace with an altitude higher than 20-30km up to the interplanetary space.

To survey geomagnetic field and geoelectrical field, the fluxgate magnetometer (FGM), search coil magnetometer (SCM), overhauser magnetometer (OHM), the magnetic fluxgate theodolite (DIM), geoelectrical field meter (GEM) and atmospheric electric field meter (AEM) were installed in 14 meridian stations. The information of the stations and instruments is shown in table 1.

***Table 1* – Information of stations and instruments**

No.	Station Name	Station Code*	Lat. (°N)	Long. (°E)	Instrument Code
01	Mohe	MHT	53.5	122.4	FGM, SCM, GEM, AEM
02	Manzhouli	MZL	49.6	117.4	FGM, SCM
03	Chanchun	NAT	44.0	125.2	FGM, SCM, GEM, AEM
04	Beijing	BJT	40.3	116.2	FGM, SCM, GEM, AEM
05	Malingshan	MLS	34.7	118.4	FGM, SCM, GEM, AEM, OHM, DIM
06	Hangzhou	HZT	30.3	120.1	FGM, SCM
07	Wuhan	JFT	30.5	114.6	FGM, SCM, GEM, AEM
08	Chendu	PXT	30.9	103.8	FGM, SCM, GEM, AEM
09	Lhasa	LST	29.6	91.0	FGM, SCM
10	Zhaoqing	ZQT	23.1	113.3	FGM, SCM, GEM, AEM
11	Shaoyan	SAY	27.2	111.5	FGM, SCM
12	Qiongzhong	QZT	19.0	109.8	FGM, SCM
13	Sanya	SYA	18.2	109.5	FGM, SCM, OHM, DIM
14	Antarctica Zhongshan	ZST	-69.4	76.4	FGM, SCM, OHM, DIM

* A special code for the Meridian Project of China.

Recently, a new plan of the second phase of meridian project has been proposed. Its main object is to build one three-dimensional solar-terrestrial space environment monitor system. In this phase, one satellite will be launched with the Langmuir probe, GPS occultation receiver, magnet field detector, electric field detector and so on. Its orbital altitude and inclination is about 450km and 90º (polar orbit) respectively. Meanwhile new station chain will been build and one is located along 100ºE and another is located along 40ºN.

2. RESULT AND DISCUSSION

The data is recorded by the fluxgate magnetometers (model GM4) and the search coil magnetometers (model LEMI-30) which have been used at all 14 stations (as shown in Table 1). GM4 magnetometers, developed by Institute of Geophysics, China Earthquake Administration, work for the frequency band DC-0.3Hz and data sampling frequency is 1Hz. LEMI-30 magnetometers, imported from Lviv Center of Institute of Space Research, Ukarine, work for the frequency band 0.001-30Hz and over which the noise level varies from 20 to 0.04pT $Hz^{-1/2}$. Its data sampling frequency is 32Hz. The raw data from LEMI-30 is passed a low pass filter which cut-off frequency is 0.3Hz and is downsampled to 1 Hz.

On 24, Jan. 2012, one large magnetic storm occurred and its maximum variation is about 180nT in H component. This magnetic storm began at UT15:04 2012-01-24 and ended about at UT06:00 2012-01-26.The GM4 magnetometer and LEMI-30 magnetometer recording data is plotted in figure 2 and figure 3 respectively.

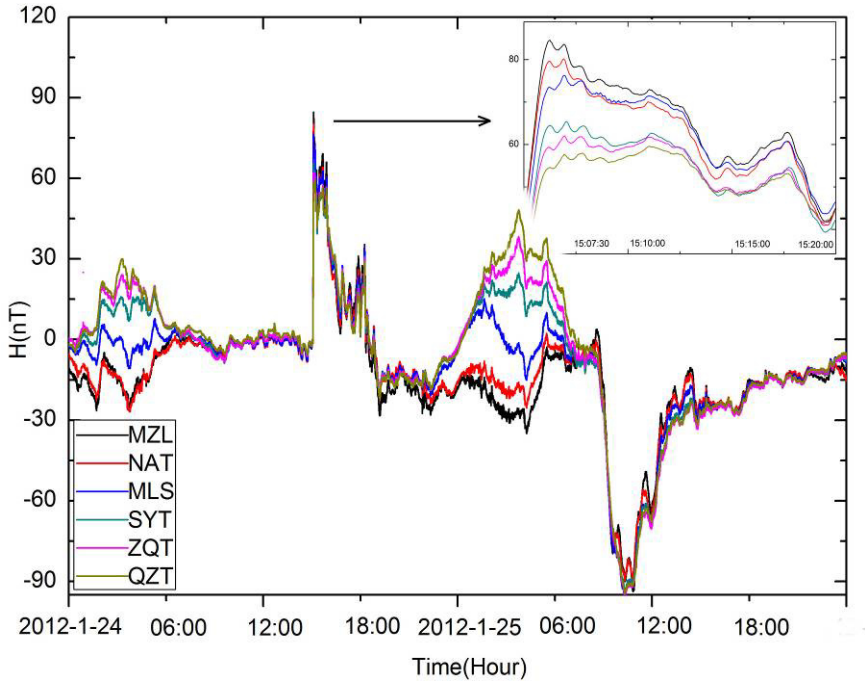

Figure 2 –H component of GM4 magnetometer. Arrow shows a partial enlarged view.

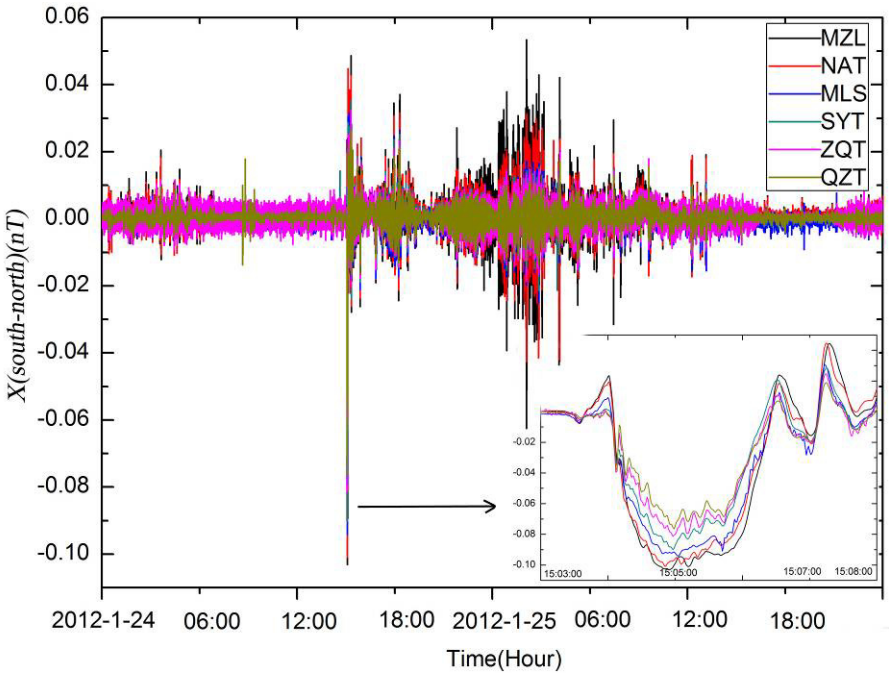

Figure 3 –X component of LEMI-30 magnetometer. Arrow shows a partial enlarged view.

In figure 2, it clearly displays initial phase, main phase and recovery phase of magnetic storm. In initial phase, there is rapid increase from about zero nT to 85 nT and the amplitude increases with the increasing latitude. In recovery phase, there is rapid decrease from about 4 nT to -96 nT and the amplitude increases with the increasing latitude.

According to the LEMI-30 magnetometer frequency characteristics, it is linear below 1 Hz and the slope is frequency f. However in figure 3 we do not transform from raw record to real magnetic value and it may be the reason the value is small. As shown in figure 3, there is rapid decrease in X component in initial phase, which is agree to increase of H component. Meanwhile the amplitude gradually increases from high latitude to low latitude in this phase. Contrary to H component in main phase, for X component, there are no obvious increase or decrease in main phase and its variation is similar to that as usual.

3. ACKNOWLEDGMENT

The authors are thankful to Institute of Geophysics, CEA for providing the fund (DQJB11B03) support and the Meridian Project for providing data. Thanks are also due to researcher at meridian stations to carry out routine observations and analysis of data.

4. REFERENCES

Wenyao, Xu (2009): " Physics of Electromagnetic Phenomena of the Earth ". *University of Science and Technology of China press, Hefei*.

Y.Kamide, A.C.-L.Chian (2010): " Handbook of theSolar-Terrestrial Environment ". *Science press, Beijing. [Translated by Wenyao, Xu]*.

SPACE WEATHER APPLICATIONS OF GEOMAGNETIC OBSERVATORY DATA

Alan W P Thomson [(1)]

[(1)] British Geological Survey, Murchison House, West Mains Road, Edinburgh EH9 3LA, UK, awpt@bgs.ac.uk

SUMMARY

Solar maximum is expected between late 2012 and early 2014. Space weather impacts on worldwide technological infrastructures are therefore likely to be at their greatest at this time. These infrastructures include power grids, pipelines, railways, communications, satellite operations, high latitude air travel and global navigation satellite systems. For example, severe magnetic storms in March 1989 and October 2003, near the peaks of previous solar cycles, were particularly significant in causing problems for a wide variety of technologies. Further back in time, severe storms in September 1859 and May 1921 are known to have been a problem for the more rudimentary technologies of the time. In this paper we review examples of these impacts, what scientific research and measurement is underway, or is still needed, and how the geomagnetic observatory community can best contribute to the ongoing efforts in developing new space weather data products. Throughout, the need for near to real-time observatory data and products to help space weather forecasters and to serve industry and government is emphasised. We also discuss how industry perceives the space weather hazard, using examples from the electrical power industry, concerned with the risk to high voltage transformers and the safe and uninterrupted distribution of electrical power.

1. INTRODUCTION

Space weather can be defined as disturbances in the solar wind that can affect Earth's space, atmosphere and surface environments and that can disrupt technologies. The Sun has a magnetic activity cycle, as measured by sunspots, of approximately eleven years. Solar magnetic activity takes the form of coronal mass ejections (CMEs) and coronal holes. CMEs (see Figure 1) are particularly significant for 'bad' space weather, when they are Earth-directed. A CME is a plasma cloud threaded by magnetic fields that is ejected from the Sun with speeds from a few hundred to a few thousand kilometers per hour. Its impact on the Earth's magnetosphere (see Figure 2) depends on whether the magnetic field in the CME is southwards pointing. In a southward configuration magnetic reconnection on the dayside of the Earth, between the magnetic fields of the CME and the magnetosphere, allows the energy and plasma of the CME to enter the magnetosphere. This boosts current systems within the magnetosphere (Figure 2), resulting in geomagnetic storms when the ring current is strengthened. Geomagnetic sub-storms occur when the magnetospheric convection that is controlled by the solar wind concentrates magnetic flux in the magnetotail. This gives rise to intermittent current discharge through field aligned currents connecting the energized magnetotail to the auroral ionosphere. CMEs should be distinguished from solar flares. The latter produces intense X-ray and EUV emissions and can give rise to radiation storms in space. However, CMEs are the driver of geomagnetic activity, for example as measured by ground-based geomagnetic observatories.

2. IMPACTS

The consequences of space weather, besides the visible aurora borealis and aurora australis, are largely impacts on technologies we rely on, for example communication, travel, navigation and power. Examples of such impacts, and an indication of some of the underlying physical causes, tied to space weather, are shown in Figure 3. One of the issues for the modern world and its exposure to space weather is the interconnectedness of many of these technologies and their reliance on uninterrupted electrical power. This is a concern for many governments at the present time.

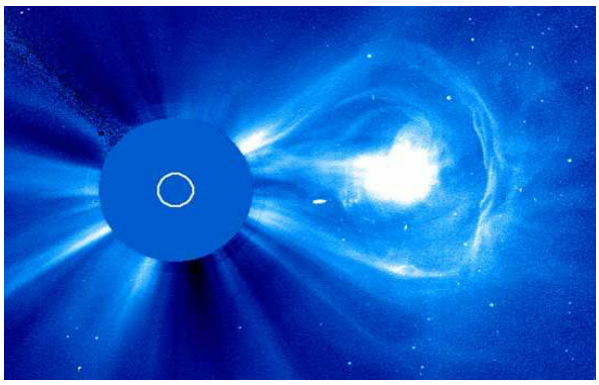

Figure 1 –A coronal mass ejection illuminated by sunlight from behind an occulting disk (blue). To scale the visible Sun is indicated by the white circle. The image is from the SOHO spacecraft, courtesy of SOHO/LASCO consortium. SOHO is a project of international cooperation between ESA and NASA. See soho.nascom.nasa.gov.

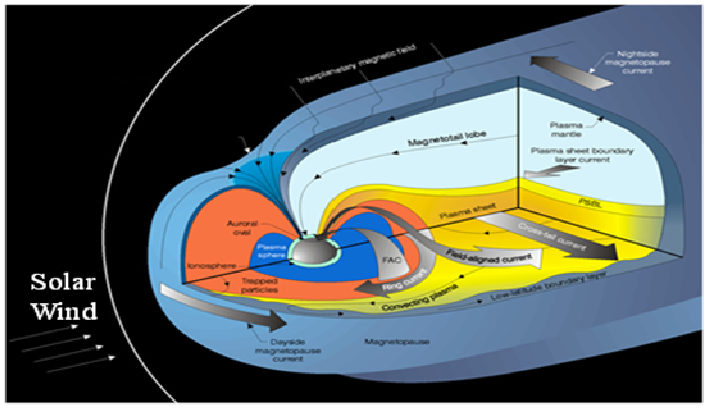

Figure 2 –A cartoon showing the major current systems of the magnetosphere (grey arrows) and major particle populations (colour). The solar wind, containing CMEs, impinges from bottom left. Figure courtesy of NASA.

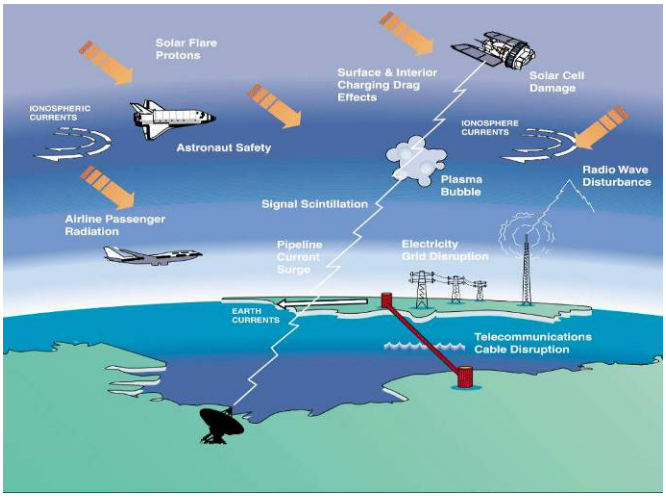

Figure 3 –Examples of space weather impacts on technology. Figure courtesy of Louis J Lanzerotti, New Jersey Institute of Technology.

3. SCIENTIFIC RESEARCH

Research into space weather, its causes and impacts, continues in many countries, particularly, but not exclusively, in countries at higher latitudes where the space weather impact is generally greater. Of particular concern are geomagnetically induced currents (GIC), that are a result of geomagnetic storm variations inducing an electric field in the conducting Earth, which in turn drives GIC through grounded networks, such as electrical transmission systems. Documented power grid impacts from GIC have been noted in places such as Sweden, USA, Canada, South Africa and the UK, indicating the range of (magnetic) latitudes where systems may be affected.

As just one example of current worldwide research in this area, in Figure 4 we show the impact of a hypothetical'extreme' event on the UK power grid. Here we have scaled the magnetic variations actually measured during the 'Halloween Storm' of October 2003. In order to estimate how big the GIC would be in the earth wire of each transformer in the UK grid, a detailed, geological map-based model of shallow surface conductivity was derived (Beamish and White, 2012). Magnetic variations were interpolated across the British Isles using the technique of 'spherical elementary current systems' (Amm, 1997), from magnetic measurements made across northern Europe. The UK National Grid company is considering the impact of these large GIC on transformers, together with government advisors.

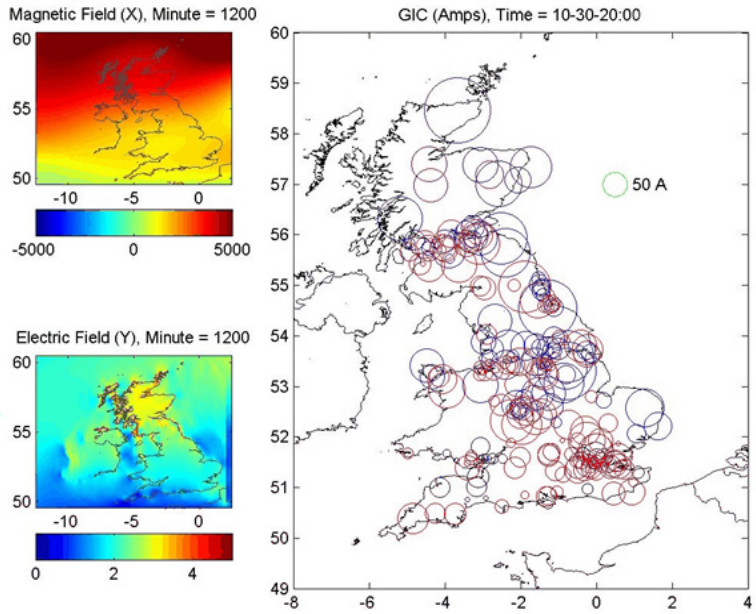

Figure 4 –Interpolated magnetic field variations (top left), calculated surface electric field (bottom left) and estimated GIC at major transformer nodes in the UK grid (main Figure: scale is 50 A) at one instant (20:00UT) on 30th October 2003, scaled to represent a 1 in 100 to 1 in 200 year event. Red (blue) denotes current flow into (out of) the grid from (into) the ground.

Of course, estimating what constitutes an extreme event is difficult, not least because the continuous geomagnetic record is only around 150 years old (depending on location and observatory) and has been digital since only about 1980. Nevertheless studies such as those by Riley (2012), Love (2012) and Thomson *et al.* (2011) have recently attempted to address this question. The latter study was used to provide the scaling factor for the example shown in Figure 4.

4. THE ROLE OF GEOMAGNETIC OBSERVATORIES

Magnetic observatories provide local measurement of local space weather conditions. At the same time through partnerships like INTERMAGNET (www.intermagnet.org), the International Space Environment Service (www.ises-spaceweather.org) and the World Data Centres for Geomagnetism (Kyoto, Mumbai, Edinburgh), free data exchange between observatories can provide vital data for analysis of space weather activity on the global and regional scale. For space weather research near-real-time magnetic data, often translated into different products (as in the example given in Figure 5), are helpful for situational awareness and for input into models that simulate or predict impact on the environment and technologies. Significant space weather events generate media and public attention, providing an excellent opportunity for geomagnetic observatory scientists to inform and educate. Increasingly, social media such as Twitter and Facebook are used, and alert systems, for example by email or SMS, can attract significant numbers of subscribers.

5. CONCLUSIONS

The potential impact of space weather on technology is growing as technology develops, for example as a consequence of the miniaturization of electrical components. Both public and private sectors of industry should therefore be better aware of the space weather hazard and consider the risk they may be exposed to. Geomagnetism science and technical expertise is in demand from industry to help with risk assessment and the relevance of the data from the worldwide geomagnetic observatory network has probably never been greater. There are therefore many opportunities for institutes operating magnetic observatories to develop local data products, based on their measurements, to address the needs of industry and the public in their countries.

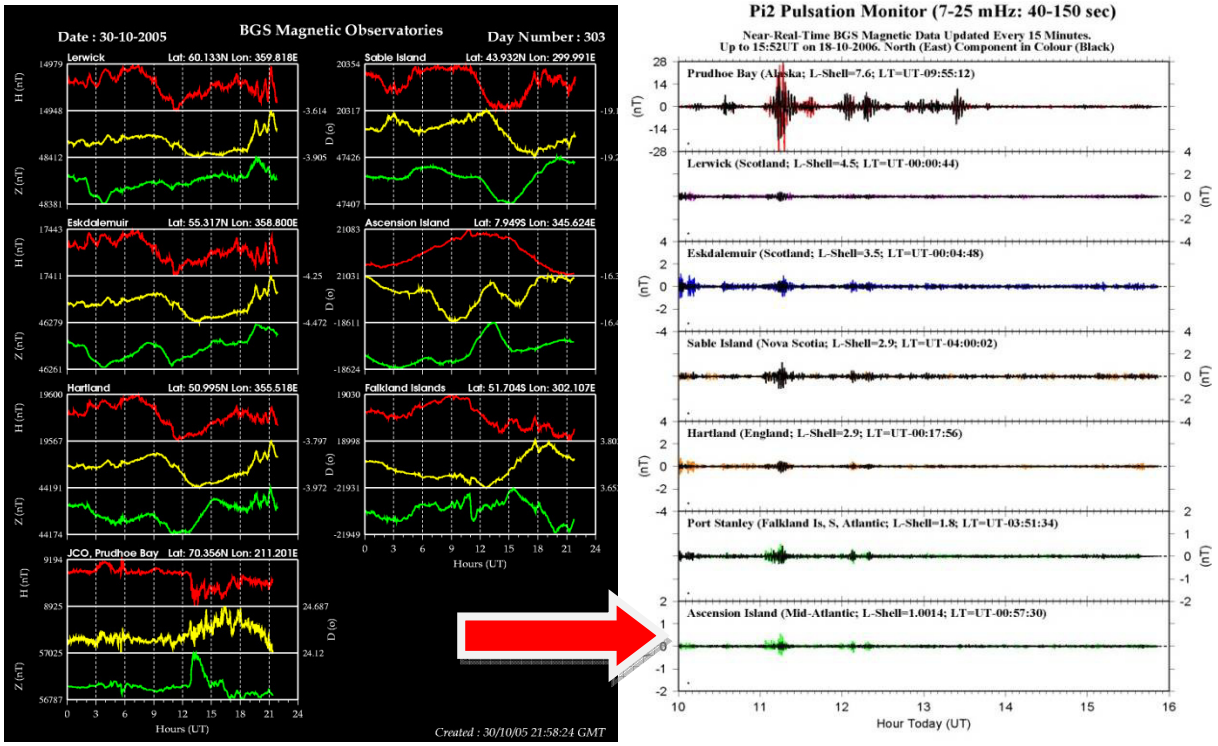

Figure 5 –Real time observatory magnetograms can be processed to provide monitoring data for different space weather processes. In this Figure magnetograms from seven BGS observatories around the world are filtered to provide a Pi2 real time monitor. Pi2 pulsations indicate substorm activity, which in this case occurs across the world at different latitudes. (Note that two different days are shown simply to illustrate the principle.)

6. ACKNOWLEDGEMENTS

The author would like to thank Ciarán Beggan, Ellen Clarke, Gemma Kelly, David Kerridge, Allan McKay, Antti Pulkkinen, Katie Turnbull, Jim Wild, Ari Viljanen and many others for collaborating over the years on space weather and, directly or indirectly, contributing to the work presented in his paper. Industry colleagues at National Grid and Scottish Power are also thanked. The research leading to these results has received funding from the European Community's Seventh Framework Programme (FP7/2007-2013) under grant agreement no 260330. This paper is published with the permission of the Director, BGS (NERC).

7. REFERENCES

Amm, O. (1997): "Ionospheric elementary current systems in spherical coordinates and their application". *Journal of Geomagnetism and Geoelectricity*, **49**, 947-955.

Beamish, D. and J. C. White (2012): "Mapping and predicting electrical conductivity variations across southern England using airborne electromagnetic data". *Quarterly Journal of Engineering Geology and Hydrogeology*, **45**, 1, 99-110, 10.1144/1470-9236/11-026.

Love, J. (2012): "Credible occurrence probabilities for extreme geophysical events: Earthquakes, volcanic eruptions, magnetic storms". *Geophysical Reseaqrch Letters*, **39**, L10301, doi:10.1029/2012GL05143.

Riley, P. (2012): "On the probability of occurrence of extreme space weather events". *Space Weather*, **10**, S02012, doi:10.1029/2011SW000734.

Thomson, A. W. P., E. B. Dawson and S. J. Reay (2011): "Quantifying extreme behaviour in geomagnetic activity". *Space Weather*, **9**, S10001, doi:10.1029/2011SW000696.

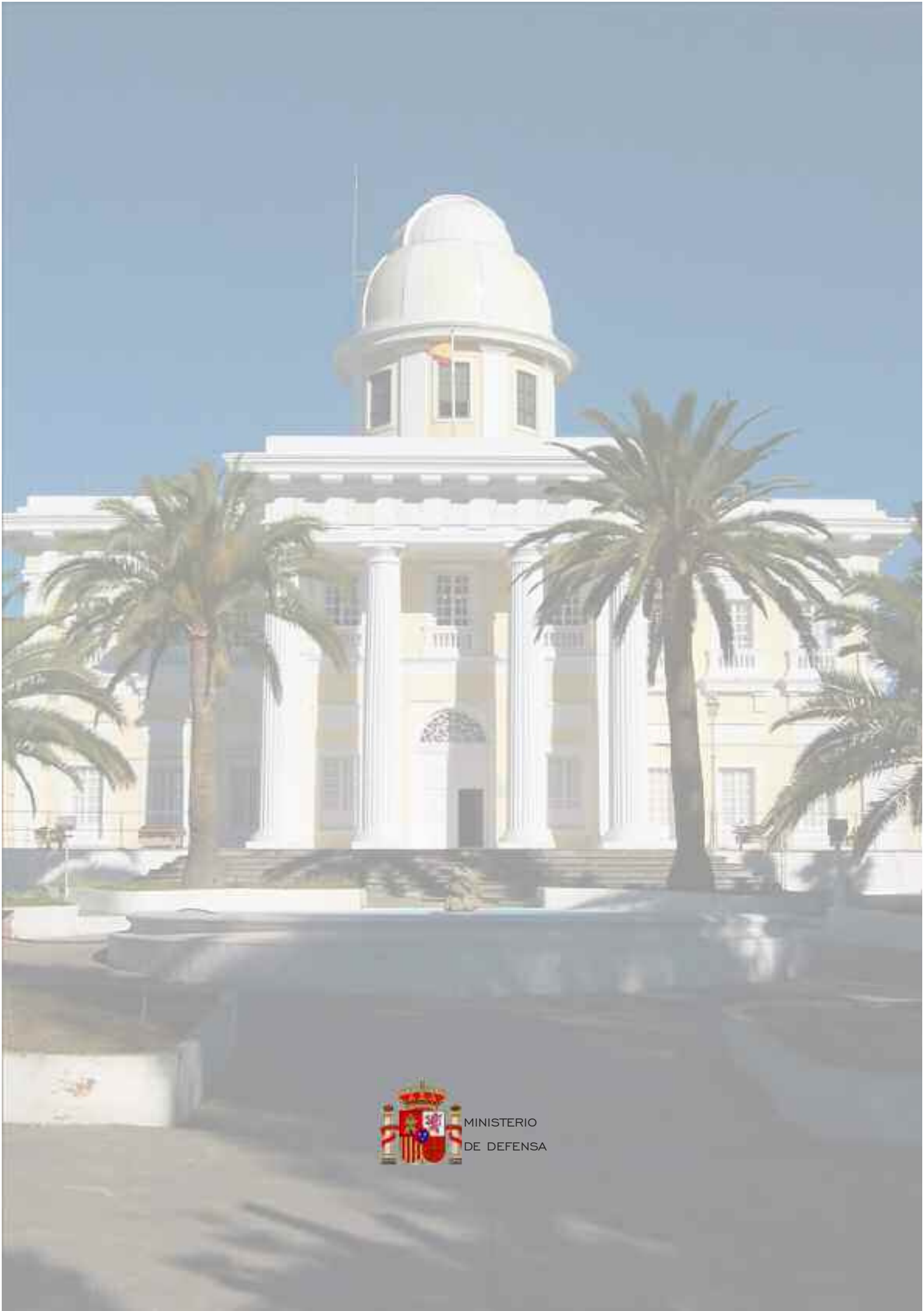

MINISTERIO
DE DEFENSA